STUDY OF AUTOMATED

RENDEZVOUS AND DOCKING

FOR ATS-V DESPIN

FINAL REPORT

VOLUME 1 OF 2

SD 71-286

Space Division
North American Rockwell

FINAL REPORT ON A
STUDY OF AUTOMATED RENDEZVOUS AND
DOCKING FOR ATS-V DESPIN

Volume 1 of 2 Volumes

February 1971   Contract NASW-2136

Prepared for

NASA Goddard Space Flight Center

Greenbelt, Maryland

SD 71-286

PREFACE

NR has completed a study in accordance with the State-
ment of Work in NASA Contract NASW-2136, "Study of
Automated Rendezvous and Docking for ATS-V Despin". Work
was performed for NASA Headquarters under the technical
direction of J. R. Burke and for the NASA Goddard Space
Flight Center under the technical direction of J. Phenix.
Their contribution and guidance to the study is gratefully
acknowledged.

This final report, SD 71-286, presents the results of
the study. It consists of 2 Volumes: Volume 1 - Text;
Volume 2 - Appendices (Calculations and pertinent reports
generated during the study). This is Volume 1 - Text.

TABLE OF CONTENTS

PRECEDING PAGE BLANK NOT FILMED

LIST OF ILLUSTRATIONS

PRECEDING PAGE BLANK NOT FILMED

LIST OF TABLES

x

INTRODUCTION, SUMMARY, & CONCLUSIONS

THE SPACE DIVISION (SD) OF NORTH AMERICAN ROCKWELL (NR) HAS COM-
PLETED A STUDY WHICH DOCUMENTS THE TECHNICAL AND ECONOMIC FEASIBILITY
OF A MISSION TO DESPIN APPLICATION TECHNOLOGY SATELLITE NO. V (ATS-V).
THE MISSION WILL PROVIDE A TIMELY, DRAMATIC DEMONSTRATION OF THE AVAIL-
ABILITY AND UTILITY OF SPACE MAINTENANCE AND REPAIR (M&R) TECHNOLOGY.
THE RECOMMENDED APPROACH WAS EVOLVED FROM AN NR PROPOSED SPACE
M&R EXPERIMENT FOR ATS F&G AND CAPITALIZES ON A UNIQUE COMBINATION
OF NR EXPERIENCE AND FACILITIES.

BACKGROUND

ATS-V was launched from Kennedy Space Flight Center on August 11, 1969. In an
otherwise perfect mission, unexpectedly large energy dissipation rates were produced by
ATS-V's heat pipes causing the spacecraft to tumble into a flat spin about an axis trans-
verse to the symmetrical spin axis before the apogee motor could be ejected (the trans-
verse axis is the stable spin axis with the apogee motor attached; the symmetrical axis is
stable after apogee motor ejection). Weeks of investigation by NASA uncovered no on-
board means to remedy the flat spin situation or bias the direction in which the spacecraft
would return to its symmetrical (stable) spin axis after apogee motor ejection. With the
probabilities about even that the spacecraft would erect properly, the apogee motor was
jettisoned -- but erection dynamics caused the spacecraft to return to the planned
symmetrical spin axis upside down and, therefore, with a reversed body coordinate spin
direction. This has prevented despinning the spacecraft since it is equipped with a spin
direction sensitive yo-yo despin system. Thus, the gravity gradient experiment and a
large part of the L-band experiment (both designed for the non-spinning mode) cannot
be conducted.

This situation developed while NR was proposing a remote maneuvering unit (RMU)
for a space M&R experiment on ATS F&G missions. RMU's are self contained spacecraft
maneuvered by "pilots" from remote locations, in this case from earth . Investigations by
NR indicated that ATS-V possessed ideal characteristics (stable spin with very slight
wobble; accessible apogee motor thrust flange for docking) to accommodate despin by a
Remote Maneuvering Unit (RMU). The ATS-V situation, then, offers an opportunity to
conduct a mission which would not only salvage unfulfilled objectives of ATS-V but at
the same time develop and qualify space M&R equipment and techniques for expanding
the versatility and utility of space operations.

A 5 month study was conducted by NR under NASA Contract NASW-2136 to investi-
gate the crucial aspects of such a mission; e.g. rendezvous, illumination, pilot-in-loop
capability, etc. This final report constitutes completion of that contract.

STUDY REQUIREMENTS

The contract required NR to "Conduct a study to ascertain the availability of re-
mote control technology to repair, maneuver, observe, and perform other functions on
synchronous orbit spacecraft. Study the application of this technology to ATS-V to
rendezvous, dock with, despin, and observe ATS-V. Study alternative applications to
observe ATS F and G antenna deployment and transfer fuel from ATS F/G to SMS". It
also stated, "Because ATS-V has a finite life of approximately 3 years, it is essential
that the mission be accomplished with existing technology and hardware." The contract
also required that the following items be addressed in the study:

Launch Requirements — definition of a nominal mission profile from liftoff
to visual acquisition. Thor Delta booster was
specified.

Rendezvous — investigation and selection of techniques to accom-
plish visual acquisition and closure to a stationkeeping
distance of 150 feet from ATS-V.

Docking — definition of docking requirements and procedures.

Despin & Separation — study of techniques to accomplish a controlled despin
of ATS-V and subsequent separation and observation
of ATS-V gravity gradient boom deployment.

Alternate Mission
Capability — consideration of other uses for the RMU after ATS-V
despin.

Integrated Spacecraft
Design — definition of a preliminary RMU configuration to
despin ATS-V.

Cost and Schedule
Plan — development of cost and schedule estimates for the
selected mission approach.

The contract schedule required submission of a final report 5 months after go-ahead.

STUDY APPROACH

Based on extensive, previous work at NR, a preliminary RMU configuration was
established as a first step in the study to serve as a basis for investigating the feasibility
of accomplishing the primary mission task: ATS-V despin. Subsequent missions for the
RMU were contemplated and provisions to perform them incorporated where such pro-
visions would not adversely impact baseline mission performance, cost, or schedule.

In all cases, to conserve cost and meet the short schedule, maximum use was made of developed, space proven components, particularly those available from the ATS-V program.

The various mission phases (launch, rendezvous, docking, despin, separation, and observation) were then studied to ascertain the suitability of the preliminary configuration and to evaluate other possible approaches. At the same time, laboratory tests were performed to investigate the applicability of various illumination, synchronization, alignment, and ranging techniques. These were factored into the preliminary configuration.

A significant part of the study was then devoted to a pilot-in-the-loop docking simulation which utilized NR's six degree-of-freedom (6 DOF) General Purpose Visual Simulator (GPVS) developed originally for Apollo docking studies. RMU Attitude Control System (ACS) and Reaction Control System (RCS) characteristics along with RMU mass properties were programmed on the GPVS analog computer; signal delays experienced in synchronous altitude transmission were incorporated; models of the ATS-V and RMU docking system were installed on the 6 DOF transport rig; and a working mockup of a pilot control console was built, complete with video monitors, hand controllers for commanding attitude and translation maneuvers, and various indicators. Using video cues and selected RMU sensor information, three "pilots" then "flew" a combined total of about 130 simulated dockings to assess the validity of the preliminary RMU equipment selection, evaluate available alternate approaches, develop statistical data on mission success probability, and provide design criteria for the docking mechanism.

Results of the piloted simulation were also used as input data (closing velocity and angular and lateral misalignments and rates) to a digital study which investigated docking and despin dynamics. Information from the digital study was also used to assess the suitability of the preliminary configuration and provide design criteria for the docking mechanism.

Detailed cost and schedule estimates were then prepared for the finalized baseline configuration. An assessment was also made of the cost and schedule impact on the baseline mission of adding capability to perform selected additional missions subsequent to ATS-V despin. Cost and schedule information was based on vendor quotes to comprehensive procurement specifications for all identified "buy" items as well as on detailed manpower estimates from NR functional groups.

As a last step in the study, this final report was prepared.

STUDY RESULTS

The baseline mission is divided into five phases as indicated in Figure 1. The nominal trajectory is generally routine state-of-the-art except for the precision needed to rendezvous. The study showed, however, that the required precision could be obtained without substantial difficulty by using only the ATS Rosman and Mojave ground tracking station (3 sigma relative position tracking errors of less than 1000 feet are predicted;

and video acquisition is possible at 10 n.mi. or more). If a third (mobile) station were added south of the equator and trilateration used to track the vehicles, the rendezvous problem would be trivial (3 sigma relative position tracking errors of less than 50 feet in each axis are predicted). In both cases, the key to achieving the exceptionally accurate relative position information is that systematic tracking errors are automatically nulled between the two spacecraft as the distance between them diminishes.

At such close rendezvous distances, the sunlit ATS-V is an easily identifiable target. If trilateration were used, the RMU would merely be pointed and the camera turned on, and ATS-V would be within the field of view. For the two station (baseline) case, a short search sequence might be required to locate ATS-V, but visual acquisition would still be readily achieved. After acquisition the "pilot"will"fly" a line-of-sight (LOS) closure similar to that previously flown on Apollo. Beginning at about 250 feet, the RMU will be maneuvered from its co-orbital view of the sunlit side of ATS-V to a view of its non-sunlit aft end. This, too, is a simple maneuver, and relative position and velocity information derived from ground tracking updated by stadia measurements from the video cue will be ample to support the closure operation.

At this point, the pilot begins the docking phase of the mission. The pilot-in-the-loop simulation showed that satisfactory scene definition can be provided to the pilot with proper selection of illumination intensity and vidicon characteristics. Also, the simulation showed that the pilot could derive the necessary alignment and range/range-rate information from video cues. The simulation also showed that a controlled "mini-pulse" translational mode was a substantial aid during the final docking approach as well as a two man (pilot and co-pilot) team to share the tasks involved in docking. Use of NR's dual purpose gyros (DPG's) was a beneficial feature since it permits quick response to attitude commands and holds precise attitudes thereafter, thus eliminating some of the pilot burden during final docking. In the simulation, pilots were consisently able to meet the docking criteria of lateral miss distance of less than 2.0 inches, angular mis-alignment of less than 3°, and closing velocity of about 0.2 fps or less.

A digital simulation showed that steady state and transient docking loads were not severe. Also, that the NR DPG control system has ample capability to stabilize the two spacecraft during docking and despin. An NR math model of the ATS-V heat pipe energy dissipation phenomenon was developed and checked against ATX-V flight data. Results validated NR's model and it was used in the digital simulation which verified the adequacy of the baseline RMU stabilization system.

The baseline RMU configuration developed to accomplish the various phases of the despin mission described above is illustrated in Figure 2. It is a conventional, solar powered spacecraft with the addition of certain mission peculiar features: a docking cage and latches which can be spun up and synchronized with the ATS-V's spin rates; a video and illumination subsystem (since sunlight will not illuminate the interior of ATS-V); and an ACS which accommodates a spin mode, a despun mode, and a dual spin mode - NR's DPG's are a key control element in the despun and dual spin modes. The spacecraft was designed for launch on a Thor Delta. It was configured only to accomplish the primary mission task of despinning ATS-V, but other missions can be performed by adding fuel.

- 4 -
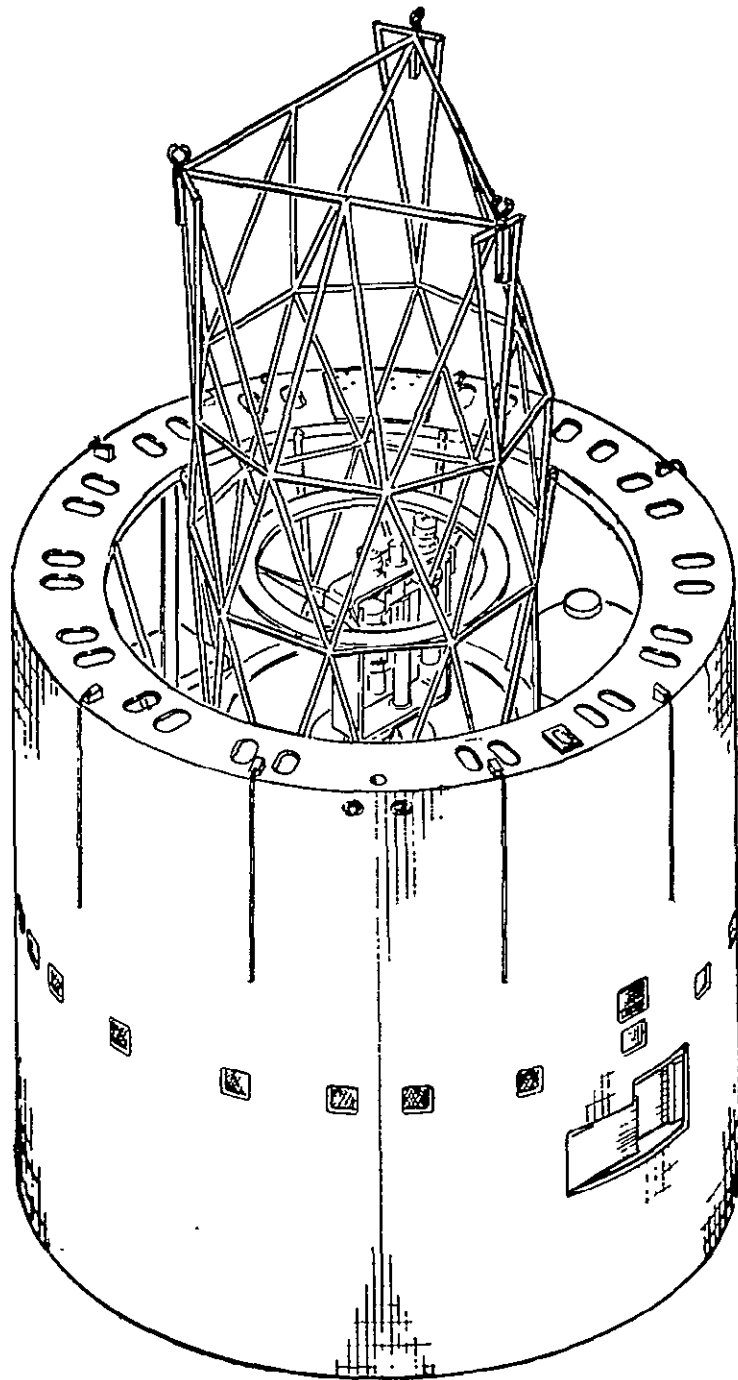
Figure 2. Baseline RMU Configuration

Cost and schedule estimates indicate the program can be conducted in 22 months or less for $10 to $11 million provided maximum use is made of available ATS-V spacecraft and ground equipment and facilities.

CONCLUSIONS & RECOMMENDATIONS

1. A low cost mission to despin ATS-V can be performed with a high probability of success.

2. The mission should be undertaken as soon as possible to maximize recoverable ATS-V life time.

3. The mission will provide valuable operational experience with remote maneuvering teleoperators, applicable to manned and unmanned maintenance, logistics and repair operation in space.

4. Maximum use should be made of available equipment and facilities from the ATS-V program to insure a minimum cost program.

5. Rendezvous can be accomplished using only the two ATS tracking stations, Rosman and Mojave, but the addition of a third (mobile) station would simplify the mission substantially. These conclusions presume ATS-V is operating; otherwise, another means of tracking ATS-V must be utilized, such as optical ground tracking with a Baker-Nunn camera. With ATS-V operable or not, no suitable radar approach was identified which would materially aid the synchronous orbit rendezvous operation.

6. Relaxed time constraints are key to performing a simple, routine type of rendezvous operation.

7. NR DPG's are ideal stabilization elements for remote, precision docking operations and, at the same time, provide ample energy dissipation in the despun section of the coupled vehicles to insure adequate stability during despin operations.

8. An acceptable video cue can be provided together with proper control power to permit ground command of the docking maneuver with the required precision.

9. A two (or more) man docking team (pilot/co-pilot) facilitates the docking operation.

10. No major technical problems are apparent, and the hardware design and fabrication phase can begin immediately; but additional work now in the following areas would facilitate a minimum cost, short schedule program in the hardware phase as well as maximize RMU usefulness:

(a) Additional digital investigation to optimize latch parameters and DPG characteristics.

(b) Preliminary latch design, fabrication of a working mockup of the cage and latches, and docking tests which simulate RMU and ATS-V mass properties and docking environment.

(c) Investigation of maximum amplitude and phase modulation which can be tolerated by the ATS R&RR ground equipment with minor or no modification; definition of a minimum cost omni C-band antenna which does not exceed the maximums established.

(d) Investigation of approaches to achieving 3 DOF video coverage instead of the essentially 2 DOF coverage provided by the base-line. Consider additional cameras, steerable mirrors, and use of a reduced frame rate transmitted via the omni C-band antenna.

(e) Review additional missions of value other than those specifically covered in the study. Consider, particularly, the equipment requirements versus the advantages of extended life.

(f) Conduct additional piloted simulation runs to investigate failure modes and optimize the video, illumination, and piloting procedures.

1.0 MISSION OBJECTIVES AND SYSTEM REQUIREMENTS

THE BASELINE MISSION OBJECTIVE IS TO PROVIDE A COST-EFFECTIVE DEMONSTRATION OF THE AVAILABILITY AND UTILITY OF SPACE MAINTENANCE AND REPAIR (M&R) TECHNOLOGY BY DESPINNING APPLICATIONS TECHNOLOGY SATELLITE-V (ATS-V) WITH A LOW-COST, STATE-OF-THE-ART REMOTE MANEUVERING UNIT (RMU).

1.1 OBJECTIVES

The primary mission task is to despin ATS-V. This will salvage several unfulfilled objectives of the ATS-V mission and at the same time provide operational experience with and design data on key M&R operations and equipment, such as: (a) ground guided rendezvous, (b) terminal line-of-sight (LOS) closure, (c) pilot-in-the-loop precision maneuvering (d) necessary pilot aids and procedures, (e) required M&R platform stability and maneuverability, (f) illumination and video gear (g) optical diagnosis, and (h) docking.

Other applications for the RMU subsequent to despinning ATS-V are possible, including rendezvous with ATS-F and -G or other synchronous satellites, use as a communication relay satellite, and use in L-band, navigation, and tracking experiments. Where these additional applications require added or different spacecraft features, they are not provided for in the baseline system, but their impact is discussed in this report.

1.2 GROUND RULES

The following ground rules have been established to facilitate achievement of mission objectives:

1. A high probability of success is required and conservative design margins will be maintained in the design of all elements.

2. The RMU must be launched at the earliest possible date to minimize degradation of ATS-V. (The three-year design lifetime of ATS-V is reached in August 1972.)

3. Available space proven components will be used to the maximum extent possible to minimize cost and development time. Weight will be sacrificed for availability where necessary, provided that total weight must be well within the capability of the Thor Delta booster.

4. Maximum use will be made of ATS-V spacecraft equipment, ground support equipment, and ground station capabilities to minimize cost and insure compatibility during rendezvous and docking operations.

5. Because the RMU is well within the state of the art and to minimize cost, only one flight article will be fabricated. It will also be used for qualification and flight acceptance testing along with one structural test model which will incorporate some active subsystems. No other system test units will be provided. Test articles at the component and subsystem level will, in general, be kept to a minimum and reused where possible on the structural model and flight unit or as spares.

6. A Quick Reaction Capability (QRC) approach will be used in the program consisting of a fully projectized, colocated operation with minimal documentation, and program management requirements.

1.3 CONSTRAINTS

The constraints imposed on the RMU mission/system as a result of the mission objectives and ground rules are related to: (a) ATS-V orbital parameters, (b) ATS-V configuration/physical parameters, and (c) required compatibility with ATS-V ground stations and software.

ATS-V is in a geostationary orbit at 107° west longitude. It is spinning about an axis which is displaced by approximately 0.9° relative to the ATS-V longitudinal axis of symmetry. As a constraint for the current study, this displacement angle was taken as 1.6° to provide a suitable design safety margin.

The spin rate of ATS-V is gradually increasing and is expected to be approximately 80 rpm at the time of the RMU mission. The spin axis is nearly normal to the orbit plane. The present orbit plane inclination angle of approximately $+2.6^\circ$ is decreasing at the rate of about 0.1°/month and will be $+0.1^\circ$ at the anticipated time of RMU launch (August 1972). The apogee motor attachment ring of the ATS-V, which will be used for RMU docking, is facing toward the south relative to earth (i.e., the RMU will approach ATS-V from the south during terminal docking closure).

Weight of ATS-V is 1003.39 pounds. Moments of inertia in roll, pitch, and yaw are $I_R = 98.6$ slug-ft^2, $I_p = 85.0$ slug-ft^2, and $I_y = 82.8$ slug-ft^2. The ratio $I_R/I_p = 1.16$ shows that the present spin configuration is stable. Heat pipes, provided to cool the solar arrays, significantly affect ATS-V dynamics due to the large rate of energy dissipation of the coolant motion in the pipes (see NASA/GSFC, "ATS-V Post Launch Report (Preliminary)", dated December 1969).

Figure 1-1 shows the aft view of the ATS-V with the apogee motor removed. The apogee motor thrust ring provides the surface to which RMU docking engagement is to be effected. Also shown are equipment packages on the structural bulkhead (at Station 2.00) that must be cleared by the RMU latching devices in docking; clearance provisions must also allow for the effects of the displacement of the ATS-V spin axis relative to its axis of symmetry. Since the thrust ring is recessed inside the ATS-V skirts, it will not be lighted by the sun, and the RMU must provide its own light ssource for docking visibility.

The ATS-V ground network currently consists of the following elements:

1. ATS Operations Control Center (ATSOCC) located at Goddard Space Flight Center (GSFC). Based on telemetry data transmitted via the tracking stations and on orbit and spacecraft attitude data provided by the Goddard Orbit Computation Facility (GOCF), the ATSOCC monitors the status of the spacecraft and issues command instructions to the tracking stations for formating and transmittal to the spacecraft.

2. The GOCF (located at GSFC) provides orbit data and "orbit correction required" data to the ATSOCC based on range and range-rate measurements obtained from the tracking stations. The GOCF also provides spacecraft attitude data to the ATSOCC as computed from (1) polarization angle (POLANG) of the C-band beacon as detected by the tracking stations, and (2) sun-sensor data received from the spacecraft telemetry link via the tracking stations.

3. Two tracking stations are currently devoted to the ATS program: Rosman, N.C. and Mojave, California. Both stations provide range and range-rate information to the GOCF using the Applications Technology Satellite range and range-rate (ATSRARR) system. This side tone ranging system utilizes ground originated C-band transmissions transponded through the spacecraft. Normal operating mode is for each station to take 2.5 minutes of such data in each hour at the rate of one measurement per second. The time interval between the sets of measurements obtained by the two stations is approximately 15 minutes.

   The two tracking stations also (1) format the command instructions received from the ATSOCC and transmit them to the spacecraft via the VHF telemetry link, (2) receive the VHF telemetry data from the spacecraft and relay the sun-sensor data to the GOCF and the spacecraft status data to the ATSOCC, and (3) measure the polarization angle of the received C-band signal and relay this information to the GOCF.

- 13 -

BLACK BOX (2 PLACES)
3 IN. FROM RING

$\theta = 118°$

$\theta = 90°$

APOGEE MOTOR THRUST
RING (DOCKING STRUCTURES)

$\theta = 0°$

$\theta = 180°$

BLACK COIL ASSEMBLIES
(2 PLACES) 4 IN. FROM RING

ALUMINIZED MILAR LOUVERS

BLACK ELECTRONICS
BOX 3.5 IN. FROM RING

$\theta = 270°$

4 IN. WIDE WHITE SKIRT RIM

$\theta = 298°$ (2) CANNON PLUGS SILVER
1.8 IN. FROM RING

BLACK INTERIOR
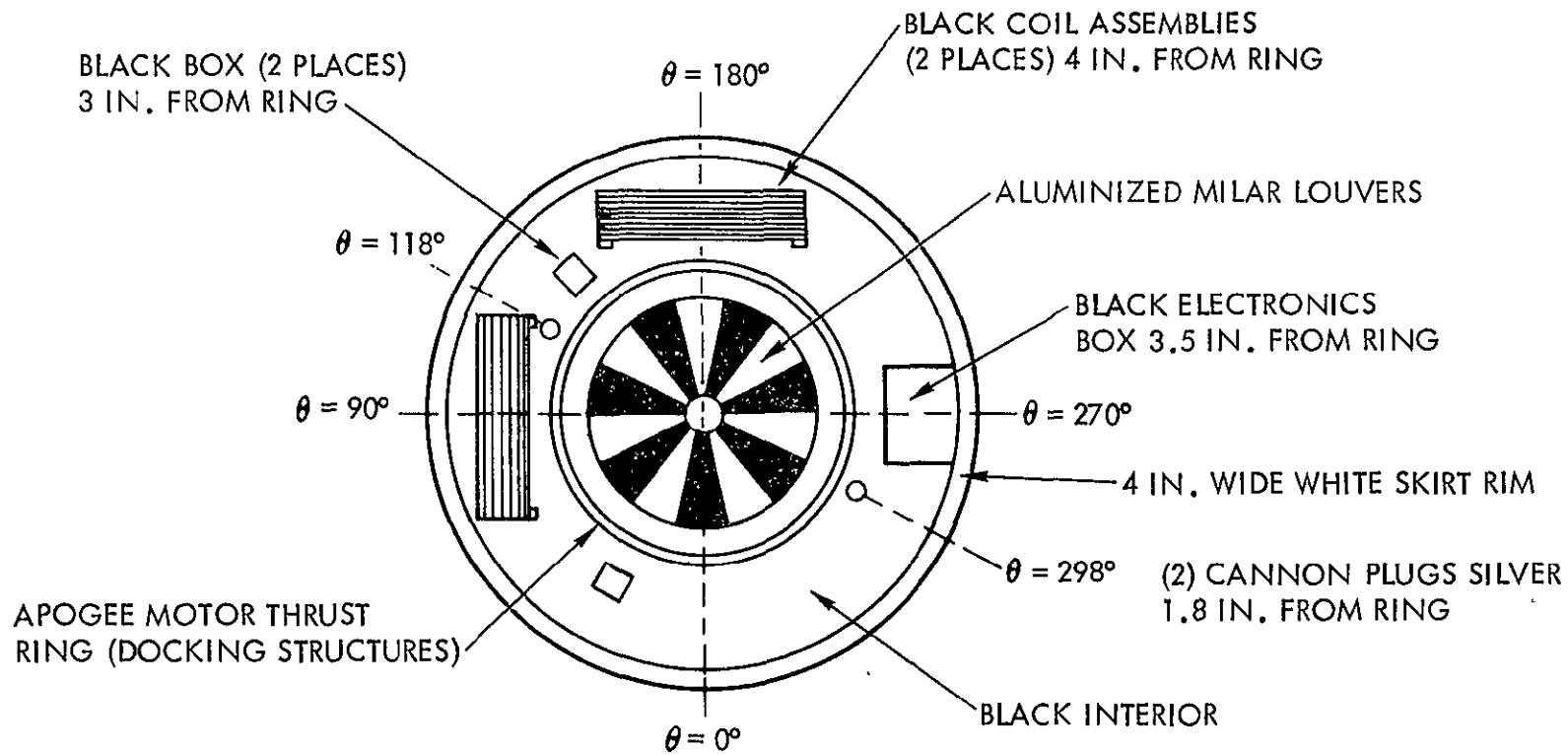
Figure 1-1: Aft View of ATS-V with Apogee Motor Separated

To minimize interface problems, the RMU will utilize the same modus operandi and facilities from launch up to visual acquisition. The baseline RMU will utilize the same up-link command frequency as ATS-V with a different address-code. The ATS-V utilizes two VHF frequencies for down-link telemetry, one of which is for transmittal of spacecraft housekeeping data, while the other is used to transmit experiment data. The baseline RMU will utilize the same two frequencies in a redundant cross-strap manner to relay all data other than the video signals. This arrangement allows RMU data to be relayed concurrently with transmitting either housekeeping or experiment data from ATS-V. The C-band up-and down-link frequencies will be identical to that of ATS-V; C-band will be used for tracking, POLANG measurements and for transmittal of video. For tracking prior to visual acquisition the C-band transponders of the two spacecraft will be commanded ON/OFF as required for alternate contact with the individual vehicles. C-band contact with either vehicle will be possible from either tracking station without reorientation of the ground antennae once the two vehicles are within 0.5 degree of each other insofar as the line-of-sight (LOS) to the ground station is concerned.

Although the baseline RMU mission will be based on utilizing only the two currently available tracking stations (Rosman and Mojave), the design of the RMU shall be compatible with the potential utilization of a third station at Santiago, Chile. This portable station, if provided, will (1) have a 15' antenna dish; (2) will not have a range and/or range-rate measuring capability -- it will, instead, relay the C-band signal received via the RMU from one of the other two stations back to the originating station via the RMU; and (3) it will not have a polarization angle measurement capability.

Once the RMU is within visual acquisition range of ATS-V, command and control of the RMU will be turned over from the ATSOCC to the Rosman, N.C. tracking station where the "pilot," utilizing the NR furnished control console, will command the RMU in real time based on video cues. The video signal will be transmitted from the RMU via the C-band down-link to the Rosman facility. This change in control authority is required since no real time wide band link suitable for video transmission exists between the tracking stations and the ATSOCC. In the ATS-V command system, commands received from the ground station are not immediately executed upon receipt; they are first relayed back to the station via telemetry and are executed only upon receipt; of an "execute" command which is transmitted from the ground as an indication of correctness of the commands. This process takes approximately 5 seconds. In the RMU command system provisions will be made to eliminate this delay for those commands which require essentially real time execution in the pilot-commanded mission phases.

1.4 BASELINE SYSTEM DESCRIPTION

In consonance with the above basic mission objectives, ground rules and constraints preliminary analyses were performed to define the baseline mission/system requirements. The results of these analyses as well as detailed descriptions of the selected baseline mission profile, selected baseline spacecraft design and baseline GSE design are given in Sections 2.0, 3.0, 4.0, 5.0 and 7.0 of this report. A brief summary of these baselines is given in the following subsection.

1.4.1 Mission Baseline

The baseline mission includes short-term observation of ATS-V after despin and terminates with a maneuver which places the RMU in a storage orbit to preclude collision with ATS-V. The mission is divided into five phases:

    a.   Launch Phase - from lift-off to visual acquisition maneuver;

    b.   Rendezvous - visual acquisition maneuver through closure to within 150 feet of ATS-V;

    c.   Precontact Docking - from 150 feet to first contact with ATS-V;

    d.   Post Contact Docking, Despin and Separation - coupled operation;

    e.   Observation and Standoff - from separation to placement in the storage orbit.

The sequences and operations in the various phases are as follows:

    a.   Launch Phase (See Section 2.0 for Details)

        The contract specified use of a Thor Delta launch vehicle, and the selected baseline is the Model 603. This model uses the Delta Inertial Guidance System (DIGS). The Thiokol TEM 442-1 has been selected as the baseline apogee motor.

        Referring to Figures 1-2 and 1-3, the baseline nominal launch phase consists of the following sequential steps:

        1.   Lift-off is due East from ETR at 9.00 a.m. local sun time; boost provided by the first and second stages of the Thor Delta result in a circular 100 n.m. orbit with an inclination angle of 28.5°.
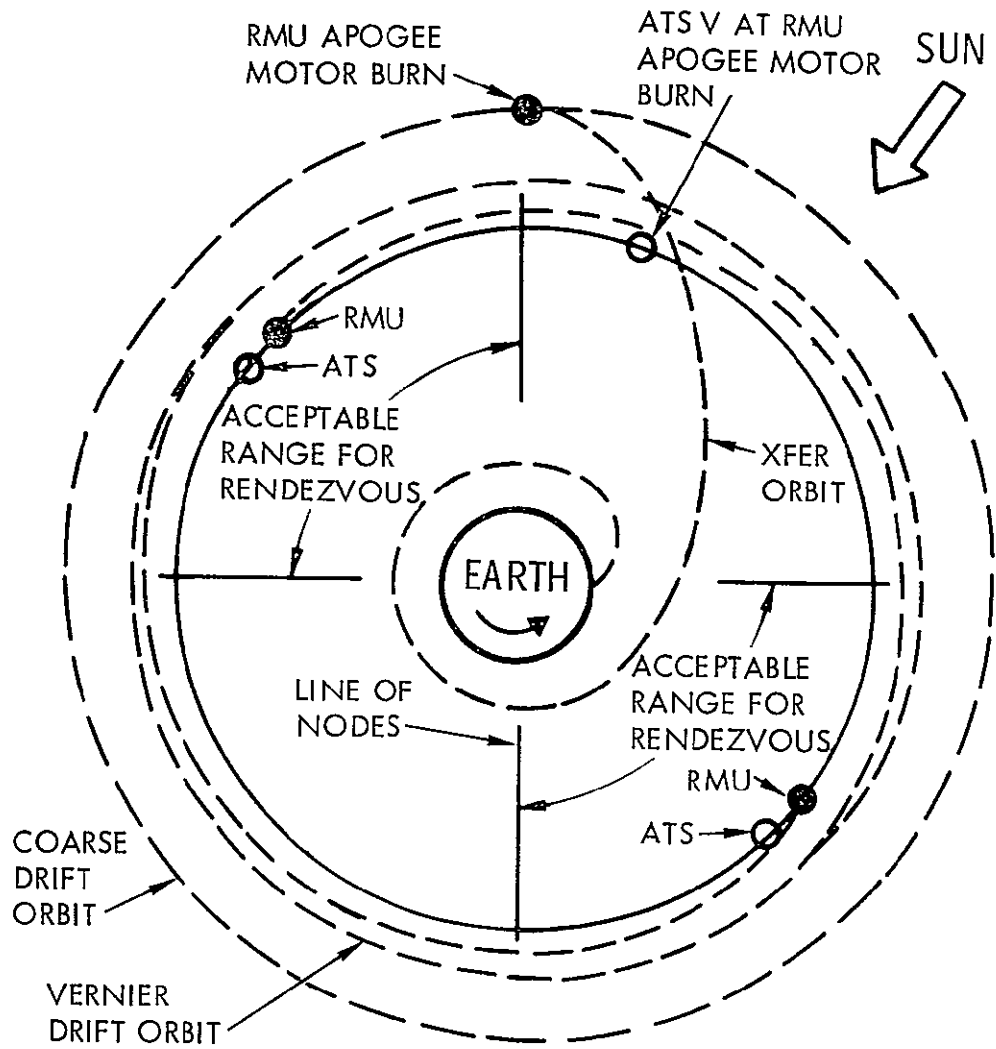
Figure 1-2. Trajectory Diagram
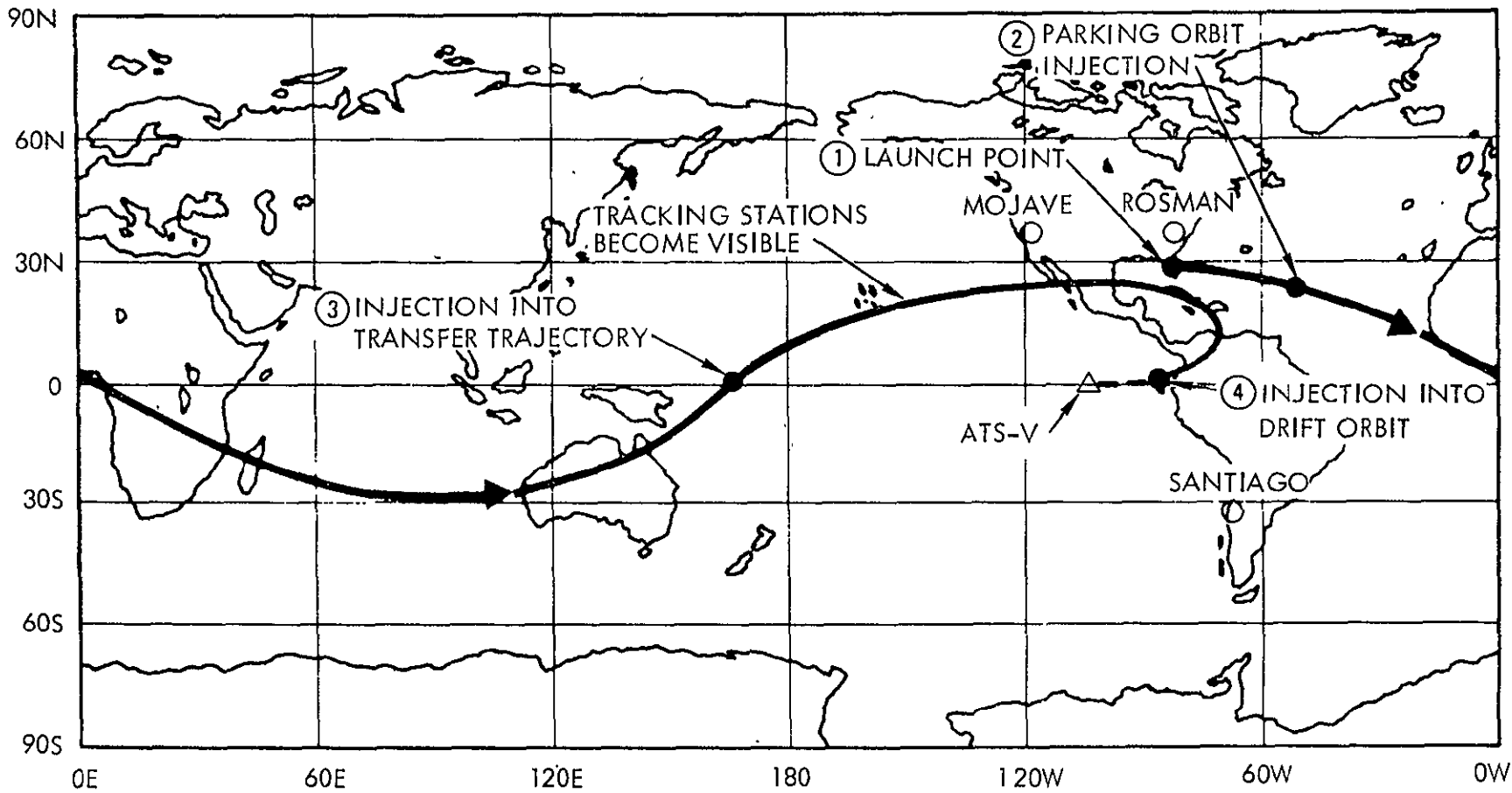
Figure 1-3. Ground Track of RMU

Space Division
North American Rockwell

2. At the first ascending node, the Thor Delta third stage places the RMU into an elliptical transfer orbit with an inclination angle of 24.5°, and an apogee altitude 84 n.m. above the altitude of the ATS-V; first apogee longitude is 87° W. The third stage is jettisoned after burnout, and the attitude control system provides active nutation control throughout the transfer orbit (the spin axis does not become the major axis of inertia until apogee motor ejection).

3. Approximately 15 minutes after third stage burn, the RMU is acquired by the ground stations on the VHF frequencies and command/telemetry links are established and the RMU is precessed to apogee firing attitude. Approximately 45 minutes after third stage burn, the ground stations will also acquire the C-band beacon of the RMU, and POLANG and RMU sun sensor data will be available for attitude determination. Before apogee is reached, any attitude error found to exist will be corrected by a second precession maneuver. The RMU will reach first transfer orbit apogee approximately 5 1/2 hours after third stage burn.

4. Upon reaching the first apogee of the transfer orbit, the apogee motor will be fired to place the RMU into a nominal circular drift orbit at 0.1° inclination and at an altitude of 84 n.m. above that of the ATS-V orbit. At first apogee, the RMU "leads" ATS-V by approximately 20° (apogee longitude is 87° W, ATS-V is at 107° W). The higher orbit of the RMU provides a drift toward ATS-V at a rate of 2° per revolution. The circular drift orbit will allow flexibility in accomplishing subsequent rendezvous at a wide range of orbital positions (see Figure 1-2).

5. After completion of apogee motor burn, the apogee motor will be jettisoned, and the RMU will be in a stable spin mode.

6. The RMU spin axis will then be precessed to a position normal to the drift orbit plane, and drift orbit maneuvers will be made to correct booster/apogee motor injection errors.

7. When the corrected drift orbit has brought the RMU to within approximately 1° of the ATS-V longitude, the delta altitude will be reduced through a Hohman transfer to produce a "vernier drift orbit" with a drift of approximately 0.2° per revolution.

8. From the "vernier drift orbit," the RMU will be placed into a final approach trajectory which will result in suitable initial conditions for visual acquisition of ATS-V. When the required initial conditions for visual acquisition of ATS-V are reached, command of the RMU is turned over to the "pilot." He commands a despin of the RMU and energizes the RMU attitude control subsystem.

b. <u>Rendezvous Phase</u> (See Section 3.0 for Details)

Preliminary calculations indicate that, with a 14° field-of-view lens, ATS-V can be acquired at distances of 10 n.mi. with sun reflection angles up to 45° (arbitrary, conservative maximum). The TV image would be indistinguishable from a star image and would not be readily recognizable until ranges less than 2000-3000 feet were achieved. To avoid mechanical steering of the TV camera or the high gain C-band antenna, ATS-V must be within the 14° pitch field-of-view of the camera; steering in the yaw plane can be accomplished since the RMU can be yawed without affecting high gain antenna earth pointing.

For three station tracking (trilateration), both in-plane and out-of-plane 3σ relative tracking errors in each axis are less than 50 feet. For these cases, a position much closer than 3000 feet range from ATS-V can easily be attained in the launch phase permitting immediate acquisition and recognition of ATS-V when the TV camera is turned on. For the baseline two station tracking case, in-plane errors are comparable, but out-of-plane 3σ relative errors grow to the neighborhood of 700 feet. Even with this error, proper geometry is easily achieved with a nominal range of less than 3000 feet, and acquisition and immediate recognition will be assured with a simple yaw search. Acquisition could also be achieved at 10 n.m. (conservatively) by performing additional operations to discriminate ATS-V from the star field background. Identification would be accomplished by making a lateral (+ Y) translational maneuver with the RMU; this will cause the ATS-V image to move on the monitor relative to the stars which are at infinity. A search in yaw (in steps of approximately 13°), may be required until the ATS-V image is identified. A very comfortable margin exists, therefore, in achieving proper initial rendezvous conditions at the termination of the launch phase. Rendezvous operations will proceed as follows:

1. The range and range-rate indicators of the pilot console will be initialized by the data provided from prior trackings; the indicators will be updated throughout this mission phase by open loop integration of all pilot-commanded delta-V maneuvers.

2. For acquisition at ranges less than 3000 feet, ATS-V will be recognized when acquired and acquisition will either be immediate or after a short search in yaw. For ranges greater than 3000, the pilot will command a translational velocity to the RMU (+ Y) and will look for an image of the ATS-V on the TV monitor (an image which has corresponding lateral motion); if the image of the ATS-V is not found, he will command a yaw maneuver (approximately 13°) and repeat the operations until the ATS-V image is identified.

3. Once the ATS-V image is located, a yaw maneuver is commanded as required to center the image on the monitor. If the image moves on the monitor, indicating the presence of relative velocity components normal to the RMU/ATS-V LOS, suitable delta-V's will be commanded to null these velocity components.

4. Next, the pilot will command a closing velocity along the RMU/ATS-V LOS of 4.0 ft/sec decreasing to 2.0 ft/sec; the latter closing rate will be maintained until the RMU is approximately 300 ft. from ATS-V as shown by the range indicator and substantiated by stadia on the TV monitor. At this point suitable delta-V firings will be initiated to reduce the closing velocity to zero as the range approaches 250 ft.

5. At the 250 ft. range lateral translation and yaw rotation will be commanded to move the RMU to a position approximately 150 ft. from ATS-V with the TV camera facing the aft end of ATS-V. The yaw and lateral maneuvers will be coordinated to keep the ATS-V image centered on the TV monitor. Once the desired position is reached, this mission phase will be concluded by stopping both the yaw and the lateral motion. Maximum elapsed time for the rendezvous phase is 3 hours.

c. Precontact Docking Phase (See Section 4.0 for Details)

Precontact docking starts at 150 feet (South) from ATS-V and ends at contact. During this phase, command of the RMU remains in the hands of the "pilot." Video will be switched to the wide angle (64°) TV camera of the RMU. The operations to be performed during this mission phase are dictated by the terminal relative alignment and velocity accuracies required for successful docking. The primary requirements are (a) angular alignment of the RMU X-axis with the ATS-V spin axis within 1.4° (this limits angular misalignment of the ATS-V thrust flange and docking latches to 3° for a 1.6° ATS-V wobble angle), (b) lateral alignment ($\pm$ Z and $\pm$ Y) of the RMU X-axis

- 21 -

with the ATS-V spin axis within 1.5 inches, (this limits the offset
of the ATS-V thrust flange from the center of the latch opening
to 2 inches for a 1.6° ATS-V wobble angle), and (c) closing
velocity of 0.1 to 0.2 ft./sec. To assure continuity of the video
down-link; the high gain C-band antenna must always point at
Earth. Once achieved, this alignment will be maintained by the
RMU's DPG's; the beam-width/ground-station geometry permits
approximately +5° tolerance on this alignment. Coarse attitude
information in pitch and roll will be provided to the pilot, as a
double-check, from the solar aspect sensors of the RMU.

The normal sequence of events in the precontact docking phase
are roughly as follows:

1. Provide rough initial RMU orientation along ATS-V centerline
   at a distance of approximately 150 feet (South) of ATS-V.

2. Translate the RMU to approximately 20 feet range, centering
   and stabilizing the TV picture.

3. Translate the RMU to the outer diameter of the ATS-V. Align
   the RMU attitude by looking across the wobbling edges of the
   ATS-V and at light reflection off the aft surface. Compare
   this observed attitude with appropriate attitude from sun/POLANG
   readings and set references.

4. Translate to the outer diameter of ATS-V at right-angles from this
   fixed location (90 degree displaced) and repeat alignment check
   for the other axis.

5. Translate RMU to center, null lateral translation, null meter
   readings, and null DPG gimbal angles, using reaction jets if
   necessary.

6. Spin-up docking cage, allowing synchronization loop to lock
   in, check and adjust the relative angular displacement of the
   latches using the despun TV image (ATS-V angular orientation
   is identifiable from high gain antenna location, sun sensor
   location, etc.).

7. Maintaining lateral translations essentially zero, translate the
   RMU at 0.1 to 0.2 fps toward the ATS until contact occurs.
   If significant lateral displacements occur prior to contact, stop
   and readjust. This operation ends the precontact docking phase
   which is expected to take less than 15 minutes.

d. Post Contact Docking, Despin, and Separation Phase (See Section 5.0 for Details)

At initial contact, the RMU's three docking clamps automatically close on the ATS-V thrust flange and couple the ATS-V and RMU into a dual spin configuration. This operation is accomplished in a damped manner, to minimize loads, and the RMU ACS system provides ample stabilization for the coupled spacecraft. Despin is initiated by pilot command immediately following docking. Despin is reacted by the RMU RCS thrusters and is complete in about 7 minutes. Following despin, the clamps are commanded open and the RMU is backed out by pilot command. Total time for this phase should not exceed 15 minutes.

e. Observation and Standoff Phase (See Section 5.0 for Details)

Having separated from ATS-V, the RMU will be commanded into suitable position(s) as needed for observation of ATS-V. The positions utilized will be limited to those (a) which do not expose the RMU's TV camera to direct sunlight, and (b) which allow ATS-V to be kept within the field-of-view of the RMU's TV camera without an RMU pitch maneuver; the latter constraint is due to the need for maintaining the Earth coverage of the RMU's high-gain C-band antenna.

Following this observation period, the RMU's TV camera and lights will be de-energized, the RMU will be commanded to orient its X-axis normal to the orbit plane and to attain a small angular velocity about its X-axis. At this point, the DPG's of the RMU will be de-energized and the spin rate about the X-axis will be increased to 40-60 rpm utilizing the RCS thrusters.

As a final operation in the mission, the RMU's RCS thrusters will be commanded to produce suitable delta-V's for placing the RMU into an orbit which assures that it will not collide with ATS-V. This entire observation and standoff phase will not exceed a one-hour time duration.

While in this no-collision orbit, the RMU solar array will recharge the RMU batteries. Thus, should telemetry indicate that the remaining N_2H_4 propellant is adequate for additional orbital maneuvers, the RMU may be utilized for subsequent orbital operations. These subsequent operations, however, are not part of the baseline mission.

- 23 -

1.4.2 RMU System Baseline

The baseline RMU spacecraft design developed to satisfy the requirements discussed in Sections 1.1 and 1.2 and the baseline mission parameters defined in Section 1.3.1 are shown on Figure 1-4. Table 1-1 summarizes baseline subsystem mechanizations. GSE is typical of synchronous satellite programs except for the addition of a pilot control console used in pilot-in-the-loop rendezvous and docking operations. The system baseline is discussed in detail in Section 7.0.
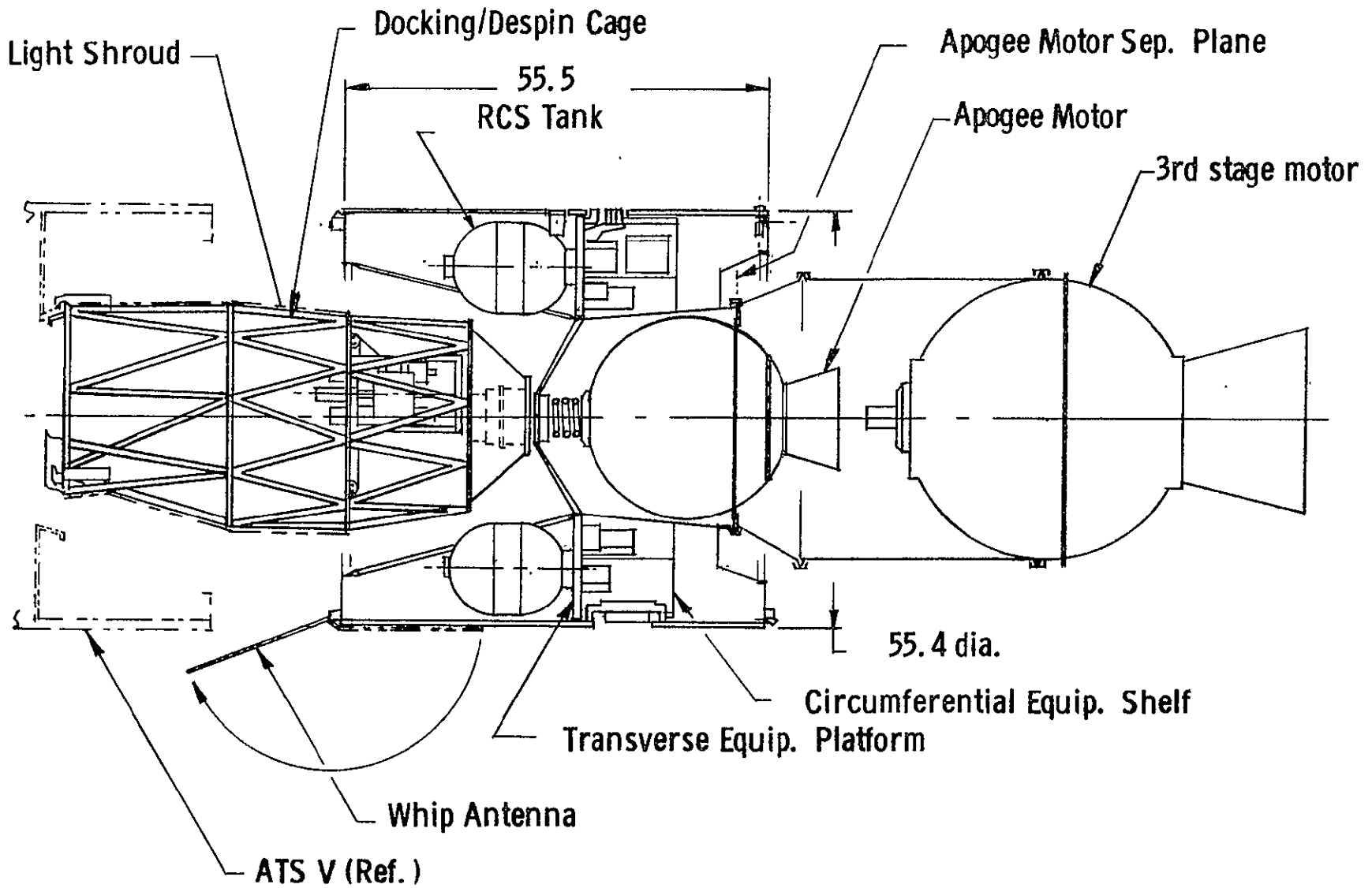
FIGURE 1-4.   BASELINE RMU CONFIGURATION

Space Division
North American Rockwell

TABLE 1-1 BASELINE SUBSYSTEMS

SUBSYSTEM	GENERAL APPROACH
STRUCTURE	• Fabrication Simplicity • Good Accessibility • Aluminum & Magnesium
ELECTRICAL POWER	• Body Mounted Solar Cells • 2 Silver-Zinc Space Qualified Batteries • Space Qualified Charger, Regulators & Status Monitors
ATTITUDE CONTROL	• ATS-V Sensors • Spin-Stabilized Up To Rendezvous • DPG's For Despun-Mode Control • DPG Energy Dissipation For Stability in Docked Mode • 6 DOF
REACTION CONTROL	• N_2H_4 Propellant • 2 Space Qualified Tanks • 12 Space Qualified Thrusters
COMMUNICATIONS	• ATS-V C-Band Equipment • New State-Of-The-Art Omni Antenna • Redundant Repeaters
TELEMETRY & COMMAND	• ATS-V Equipment • Redundancy With Cross-Strapping
VIDEO & ILLUMINATION	• 2 Redundant ATS-V TV Cameras • Wide Angle & Telephoto Lenses • Redundant Cold Cathode Lamps
DOCKING	• 3 Latches Based on Apollo Technique
PROPULSION	• Space Qualified Thiokol TEM-442-1 Apogee Motor
THERMAL	• Passive With Radioisotope Heaters For RCS Jets & TV Cameras

2.0 LAUNCH PHASE

THE RMU CAN BE LAUNCHED IN A STRAIGHTFORWARD SEQUENCE OF BOOST, PARKING ORBIT, TRANSFER ORBIT AND SYNCHRONOUS DRIFT ORBIT PHASES INTO RENDEZVOUS PROXIMITY OF THE ATS-V USING DEVELOPED SPACECRAFT EQUIP-MENT AND AVAILABLE GROUND TRACKING CAPABILITY.

2.1 REQUIREMENTS

The launch phase commences with lift-off from ETR and continues through the various orbital maneuvers until the RMU is within acquisition range of ATS-V. The RMU must be brought safely through main boost, parking orbit, and perigee burn for the transfer orbit to synchronous altitude. It must provide for attitude orientation during the transfer orbit to enable proper apogee boost for initiating phasing orbits. Engine capability for a payload of about 500 pounds must be provided together with proper selection of launch parameters. Following synchronous orbit injection, properly phased drift orbits must be determined and controlled to deliver the RMU to the proper rendez-vous acquisition position relative to ATS-V. Although the parameters related to this acquisition portion are discussed in detail in Section 3.0, they are briefly reviewed here in light of their impact on the launch phase requirements.

The method used for ATS-V detection impacts launch operations by defining the geometry which must exist at the end of the launch phase. As indicated in Section 3.0 and 7.0, a non-steerable video sensor was selected as the baseline acquisition sensor. This coupled with a non-steerable high gain antenna for video transmission constrains the TV to viewing essentially along a single plane which is tangent to the orbit path and normal to the orbit plane. This, in turn, demands that altitude difference (ΔR) between ATS-V and the RMU be kept relatively small because the TV camera cannot be steered in pitch without loss of TV transmission at the ground station. The out-of-plane errors (ΔN) are not as constraining since a search can be conducted in yaw by rotating the RMU without affecting the high gain antenna LOS to ground.

The video can detect the RMU if it is within the camera field-of-view at dis-tances out to 10 n.m. For immediate recognition (relative to a star), the range must be less than 3000 feet. In the intermediate ranges between 10 n.m. and 3000 feet RMU translational maneuvers may be required for distinguishing the ATS-V image from a star. Also, the sun-RMU-ATS-V geometry must be such that adequate sunlight is re-flected by the ATS-V toward the RMU. This can be attained by assuring that the RMU arrives at the acquisition point at the proper local sun time with a tolerance of, say, 1 hour, with the RMU on the sunlit side of ATS-V.

Finally, relative velocity must be sufficiently small (on the order of 1 to 2 fps) to maintain proper geometry during the period between RMU despin and target acquisition.

All of these requirements are easily met with existing ground tracking capabilities since the rendezvous operation is not time constrained to any significant degree. The selected baseline acquisition sensor does not impose any unusual or difficult accuracy requirements.

2.2 ALTERNATE APPROACHES/TECHNICAL CONSIDERATIONS

Several trade-offs were made in the evolution of the selected launch phase approach for RMU. Some of the basic considerations are discussed below.

2.2.1 Launch Vehicle and Apogee Motor Selection

Launch vehicle selection was restricted to the Thor-Delta series by the study contract. Figure 2-1 shows payload injected into the transfer orbit versus transfer orbit inclination for the Model 603, 903 and 904 Thor Delta series launch vehicles. The corresponding curve for the Model 303 booster is not shown since its payload capability is inadequate for an RMU class vehicle.

A series of apogee motors was originally selected for consideration: The Thiokol TEM 442-1 and TEM 531, and Aerojet SVM-2. The payload capabilities of these motors are also shown on Figure 2-1 as a function of transfer orbit inclination angle; the payload capability of each motor is given for a post-apogee-burn inclination angle of zero degrees (i.e. nominally no orbit inclination change to be made by the RMU reaction control subsystem).

As expected, the booster injected weight capability reduces sharply as the inclination angle decreases from the initial 28.5°, whereas each apogee engine with a fixed amount of propellant is seen to carry an increased payload as the transfer orbit inclination (and hence required apogee ΔV) decreases. The figure shows that the maximum useful payload deliverable by the Delta 603/TEM 442-1 combination is 510 pounds at an inclination angle of 24.5°.

Although this payload capability meets the basic requirement, some consideration was given to the possibility of providing greater payload margin by off-loading an initially larger apogee engine or adding propellant to the TEM 442-1. The results of off-loading the JPL SR28-3 motor as well as stretching (by adding a central cylindrical section to the propellant sphere) of the TEM 442-1 motor are shown in Figure 2-2, which is effectively an enlargement of Figure 2-1 in the area of 20° to 30° inclination angle and 500 to 650 pounds payload. A higher I_{sp} is shown for the modified TEM 442-1 motor because of assumed natural companion modifications. Appreciable payload margin is realizable by these techniques but at some expense; e.g., the JPL SR 28-3
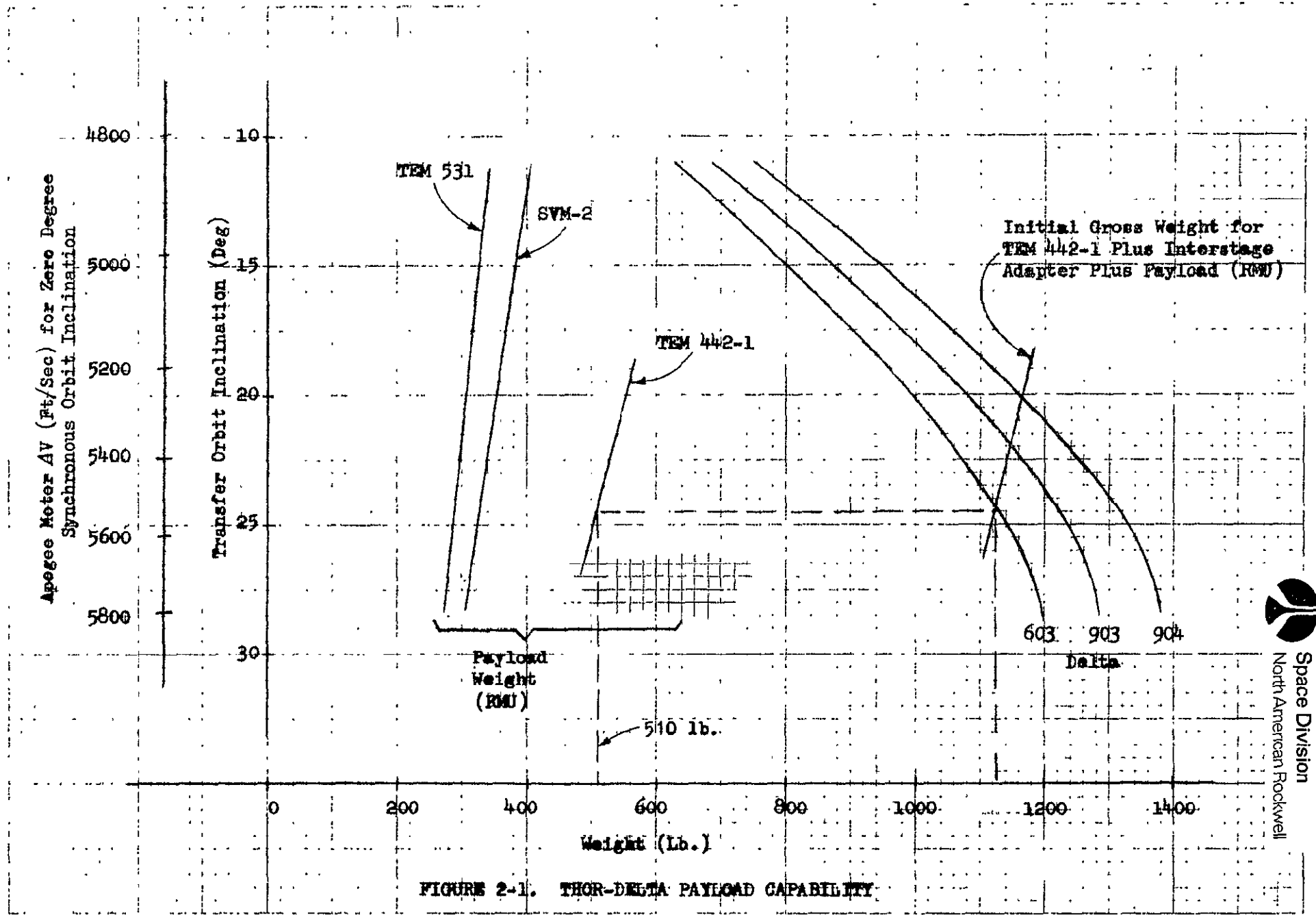
FIGURE 2-1.   THOR-DELTA PAYLOAD CAPABILITY

Space Division
North American Rockwell
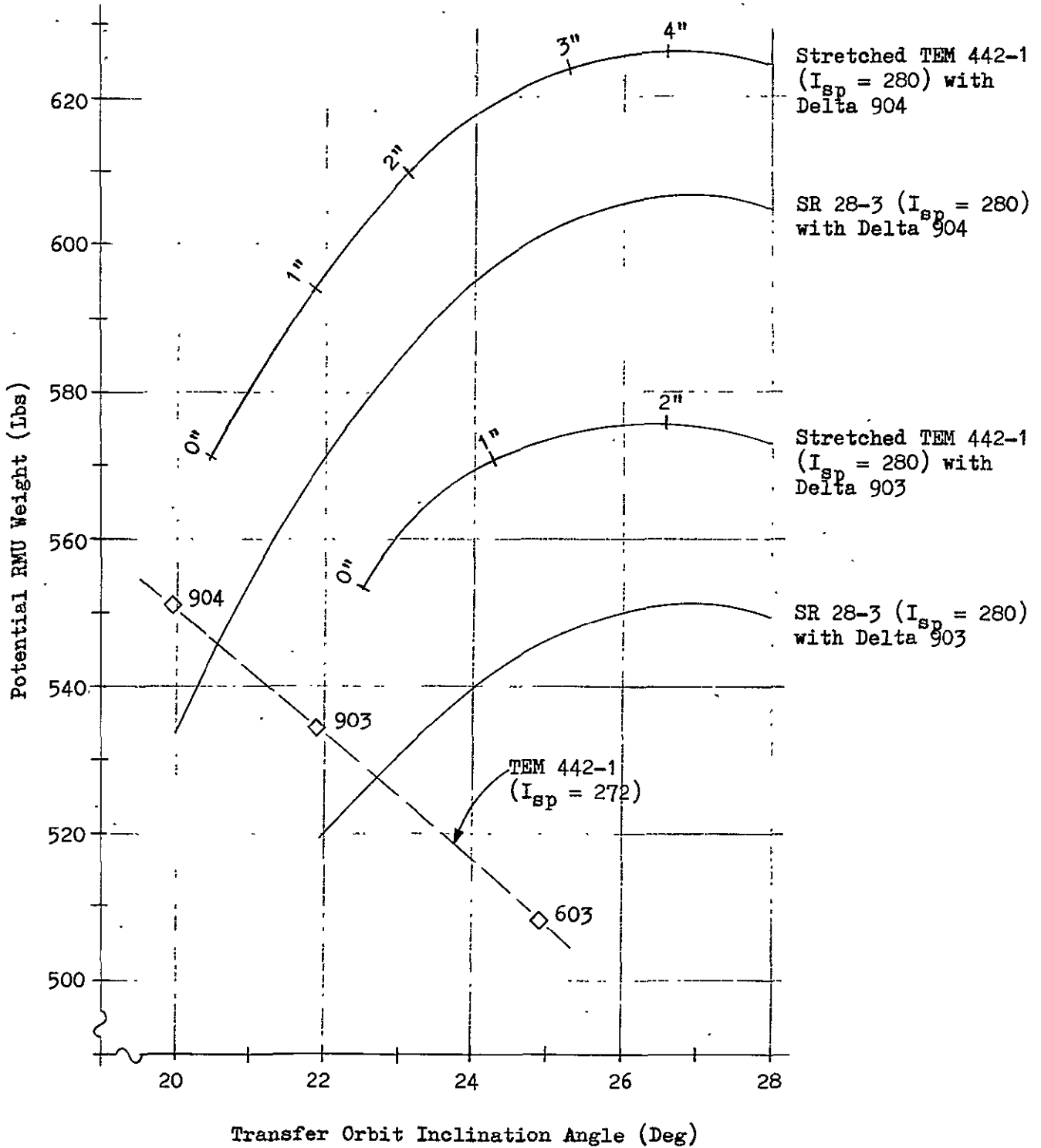
Figure 2-2   Payload Potential Comparisons

presents packaging problems since it is 24 in. longer (as well as wider) than the TEM 442-1, while redesign and requalification of a stretched TEM 442-1 would involve additional cost. Thus the Thor-Delta 603 booster and the Thiokol TEM 442-1 apogee motor were selected for the baseline because of size, cost, availability, and payload adequacy considerations.

2.2.2 Attitude Determination and Control

The Thor-Delta imparts a spin rate to its third stage as a means of eliminating active thrust vector control during third stage burn. The RMU is, thus, injected into the transfer orbit in a spinning mode. Configuration analysis described in Section 7.0 has shown that envelope constraints cause the RMU plus apogee motor combination to be unstable in the spinning mode and active nutation control (ANC) is required. However, ANC propellant requirements are not significant, and the decision was made to leave the vehicle in the spinning mode through apogee burn since this approach is compatible with ATS normal operation and minimizes apogee thrust misalignment effects without active control. After apogee motor ejection the RMU is in a stable spin configuration and, since this mode of operation offers a simple approach to attitude control, the vehicle remains spinning throughout the remainder of the launch phase.

Maximum compatibility with existing ground station software and hardware is desired for a low cost approach, and the baseline concept utilizes the same attitude determination technique as that employed on ATS-V; i.e. during the launch phase RMU attitude is determined from (a) telemetered sun sensor data and (b) the polarization angle (POLANG) of the received C-band signal.

2.2.3 Injection Point Selection

For thermal reasons, the third stage of the Delta launch vehicle must be ignited either at the first descending node or the first ascending node of the parking orbit. The first descending node occurs at about 3° east longitude and the first ascending node occurs at about 172° east longitude. Between injection at perigee and arrival at apogee of the transfer orbit, the RMU advances in longitude a total of 101.3° so that the apogee arrival longitudes for injection at the descending and ascending nodes are 104.3° and 273°, respectively. Since the target is nominally at 253° (107°W) the ascending node injection point is preferable. The use of the ascending node causes the RMU to traverse the northern hemisphere during the transfer orbit, providing early initial tracking station acquisition and continuous contact capability during the remainder of the mission. In contrast, the descending node injection places the transfer orbit and the first apogee out of view of the U.S. tracking stations; this would necessitate waiting an additional 10.5 hours for satisfactory tracking station geometry at the second apogee incurring an increased risk of system degradation and an increased propellant consumption for nutation control.

For these reasons transfer orbit injection at the first ascending node was selected for the baseline mission. The resultant trajectory also offers a relatively early second opportunity for apogee motor burn as a contingency mode of operation, i.e., should circumstances necessitate postponement of the burn from first apogee, the third apogee again offers satisfactory ground station coverage.

2.2.4 Tracking Technique

To effect rendezvous of the RMU with the ATS-V, the relative state (position and velocity) of the RMU with respect to the ATS-V must be determined with a relatively high degree of precision. The accuracy of the absolute state estimates of the RMU and ATS-V is not critical for the purposes of rendezvous. The relative state estimation accuracy is dependent upon several significant parameters of the tracking configuration which are:

1. Type of measurements – range, range-rate, angular, etc.

2. Rate of measurements – number of measurements processed per unit time.

3. Duration of tracking – time since initiation of tracking.

4. Accuracy of measurements – random errors, bias errors, station location errors, etc.

5. Location of tracking stations – tracking geometry.

6. Number of tracking stations.

7. Mode of tracking – sequential or simultaneous.

The selected tracking approach is based upon a "matched" tracking mode where both the RMU and ATS-V will be tracked by the same tracking stations with a minimum of time delay between tracking the two vehicles. This approach is taken to minimize the effects of systematic errors in the relative state estimation which are inherent in tracking the RMU and ATS-V with separate tracking stations. That is, the state estimate bias errors which result from "external" systematic errors (range measurement biases, tracking station location errors, atmospheric effects, etc.) can be closely equalized for the two vehicles by using matched tracking. The two vehicles are also assumed to be in close proximity during tracking; i.e., the tracking accuracy of the relative state is of major concern during the final RMU vernier drift orbits when the RMU and ATS-V angular separation is on the order of one degree or less. In this manner, the relative state estimate will have a negligible resulting bias error and is, therefore, primarily a function of the random measurement errors which are greatly reduced by the use of the redundant data available.

- 32 -

Although a specific tracking configuration and technique will be further developed as the program progresses, the following remarks pertain to selection of a system which can be considered baseline and is fully adequate to meet mission objectives. For compatibility with ATS ground stations, use of the ATSR&RR tracking system was assumed. Although range rate information will assist, particularly early in the tracking period, utilization of range only information has been found to suffice (see data in later section). Based on current NASA ATS ground tracking operations and capabilities, measurements are assumed to be taken one per second for intervals of 2-1/2 minutes (150 range measurements per interval). These intervals will then be repeated at a frequency not to exceed three per hour, but at least one per hour. Since adequate time is available in the drift orbit for Hohman transfer type orbital maneuvers, twelve hours will separate ΔV corrections providing more than adequate time to reduce state estimate errors to acceptable values.

Although accuracies and response time of the tri-lateration technique (three ground stations tracking simultaneously) constitute a distinct improvement, analysis shows that the two existing ATS stations within the continental U.S. (Mojave and Rosman) are capable of providing acceptable performance; therefore, the two-station configuration is considered baseline. Finally, whereas sequential tracking (one ground station at a time) and simultaneous tracking produce essentially comparable performance for the total number of measurements, simultaneous tracking is utilized for the baseline mission because it can readily be mechanized and enables as many as three full tracking cycles (information from both stations for both RMU and ATS-V) to be accomplished in one hour; this results in more rapid convergence and data smoothing.

2.2.5 Tracking Accuracy

Good tracking accuracy is key to guiding the RMU to a satisfactory ATS-V acquisition point. Utilizing a computer program previously developed by NR, a detailed analysis was made of the tracking accuracy obtainable during the critical drift orbit phase of the RMU mission. The assumptions, groundrules and methods utilized in this analysis as well as the results obtained are described below. In this discussion, unless otherwise noted, all errors are considered one sigma.

Errors, reflecting the current capability of the ATS ground stations to fix the orbital parameters by tracking were supplied by NASA. They consist of a 1000 ft. position error and a 0.1 ft per second velocity error, predicated upon 12 hours tracking time. Although these orbit determination accuracy numbers are representative of demonstrated ground station capability, relative ATS-V/RMU position and rate determination will be better because of the effective cancellation of systematic errors when only relative information is important. Accordingly, this discussion deals with the investigation of system performance in these relative rather than absolute terms.

Certain assumptions were tacitly made which minimize the effects of systematic errors in the determination (estimation) of the relative state of the RMU and ATS-V. The primary assumptions are that the RMU and ATS-V are in near synchronous circular orbits with a phase angle of a few degrees and the measurements taken from available tracking stations are the same for both vehicles, within tracking facility constraints.

The tracking measurement data assumed in the analysis are as follows:

.   Measurement Type - Range Only

.   Measurement Rate - One per Second During Tracking Periods

.   Measurement Error - 30 ft (1σ)

All tracking modes considered are characterized by the 20-minute measurement format with respect to time as depicted in Figure 2-3. These modes differ only in whether one station at a time (sequential method) or all stations together (simultaneous method) follow the 20-minute measurement format of Figure 2-3. In either event, a tracking cycle constitutes a set of all stations involved tracking the two targets. Two or three tracking stations were considered as follows:

Two Stations - Mojave and Rosman

Three Stations - Mojave, Rosman, and Santiago

Several particular cases of tracking were considered as defined in Table 2-1.

The RMU/ATS-V relative state determination accuracy data for cases 1 through 6 are presented in Tables 2-2 through 2-7, respectively. The R, T, N components of error represent Radial (R) and Tangetial (T) in-plane errors, and Normal (N) out-of-plane errors. Moreover, the data presented correspond to the end of the tracking hour for which the data are given. In this manner, the data reflect the effects of error propagation from the time that measurements are completed to the end of the tracking hour considered.

The data presented in Tables 2-2 through 2-7 show that a relatively high degree of accuracy can be expected in estimating the relative state of the RMU and the ATS-V. These results are dependent upon the minimization of the effects of systematic errors in the relative estimate of the RMU and ATS-V states; that is, the effects of ground tracking station location errors and measurement biases will be nearly equal for the two vehicles. However, systematic errors which are unique to the two vehicles will not equalize. These errors will produce a "residual" bias in the relative estimate of the two vehicles which is dependent upon the particular values of the systematic errors that are unique to the two vehicles. To assess the effects of these residual bias errors, bias sensitivities were determined in the tracking analysis. These sensitivities are presented in Table 2-8 for the six cases considered. The data presented are the largest bias

- 34 -

| LOCK-ON/CALIBRATE STATION
TO FIRST SPACECRAFT | TRACK 1ST
SPACECRAFT | LOCK-ON 2ND
SPACECRAFT | TRACK 2ND
SPACECRAFT |

←————————10 MIN————————→ ←—2½ MIN—→ ←————5 MIN————→ ←—2½ MIN—→

0 1 2 3 4 5 6 7 8 9 10 11 12 13 14 15 16 17 18 19 20

←——————————————————— 20 MIN. ———————————————————→
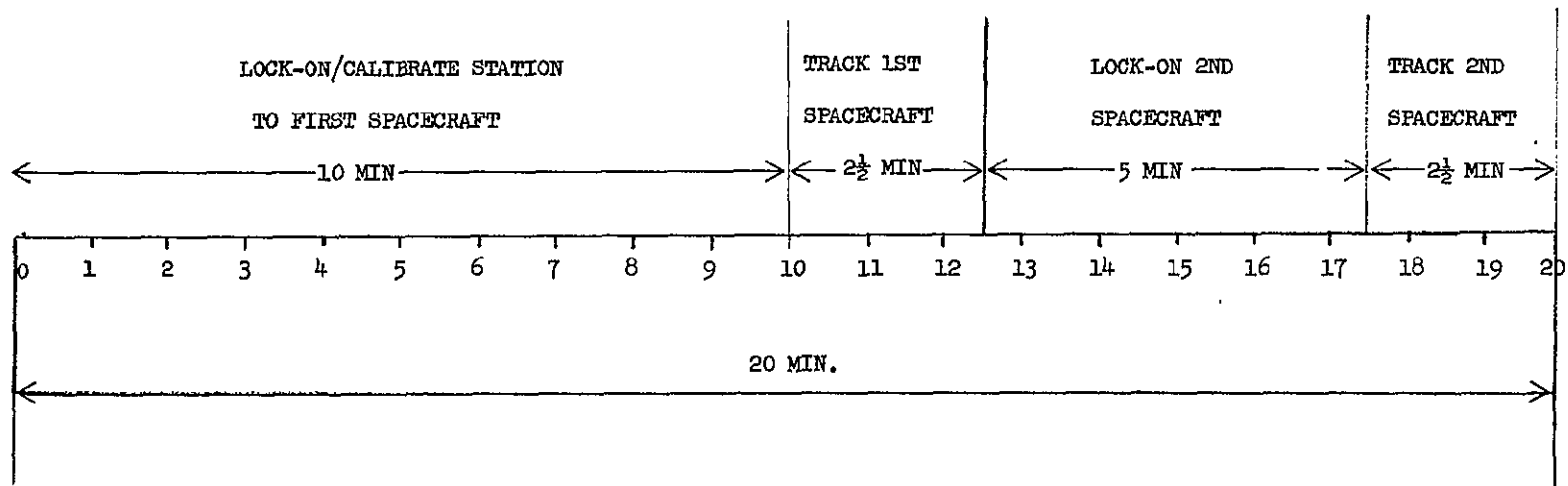
FIGURE 2-3. TRACKING FORMAT

TABLE 2-1

TRACKING CASES ANALYZED

CASE NO.	TRACKING STATIONS	TRACKING MODE	TRACKING CYCLES PER HOUR
1	2	Sequential	1
2	2	Simultaneous	1
3	3	Sequential	1
4	3	Simultaneous	1
5	2	Simultaneous	3
6	3	Simultaneous	3

TABLE 2-2

CASE 1 TRACKING ACCURACY

| TIME (HOURS) | RELATIVE ERRORS (1σ) | | | | | |
| | POSITION (FT) | | | VELOCITY (FT/SEC) | | |
	R	T	N	R	T	N
1	30807.0	4859.7	311079	8.5129	1.6499	81.515
2	7656.3	1864.6	77300	1.9383	.5275	18.520
3	396.3	133.6	4042	.0801	.0307	.748
4	216.8	99.1	2218	.0335	.0166	.291
5	143.8	83.5	1474	.0185	.0109	.145
6	104.0	73.8	1069	.0118	.0078	.082
7	79.1	66.8	815	.0083	.0059	.049
8	62.2	61.4	642	.0062	.0046	.031

2 Stations - Sequential - 1 Cycle/Hour

TABLE 2-3

CASE 2 TRACKING ACCURACY

| TIME (HOURS) | RELATIVE ERRORS (1σ) | | | | | |
| | POSITION (FT) | | | VELOCITY (FT/SEC) | | |
	R	T	N	R	T	N
1	31513.0	4446.8	309580	8.8215	1.5740	81.212
2	7727.8	1935.4	78741	2.0556	,6050	19.726
3	132.7	161.6	4442	.0811	.0337	.738
4	231.1	114.4	2378	.0341	.0177	.285
5	150.8	93.6	1556	.0189	.0115	.141
6	107.9	88.1	1115	.0121	.0081	.079
7	81.3	72.3	842	.0085	.0061	.047
8	63.4	65.7	658	.0064	.0047	.029

2 Stations - Simultaneous - 1 Cycle/Hour

37

TABLE 2-4

CASE 3 TRACKING ACCURACY

TIME (HOURS)	RELATIVE ERROR (1σ)					
	POSITION (FT)			VELOCITY (FT/SEC)		
	R	T	N	R	T	N
1	130.25	1262.5	989.00	.1051	.43803	.6901
2	6.46	53.30	40.63	.0038	.00713	.0115
3	4.30	36.93	29.19	.0027	.00190	.0049
4	3.54	30.49	24.03	.0022	.00078	.0027
5	3.09	26.56	20.68	.0019	.00039	.0018
6	2.76	23.77	18.14	.0017	.00321	.0013

3 Stations - Sequential - 1 Cycle/Hour

TABLE 2-5

CASE 4 TRACKING ACCURACY

TIME (HOURS)	RELATIVE ERRORS (1σ)					
	POSITION (FT)			VELOCITY (FT/SEC)		
	R	T	N	R	T	N
1	1020.40	3644.90	1940.00	.3745	1.32960	.7071
2	35.80	106.78	58.02	.0096	.02044	.0115
3	7.59	37.08	32.12	.0028	.00202	.0041
4	5.15	30.17	25.66	.0022	.00073	.0025
5	4.09	26.29	21.59	.0019	.00033	.0017
6	2.59	16.67	13.21	.0012	.00013	.0013

3 Stations - Simultaneous - 1 Cycle/Hour

TABLE 2-6

Space Division
North American Rockwell

CASE 5 TRACKING ACCURACY

TIME (HOURS)	RELATIVE ERRORS (1σ)					
	POSITION (FT)			VELOCITY (FT/SEC)		
	R	T	N	R	T	N
1	631.11	65.49	6425.3	0.6796	0.0654	6.9274
2	258.20	51.05	2636.9	0.0940	0.0213	0.9473
3	149.26	46.00	1528.2	0.0330	0.0117	0.3215
4	99.32	42.12	1019.4	0.0162	0.0076	0.1480
5	71.51	38.94	735.7	0.0094	0.0054	0.0794
6	54.12	36.28	558.0	0.0062	0.0041	0.0465
7	43.22	32.88	437.7	0.0045	0.0030	0.0287
8	33.95	31.96	351.5	0.0033	0.0025	0.0185
9	27.69	30.16	287.2	0.0027	0.0020	0.0123
10	22.87	28.52	237.6	0.0022	0.0017	0.0085

2 Stations - Simultaneous - 3 Cycle/Hour

TABLE 2-7

CASE 6 TRACKING ACCURACY

TIME (HOURS)	RELATIVE ERRORS (1σ)					
	POSITION (FT)			VELOCITY (FT/SEC)		
	R	T	N	R	T	N
1	5.35	45.70	28.89	0.00445	0.01921	0.01489
2	3.17	26.40	19.60	0.00205	0.00286	0.00451
3	2.48	20.49	15.79	0.00153	0.00094	0.00233
4	2.09	17.30	13.41	0.00128	0.00041	0.00146
5	1.83	15.20	11.67	0.00112	0.00021	0.00102
6	1.64	13.65	10.29	0.00101	0.00011	0.00078

3 Stations - Simultaneous - 3 Cycle/Hour

TABLE 2-8

RESIDUAL BIAS SENSITIVITIES FOR SYSTEMATIC ERRORS

CASE	POSITION		
	R	T	N
1	0.59	0.22	4.45
2	0.61	0.24	4.20
3	0.97	1.21	0.45
4	0.96	1.29	0.43
5	0.73	0.29	3.06
6	0.96	1.18	0.40

sensitivities for the two vehicles. These data represent sensitivity coefficients which directly assess the residual bias effects. For example, if the equivalent measurement bias is one foot for each vehicle, then for Case 1, the out-of-plane (N) component of residual bias would be approximately $\sqrt{2} \times 4.5 = 6.3$ ft (RMS) value.

For a baseline system consisting of two ground stations, employing simultaneous tracking, Tables 2-3 and 2-6 (cases 2 and 5) indicate that, for three measurements per hour for eight hours, relative position accuracy (1σ) will be better than 240 ft. and relative velocity accuracy (1σ) better than 0.009 ft/sec in the axis of least accuracy (normal to orbital plane). This accuracy enables precise control of phasing orbits to achieve desired ATS-V rendezvous conditions.

2.3 NOMINAL LAUNCH PHASE

The events occuring in the launch phase of the RMU mission are outlined in sequence in this section.

2.3.1 Boost and Parking Orbit

The RMU will be launched on a Delta 603 launch vehicle from Cape Kennedy (nominal launch date August 1, 1972) with a launch azimuth between 90° and 95°. The nominal launch time has been tentatively designated at 9:00 a.m. to provide satisfactory sun angles for attitude determination in the transfer orbit. Inasmuch as circular drift (phasing) orbits are planned, the orbital time phasing between drift orbit insertion and ultimate acquisition is unconstrained. Although not critical, this launch time also places the transfer orbit line of nodes between best target acquisition and best attitude information locations on the orbit.

The vehicle is boosted into the 100 n.m. parking orbit (Figure 2-4) with an inclination of approximately 28.5°. The parking orbit phase is concluded when the vehicle reaches the first ascending mode at 172°E, approximately 70 minutes after lift-off, and is injected into the transfer orbit by the booster's third stage. The sequence of events, up to and including this injection, is given in Table 2-9.

2.3.2 Transfer Orbit

At the first ascending node the RMU is injected into a $24\frac{1}{2}°$ transfer orbit by the solid propellant Delta third stage which is spin-stabilized (40-60 rpm). The task of changing inclination from that of the parking orbit to that of the transfer orbit is accomplished by the third stage of the launch vehicle when it provides the transfer orbit injection. An elliptical 180° transfer from the parking orbit to synchronous altitude is employed because it combines simplicity of implementation with economy of propellant and has been successfully used in other space missions, such as the ATS-V. The 180° transfer is a long-duration trajectory but the RMU mission does not require a short transient time. In fact, the long transit time is beneficial because it allows added time for smoothing and processing of tracking data and for reorienting the RMU for the apogee motor burn.

41

h = 100 n.m.
i = 28.5°
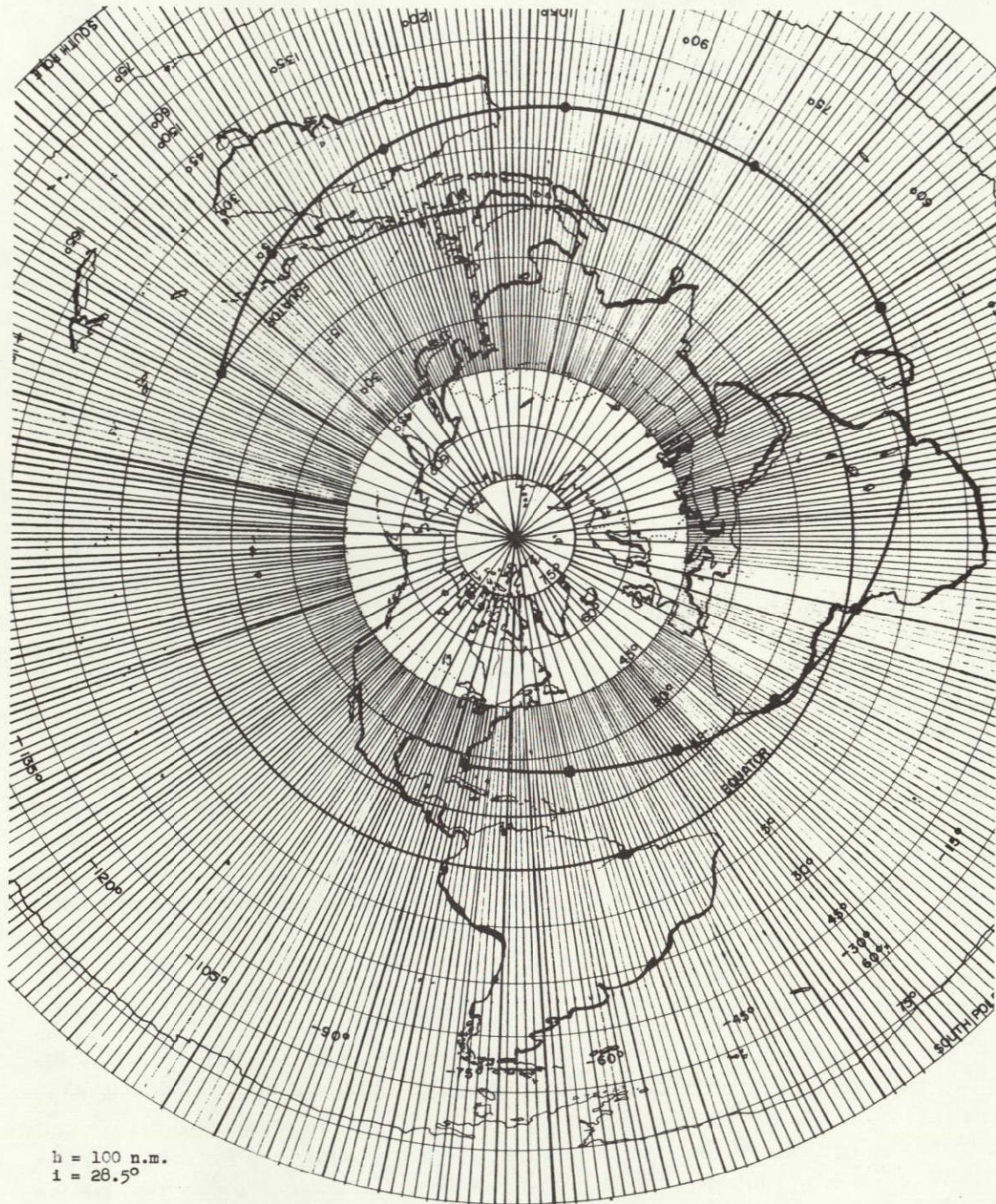
FIGURE 2-4. RMU PARKING ORBIT

TABLE 2-9

SEQUENCE OF EVENTS THROUGH TRANSFER ORBIT INJECTION

EVENT	TIME (SEC.)
Solid Motor Ignition, Sets #1 and #2	0 (Approx.)
Start Solid Motor Timers #1, #2	
Liftoff Signal to Guidance System	0.0
Initiate First Stage Open Loop Guidance	2.0
Solid Motor Separation Command, Set #1	90
Solid Motor Separation Command, Set #2	95
Initiate First Stage Closed Loop Guidance	102
Main Engine Cutoff (MECO)	220.5
Blow Stage I/II Separation Bolts	224.5
Start Stage II Engine	
Transfer Guidance Control to Stage II	
Initiate Second Stage Open Loop Guidance	226.5
Fairing Separation	261.5
Second Stage Engine Cutoff Command #1	522.5
Initiate Second Stage Coast #1 Guidance	620.5
Restart Conditioning	4053.5
Turn on Hydraulic Pump	
Initiate Ullage Jets	
Engine Restart	4093.5
Second Stage Engine Cutoff Command #2	4121.5
Fire Spin Rockets	4123.5
Start Stage III Ignition Time Delay Relay	
Start Stage III Sequence Timer	
Fire Stage III Ignition Wire Cutters	4124.5
Blow Stage II/III Separation Bolts	4125.5
Second Stage Retro	
Stage III Ignition	4138.5
Stage III Burnout	4182.5
Payload Separation	4273.5

43

The transfer orbit (Figure 2-5) has a nominal apogee altitude 84 n.m. above the orbit of the ATS-V (approximately 19,330 n.m.). The transit time from injection to apogee (1/2 orbit) is 5.25 hours. In this period of time, the RMU must acquire the sun, establish contact with the ground stations, and reorient for the apogee maneuver. The RMU comes into view of the Mojave station about eight minutes after transfer orbit injection (TOI) and can be seen by Rosman 16 minutes after TOI (assuming a 5° mask angle).

When the RMU arrives in the region of apogee, the TEM 442-1 apogee motor is fired at an angle of 45.8^o to the direction of motion and in the local horizontal plane. The impulse of 5724 ft/sec will place the RMU into circular orbit 84 n.m. above synchronous altitude. The necessary orientation of velocity and thrust vectors associated with the orbit transfer is illustrated in Figure 2-6. As illustrated, during the 5.25 hour flight from the parking orbit to the transfer orbit the RMU spin axis must be rotated 148° about the line of nodes into the correct orientation for apogee motor firing.

The initiation of the vehicle reorientation maneuver will occur about 1/2 hour after transfer orbit injection, approximately 22 minutes after the RMU has come into view of the ground station, so that all systems will have been activated and checked out and the reorientation command given from the ground. The torque vector is applied along an axis normal to the major axis of the transfer orbit, normal to the spin vector, in the plane of the desired precession so that the vehicle is precessed about the major axis of the transfer ellipse (line of nodes). Since the RMU is spinning at the rate imparted by the launch vehicle, it must be reoriented by means of periodic synchronized precessional torque impulses. The angular velocity of the RMU about the spin axis W_x, will be between 40 rpm and 60 rpm. The sun sensor will be used to synchronize the cycling of the applied couple.

Development of a technique for accomplishing this maneuver, and an assessment of its performance and accuracy are presented in Appendix A. From that analysis, a plot of time and propellant required as a function of pulse durations (in terms of torque actuation half angle) is shown in Figure 2-7.

The error analysis given in Appendix A indicates a total 3σ attitude error of approximately 3° following the 148° open loop precession. A correction will be applied after sufficient POLANG attitude sensing smoothing in accordance with the time-line of Figure 2-8. The resulting error (3σ) following the correction is shown to be approximately 0.84^o (Appendix A). Since this error is due primarily to attitude sensing, a second correction is not planned at this time. As shown in Figure 2-8, however, time is available for such a second correction should the need arise. Such a final correction at five hours can include increments reflecting measured orbital errors (based on tracking) to reduce to some extent subsequent ΔV requirements.

44
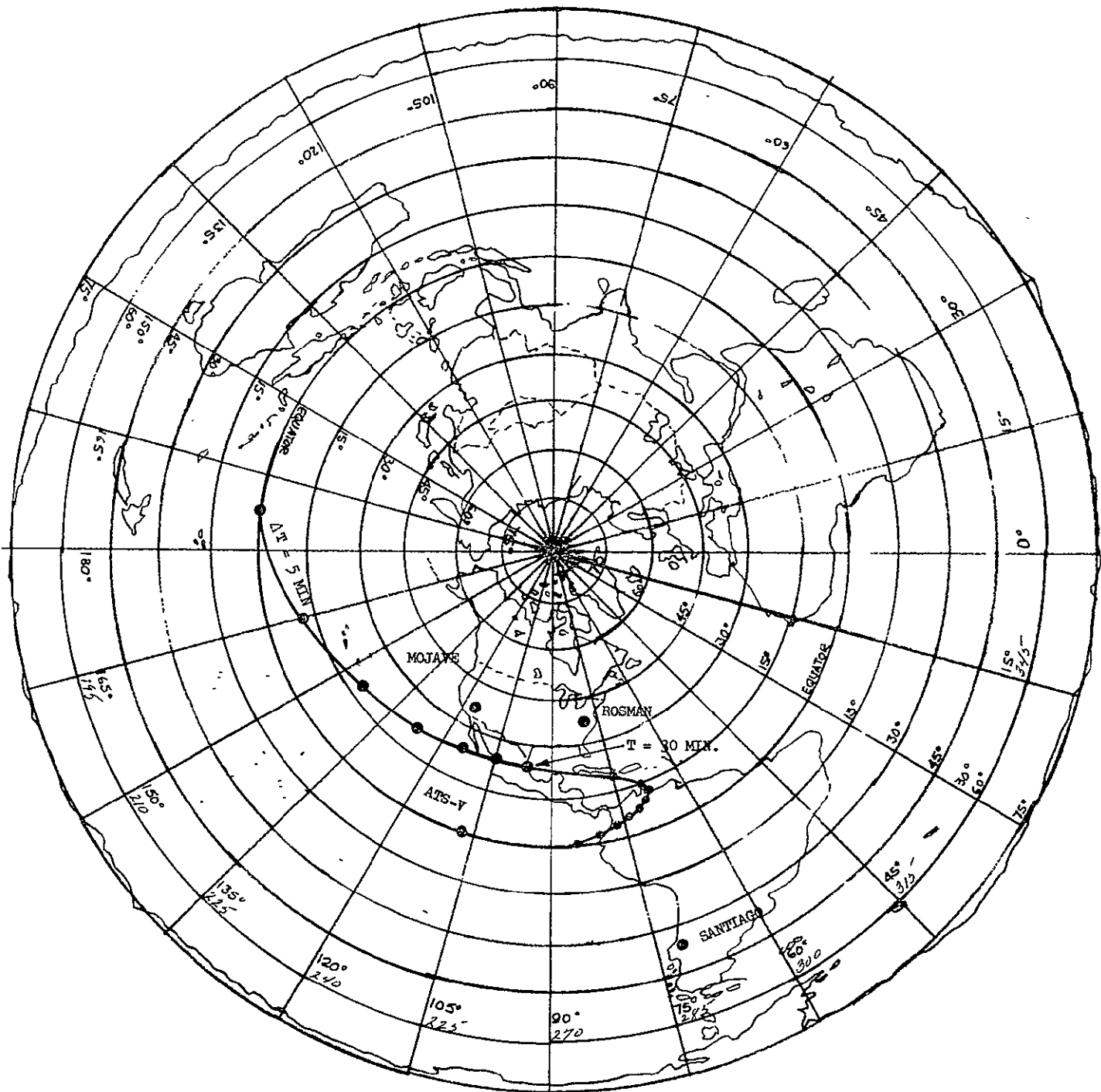
FIGURE 2-5. RMU TRANSFER ORBIT - FIRST REVOLUTION

North Pole

Rotation Angle $\Delta\phi = 180° - \phi_2 + \phi_1 + i_t - i_p$

Perigee

V_1

ϕ_1

V_2

Apogee

i_p

i_t

V_4

Equatorial Plane

ϕ_2

V_3

Line of Nodes
(Normal to Paper)

Viewed from
Apogee side of
earth
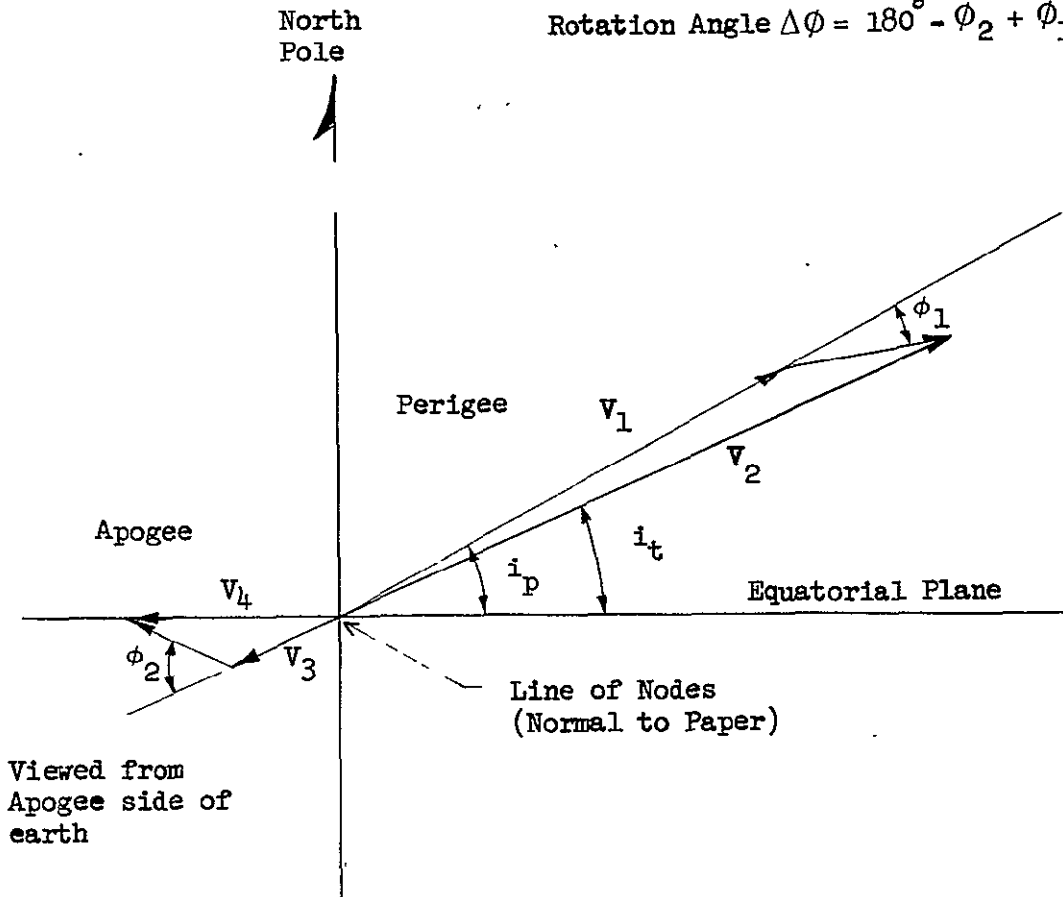
LEGEND

V_1	25582.0 ft/sec	Orbital Velocity, Parking Orbit
ΔV_1	8397.6 ft/sec	Third Stage Impulse, Perigee
ϕ_1	18.3^c	Firing Angle, Third Stage
V_2	33657.4 ft/sec	Perigee Velocity, Transfer Orbit
V_3	5232.4 ft/sec	Apogee Velocity, Transfer Orbit
ΔV_2	5700 ft/sec	Apogee Motor Impulse
ϕ_2	45.8^c	Firing Angle, Apogee Motor
V_4	10068 ft/sec	Perigee Velocity, Drift Orbit
i_p	28.5°	Parking Orbit Inclination
i_t	24.5°	Transfer Orbit Inclination

FIGURE 2-6.   GEOMETRY OF TRANSFER MANEUVERS
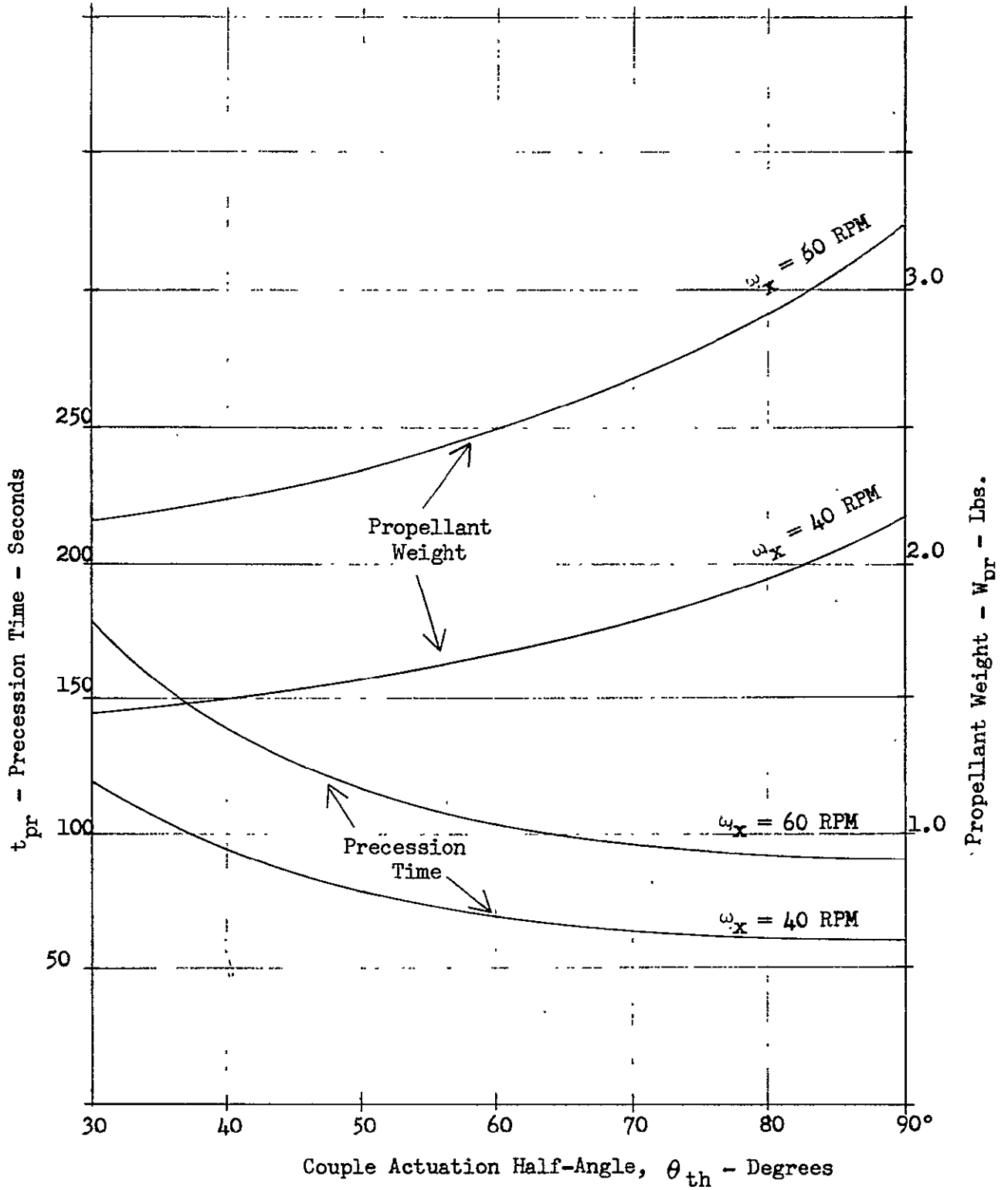
Fig. 2-7. Precession Time and Propellant Requirements
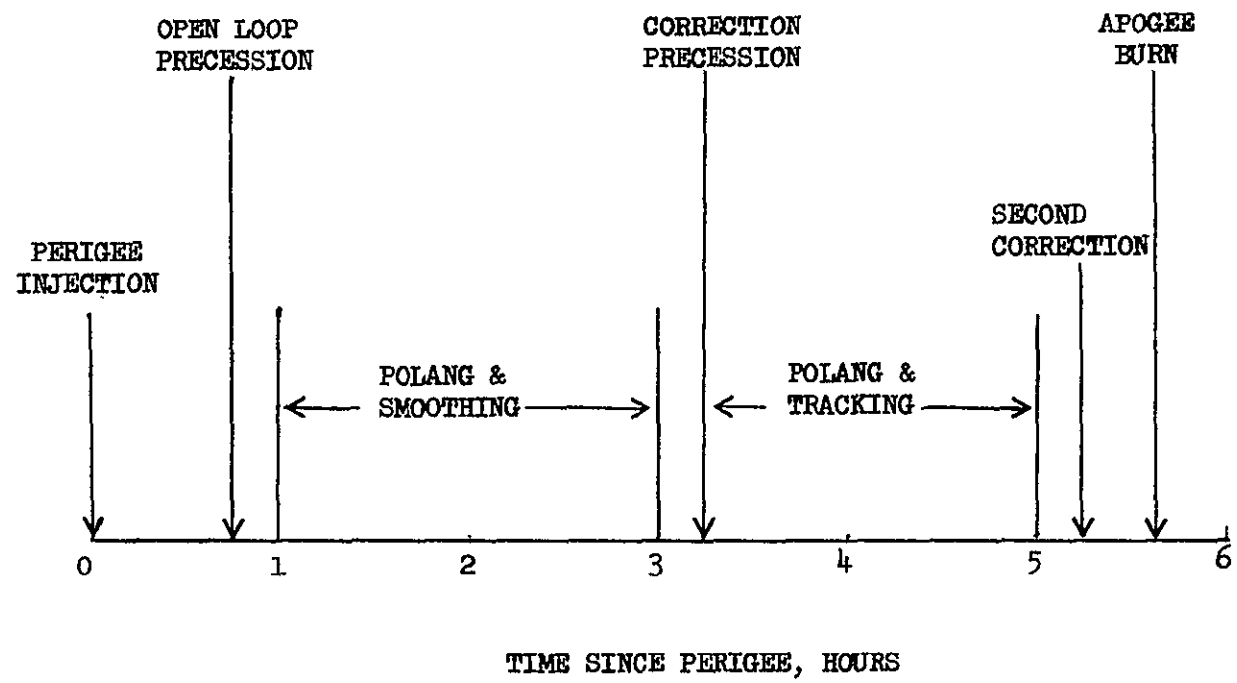
FIGURE 2-8. ATTITUDE ORIENTATION FOR APOGEE BURN

The first apogee of the nominal transfer trajectory is at 273°E longitude (87°W) approximately 20 degrees east of the target. If, due to unexpected circumstances, the apogee motor cannot be fired on the first apogee, the firing can be delayed until the third apogee (the second apogee must be by-passed because it is not in view of the tracking stations). Figure 2-9 is the ground trace of the approach to the third apogee in the transfer orbit. The third apogee occurs at approximately 41°W longitude, 46° to the east of the first apogee.

The RMU is in continuous sunlight during the transfer to synchronous altitude. While the vehicle is oriented as for transfer orbit injection (10.2° up from the equatorial plane) the sun/spin axis angle (θ_1) is 45° (Figure 2-10). After the spin axis has been rotated 148° in a plane normal to the equatorial plane, in preparation for the apogee impulse, the spin axis is 21.8° out of the equatorial plane and the sun/spin axis angle (θ_2) is 120°. Except for this change due to spin-axis reorientation, the angle between the sun line and the spin axis does not change during the transfer to synchronous altitude. Communication between the spacecraft and the ground stations is required during the transfer phase of the mission orbit for telemetry, command, tracking, and POLANG measurements. The continuing change in spacecraft orbital position, combined with the attitude reorientation requirements results in a variation in the RMU line of sight with respect to the ground stations. Figure 2-11 shows the angle (θ) between the RMU spin axis and the line of sight to the Mojave station with respect to time, assuming that the RMU is oriented for apogee burn. The data for the first half hour is omitted because the line of sight to the tracking station is obstructed by the earth for about 10 minutes and the vehicle is undergoing an attitude maneuver during the remaining 20 minutes. The satellite altitude and its range to the tracking station are also shown in Figure 2-11.

2.3.3   Drift Orbits

After the apogee motor fires (5.25 hours after transfer orbit injection) and is ejected, the RMU is in an essentially equatorial orbit in a stable spin mode, and its spin-axis is positioned normal to the orbit (equatorial) plane by precession through 68.2°. The angle between the spin axis and the sun line thus becomes equal to the declination of the sun. The declination of the sun at nominal lift-off time is 17.5° and is decreasing at approximately .3° per day. Over a two-week mission duration, therefore, the angle between the sun and the spin axis will reduce from 17.5° to about 13.3°. Since the minimum angle for continuous sunlight at synchronous altitude is 8.7°, the RMU will be in continuous sunlight for the remainder of the nominal baseline mission. This condition will exist for about 29 days after the nominal launch date. Figure 2-12 shows the variation in the declination of the sun with time.

At apogee motor burn the RMU is nominally 20°E of (leading) the target in a circular orbit, and because of its higher altitude (approximately 84 n.m.) is reducing the angular difference at a rate of 2° per orbital revolution. The simple technique of accomplishing rendezvous with minimum fuel requirement can be visualized with the

49
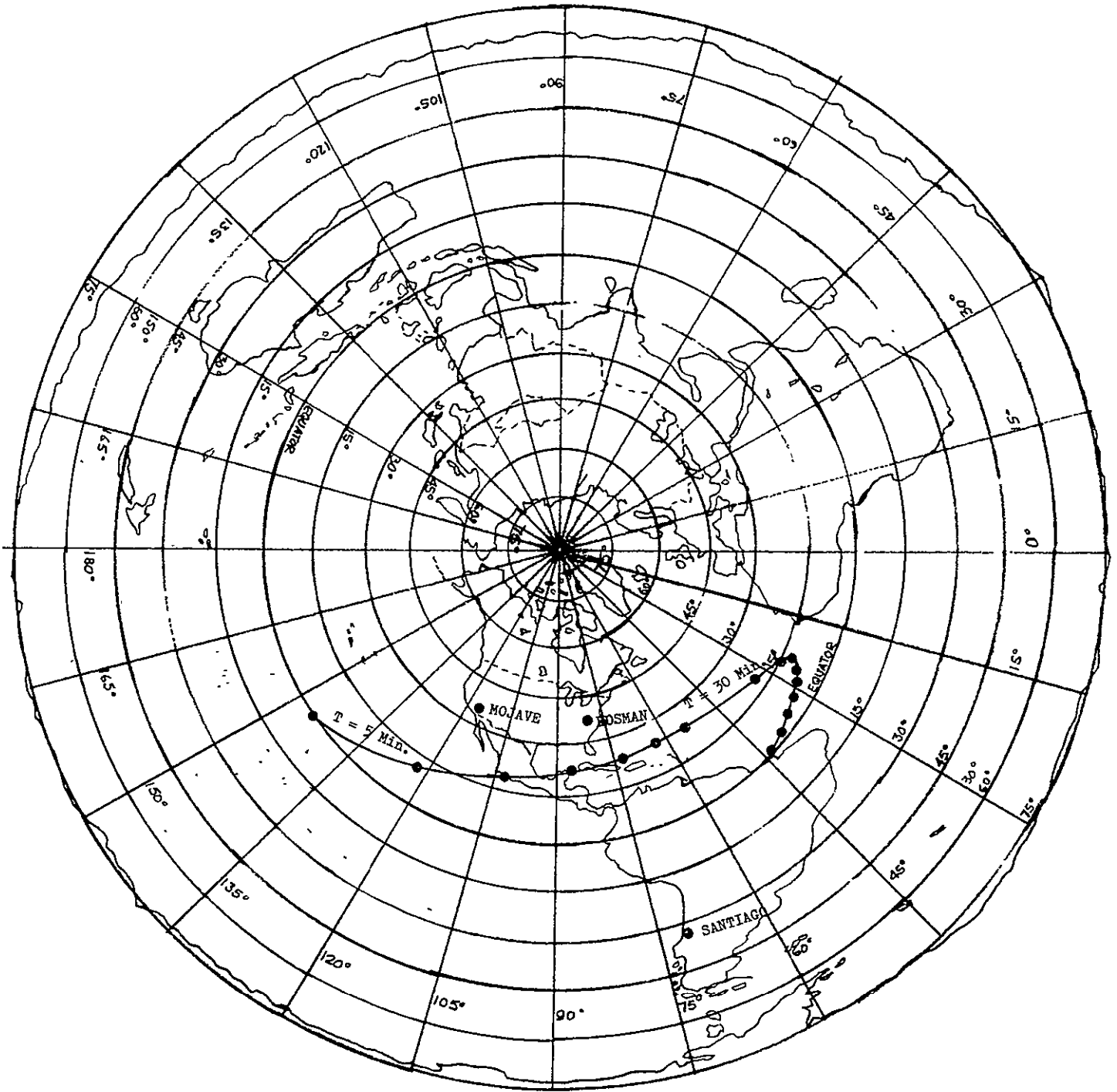
FIGURE 2-9   RMU TRANSFER ORBIT - THIRD REVOLUTION
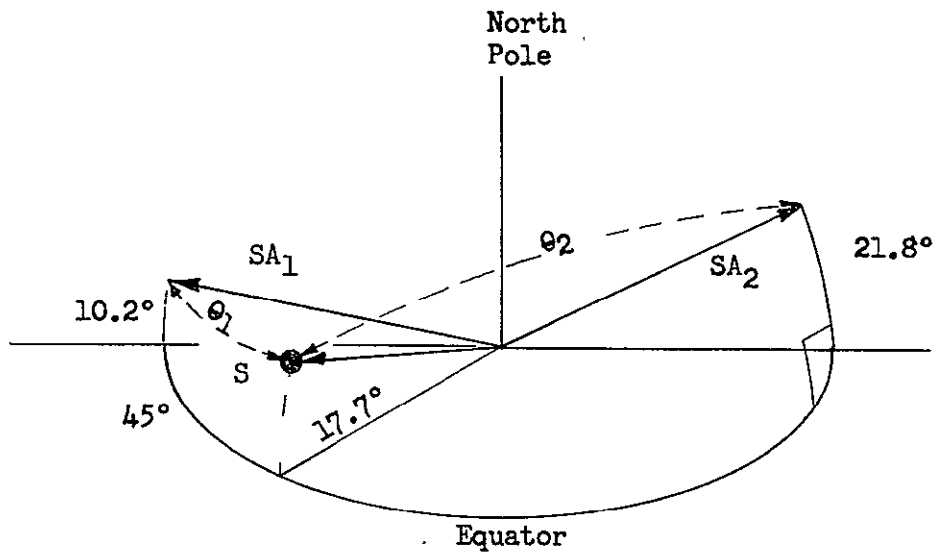
FIGURE 2-10. SUN/SPIN AXIS ANGLE (θ_1, θ_2)
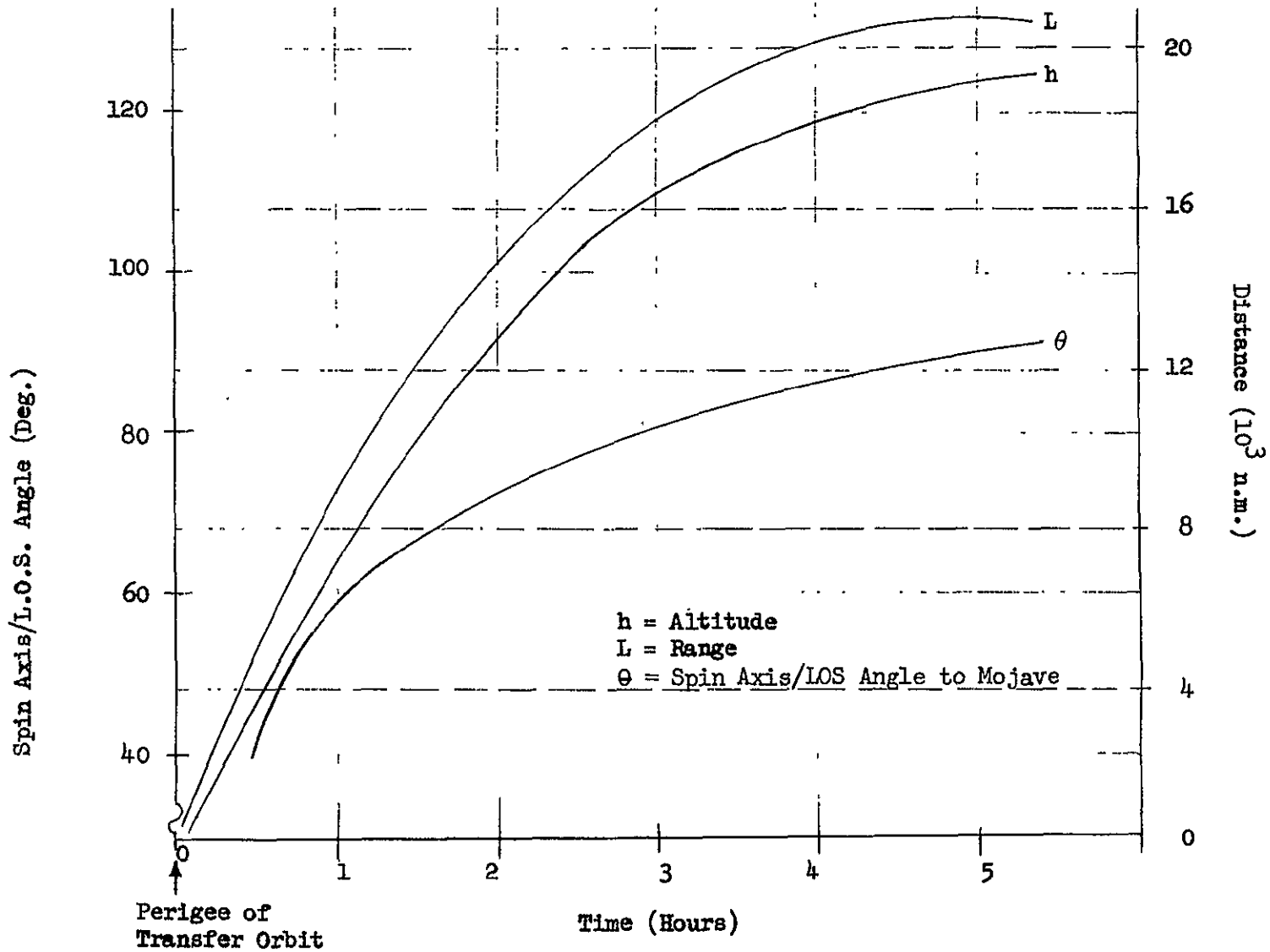
FIGURE 2-11. ALTITUDE & SPIN AXIS/L.O.S. ANGLE TO MOJAVE

h = Altitude
L = Range
θ = Spin Axis/LOS Angle to Mojave

Space Division
North American Rockwell
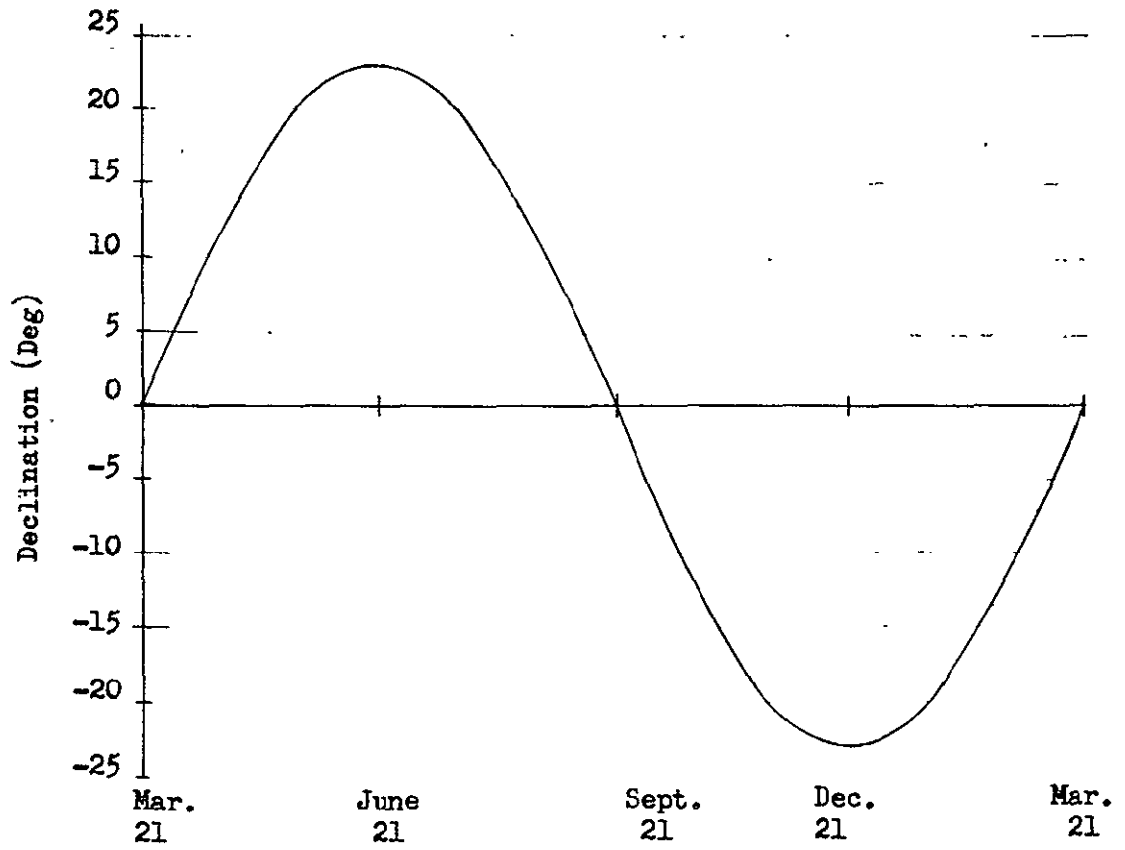
FIGURE 2-12   DECLINATION OF THE SUN

aid of Figures 2-13 and 2-14 which provide numerical and geometrical correspondence for key identified trajectory points. Figure 2-13 is a plan view (from the North) of the drift trajectory geometry, showing that target acquisition can best be accomplished at 6 p.m. orbital sun time (because of target visibility), while the apogee boost is planned to occur at 3 p.m. Figure 2-14 is a plot of orbital lead angle (longitude difference) plotted against number of orbits from the nominal ATS-V acquisition point.

Referring to Figure 2-13, a closing velocity of approximately 1 ft/sec (actually 0.935 ft/sec) at acquisition (point (a)) can be achieved by a Hohman transfer from a circular orbit corresponding to approximately a 0.2^{o}/rev slower orbit by applying a 0.935 ft/sec ΔV at the transfer ellipse apogee; i.e., 1/2 orbit prior to acquisition (point (b)). The average drift rate during this 1/2 orbit is 0.1^{o}/rev; thus for an intercept the ΔV applied at point (b) should occur with the RMU leading ATS-V by 0.05^{o}. In reality a slight lag is desired at point (a) rather than an intercept to allow viewing of ATS-V from the sunlit side. Thus, for a lag of say, of 2500 ft at point (a) the lead at point (b) would have to be approximately 0.0485^{o}.

Any error in the knowledge of the lead angle at point (b) will translate into an equal error in the lag at point (a); from Table 2-6 the 3 sigma tangential tracking error is less than 100 ft. Thus, this error source is not significant. An error of 0.1 sec in the timing of the impulse at point (b) amounts to only 5 ft of error at point (a) and is also not of concern. Any error in impulse magnitude at point (b) can be reduced by at least an order of magnitude by applying a correction between point (b) and point (a). Table 2-6 shows good tracking data to be available in ample time for such a correction, and therefore, this error source can be kept small relative to the nominal acquisition range. The only other error source of interest in this regard is the possibility of arriving at point (b) with an incorrect lead angle. The probability of this occuring is negligible in view of the time available for refining the drift orbit parameters and could be compensated, in any event, by adjusting time of ΔV burn at point (b). In short, guidance accuracy can readily support visual acquisition requirements.

The line (b)-(c) on Figure 2-14 represents the closure in the final vernier drift orbit at 0.2^{o}/rev. Nominally four and one-eight full vernier orbits are planned to provide ample time for fine corrections and to allow the ΔV impulses for transfer from the larger drift orbit to occur at 3 p.m. and 3 a.m. (corresponding to original boost transfer orbit line of nodes). Allowing 1/2 orbit following apogee burn for tracking and computation, 9 full drift orbits at a relative rate of 1.85^{o}/rev (78 n. m. above the ATS-V orbit) provide a properly phased closure.

The inherent flexibility of the nominal plan shown in Figures 2-13 and 2-14 indicates that the expected dispersion resulting from boost uncertainties can be accommodated by drift orbit adjustments (number of orbits and drift rate). For

54
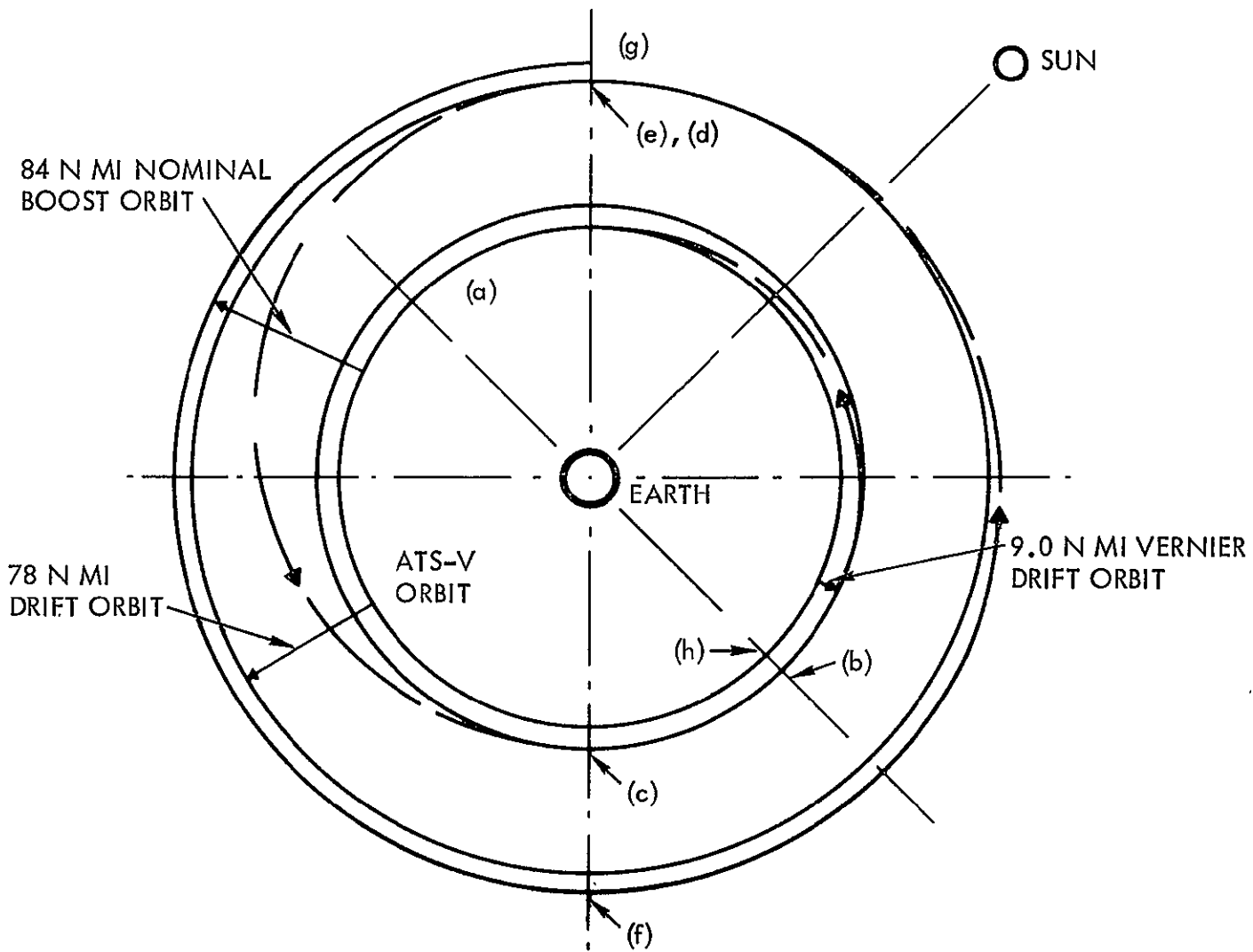
FIGURE 2-13. PHASING DRIFT ORBITS (PLAN VIEW)

Space Division
North American Rockwell
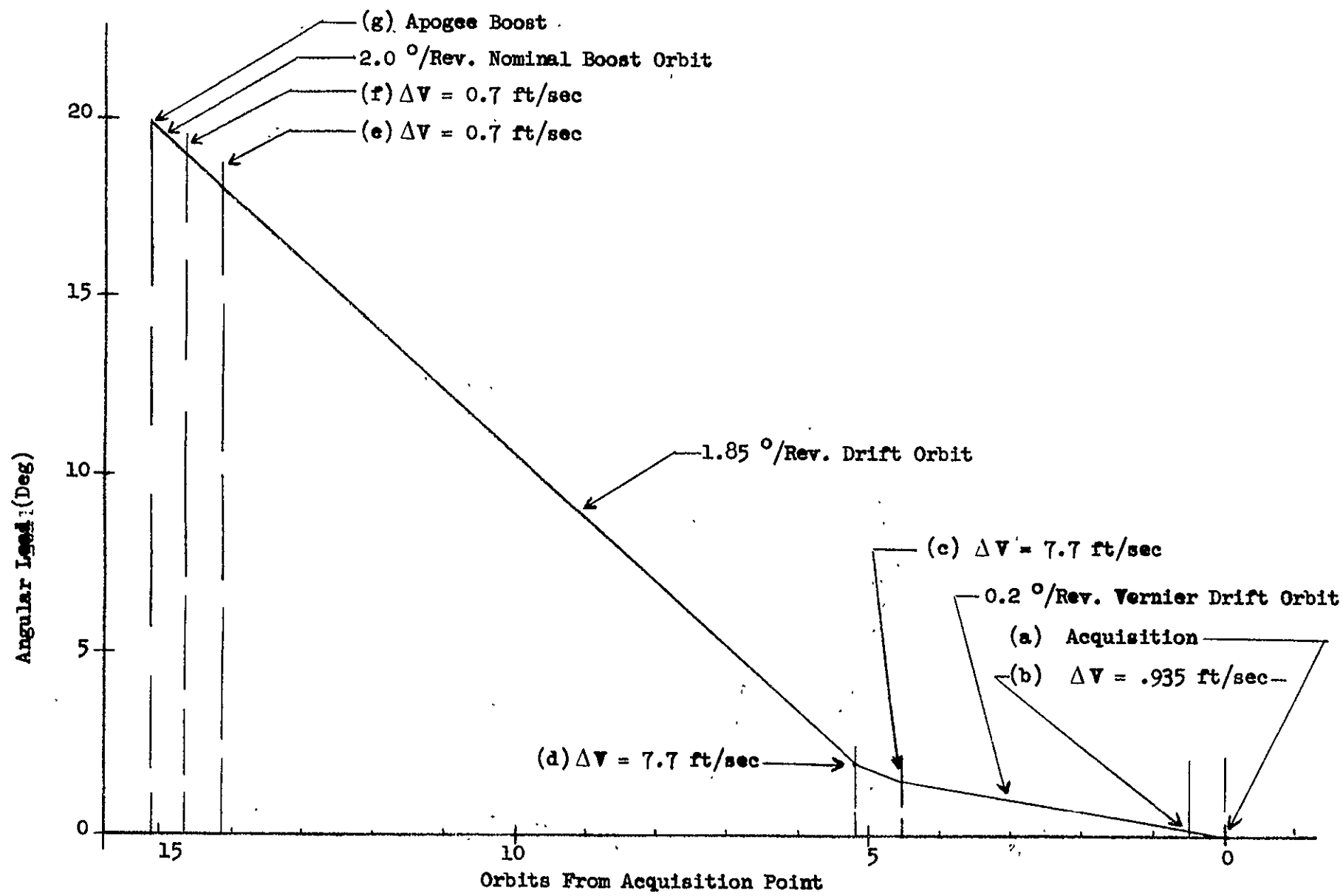
FIGURE 2-14. PHASING ORBIT CLOSURE

Space Division
North American Rockwell

originally elliptic orbits, unequal ΔV's at points (e) and (f) will be provided, at no loss in efficiency. Boost dispersion could conceivably cause large enough drift rates to radically reduce the angle between the RMU and ATS-V, even reverse their positions in as little as one revolution. However, in 12 hours tracking will permit good definition of the orbit and allow for any corrections needed to maintain the basic condition of RMU leading ATS-V. These straightforward calculations of drift orbit definition can readily be made during the first 12 hours following apogee boost.

A summary of the essentially linear relationships for a range of phasing orbits is shown in Figure 2-15. The nominal drift orbit and vernier drift orbit are indicated by small dashes.

2.4 DELTA-V REQUIREMENTS

A guidance analysis has been performed for the RMU rendezvous mission to (1) assess the orbital corrections required to compensate for launch dispersion, and (2) size the propellant necessary to provide the corrections.

This analysis was based upon four error categories. In this discussion all errors will be considered one sigma unless otherwise noted. The error categories assumed were:

1)   Transfer Orbit Injection

These data were provided by McDonnell Douglas Corporation for three particular transfer orbits characterized by varying inclination angles; i.e., 28.8°, 22.5°, and 16.3°. Errors were transmitted in the form of covariance matrices (Table 2-10) of the cartesian positions and velocities occurring at transfer orbit insertion (perigee). In the table, the NASA right-handed X Y Z system of nomenclature was utilized; i.e., Z-axis pointed along radius toward earth, X-axis normal to the earth radius vector in the plane of orbital motion, and Y-axis normal to the plane of motion.

2)   Apogee Motor Burn

These errors resulted from a 0.3° pointing error (See Appendix A) and a thrust impulse magnitude error of 0.5% (quoted by the Thiokol Chemical Corp).

- 57 -
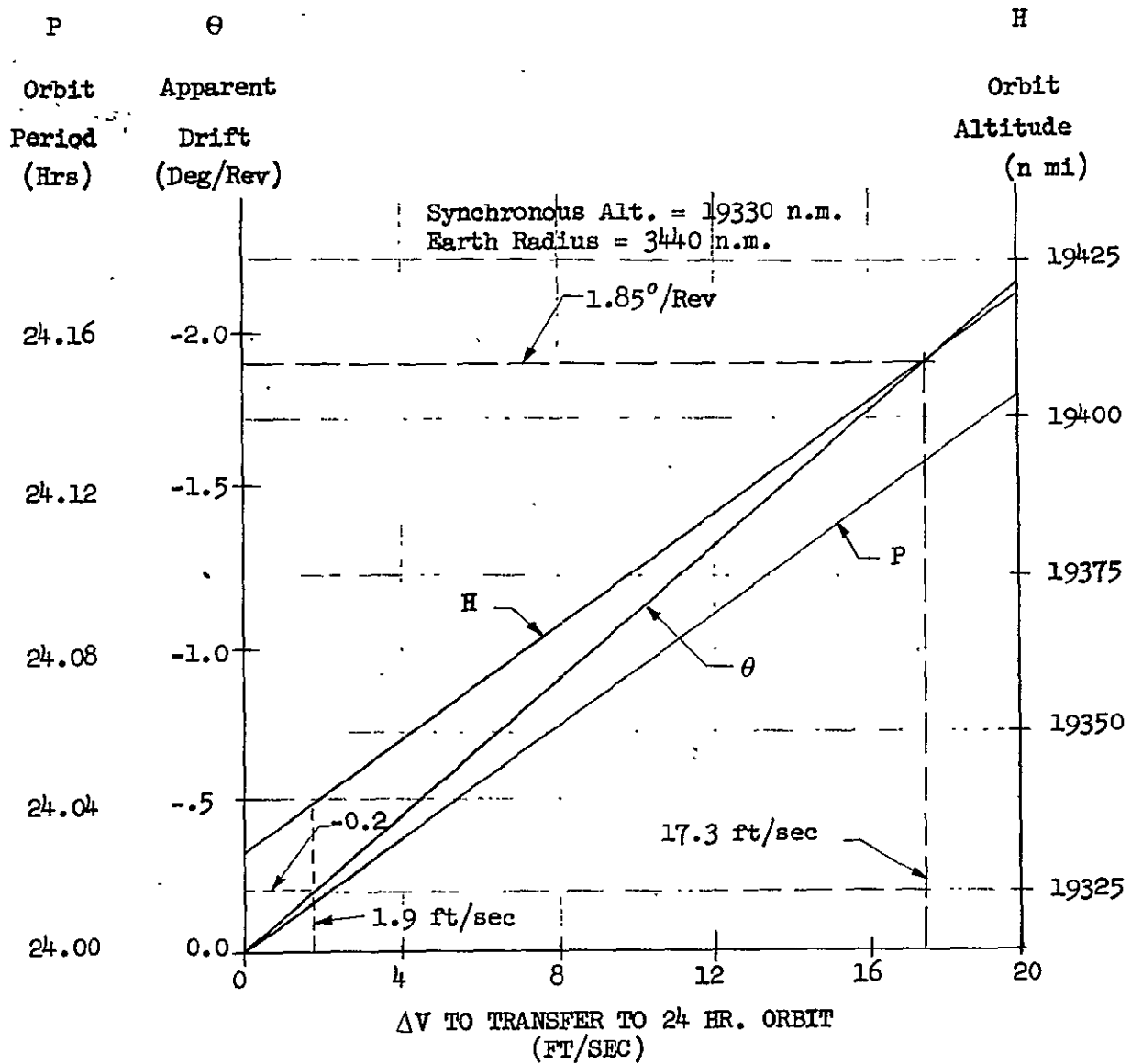
FIGURE 2-15. PHASING ORBIT CHARACTERISTICS

TABLE 2-10
TRANSFER ORBIT INJECTION ERRORS (NASA XYZ SYSTEM

X	Y	Z	Ẋ	Ẏ	Ż
0.1116677?D 09	-0.1967892CD 08	-0.982198600 08	0.1137435CD 06	-0.809013700 05	-0.184516300 06
-0.1967892CD 08	0.46433550D 08	0.211978500 08	-0.799329500 05	0.110503800 06	0.391304100 05
-0.982198600 08	0.211978500 08	0.177120100 09	-0.982546100 05	0.182033100 05	0.426649200 06
0.1137435CD 06	-0.799329500 05	-0.982546100 05	0.252408800 04	-0.332034900 04	-0.391738600 03
-0.809013700 05	0.110503800 06	0.182033100 05	-0.332034900 04	0.576127900 04	-0.116319200 03
-0.184516300 06	0.391304100 05	0.426649200 06	-0.391738600 03	-0.116319200 03	0.824570800 04

TRANSFER ORBIT INCLINATION ANGLE = 16.3 DEG.

X	Y	Z	Ẋ	Ẏ	Ż
0.121094800 09	-0.115781700 08	-0.108532400 09	0.895948100 05	-0.392558400 05	-0.214421400 06
-0.115781700 08	0.364234700 08	0.124104700 08	-0.410762800 05	0.103443800 06	0.177992800 05
-0.108532400 09	0.124104700 08	0.181919300 09	-0.110405200 06	0.100382400 05	0.407857100 06
0.895948100 05	-0.410762800 05	-0.110405200 06	0.906761100 03	-0.157679200 04	-0.610673700 03
-0.392558400 05	0.103443800 06	0.100382400 05	-0.157679200 04	0.528004000 04	-0.125465900 03
-0.214421400 06	0.177992800 05	0.407857100 06	-0.610673700 03	-0.125465900 03	0.623019300 04

TRANSFER ORBIT INCLINATION ANGLE = 22.5 DEG

X	Y	Z	Ẋ	Ẏ	Ż
0.107571000 09	-0.335678300 06	-0.953913000 08	0.651810300 05	-0.446416800 04	-0.181775500 06
-0.335678300 06	0.348237300 08	0.760638100 06	0.726503100 03	0.100301800 06	0.609106500 03
-0.953913000 08	0.760638100 06	0.170922900 09	-0.904287000 05	0.225108300 04	0.377574700 06
0.651810300 05	0.726503100 03	-0.904287000 05	0.333523000 03	0.721238200 02	-0.862767200 02
-0.446116800 04	0.100301800 06	0.225106300 04	0.721238200 02	0.529612400 04	0.107079100 02
-0.131775500 06	0.609106500 03	0.377574700 06	-0.862767200 02	0.107079100 02	0.574370600 04

TRANSFER ORBIT INCLINATION ANGLE = 28.8 DEG

UNITS: POSITION - FT
          VELOCITY - FT/SEC

3)   Orbit Determination Errors

These errors, reflecting the capability of the ground stations
to fix the orbital parameters by tracking, were supplied by
NASA. They consist of a 1000 ft. position error and a 0.1
ft per second velocity error, predicated upon 12 hours tracking
time.

4)   RMU Δ Control Errors

This error was taken as 1% of the commanded control impulse.

In the tables presented in the following discussion, all errors are resolved into the
radial R (Z), tangential T (X), and normal N (Y) directions. The error analysis was
conducted for the three inclination angles indicated above, to provide coverage for
any anticipated inclination angle.

The RMU initial drift orbit errors propagated from the transfer orbit injection
errors are presented in Table 2-11. These data are the standard deviations (1σ) of
the position and velocity components of the RMU before apogee burn. In general terms,
the cases of higher transfer orbit inclination angles yield smaller initial orbit errors.
In Table 2-12, the velocity errors due to apogee burn errors are given for each transfer
orbit inclination angle considered. The higher inclination angles result in larger
velocity errors. This is due primarily to the greater apogee burn magnitude required
for the higher transfer orbit inclination angles. The combined results of the transfer
orbit injection errors and the apogee burn errors are shown in Table 2-13. In these
data, the two error sources are assumed statistically independent and the position errors
occurring from the apogee burn are assumed negligible. The combined errors are
smaller for the higher transfer orbit inclination angles.

In Table 2-14, the errors presented in Table 2-13 are expressed in terms of par-
ticular in-plane orbit parameter errors of concern for the RMU initial orbit. Of
particular interest are the period and initial drift rate errors. The drift rate errors
are significantly greater than a nominal drift rate of two degrees per orbit. Moreover,
if an orbit of the RMU is required to complete initial orbit tracking and correcting, then
the angular separation between the RMU and ATS-V can vary appreciably from a nominal
value of 20 degrees.

The ΔV requirements to correct the in-plane RMU orbit period and shape are
shown in Table 2-15. These data are computed on the basis of a 180 degree transfer
correction orbit (at line-of-apsides) from the actual to the corrected RMU orbit.
These data are representative of the requirement to correct for the effects of transfer
orbit injection and apogee burn errors.

TABLE 2-11

INITIAL DRIFT ORBIT ERRORS DUE TO TRANSFER ORBIT
INJECTION ERRORS (1σ)

TRANSFER ORBIT INCL. ANGLE (DEGREE)	POSITION (1000 FT)			VELOCITY (FT/SEC)		
	R	T	N	$\dot{R}$	$\dot{T}$	$\dot{N}$
16.3	3041.	2844.	839.9	398.6	100.2	40.5
22.5	1780.	1606.	672.7	231.4	54.9	32.6
28.8	1067.	1160.	638.5	146.5	33.6	20.1

TABLE 2-12

APOGEE BURN VELOCITY ERRORS (1σ)

TRANSFER ORBIT INCLINATION ANGLE (DEGREE)	APOGEE BURN ERRORS (FT/SEC)		
	R	T	N
16.3	27.5	26.3	27.3
22.5	29.2	28.2	29.1
28.8	31.5	30.4	31.2

TABLE 2-13

INITIAL DRIFT ORBIT ERRORS
(AFTER APOGEE BURN) (1σ)

TRANSFER ORBIT INCL. ANGLE (DEGREE)	POSITION (1000 FT)			VELOCITY (FT/SEC)		
	R	T	N	$\dot{R}$	$\dot{T}$	$\dot{N}$
16.3	3041	2844	839.9	399.6	103.6	48.9
22.5	1780	1606	672.7	233.2	61.7	43.7
28.8	1067	1160	638.5	149.8	45.3	37.2

TABLE 2-14

INITIAL DRIFT ORBIT PARAMETER ERRORS (1σ)

TRANSFER ORBIT INCL. ANGLE (DEGREE)	SEMI MAJOR AXIS (1000 FT)	ECCENTRICITY ($\times 10^{-3}$)	PERIOD (SEC)	DRIFT RATE (DEG/REV)
16.3	3395	5.601	3178.1	13.229
22.5	2192	5.942	2052.2	8.575
28.8	1489	6.236	1394.1	5.825

TABLE 2-15

ΔV REQUIREMENT FOR
IN-PLANE CORRECTIONS (1σ)

| TRANSFER ORBIT INCL. | ΔV REQUIRED (FT/SEC) | |
ANGLE (DEGREE)	APOGEE	PERIGEE
16.3	55.10	70.22
22.5	32.27	50.62
28.8	19.34	39.67

TABLE 2-16

RESIDUAL ERRORS AFTER
INITIAL ORBIT CORRECTION (1σ)

TRANSFER ORBIT INCL. ANGLE (DEGREE)	SEMI MAJOR AXIS (1000 FT)	ECCENTRICITY ($\times 10^{-3}$)	PERIOD (SEC)	DRIFT RATE (DEG/REV)
16.3	2.486	0.178	23.27	0.0972
22.5	1.691	0.121	15.83	0.066
28.8	1.265	0.090	11.84	0.049

In Table 2-16, the residual errors after the RMU orbit corrections are made are shown. These residual errors reflect the effects of the RMU orbit determination and ΔV control errors in correcting the RMU initial orbit. The factor of reduction of the RMU orbit errors is comparable to the 1% RMU ΔV control errors which indicates that these errors are the significant residual errors as compared with the RMU orbit determination errors. The results indicate that the drift rate errors can be reduced to 0.05 to 0.1 deg/orbit (1 σ) depending upon the transfer orbit inclination angle used.

In Figure 2-16, the out-of-plane ΔV requirement is shown as a function of transfer orbit inclination error and percent probability of occurrence. The determination of this ΔV requirement is based upon the initial orbit angular momentum vector pointing error, which is a direct measure of the plane change angular correction required to correct the out-of-plane position and velocity errors as shown in Table 2-13.

The error data presented herein are derived on the basis of a linear error model. That is, the RMU drift orbit errors are defined as "first-order" variations, or pertubations, of the nominal drift orbit, and the delta-velocity (ΔV) corrections to correct orbit errors are defined on the basis of a "first-order" linear relationship to orbit errors. In this manner, the orbit errors and ΔV corrections are linear functions of the causative error sources indicated. If these causative errors are assumed as Gaussian random variables, then, using the linear error model, the resulting orbit errors and ΔV corrections are Gaussian random variables; moreover, if the first and second statistical moments of the causative error sources are known, then, the resulting orbit errors and ΔV corrections are specified by their first and second statistical moments using the relationships of the linear error model. Under these conditions, the joint probability density functions of the resulting errors are known, which provide a basis for assessing the probability of occurrence of the orbit errors and ΔV corrections.

The resulting orbit errors and their affect on the mission can be assessed directly on the basis of a joint Gaussian probability density function of the orbit errors. The error data resulting from this analysis are the standard deviations which specify the orbit error joint probability function where the causative error sources are assumed unbiased (zero first statistical moment); this yields unbiased orbit errors.

Likewise, the ΔV corrections can be assessed on the basis of a Gaussian joint probability function and the resulting data are the standard deviations. However, the fuel requirement to provide the ΔV correction is not a Gaussian random variable since it is not a linear function of the ΔV corrections. i.e., the fuel requirement (lbs) is a monotonically increasing function of the modules of the ΔV corrections. Thus, in sizing the fuel requirement, some discretion must be exercised in assessing the probability of occurrence of the fuel requirement when the statistical moments for the ΔV corrections are used.
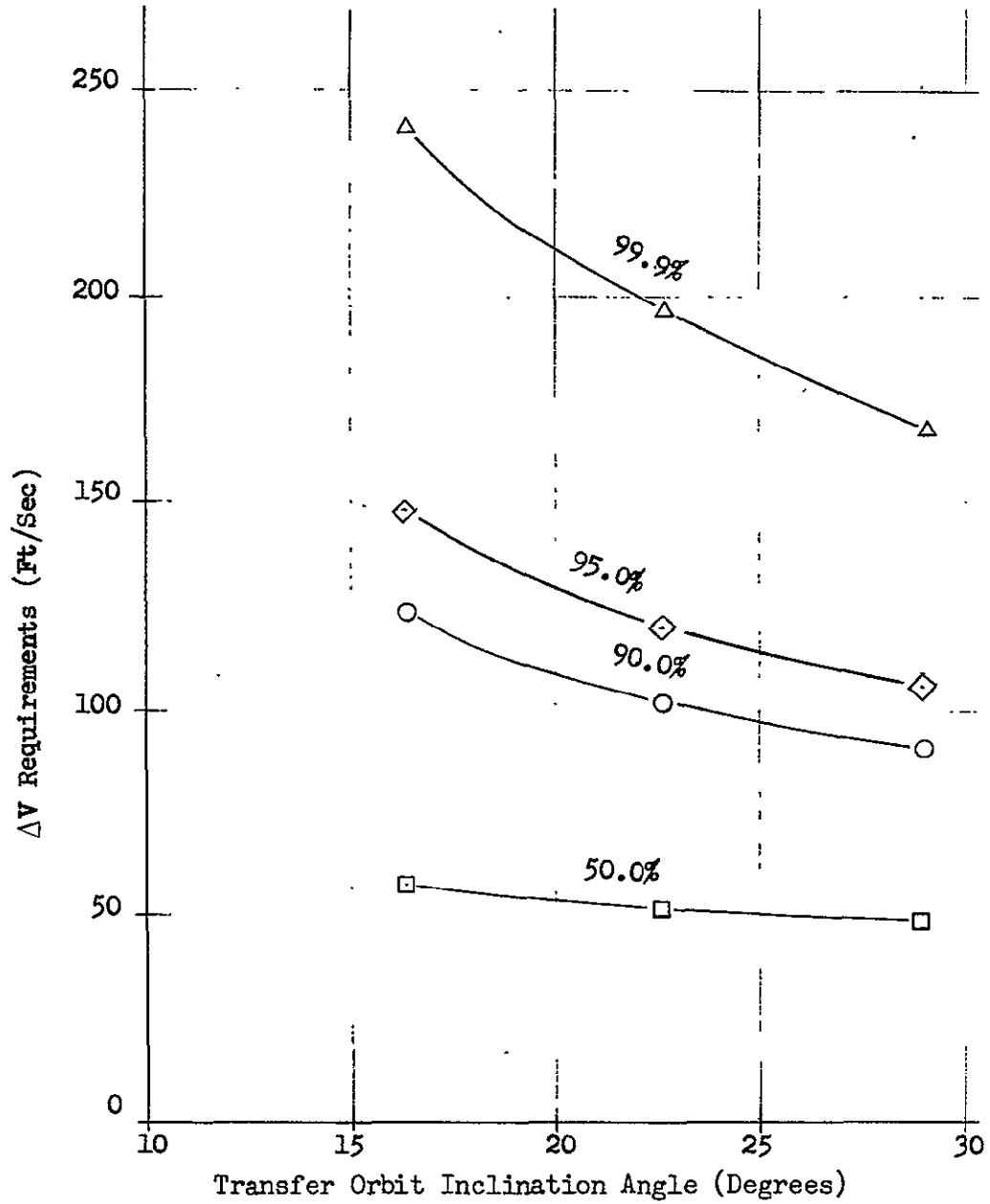
Figure 2-16. Out-of-Plane ΔV Requirement

On the other hand, the fuel requirement can be assessed on a conservative basis by simply adding the requirements for each correction for a given probability of occurrence. That is, the fuel requirement for the in-plane ΔV corrections can be "sized" using the sum of the "three-sigma" (σ) cases for the various ΔV corrections, which then sizes the total fuel requirement on the basis of at least (actually well over) 99.7% of the occurrences.

The out-of-plane fuel requirement, in turn, can be sized on the basis of a single ΔV correction to be made at the line-of-nodes of the perturbed and nominal orbits. This ΔV correction is directly proportional to the perturbed orbit inclination angle with respect to the nominal orbit plane. This angle, in turn, can be determined on the basis of the two orthogonal components of the perturbed angular momentum vector as shown in Figure 2-17. The approximations are as follows:

$$\alpha \simeq \frac{\Delta H_{xy}}{M}$$

$$\Delta H_{xy}^2 = \Delta H_x^2 + \Delta H_y^2$$

To assess the out-of-plane ΔV correction, ΔV_N, the occurrence of the perturbed orbit inclination angle α must be specified. This, in turn, requires a specification of the occurrence of the vector sum of the two orthogonal components, ΔH_x and ΔH_y.

Now, the in-plane angular momentum vector errors, ΔH_x and ΔH_y, are Gaussian random variables, assuming a linear error model of the first-order perturbations. On this basis the occurrence of ΔH_{xy} can be assessed by using a set of principal error coordinates that are defined by the model matrix of the ΔH_x and ΔH_y covariance matrix, which defines a trace invariant transformation to principal error coordinates. The principal errors are statistically independent and their vector sum can be assessed using tabulated data for the probability of occurrence. This is the basis by which the out-of-plane ΔV requirement was derived. The requirement is essentially based upon the perturbed orbit inclination angle which is assessed on the basis of the vector sum of in-plane angular momentum vector perturbations.

Now, the total fuel requirement, including in-plane and out-of-plane requirements, can be sized by adding the in-plane and out-of-plane requirements for a particular probability of occurrence. In this manner, a total requirement can be sized on a relatively conservative basis, however, the conservative "margin" depends upon the degree of correlation which exists between the various ΔV corrections and as the correlation approaches unity the sizing approaches the exact value, i.e. the margin decreases. In the present analyses the ΔV correction correlations were found to be on the order of 0.6, or less.

x - y nominal plane-of-motion

$\Delta V_n \simeq \alpha\, V$

V = total velocity of circular orbit

x, y Initial plane-of-motion
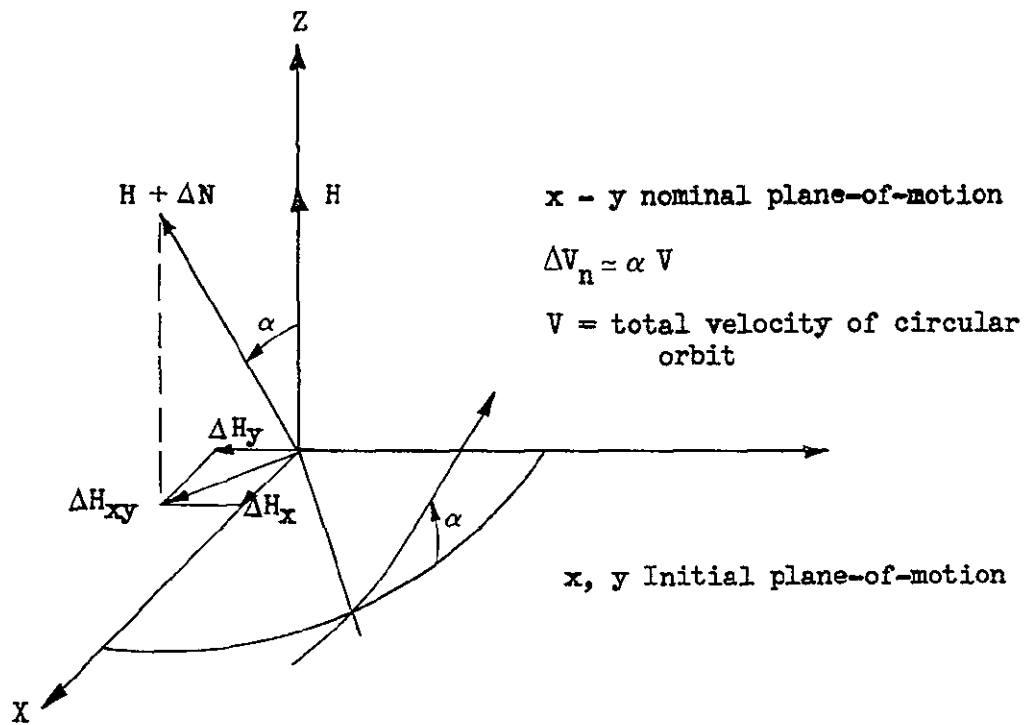
Fig. 2-17. Orbital Inclination (out-of-plane) Correction

For the purpose of establishing a preliminary propellant budget for the RMU baseline reaction control subsystem, the ΔV requirements for correcting in-plane and out-of-plane errors were estimated on the above conservative basis (i.e. for full correlation). On this basis, interpolating between the values given in Table 2-15, the 3 sigma ΔV requirement for correcting in-plane errors was estimated as 210 ft/sec. Using Figure 2-7, the ΔV requirement for correcting out-of-plane errors (for 99.7% probability of occurence) was estimated as 185 ft/sec. Thus the total drift-orbit correction requirement was estimated as 395 ft/sec resulting in a very conservative propellant budget.

Propellant requirements for precession of the RMU spin axis for changing space-craft attitude during the launch phase were estimated on the basis of Appendix A as 621 lb-sec of impulse. Propellant needs for active nutation control were estimated on the basis of ATS data with adjustments for relative magnitudes of mass properties, energy dissipation rates, and related factors; on this basis the preliminary requirement was estimated as 120 lb-sec of impulse.

The ΔV required for reducing the drift-orbit altitude to the ATS-V orbit altitude as the visual acquisition point is approached, was estimated on the basis of Figure 2-15 as 18 ft/sec.

2.5 CONCLUSIONS AND RECOMMENDATIONS

A trajectory profile, vehicle configuration, and operational procedure have been developed which are compatible and combine to represent a feasible method for achieving the initial conditions required for rendezvous acquisition with the ATS-V. Adequate design and performance margin exists in the important areas of payload capability, reaction fuel capacity, and vehicle orientation and trajectory control. The RMU/ATS-V rendezvous acquisition range and time can be controlled to a high degree of accuracy using RMU and ATS-V relative tracking and orbit corrections after the transfer maneuver from initial to final drift orbits.

3.0 RENDEZVOUS

THE RMU CAN RENDEZVOUS WITH THE ATS-V IN A SIMPLE, ORDERLY
SEQUENCE WITH WIDE MARGINS OF TARGET ILLUMINATION ADEQUACY AND
TRAJECTORY CONTROL ACCURACY.

3.1 REQUIREMENTS

The rendezvous sequence begins with the despinning of the RMU at the termination
of the final vernier drift orbit and ends with the placement of the RMU approximately
150 feet south of the ATS-V ready for final approach and docking. During this mission
·phase, the RMU must be despun and the TV axis rotated to the general direction of the
ATS-V. The high gain C-band antenna must be pointed to earth for adequate TV trans-
mission and the TV must be pointed to acquire the ATS-V target. If the acquisition
range exceeds that where image size would permit immediate recognition, validation
maneuvers must be accomplished to insure detection of the proper target. Upon valida-
tion, the RMU must be translated to the immediate vicinity of the ATS-V with minimum
fuel consumption and then translated and rotated to a position directly south of the
ATS-V (along its spin axis), all while maintaining uninterrupted TV coverage of the
ATS-V. The entire rendezvous operation, to minimize power utilization and equipment
heating, should be accomplished within a very few hours. Three hours has been set as
a maximum for this phase to assure minimum impact on equipment.

3.2 ALTERNATE APPROACHES/TECHNICAL CONSIDERATIONS

Some of the items affecting the basic rendezvous procedure and/or system configura-
tion, are discussed below.

3.2.1 Acquisition Time

The most favorable time during the ATS-V orbit for acquisition is affected by two
factors. Referring to Figure 3-1, the first consideration is that of assuring good target
illumination by proper geometrical orientation relative to the sun. If, for example, the
acquisition (wherein the RMU is overtaking the ATS-V from behind) were to occur at
6 p.m. sun time, the sun would be behind the RMU, thus providing best reflections
between 3 p.m. and 9 p.m. sun time. The second consideration is that of sensing RMU
attitude information from on-board sun sensors and from POLANG. As depicted in
Figure 3-2, a sun sensor located at point P can provide attitude information about any
axis lying in a plane perpendicular to the line P-S to the sun. The POLANG measure-
ment provides a single axis sensitivity about line P-E directed toward the earth tracking

Best Rendezvous Region
(Sun Illumination)

Selected Rendezvous
& Docking Region

Best Docking Region
(Full Attitude
Information)

3 Hrs.

3 Hrs.

Earth

Sun

Space Division
North American Rockwell
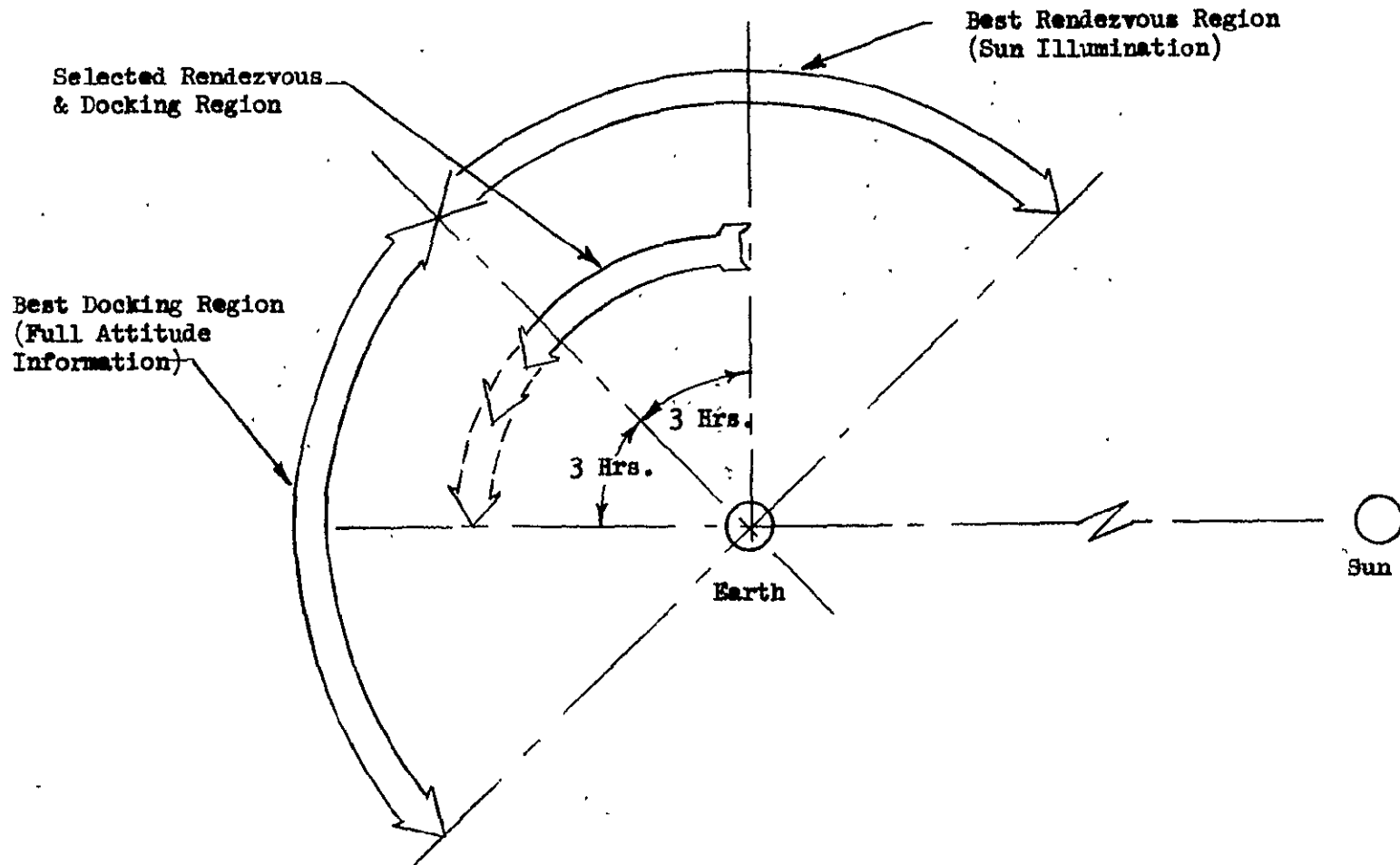
FIGURE 3-1.   SELECTION OF ORBITAL PHASES FOR RENDEZVOUS & DOCKING
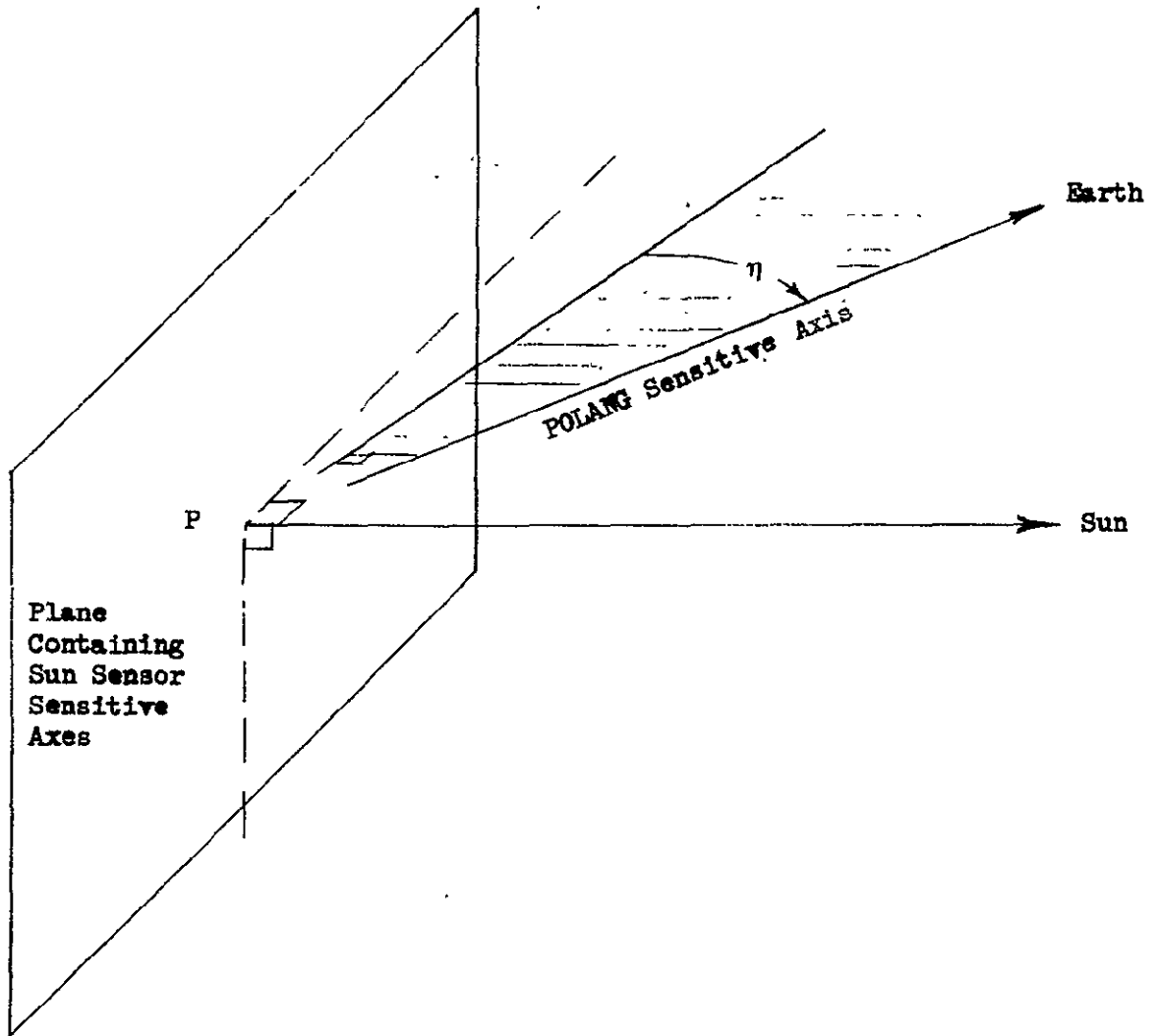
FIGURE 3-2. ATTITUDE MEASUREMENT SENSITIVITY

station. Accordingly, no sensitivity exists for a measurement about the sun line when the earth is in the plane normal to the sun line. In short, poor attitude sensitivity about the sun line exists at 6 p.m. (and 6 a.m.) while best attitude capability is provided at 12 p.m. (and 12 a.m.) as shown in Figure 3-1.

The inherent RMU attitude-measuring capability is further depicted in Figure 3-3, wherein measurement accuracy for each of the three major axes is plotted against orbital position, assuming sun at zero declination. Specifically, pitch angle θ is always directly measured only by sun sensor; yaw angle is always measured by POLANG and supported with varying sensitivity by sun sensor (statistical combination providing improved accuracy, particularly at 6 p.m. and 6 a.m.); and roll angle ϕ provided with varying sensitivity only by sun sensor (becoming totally insensitive at 12 p.m. and 12 a.m.). Changes in declination merely tip the axis of zero sun sensor sensitivity.

Initial RMU attitude is known from prior POLANG/sun-sensor data accumulated in the drift orbits. Pointing of the high gain antenna to earth at the end of the RMU despin operation is readily accomplished by observing received C-band signal level on the ground. Although during subsequent operations the TV transmission will be the primary source of attitude information, maneuvers requiring precision attitude information (such as docking) should be accomplished closer to 12 p.m. to take advantage of the RMU sensor-derived information. Accordingly, as indicated in Figure 3-1, acquisition is planned to start at 6 p.m. when best target illumination is provided and the docking maneuver several hours later to assure good attitude information from the sun sensors. Since the video cue will provide the primary source of relative attitude information, the sun sensor attitude sensing consideration is non-critical.

3.2.2 Acquisition Range and Geometry

The relationship between geometrical constraints and guidance accuracy, as it affects selection of nominal acquisition positioning, is shown in Figure 3-4. Referring to the side view geometry (viewed from the north), the relative position error must be within an angle defined by the high gain antenna beam width and the TV camera field of view. Further, to eliminate the requirement for search scanning about the pitch axis , knowledge of relative ATS-V position (tracking accuracy) must be within the TV camera FOV. Referring to the top view geometry, the out-of-plane position error, assuming no azimuth search limitations, is constrained only by illumination adequacy (a maximum acceptable viewing offset angle of 45° is arbitrarily taken). Considering the above, the smaller the nominal acquisition range, the greater the navigation accuracy requirement because of the geometry constraints.

Two categories of target acquisition range are possible: one where the target is detected but unresolved, and a validation sequence must be employed to distinguish ATS-V from the star background; the other where ATS-V is immediately recognizable once acquired. A plot showing the number of TV lines subtended by the side-viewed ATS on a $14° \times 15°$ field of view 525 line camera is presented in Figure 3-5. As shown, the image becomes marginally resolved (> 4 lines) at R = 3,000 feet and definitely
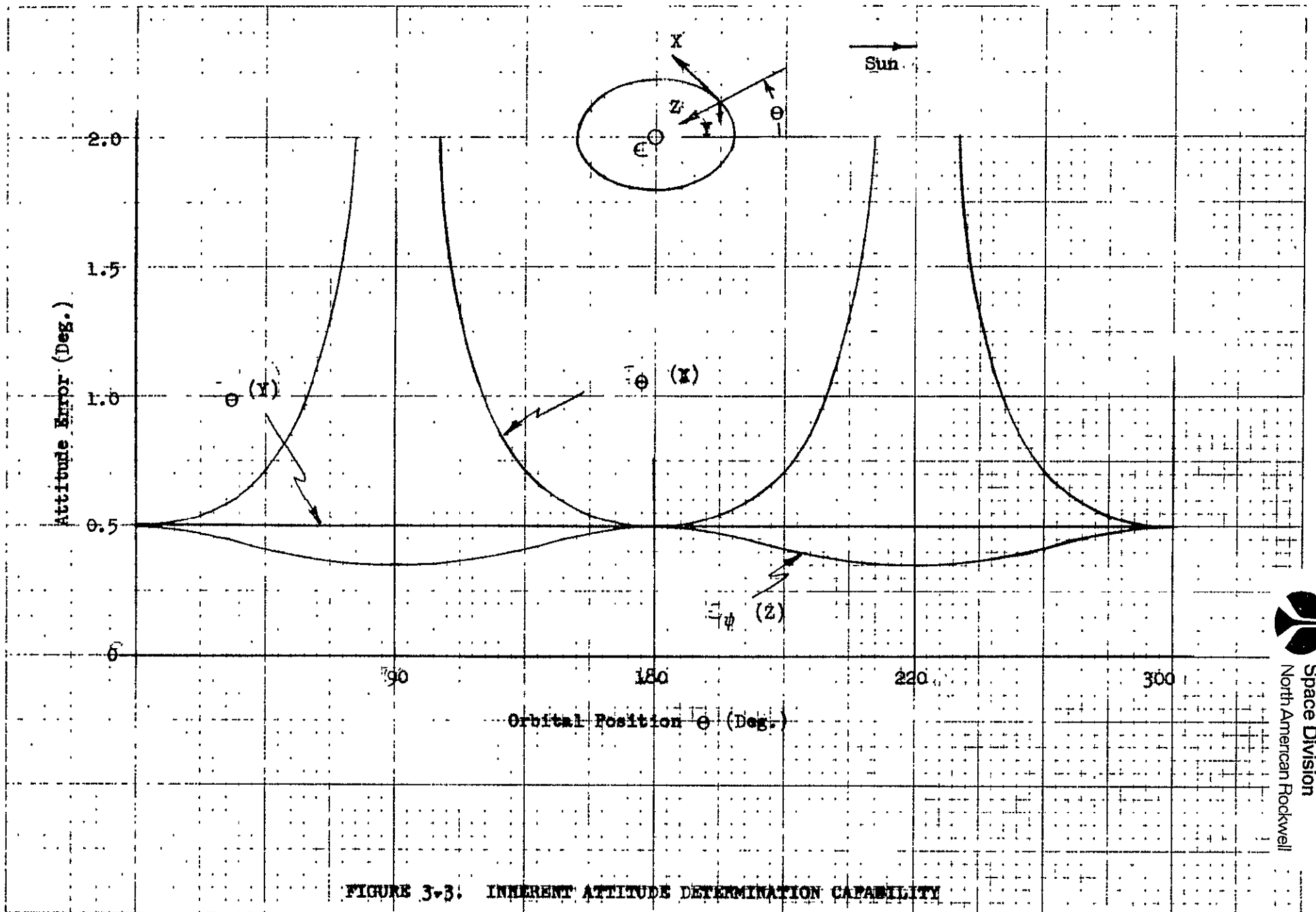
FIGURE 3-3. INHERENT ATTITUDE DETERMINATION CAPABILITY
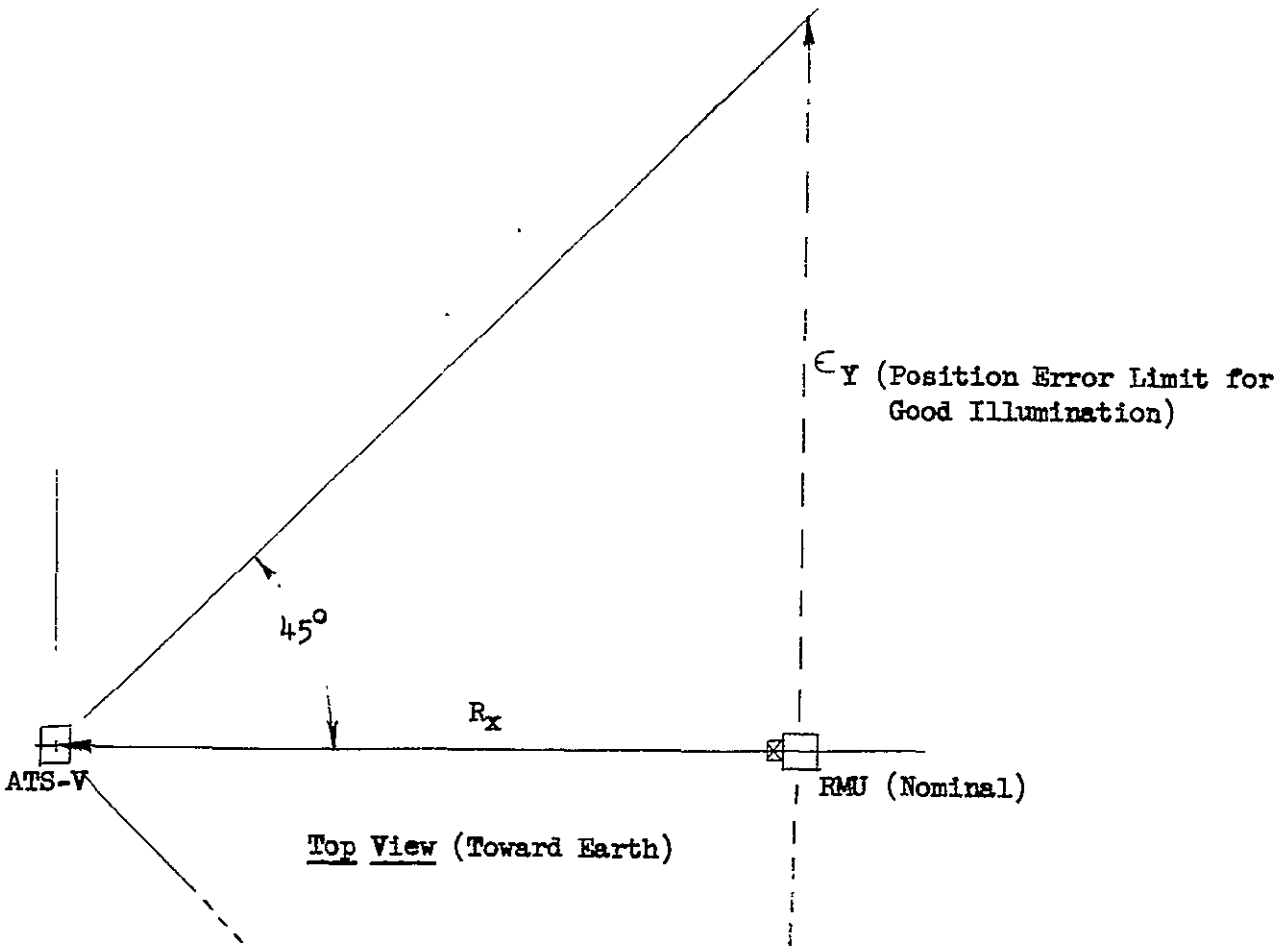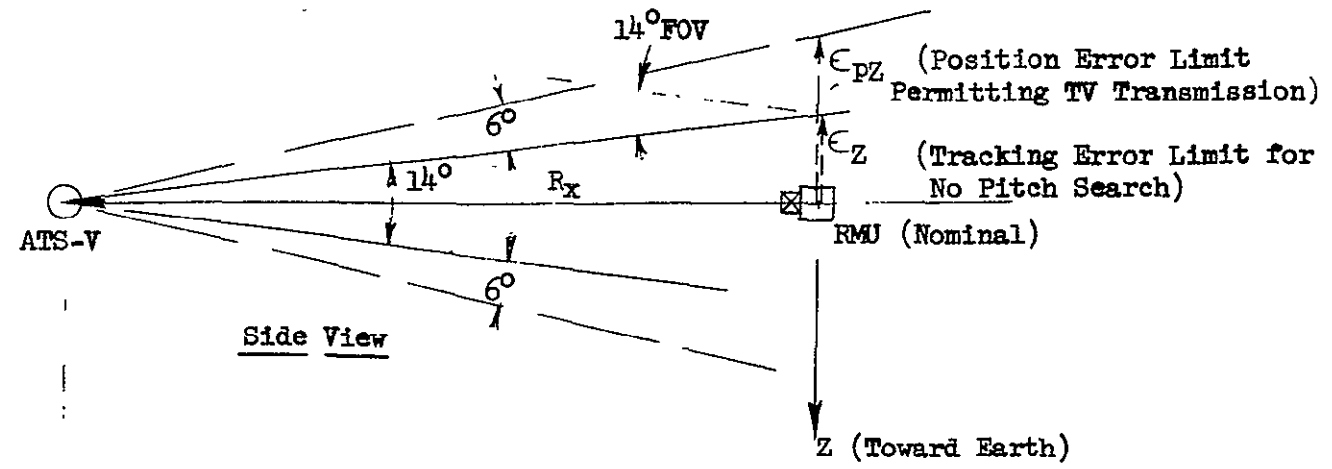
FIGURE 3-4. ACQUISITION GEOMETRY
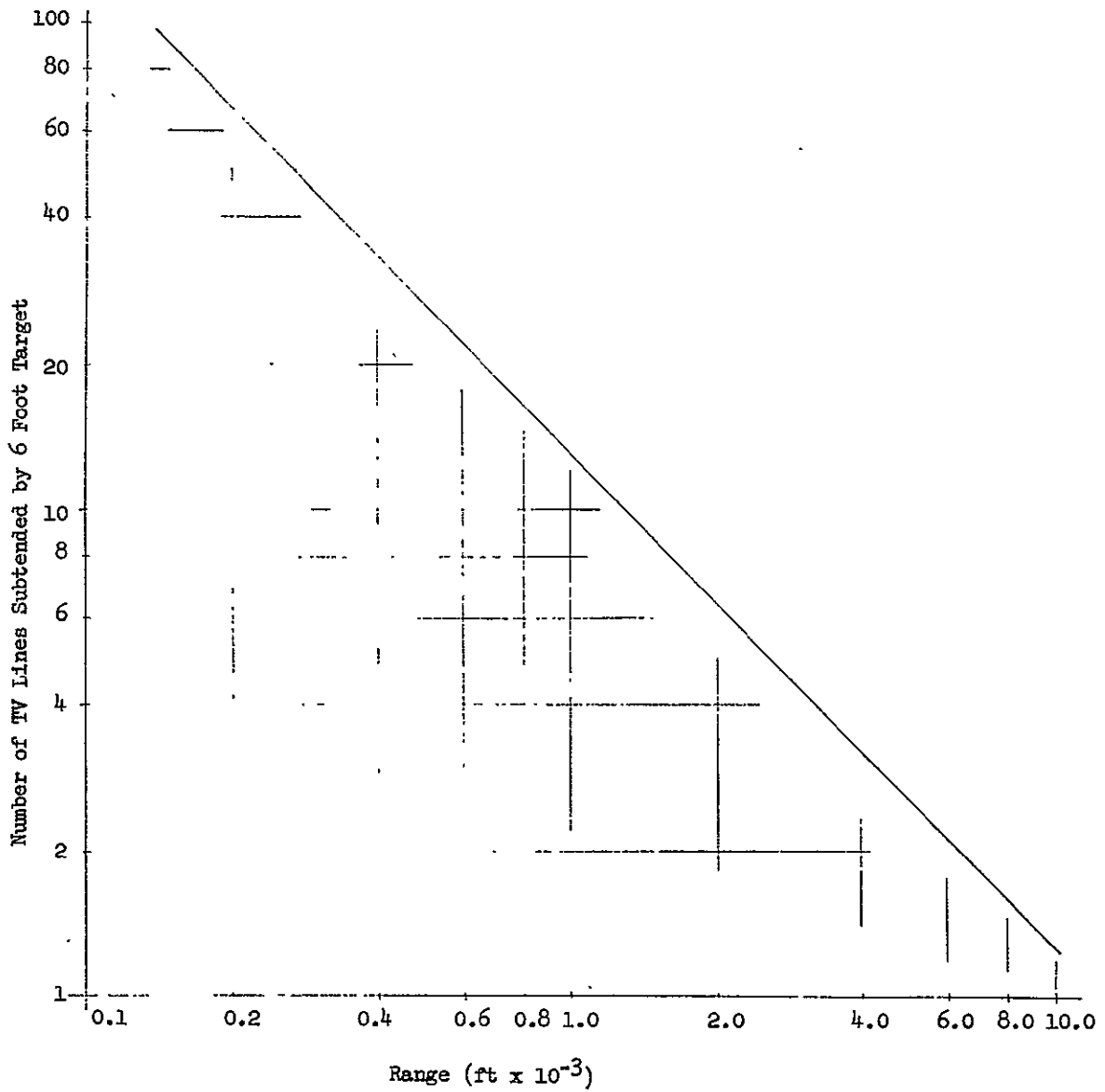
Figure 3-5 ATS-V Image Size vs. Range

resolved (>6 lines) at R = 2,000 feet. The ATS-V unresolved target can conservatively be detected at ranges up to 10 n.mi. as indicated below, but will require validation maneuvers at ranges much greater than 3,000 feet to distinguish the ATS-V image from the star background.

The range at which the ATS-V can be detected is dependent upon many factors but initial calculations indicate that the target spacecraft can be detected by the TV sensor at a range which greatly exceeds the range at which the spacecraft is resolved. At ranges greater than the resolution range the ATS-V appears as a point target which is in general much more intense than the star background. This conclusion is based on the following calculations which are purposely conservative.

Detection is assumed to take place under conditions of target reflected sunlight with observation geometry such that the field of view of the TV sensor is positioned in the radiation field of the reflected sunlight. For calculation purposes the solar constant at earth distance from the sun is taken as broadband spectral radiation which equals or exceeds the spectral response of the TV sensor. The solar constant, I, has the value

$$I = 1.3 \times 10^5 \text{ candles/m}^2 .$$

In photometric terms the incident radiation is referred to as the illuminance. Part of the incident radiation is reflected by the target. The reflected radiation is termed the target luminance or target photometric brightness in the same units as the illuminance. The luminance, B, is given by

$$B = \frac{I \rho}{2 \pi} \text{ cd/m}^2$$

where ρ is the reflectivity of the target ($0 \le \rho \le 1$). The quantity 2π is included to account for the unknown scattering characteristics of the target. Without a detailed knowledge of the target's reflective characteristics, the incident radiation is assumed scattered non-preferentially into a hemisphere.

At a distance, R, the target has an illuminance, E, determined by the luminance B, the projected area of the target in the direction of measuring and the distance from the target in the form:

$$E = \frac{B A_T \text{ Cos } \emptyset}{R^2} \text{ cd/m}^2$$

where: E is the illuminance of the aperture of the TV optical system

B is the target luminance

A_T is the target area in m^2

$\emptyset$ is the angle of observation from the normal to the illuminated target surface

R is the range from the target to the TV optical aperture in meters.

The target area, A_T, which intercepts the solar radiation is also dependent upon the geometry so that

$$A_T = A_T' \, \text{Cos} \, \theta$$

where: A_T' is the geometric cross section of the target which is assumed to be rectangular

θ is the angle between the normal to A_T' and the direction of the incident solar radiation.

For calculation purposes the target area, A_T', is assumed to be a rectange 5 ft. high by 8 ft. long with a maximum area of 40 ft.^{2} (3.7 m^2). However, to account for the decrease in target area due to geometric factors a value of one square meter will be used to calculate detection range, that is,

$$A_T = A_T' \, \text{Cos} \, \theta = 1m^2 .$$

Target reflectivity has a marked effect on detection range. To obtain a conservative estimate of range a value of 0.1 is used for reflectivity although it may be as high as 0.5.

If the values given above are substituted into the expression for target illuminance we obtain

$$E = \frac{1.3 \times 10^5 \times 10^{-1} \times 1}{2 \pi \quad R^2} \, \text{Cos} \, \emptyset \, \text{cd/m}^2$$

$$E = \frac{2.37 \times 10^3}{R^2} \, \text{Cos} \, \emptyset \, \text{cd/m}^2 .$$

The significant parameter for detection of a point target by a TV camera tube is the illuminance in the image plane. No precise figures are available for this quantity since it is determined by the sensitivity of the photosurface and the thermal noise in the video amplifier of the output. Space rated vidicon cameras have minimum detectable illuminances on the order of 0.03 cd/ft^2 and since the proposed camera will have at least an equivalent sensitivity, a value of minimum illuminance for a 30 db output signal to raise ratio could be as small as

$$E_{i(min)} = 3 \times 10^{-2} \, \text{cd/ft}^2 = 3.24 \times 10^{-1} \, \text{cd/m}^2$$

SD 71-286

where E_i is the image plane illuminance. However, to account for spectral mismatch of the illumination and the detector sensitive surface, and transmission loss in the optics a value of

$$E_{i(min)} = 1 \text{ cd/m}^2$$

will be used.

To connect the illuminance at the optical aperture to illuminance in the image plane, the optical characteristics of the camera system must be considered. This conversion is established by multiplying the illuminance of the aperture by the ratio of area of the aperture to the area of the "airy" disc of the optical system in the image plane. Thus

$$E_i = E \frac{A_r}{A_D}$$

where: A_r is the area of the optical aperture

A_D is the area of the airy disc in the image plane.

For an aperture of diameter, d,

$$A_r = \frac{\pi}{4} d^2$$

and the area of the airy disc is

$$A_D = \frac{\pi}{4} d_i^2 .$$

The quantity, d_i, is the diameter of the airy disc. It is not unique for broadband spectral illumination since it is determined by the diffraction of the aperture which is wave length dependent. Common practice uses a wave length which is near the center of the spectral band and which is determined by the average illuminance over the spectral band. For calculation purposes an average wave length value of

$$\lambda = 0.56 = 5 \times 10^{-7} \text{meter}$$

is used. From diffraction theory the angle subtended by the airy disc in the image plane is

$$\alpha_D = 1.22 \frac{\lambda}{d}$$

where d is the optical aperture and λ is the average wave length of the illumination. From simple geometry it follows that the diameter of the airy disc is

$$d_i = 2f\alpha_D$$

where f is the focal length of the optical system. Substituting for α_D the diameter becomes

$$d_i = 2.44 \frac{f}{d}$$

But, since the aperture ratio or f/number, N, is

$$N = \frac{f}{D}\lambda$$

$$d_i = 2.44 \, N\lambda$$

therefore

$$A_D = \frac{\pi}{4} d_i^2 = \frac{\pi}{4}(2.44 \, N\lambda)^2 .$$

Substituting into the expression for E_i we obtain

$$E_i = E \frac{d^2}{6N^2 \lambda^2}$$

To complete the calculation two additional quantities must be specified, that is the optics diameter, d, and the aperture ratio N. For computation purposes a diameter of one inch is assumed, that is

$$d = 1 \, in = 2.54 \times 10^{-2} \, meters.$$

For target search, a field of view of 14 deg. is to be used and from simple geometry

$$\tan \theta/2 = \frac{d/2}{f} = \frac{1}{2N}$$

so that the aperture ratio is

$$N = \frac{1}{2 \tan 7°} = 4 .$$

- 79 -

SD 71-286

If the numerical values are substituted into the expression for the image plane illuminance we obtain

$$E_i = \frac{2.37 \times 10^3 \times 6.46 \times 10^{-4}}{6.0 \times 16 \times 3.13 \times 10^{-13} R^2} \, \text{Cos} \, \phi$$

$$E_i = \frac{0.510 \times 10^{11}}{R^2} \, \text{Cos} \, \phi \, \text{cd/m}^2$$

and since $E_{i(min)} = 0.1 \, \text{cd/m}^2$

we obtain

$$R^2 = 0.510 \times 10^{11} \, \text{Cos} \, \phi$$

or

$$R = 2.26 \times 10^5 \sqrt{\text{Cos} \, \phi} \quad \text{meters}$$

and

$$R = 122 \sqrt{\text{Cos} \, \phi} \quad \text{naut. mi.}$$

For an angle of view, ϕ, as large as 85 deg. off the normal, the detection range is on the order of 36 nautical miles so that there does not appear to be any real difficulty in detecting the ATS-V at extended range in spite of the fact that the spacecraft will not be resolved by the TV system until a much shorter range is reached.

While the calculations given are not intended to be definitive they do indicate that even with generally pessimistic assumptions the target can be detected at long range. Conservatism in establishing the range is also dictated by the fact that the solar cells covering most of the ATS-V surface may, to some extent, act as a specular reflector; this characteristic would reduce the photometric brightness of the observed target. Thus a maximum detection range of 10 n.m. is assumed in this report for obtaining an unresolved image. Tracking accuracy is such that rendezvous at less than 1/2 n.mi. range is easily supported, and the 10 n.m. maximum detection range provides a comfortable margin to insure that rendezvous will be accomplished without difficulty.

Provided the immediate recognition category could be supported by tracking capability, it will be selected as the nominal approach since search time, recognition/target validation time, and closure time would be minimized (thus conserving both power and fuel). If tracking accuracy were insufficient to support the immediate recognition category, a nominal range as close as geometry permitted would be selected and validation maneuvers anticipated.

The technique employed to accomplish target acquisition, then depends upon the initial errors in relative ATS-V/RMU location. Potential errors in ground tracking relative position data in the terminal phase of the drift orbit are tabulated in Table 3-1 as functions of assumed tracking condition (excerpted from Section 2).

Early tracking accuracy assessments indicated that condition 4 accuracy (Table 3-I) might be the best available and a minimum range of approximately 5,000 feet would result based on the 45° maximum viewing offset angle limitation. As a conservative approach, investigation of rendezvous techniques applicable to a 12,000 foot acquisition range was conducted. More recent information indicates that condition 2 accuracy (Table 3-1) can be achieved readily and the two geometric constraints of Figure 3-4 will not be exceeded at 3,000 foot R_x for $\epsilon z < 70$ feet and $\epsilon y < 720$ feet. Thus, ultimate adoption of an immediate recognition category nominal range $\leq 3,000$ feet is anticipated. However, much of the subsequent discussion concerns a 12,000 foot nominal acquisition range to illustrate an acquisition requiring validation maneuvers.

3.2.3 Search Patterns

Another important consideration is the selection of the related parameters affecting target search. These are TV field of view, search ranges employed, and search patterns. These parameters depend upon assumed tracking accuracy, time and energy limitations, and common requirements relating to other mission phases. A search TV field of view of 14° (available lens) was selected to augment the 64° wide angle field of view selected for docking; this provides a sufficiently wide field of view for maneuvering and yet is narrow enough to provide for early target resolution. An acquisition range of 12,000 feet is consistent with this selection, and search patterns geared to tracking uncertainties (with considerable conservatism) are conveniently outlined below for this as well as shorter search ranges.

Considering the relative geometry of acquisition, the RMU body axes x, y, z are nominally coincident with the corresponding spatial axes X, Y, Z (see Figure 3-6). The accuracy with which this orientation can be obtained is such that the total pointing deviation is less than 1° from nominal for sun sensor direction errors of 0.5°. Using the values of Table 3-1 for the 3σ out-of-plane (Y) and altitude (Z) position errors, the required search half-angles as a function of R_X become

$$(\Delta\psi)_{3\sigma} = \arctan \frac{\epsilon_Y}{R_X}$$

$$(\Delta\theta)_{3\sigma} = \arctan \frac{\epsilon_Z}{R_X}$$

for the vertical (pitch) and horizontal (yaw) search half-angle, respectively.

TABLE 3-1 TRACKING ACCURACY

Condition	3σ Error (Feet)		
	z (Altitude)	x (Tangential)	y (Out-of-Plane)
1. 3 ground stations, each tracking hourly for six hours. (Ref. Tables 2-4 & 2-5)	8	50 to 70	40 to 55
2. 2 ground stations, each tracking 3 cycles per hour for ten hours. (Ref. Table 2-6)	70	90	720
3. 2 ground stations, each tracking hourly for eight hours. (Ref. Tables 2-2 & 2-3)	190	190	2000
4. 2 ground stations, each tracking hourly for five hours. (Ref. Table 2-2)	450	250	4200
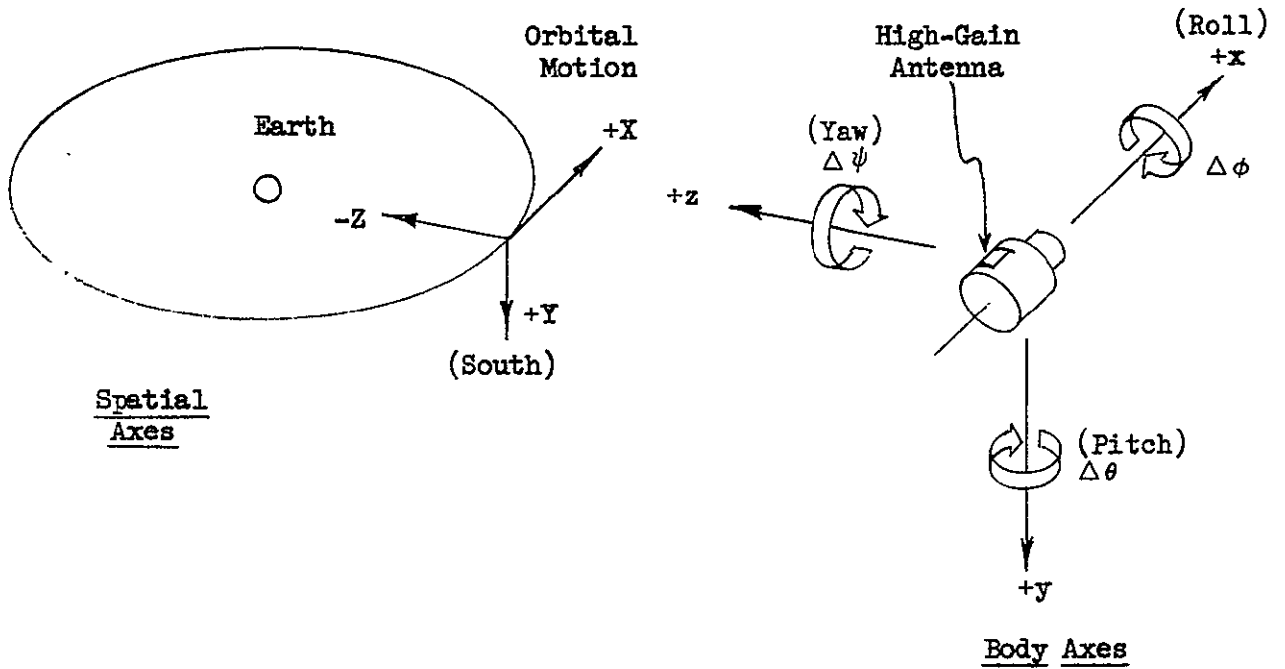
FIGURE 3-6.   AXES DEFINITIONS

For the expected condition 2 tracking accuracy (Table 3-1) the immediate recognition rendezvous category would be used, and the requirement for more than one (1/2 FOV) search extent in the pitch direction will not occur as long as acquisition takes place at $R_{X_o} \geq 600$ feet. This results from setting $\Delta\theta = 7°$, and $\epsilon_z = 70$ feet. However, the 45° maximum view offset angle limitation requires $R_X \geq 720$ feet. Thus a 720 - 3,000 ft. initial acquisition point would allow immediate recognition with a yaw search and will be consistent with the geometrical constraints. The nominal point would be set as close to 3,000 feet as possible to minimize the yaw search and the viewing offset angle. The yaw search would be a continuous rotation of the RMU since recognition of ATS-V would be easily accomplished without pausing at a given view. Thus, with condition 2 tracking capability (Table 3-1), the acquisition process is extremely simple.

For condition 4 tracking accuracy (Table 3-1) the requirement for more than one (1/2 FOV) search extent in the pitch direction (no rotation about Y) will not occur as long as acquisition takes place at $R_X \geq 3600$ feet. This results from setting $\Delta\theta = 7°$, and $\epsilon_z = 450$ feet. However, to meet the 45° maximum view offset angle limit, with $\epsilon_y = 4200$ feet R_X must be 4200 feet minimum. Since at this range immediate recognition of the target is not possible (unresolved TV image case), the yaw search cannot be a continuous yaw rotation of the RMU. The technique selected to allow recognition of the target (as opposed to a star) is described in Subsection 3.2.4; it necessitates that the yaw attitude of the RMU be held constant for each FOV to allow examination of the image; thus the yaw search must be conducted in incremental steps of one FOV each.

A plot of the required yaw search pattern for $\epsilon_y = 4200$ feet is given in Figure 3-7; as shown 4 to 5 FOV's would assure detection. The proposed acquisition search pattern consists of viewing integral FOV patterns which are angularly positioned to be contiguous with a, say, 1° overlap to eliminate holes due to attitude uncertainties.

Figure 3-8 shows such a set of patterns, with the projection of the error ellipsoid in the viewing plane sketched for two values of R_X. To make an assessment of the time allocations for each FOV segment, consider the cumulative normal distribution function, F_N, for locating the ATS-V target within a given search angle, $2\Delta\psi$:

$$F_N(\Delta\psi) = \frac{1}{\sqrt{2\pi}} \int_{-\infty}^{\Delta\psi/\sigma} \exp\left(-\frac{\tau^2}{2}\right) d\tau$$

where:

$$\sigma = 1/3 \arctan\left(\frac{\epsilon_Y}{R_X}\right)$$

and, for this analysis, ϵ_Y is taken at its 3σ value of 4200 feet.
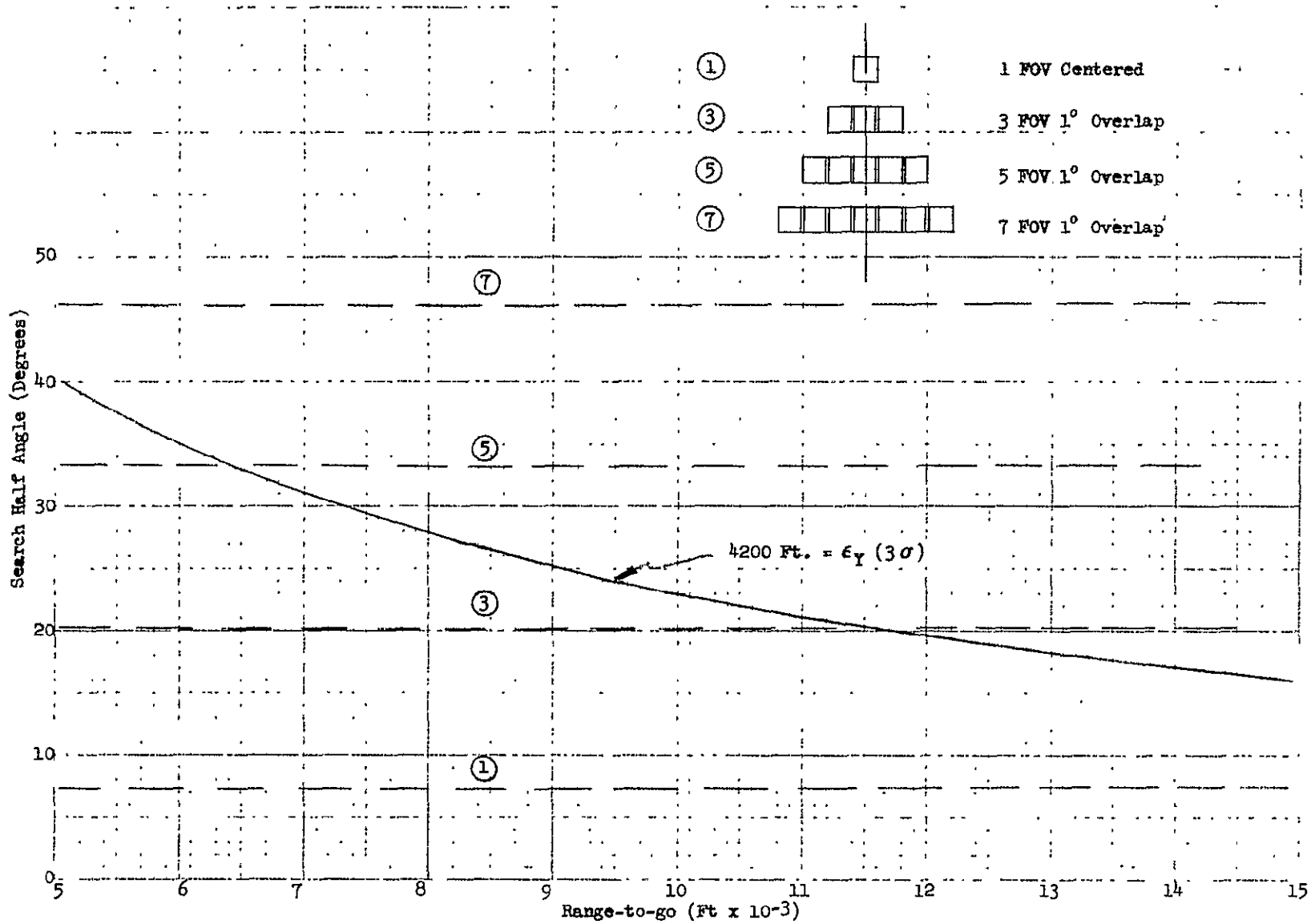
Figure 3-7 Yaw Search Angle Requirements

Space Division
North American Rockwell

14°

7°

Y

+Z (Toward Earth)

1 - FOV Pattern

-3σ - Error Ellipse

Y

20°

+Z (Toward Earth)

3 - FOV Pattern
R_x = 12,000 Ft.

-3σ - Error Ellipse

Y

33°

+Z (Toward Earth)
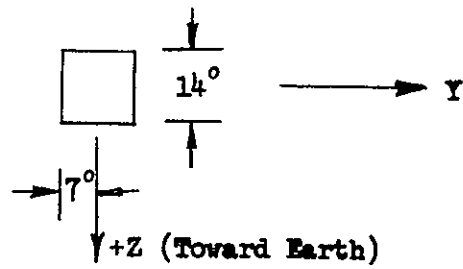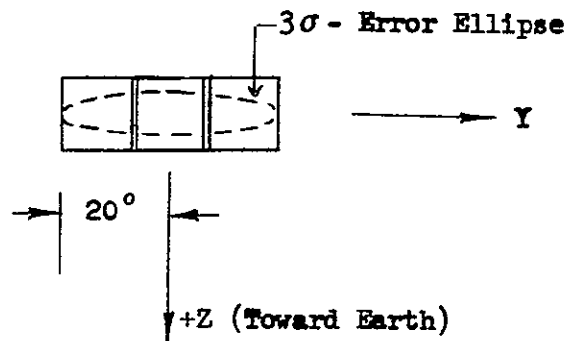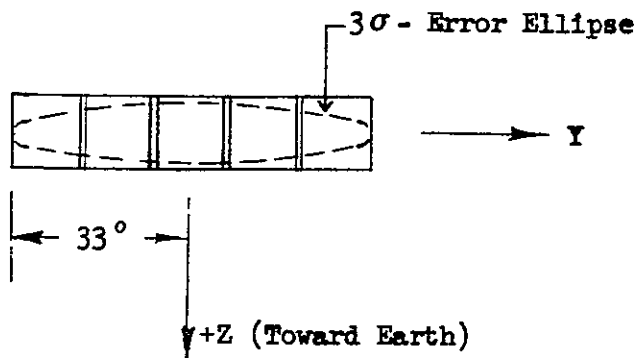
5 - FOV Pattern
R_x = 6,600 Ft.

FIGURE 3-8. TV - ACQUISITION SEARCH - PATTERNS
VIEWED TOWARD TARGET

Thus, the probability of target location in the center FOV as a function of R_X is then:

$$P_1 = F_N (7^O) - F_N (7^O) .$$

Similarly, the probability of target location in either of the two adjacent FOV's, excluding the 1^O overlap is:

$$(P_3 - P_1) = \left[F_N (20^O) - F_N (-20^O) \right] - P_1 .$$

Analogously, the probability of target location in either of the outer two FOV's in the 5 FOV pattern is:

$$(P_5 - P_3) = \left[F_N (33^O) - F_N (-33^O) \right] - P_3 .$$

A plot of these probabilities of location vs. R_X is given in Figure 3-9.

The viewing frequency of a given FOV for an extended search pattern can thus be tied to Figure 3-9 while the pattern extent required is given in Figure 3-7, both as a function of range-to-go.

Roll error (about X-axis) is limited by the high gain antenna beam width to approximately 6°, and, therefore, causes negligible distortion of the search pattern and has negligible affect on the search effectiveness.

3.2.4 Target Validation

The detection of the presence of an unresolved image on the TV display does not guarantee that the target detected is the ATS-V rather than a star image. Although the presence of a large star (visual Mag. (-3) or larger) is not possible within the search area projected on the celestial sphere in August, a sufficient number of lesser magnitude stars are visible in the viewing area to make a false image detection possible, though unlikely.

While a detailed visible star map superimposed on the display would be an aid in establishing whether or not a given image may be a star image, it would not unambiguously establish the converse condition. However, a simple and quick procedure can be pursued to validate an unresolved image. Consider a translational maneuver of the RMU along the Y-axis. This maneuver consists nominally of:

1. A ΔV increment of 1.0 ft/sec in the above described direction.

2. A two-minute (120 sec) translation period (per FOV to be examined).

3. An opposing ΔV increment of 1.0 ft/sec.

- 87 -
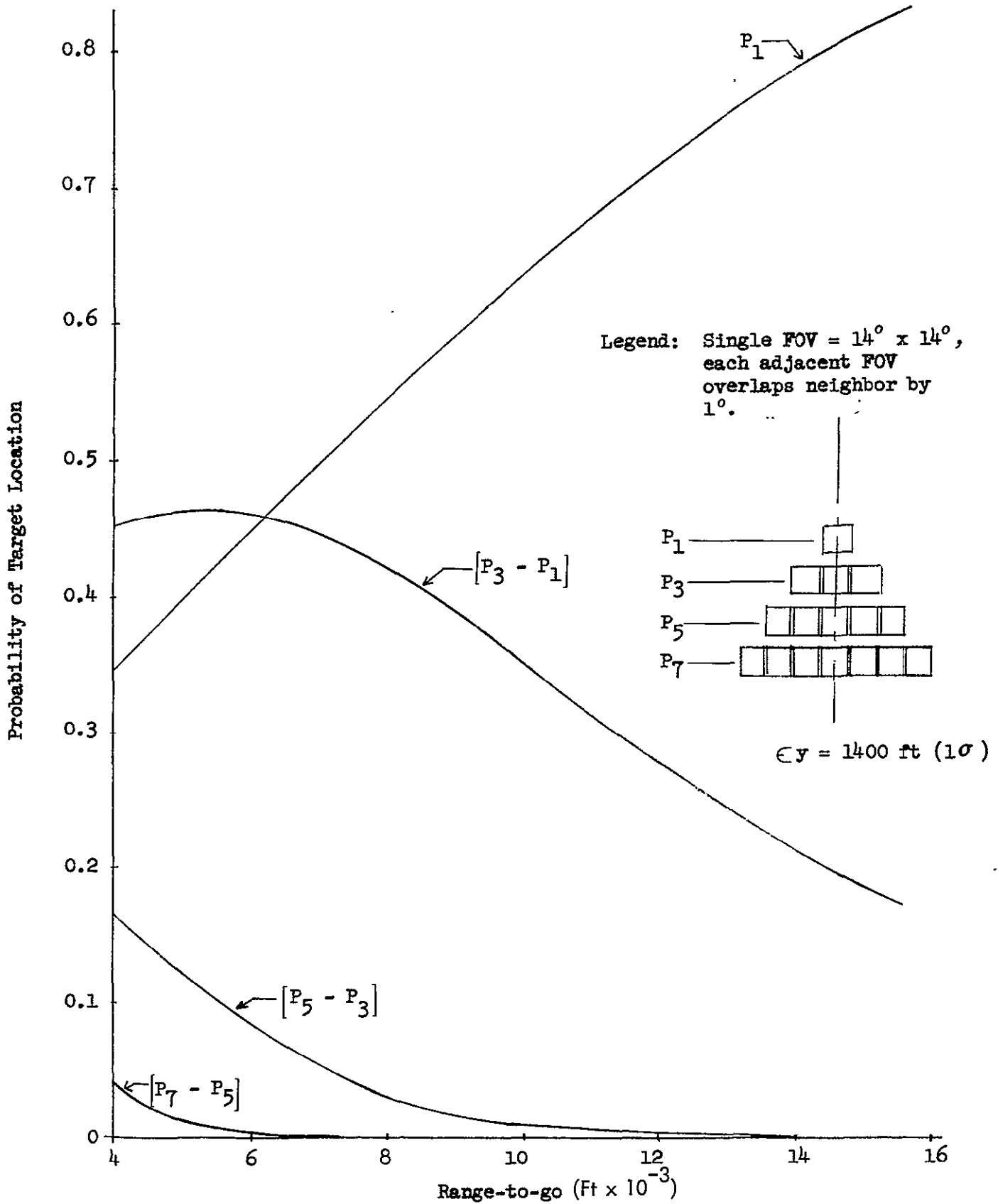
FIGURE 3-9.   PROBABILITY OF TARGET LOCATION IN VARIOUS FOV SEGMENTS

The result is a translation of the RMU along its Y-axis for 120 ft. for each FOV of interest. Even at a rendezvous range of 12,000 ft., this corresponds to 10 mr in angle or the equivalent of approximately 22 lines on the 14^0 FOV TV display. This is the displacement the ATS-V image would experience while any star image would remain fixed. The validation maneuver direction would be chosen to reduce the target out-of-plane error in the process of validation.

In the time interval during which the 1.0 ft/sec ΔV buildup takes place (approximately 6.5 sec), an image shift on the display may be caused by an RMU rotation developed from any force unbalance between the two jets actuated for this ΔV. The impact of this can be assessed as follows.

For any disturbance torque, the spacecraft will (because of the effective rate feedback of the DPG's) achieve an angular rate approximated by

$$\omega = \frac{B}{H^2} \, T_\epsilon$$

where ω = RMU angular rate, rad/sec

   B = DPG damping factor, 0.06 lb ft/sec

   H = DPG angular momentum, (one axis) 1.2 slug ft^2/sec

   T_ϵ = Disturbance torque, ft-lb

With a 54 inch distance between the two RCS thrusters, each operating at 1.2 lb of thrust, assuming an average error of 4.5% in thrust level, the disturbance torque (T_ϵ) is 0.23 ft-lb. Thus, ω = 0.0096 radians per second; over the 6.5 sec thrusting period this amounts to a total attitude shift of 3.5 degrees (3 sigma).

This rotation of the display axes when thrusting normal to the LOS for target validation takes place during the initial few seconds of the validation maneuver. Thus, the image displacement on the display due to this unbalanced force couple is readily discernible as such by the operator. Following the initial transient, the operator marks the TV location of the observed target. No confusion with image motion due to the RMU displacement over the succeeding two-minute period results. This display geometry for the validation procedure is shown in Figure 3-10.

If the observed target is proven to be a star (false alarm) the search mode is then reinitiated with an other FOV position until validation is accomplished and ATS-V closure initiated. The lateral (Y) motion of the RMU is not stopped until the validation has occurred.
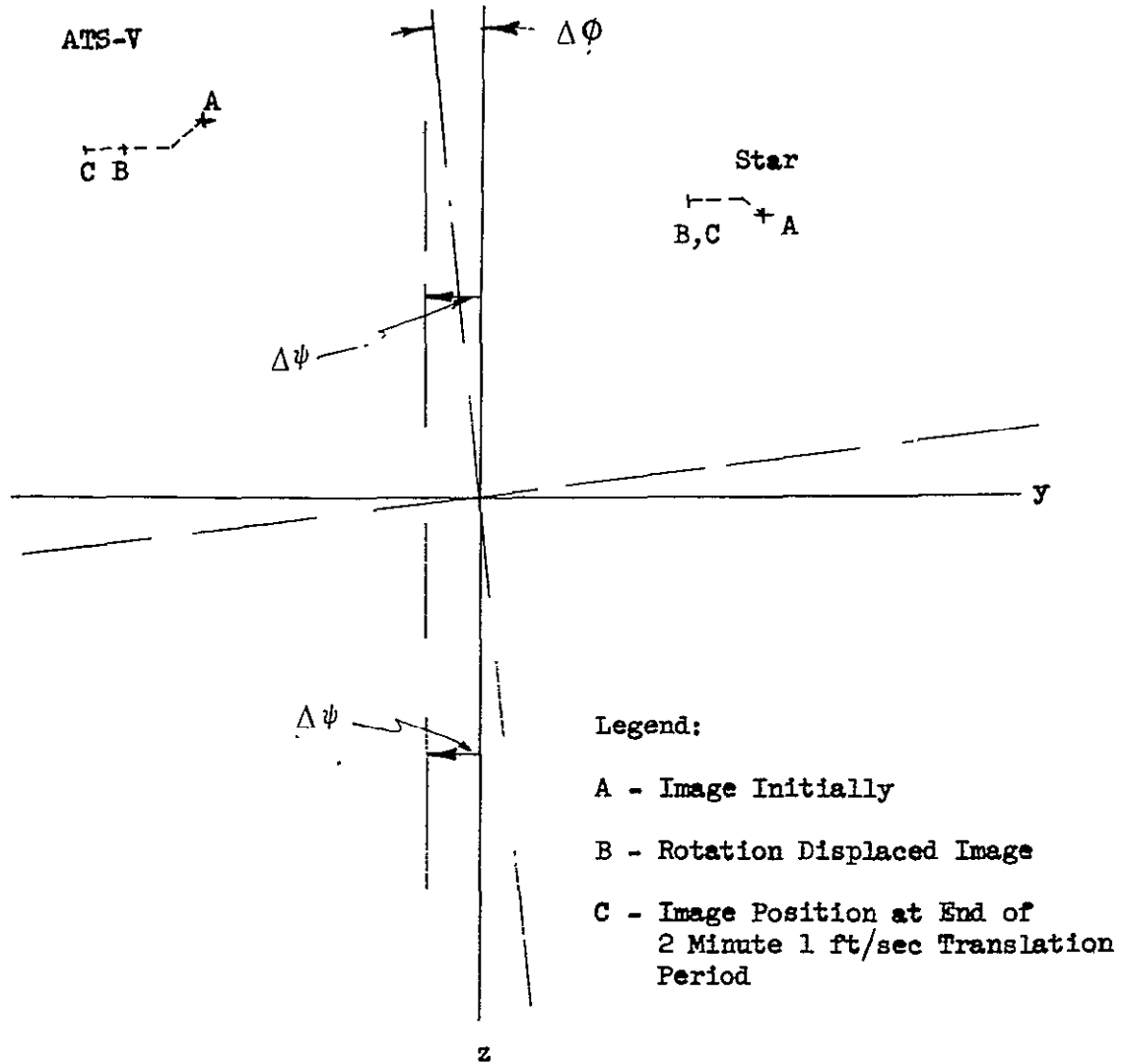
FIGURE 3-10. TV TARGET VALIDATION DISPLAY GEOMETRY

Legend:

A - Image Initially

B - Rotation Displaced Image

C - Image Position at End of
    2 Minute 1 ft/sec Translation
    Period

3.2.5 Relative Velocity at Acquisition

The only restriction on relative velocity at acquisition is that the RMU must not drift out of acceptable geometry relationships relative to ATS-V during the despin, search and acquisition process. This process at a 12,000 foot nominal will take approximately 15 minutes and a 1 fps relative velocity would consume 900 feet which should not invalidate geometry constraints. Similarly for a 3,000 foot R_X, the acquisition process should be completed within 5 minutes or less and a 1 fps relative velocity would consume no more than 300 feet which, again, should not affect proper geometry.

A 1 fps relative velocity is not difficult to achieve since ground tracking velocity determination accuracies of better than 0.1 fps are expected (see Section 2.0) and ΔV corrections of 0.1 fps and smaller are possible.

3.2.6 ATS-V Closure

The closing approach to the target is time-constrained to take place within, say, three hours. This restriction is mild enough to permit maximum closing rates as low as, say, four ft/sec without danger of exceeding or even approaching this time limit. Although the stopping distance of the RMU is trivial even for much higher maximum closing rates than 4 ft/sec, this value is used to minimize the propellant mass required for rendezvous.

Closing direction is controlled basically as a proportional navigation approach. The closing thrust is applied in the vehicle x-direction after the RMU attitude is oriented so that the x-direction is toward the target. The geometry in one plane is shown in Figure 3-11. Following the x thrust, RMU attitude is reoriented to spatial references X, Y, Z, using solar sensors so that minute y and z thrust pulses can cause the target blip to drift slowly toward TV center.

A further simplification in the closing procedure can be made for the case where the validated target offset from the X direction is small. Then the validation maneuver ΔV of 1 ft/sec can be continued to bring the image to the display origin without consuming much additional time and thus eliminate the requirement for RMU angular reorientation maneuver prior to closing thrusting.

During the closing maneuver, the range-to-go, $|R|$, made available to the operator, is obtainable from two independent sources. First, it exists as the extrapolated position from the last ground system indicated range-to-go updated by the open loop integrated ΔV applied. Second, it exists from stadiametric measurement based on image size of the resolved target.

The 3σ error in the first range-to-go estimate can be described as a function of $|R|$ by expressing the open loop estimating error (ϵ_o) as

VIEWED FROM NORTH
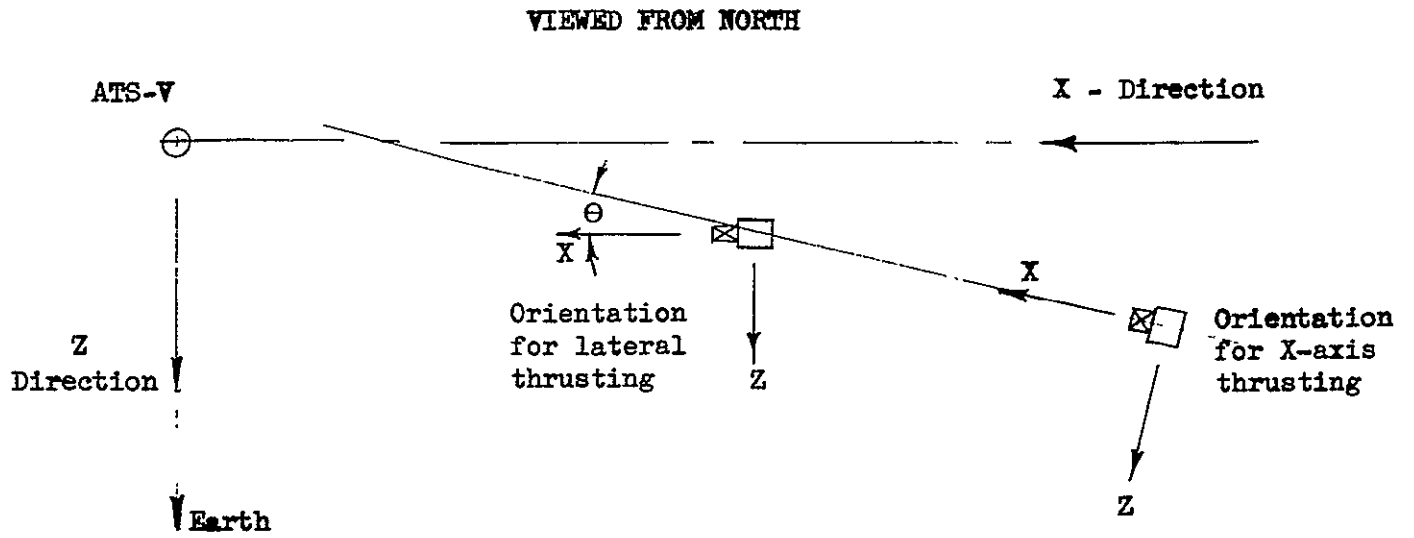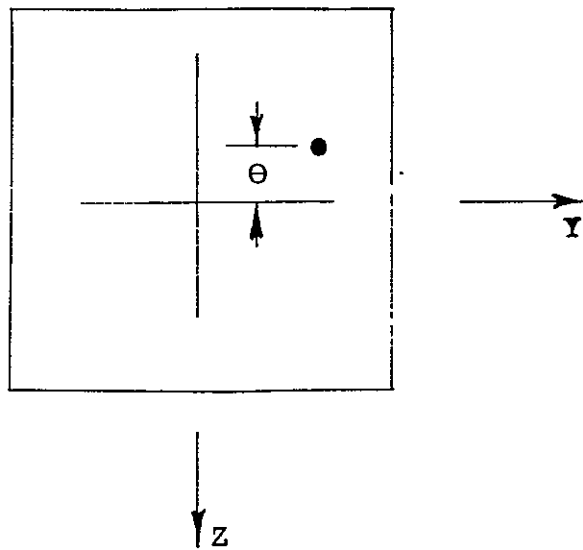
FIGURE 3-11   RENDEZVOUS CLOSURE GEOMETRY (Z-DIRECTION)

$$\epsilon_o = \left\{ (\epsilon_x)^2 + \left(\frac{\epsilon_{\Delta V}}{\Delta}\right)^2 \left[R_{x_o} - |R| \right]^2 \right\}^{1/2}$$

where the term

$$\frac{\epsilon_{\Delta V}}{\Delta V} = \text{error in applied closing } \Delta V.$$

Assuming this error as 4%, taking R_{x_o} as 12,000 feet and ϵ_x as 250 feet (from Table 3-1)

$$\epsilon_o = \left\{ 250^2 + (.04)^2 \left[12000 - |R| \right]^2 \right\}^{1/2} \quad (1)$$

. An estimate of the 3σ error in the stadiametric estimate of $|R|$ is composed of two independent contributors: the uncertainty of the true stadiametric size with respect to the indicated size due to illumination effects, and the operator error in determining the image size.

With a 10% error (3σ) assigned to the image size uncertainty and a 2 TV line error assigned to the second contributor (using a 525 line TV system with a 14% FOV), the resulting 3σ stadiametric ranging error is described by

$$\epsilon_{TV} = \left\{ (0.1 R)^2 + \left(\frac{R^2}{6450}\right)^2 \right\}^{1/2} \quad (2)$$

A plot of equations (1) and (2) is given in Figure 3-12. As shown, the open loop estimate of range-to-go is far preferable to the stadiametric estimate until $|R| < 2000$ ft. After that point, however, the stadiametric indication of range becomes accurate very rapidly. For this reason, the closing velocity is reduced to 1.5 ft/sec at $|R| = 2000$ ft. to give the operator ample time in gauging the increasing image size.

Similarly, analyzing error magnitudes in range rate, generated from the same two sources (i.e., open loop addition of ΔV's to initial tracking data, and stadia measurements) a comparison can be shown as in Figure 3-13. As expected, since open loop rate determination (compared with range) eliminates an integration, and stadiametric rate determination requires an additional differentiation, the former technique is much preferred, as suggested by the cross-over in the neighborhood of 350 feet.
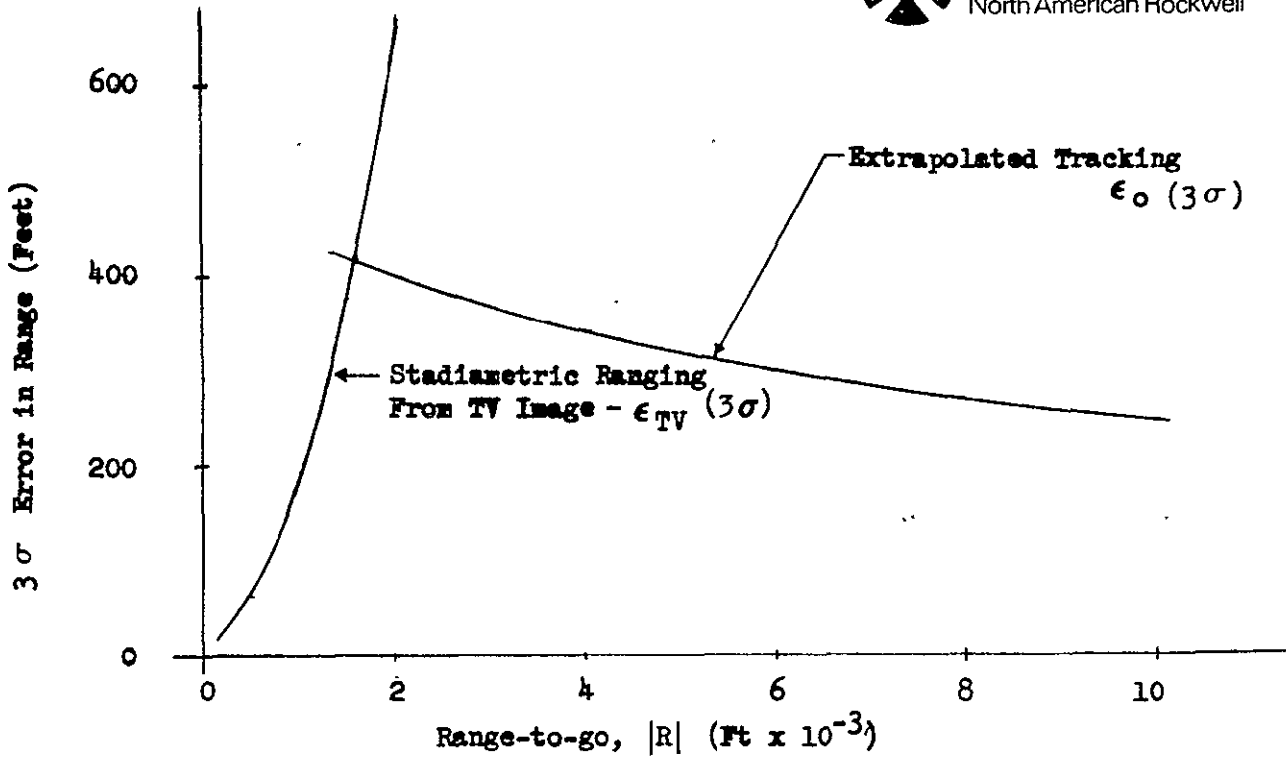
FIGURE 3-12   ANTICIPATED RANGE ERROR
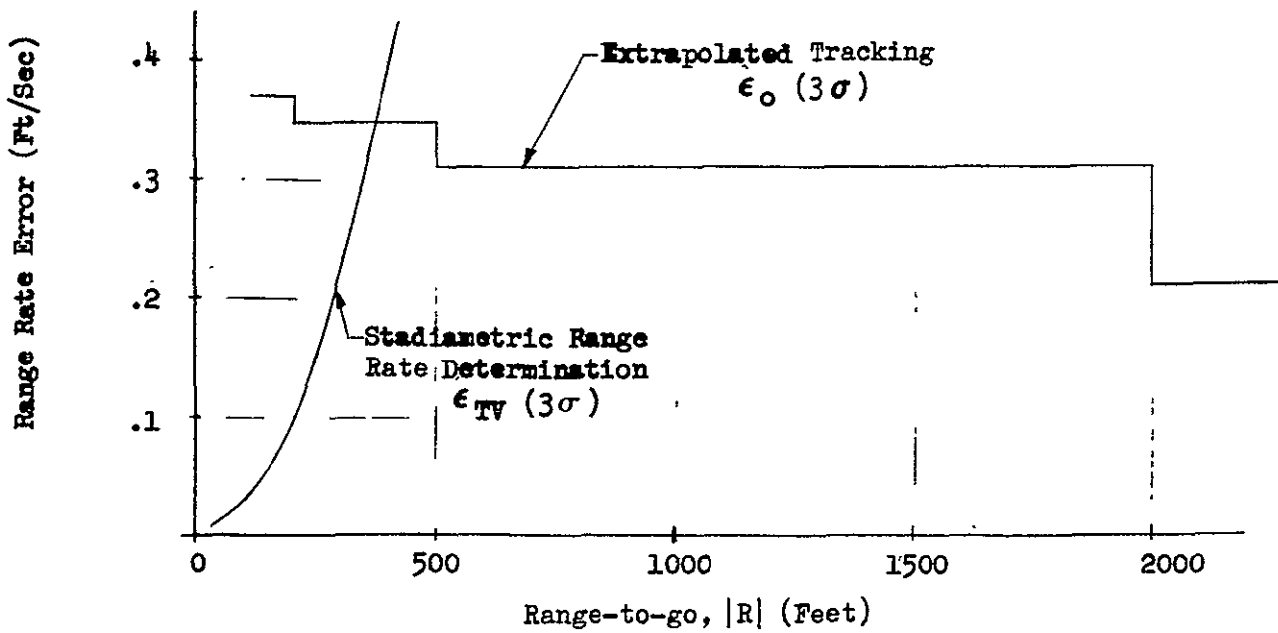
FIGURE 3-13   ANTICIPATED RANGE RATE ERROR

3.3 NOMINAL RENDEZVOUS SEQUENCE

On the basis of the requirements and technique consideration discussed in the preceding, a rendezvous sequence has been selected as described in the following. The RMU body coordinates (x, y, z) and the spatial coordinates (X, Y, Z) referred to in this discussion are defined in Figure 3-6.

3.3.1 RMU Despin and Orientation

The RMU at the start of rendezvous is in a stable spin about its body x-axis (spatial Y axis) with its TV camera pointing northward; it is located a nominal distance behind the ATS-V in its orbital path, and is closing at approximately one foot per second. The time is close to 6 p.m. orbital sun time for optimum lighting conditions. Initial operations will consist of the following:

1. By employing roll reaction jets, the RMU spin is nearly stopped. During the final phases of the spin, RMU body roll (body x-axis) attitude rate is noted by sun sensor signals, so that the stopping process can be controlled.

2. The DPG's are turned on just prior to total despin to establish an attitude reference base in pitch and yaw (body y and z axes); the roll DPG will now automatically stop roll rate and will command the reaction jets as needed in the process.

3. With the DPG's holding the yaw and pitch attitude constant, the roll DPG will be commanded to produce a roll rate as needed to attain lock-on on the high-gain C-band antenna of the RMU. Roll attitude will be optimized on the basis of monitored signal strength received by the ground station.

4. The TV camera aligned with the 14° FOV lens is turned on and its operation is checked out.

5. By commanding the yaw DPG (z body axis) a 90° turn is made about the spatial Z axis. This rotates the RMU x body axis into alignment with the spatial X-axis (pointing approximately toward ATS-V). At this point the x, y, and z RMU body axes are nominally coincident with the X, Y, and Z spatial axes. This RMU attitude is verified on the basis of combined data from the solar aspect sensors in yaw and pitch (z and y body axes), the TV camera signal ground reception in roll and pitch (x and y body axes) and by POLANG measurements in yaw (z body axis). Since the DPG command input level is 1°/sec, this rotation will require approximately 1-1/2 minutes.

3.3.2 Search, Acquisition and Validation

As previously discussed, two alternates can be considered: (a) where ground tracking accuracies can support an initial rendezvous range of less than 3000 feet (condition 2 of Table 3-1) thus assuring that the TV image of ATS-V will be large enough for immediate recognition once acquired, and (b) where condition 4 type tracking accuracies (Table 3-1) will only be adequate for attaining an unresolved point image of ATS-V upon acquisition. These two cases are discussed below.

1. With an initial range of 3000 feet or less, at the worst case, a brief yaw search may be necessary to acquire ATS-V. Once acquired, validation will be immediate due to the distinct size of the image relative to stars. The search will consist of a continuous yaw rotation at 1.0°/second until the ATS-V image appears in the camera FOV.

2. With initial ranges much in excess of 3000 feet validation of the target image will probably not be possible without observing each potential target image as to drift in the FOV in the presence of a lateral RMU velocity (along the y body axis). Thus, the search maneuver will start with application of a 1.0 ft/second ΔV to the RMU along the y body axis. Next, the TV monitor will be observed for approximately 2 minutes to note whether a drifting object is or is not present in the FOV. If such object is not found in the first FOV, a yaw rotation of 13° will be commanded via the DPG at 1.0°/second and the next FOV will be observed in the same manner. This process will be repeated until an object can be validated as the ATS-V by noting its drift in the FOV. When this occurs the search, acquisition and validation operations will have been concluded.

3.3.3 Closure to ATS-V

Once the target has been acquired and validated, the pilot will command suitable attitude rotations to align the target's image with the crosshairs of the TV camera lens; this will align the RMU body x-axis along the line-of-sight (LOS) to the ATS-V. Next he will command a ΔV toward the ATS-V; the magnitude of this ΔV will be adjusted based on tracking data (regarding initial closing velocity provided by the drift orbit approach trajectory) to provide a total closing velocity of 4.0 feet/second. Lateral ΔV's will now be applied along the z and y body axes as needed to keep the image of the ATS-V aligned with the crosshairs; this will eliminate relative velocities normal to the LOS thus assuring a proper rendezvous trajectory. During this period a constant pitch rate will be commanded from the ground to compensate for the inertial rotation of the LOS (15°/hour) due to orbit mechanics. This will necessitate occasional trimming of the lateral relative velocity observed by the pilot along the body z-axis. When the range is reduced to 2000 feet, as determined by updating of initial tracking data

per ΔV commands, the closing velocity will be reduced to 1.5 feet/second; this will allow time for accurate assessment of stadia for range determination during the final stages of the approach. Finally, when the range is reduced to 300 feet, the relative velocity will be gradually reduced to zero at a range of 250 feet. Typical range and range-rate profiles for an approach from an initial range of 12,000 feet are shown on Figure 3-14. As shown, the 3 hour time allocated to the rendezvous maneuver for power and thermal design purposes, is conservative even with an initial range of 12,000 feet.

3.3.4 Approach to Aft-End of ATS-V

At a range of 250 feet the RMU x, y, and z body coordinates are carefully aligned with the spatial X, Y, and Z coordinates. Next, as illustrated on Figure 3-15, 1.0 ft/second ΔV's are imparted along the +x and -y body axes resulting in a total relative velocity of 1.4 feet/second along the diagonal. The RMU is now rotated by command about the Z spatial axis to maintain the target at TV center. Because of the alignment, a command to only the z-axis (yaw) DPG is required. The translation is controlled such that the line-of-sight rotation does not exceed the attitude rate command input level of 1°/sec. When the range becomes about 180 feet, y and x (body axes) thrust increments are added to stop the Y spatial velocity, as shown in Figure 3-15. The translation continues in the X spatial direction until the x body axis becomes approximately aligned with the Y spatial direction. Translation is then halted with a ΔV applied along the +y body axis. Any number of alternate rotational techniques could be followed, as long as the overall translational and rotational objectives are met and uninterrupted TV coverage is provided.

3.4 DELTA-V REQUIREMENTS

The total propellant requirement for the rendezvous phase was conservatively estimated at 1.8 lb. This was based on an impulse requirement of 180 lb-sec for despinning the RMU and on a ΔV requirement of 10 ft/sec for the translational maneuvers. The latter was based on the approach profile shown in Figure 3-14 which assumed a need for search and validation maneuvers as well as an initial range of 12,000 feet.

3.5 CONCLUSIONS AND RECOMMENDATIONS

The ATS-V rendezvous can readily be accomplished with straightforward control techniques. Tracking accuracy, attitude control stability, illuminated target reflection, and search coverage are all significantly greater than required. The entire rendezvous can easily be accomplished under two hours, with a fuel utilization under two pounds.

Time History Legend

1 - 12 min., 3-FOV Search, Sequence
2 - 3 min., Validation and Closing Orientation
3 - 41 min., Closing at 4 fps to R=2000 ft
4 - 41 min., Final Closing
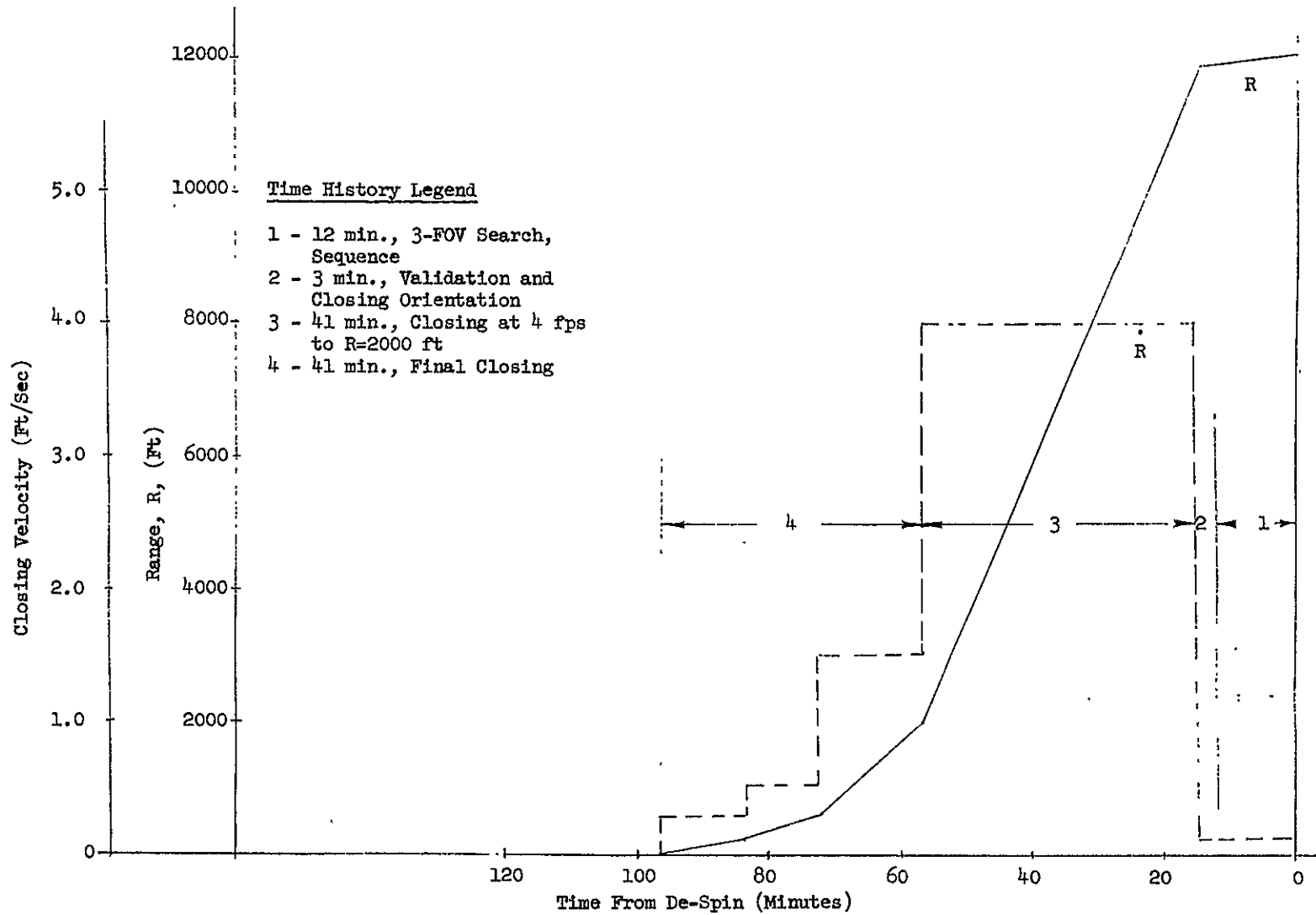
FIGURE 3-14.   NOMINAL CLOSING VELOCITY AND RANGE TIME HISTORIES

Space Division
North American Rockwell

North

ATS-V

X   250 ft

+x

RMU

-y

V=1.4
ft/sec

150 ft

179 ft

-y

V=1 ft/sec

Viewed From Earth

Space Division
North American Rockwell
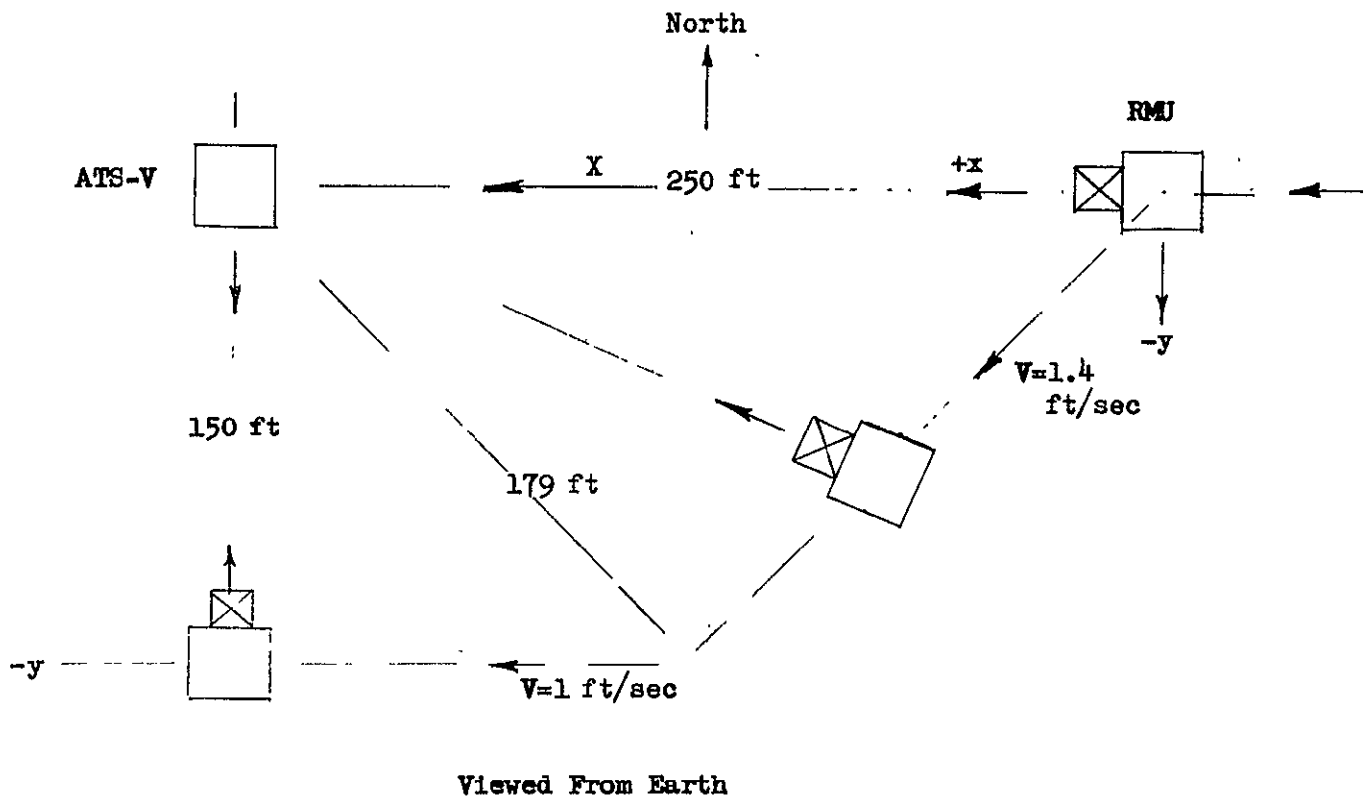
FIGURE 3-15   FINAL RMU RENDEZVOUS ROTATION

4.0 PRECONTACT DOCKING

THE RMU CAN BE BROUGHT SAFELY INTO DOCKING CONTACT WITH THE ATS-V BY A CAREFUL PROCEDURE OF REMOTE CONTROL, AIDED BY SELECTIVE DISPLAY INFORMATION AND CONTROL INPUTS.

4.1 REQUIREMENTS

The precontact docking phase for the baseline docking approach begins with the RMU below (South of) the ATS-V at a distance of approximately 150 feet with the ATS-V in TV view; it ends when the RMU docking mechanism contacts the ATS-V docking interface. The precontact docking phase includes those operations just prior to docking which must be performed to support the baseline docking approach. This approach involves rigidly attaching to ATS-V without damaging it and providing for complete disengagement when despin is complete. The general requirement is (a) to align the RMU axis closely to the ATS-V spin axis to avoid excessive impact and gyroscopic forces during docking, (b) to synchronize the spin speed of the docking device with that of the ATS-V to preclude damage due to relative motion at contact, (c) to close fast enough to minimize lateral drift during final closure, and (d) to close slowly enough to avoid excessive impact forces and rebound at contact while the RMU docking mechanism is actuated. To support this general requirement requires the generation of sufficient information to permit the pilot to command the docking operation from the ground. This, in turn, requires video, illumination, and other spacecraft status sensors. The design values for alignment ' and closure tolerances are based on a combination of physical clearance considerations, . pilot proficiency, and docking forces and operations for various initial contact conditions and docking device mechanizations. Selected values shown below are based on the results of the extensive pilot in the loop simulation (See Appendices B & C0 and a comprehensive digital docking dynamics analyses (See Appendix D); also, most of the material in this section has been contrasted for these studies.

Synchronization Accuracy - 0.1% of ATS-V spin rate (approximately 0.001 revolutions/second). This value was selected because it prevents collision with "black boxes" on ATS-V by keeping relative angular motion within clearance limits during the final docking closure. Also, the required rate feedback system can be easily mechanized.

Closure Velocity - 0.200 fps is set as a nominal requirement based on pilot performance and because docking loads are not severe at this value.

Lateral Velocity - 0.02 fps is set as a design limit based on pilot performance and because docking loads are not severe at this value.

PRECEDING PAGE BLANK NOT FILMED

Angular Misalignment - $\pm 3°$ (combined pitch and yaw) is selected as a latch angular misalignment tolerance design criterion to accommodate pilot error and $1.6°$ (conservative) ATS-V wobble.

Lateral Misalignment - ± 2 inches (combined Y and Z miss) is selected as a latch lateral misalignment tolerance design criteria to accommodate pilot error and 0.46 inches offset caused by $1.6°$ (conservative) ATS-V wobble.

To avoid draining available battery power and equipment overheating prior to mission completion, the docking operation must be accomplished in a relatively short duration. Although not critical, a period of one hour should not be exceeded for this operation.

4.2 TECHNICAL APPROACHES/CONSIDERATIONS

Key requirements associated with this mission phase center around the video cue, maneuvering precision, and spacecraft attitude and spin speed determination. Various elements involved in setting and meeting the requirements are discussed below:

4.2.1 Docking Mechanism Characteristics

Early consideration was given to various docking schemes in an attempt to minimize the precision requirements of the docking maneuver. As discussed in Sections 5.0 and 7.0, the approach which provided the best compromise between operational suitability, low development risk, and reasonable maneuvering precision is the baseline three latch concept. This concept is compatible with the alignment and synchronization requirements listed previously.

4.2.2 Video Cue

Because ATS-V is spinning relative to the RMU, the TV image could be either stationary or spinning, depending upon camera mounting and optical processing. A despun image enables a good view of the relative latch/docking ring orientation while the spinning image provides a better feel for control necessary to provide translational alignment. Again, both spun and despun images appear desirable for best ground crew performance.

In the baseline concept, the camera does not spin, and a spinning image of ATS-V is transmitted to ground and presented to the pilot. The co-pilot is presented a despun image of ATS-V which is generated optically on the ground. This approach was selected over use of a spinning TV camera on the RMU or use of derotation optics on the RMU to avoid unnecessary rf, mechanical, and image presentation complexities.

4.2.3 Spin Speed Synchronization

As previously indicated, the RMU docking latches must be synchronized with the ATS-V spin rate and properly phased to avoid the two Cannon plugs and "black boxes" which are adjacent to the ATS-V thrust flange (the ATS-V docking interface). Good speed synchronization can be achieved based solely on video cue by nulling observed motion between the latches and two Cannon plugs. Phasing is somewhat more difficult because the two Cannon plugs are symmetrically located and the unsymmetrically located "black boxes" cannot be seen. Thus, some data in addition to video cue would be desirable for this operation. Use of ATS-V sun sensor data coupled with magnetic pick-off data on the RMU docking cage spin rate and angular position was considered and appears suitable to assist in the manual synchronization and phasing operation. This approach as indicated later might be mechanized to provide both automatic synchronization and phasing; a co-pilot override would permit final adjustments for any bias or other errors detected from the video cue.

4.2.4 Illumination

Since the sun will be above a plane normal to the ATS-V spin axis, some special technique must be provided for lighting the docking ring area inside the ATS-V shroud. Both sun reflection techniques and lamp techniques have been considered. Because of the simplification of light control and the availability of ample power, the installation of lamps appears to provide the simplest solution.

4.2.5 Attitude Determination/Control

Relative attitude information for the two vehicles is available from sun sensors, polarization angle measurement (POLANG), and visual observations along the wobbling edge of the ATS-V. POLANG provides angular information about the Earth to ATS (or RMU) line of sight. The sun sensor provides angular information except about the sun to ATS-V (or RMU) line of sight. Both of these measurements, as noted in Section 2.0, can be considered to be accurate to approximately 1/2 degree. The POLANG measurement requires some smoothing to assure accuracy of absolute attitude data.

The piloted simulation has indicated that pilots can utilize light wedge reflections on the ATS-V aft ring along with ATS-V edge observations to align the vehicles closely. This will be the basic alignment technique (see Appendix C). Also, because of the ready availability of the POLANG and sun sensor derived measures of relative RMU/ATS-V attitude, this information will be provided to the crew as a check on the alignment achieved visually.

Also relative to attitude displays, good insight into change in vehicle attitude can be obtained by monitoring and integrating the time history of the gimbal angles of the DPG's. This alternately could be used to monitor angular alignment after an original alignment has been accomplished. Additionally, the gimbal angle provides a valuable indication of any impending attitude change caused by DPG saturation and resulting RCS action.

Another design consideration is the magnitude of the basic commanded angular rate. This magnitude is, of course, a matter of pilot opinion and a magnitude of one degree per second appears (in the simulation – Appendix C) to represent a good value.

4.2.6 Lateral Displacement Control

Because of the very slow translation movement required, adequate control of translational rates is difficult. To aid in this control, the commanded velocity increments can be integrated and presented to the pilot. The error in open loop estimation of actual velocity increments can be significant (say, greater than 10% for small impulses). Nevertheless, the simulation indicated that such a display can be of significant help in controlling translation since it can be zeroed at the crew's discretion. Another aspect of translation control is the selection of a minimum impulse bit, enabling the crew to make very small adjustments to observed translational velocity. This also becomes a matter of pilot opinion although a value in the neighborhood .035 to .05 lbs.-sec. of impulse per jet (corresponding to .054 and .077 inches per second) appears to be satisfactory. (Reference Simulation Report, Appendix C.)

4.2.7 Range Determination

Various means have been considered to determine ATS-V/RMU range, including high frequency radar tracking, multiple camera stereo techniques, and the angular extent of known geometrical sizes stadiametrics). Because of simplicity and adequacy, the use of stadia lines marked on the TV monitor appears to be the best solution.

4.2.8 Crew Assignment

Since the crew will be operating at a ground base, the usual reason for limiting their number disappears and the primary consideration is the tradeoff between task simplification and the necessary coordination and interfacing among multiple crew members. During the simulation, two crew members, a pilot and co-pilot, were the maximum employed at the control console, largely because of the control console arrangement. They were assisted by other personnel involved in tuning the simulation equipment and monitoring the video system. After a small amount of training, the pilot/co-pilot arrangement appeared to be quite satisfactory, although specific human factors studies, if pursued in greater depth, might indicate an increased crew complement at the console to be an improvement. For instance, a Flight Status Engineer at the console may improve the operation by relieving the pilot and co-pilot of some monitoring tasks. A Visual Systems Engineer will also be required to monitor operation of the video system.

4.3 NOMINAL DOCKING IMPLEMENTATION

4.3.1 TV Configuration

The baseline configuration has been evolved to consist of two TV cameras, one 64 degree field-of-view centerline mounted camera (used primarily for docking) and an off centerline 14 degree field-of-view camera (for rendezvous operations). The TV image is presented both directly (spinning image) and as projected through a dove prism which is rotated to remove the spin; i.e., a despun image. As indicated previously, the spinning image is best used for primary lateral translation control while the despun image can be used for spin synchronization and latch orientation. Illumination is provided by redundant cold-cathode tubes immersed in a doughnut-shaped ring, to provide light near the periphery of the ATS-V docking ring.

4.3.2 Spin Synchronization

Manual spin synchronization was used in the pilot simulation (Appendix C) by visually comparing (on an oscilloscope presentation) pulses from the simulated ATS-V sun sensor and the RMU spin cage magnetic pulses. The RMU spin rate was then manually adjusted to synchronize the pulses. This method proved satisfactory for meeting the selected design synchronization criterion and could be used in the actual mission.

Automatic spin synchronization might also be provided as functionally depicted in Figure 4-1.though the system shown has not been mechanized. This block diagram shows the manner in which basic angular rate commands are transmitted to the RMU cage spin speed control loop. Pulses from the ATS-V sun sensor and the RMU spin cage magnetic pulser are compared in relative phase (counter circuit) to generate a rate command signal such that the desired phasing is maintained. A nominal adjustment is furnished for the crew to provide vernier corrections to the relationship based upon despun image observation.

4.3.3 Attitude Control

As previously indicated, relative attitude meters are provided to the crew driven from differential sun sensor and POLANG information.

4.3.4 Translation Control

To enhance translation control, translation rate meters are provided for each of the three axes to display velocity as the integral of commanded delta-V impulses. These meters can be reset to zero individually whenever the rate is observed to be zero. A range meter can also be provided by integrating the velocity in the along-axis direction. This meter also can be set to any observed value at any time by the crew, and the pilot simulation indicated this double-integration meter was an aid even though accurate to only 10%.
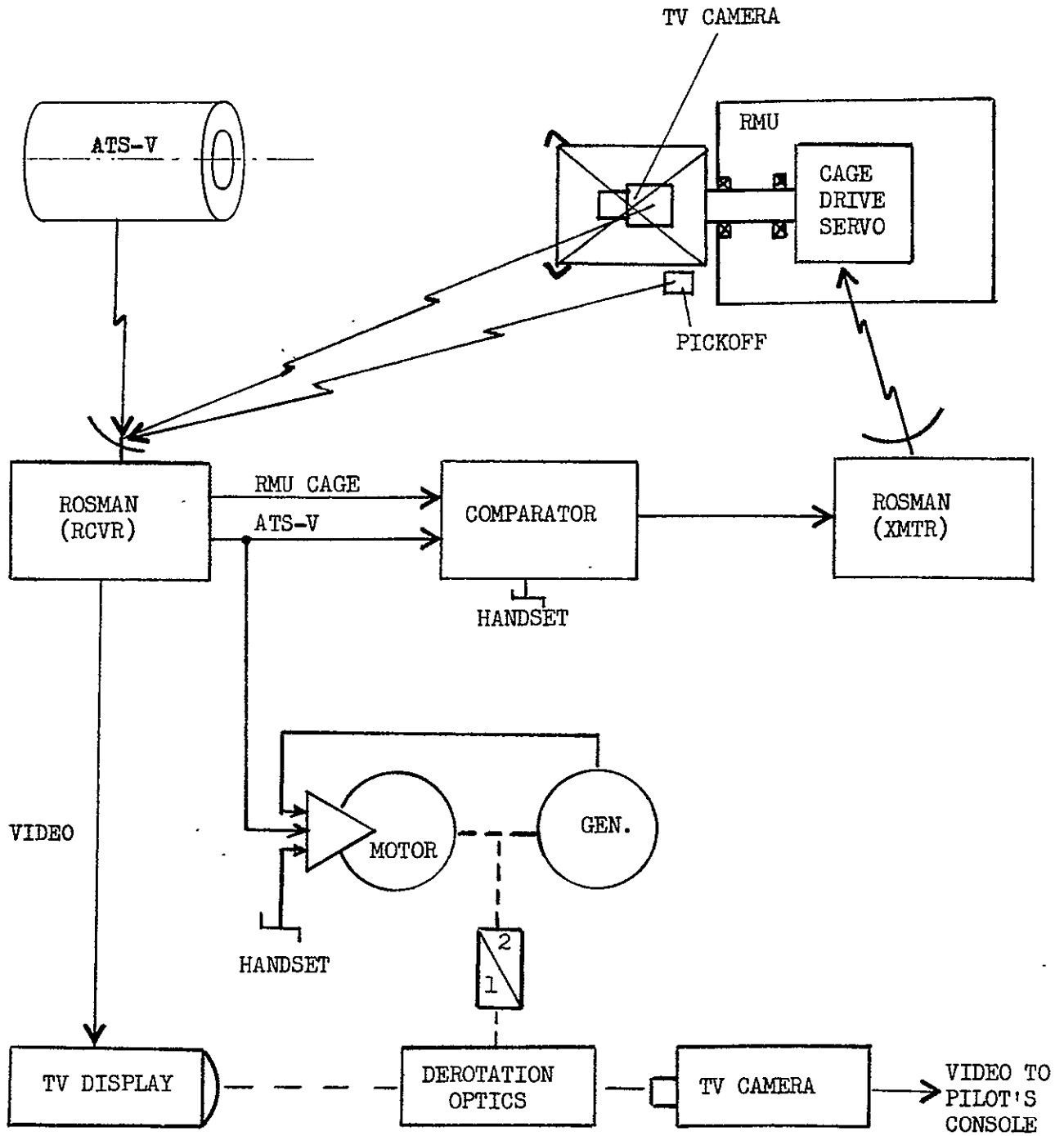
FIGURE 4-1   SPIN SYNCHRONIZATION

4.3.5 Nominal Precontact Docking Sequence

The nominal sequential maneuvers, performed within approximately 1 hour, are as follows as excerpted from the Simulation Report (Appendix C):

1. Between 200 and 100 ft. of range establish zero DPG gimbal angles (status engineer task).

2. Decelerate closing velocity with 5 seconds X command at 100 to 50 ft. range as indicated by satellite size with respect to stadia on the TV monitor (pilot's task).

3. Gross align with the docking end of the ATS at a stadia range of 10 ft. and null translational rates (2 sec. -X command) to visual zero. Turn on RMU lights (pilot's task).

4. Activate rate meters and minimum impulse translation command switch (pilot's task).

5. Translate to sun lighted edge of the ATS at .1 fps and null translation rates with rate meters (pilot's task).

6. Align front and rear edges of the ATS with the monitor crosshair until the front and rear edges appear to oscillate (due to ATS off axis spin) an equal distance either side of the crosshair (see Figure 4-2). Each attitude correction must be followed by a translation back to align crosshairs with the ATS edges (pilot's task).

7. Rotate the RMU docking system such that the pilot can see the ATS center hub while the crosshairs are aligned on the ATS edge (co-pilot's task).

8. Correct any attitude error in the other axis by observing where the RMU light reflection is with respect to the crosshairs. Command rotation to fly the crosshair to the light reflection such that the crosshair is centered on the reflection. Each attitude correction must be followed by a translation back to align crosshairs with the ATS edge and one ray of the crosshair with the ATS center hub. Verify attitude alignment with backup pitch/yaw meter (pilot's task).

9. Null translation rates and reset rate meters (pilot's task).

SPIN AXIS
OF ATS-V

AFT EDGE OF ATS-V

ATS-V

FRONT EDGE OF ATS-V

BORE-SIGHT OF RMU'S TV
CAMERA WHEN RMU'S X-AXIS
IS PARALLEL TO SPIN AXIS
OF ATS-V

VIEW ON TV
MONITOR

CROSS-HAIRS

RMU

'AFT EDGE
OF ATS-V

FRONT EDGE
OF ATS-V
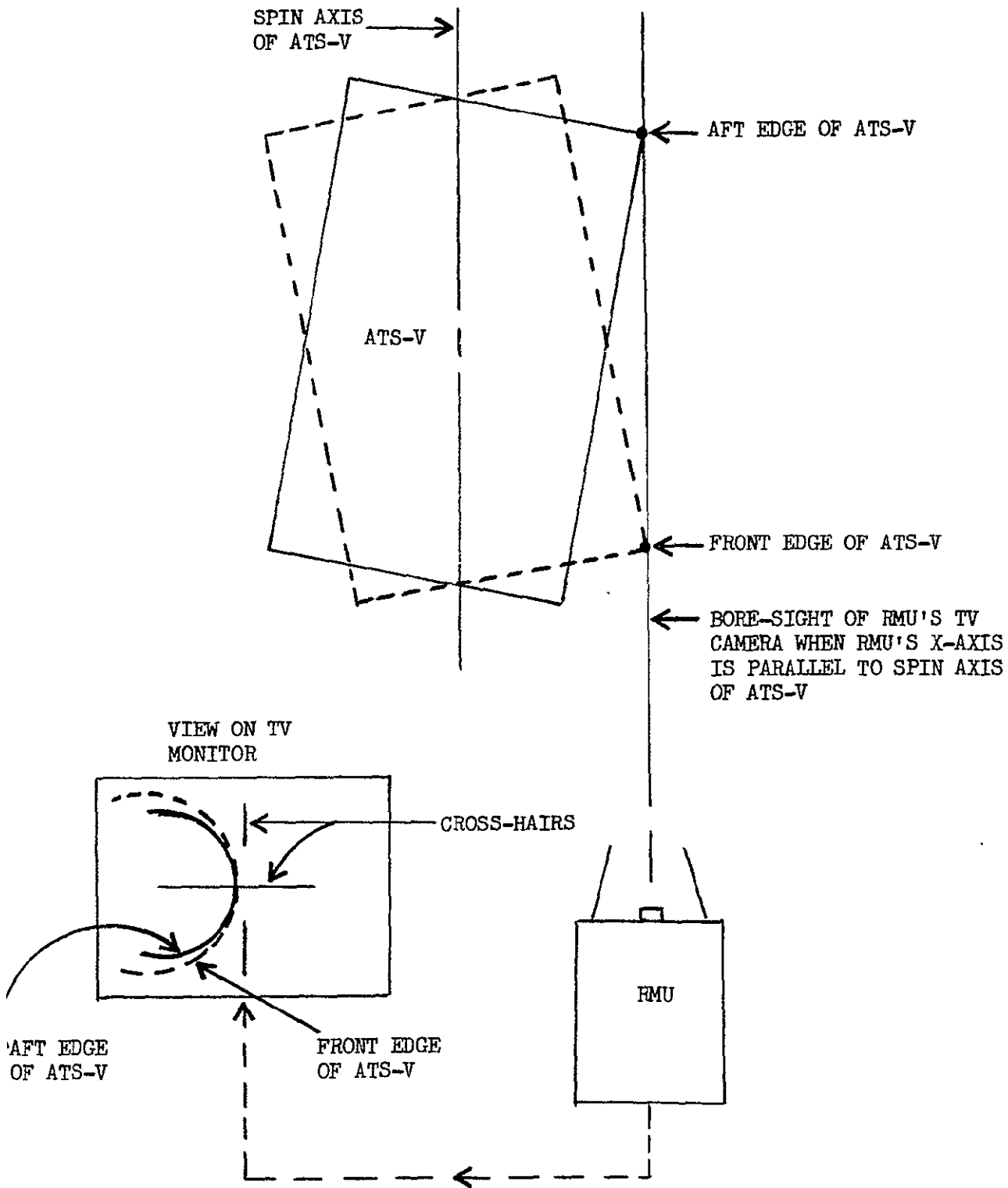
FIGURE 4-2   ALIGNMENT OF RMU X-AXIS

10. Translate to ATS edge 90° from first alignment and null translation rates with rate meters (pilot's task).

11. Check attitude alignment and make corrections as in steps 6, 7 and 8 as required (pilot's task, co-pilot's task).

12. Null translation rates and reset rate meters (pilot's task).

13. Translate to center RMU crosshairs on center hub of ATS at .1 fps and null translation rates with rate meters. Ask co-pilot for spinup when ready (pilot's task).

14. Switch on and fine vernier derotation optics to synchronize and de-rotate TV image on co-pilot's monitor (co-pilot's task).

15. Switch on and fine vernier cage spin motor to synchronize and index the docking system using the index scope to align the RMU roll angle discrete with the ATS roll angle discrete (co-pilot's task).

16. Check despun view for visual index with respect to the ATS Cannon plugs. On verification, ask pilot to complete docking (co-pilot's task).

17. Check DPG gimbal angle status and inform pilot if gimbal saturation in roll is imminent (status engineer's task).

18. If not, correct roll attitude error caused by docking system spinup (pilot's task).

19. If imminent, request roll gimbal desaturation and correct resulting roll attitude to zero (pilot's task).

20. Center crosshairs on ATS center hub. Null translation rates to visual zero. Reset rate meters (pilot's task).

21. Command + X translation to close to docking contact at .15 to .2 fps (pilot's task).

22. Maintain RMU crosshairs on ATS center hub through latching. Check against despun image on co-pilot's console by observing latch con-centricity and reduced ATS center hub traverse (pilot's task).

23. Latch indicator light "ON" indicates docking complete if ATS image remains fixed.

24. Start despin procedure (co-pilot's task).

- 109 -

The above procedures can be interrupted at anytime if the pilot decides to repeat the angular alignment process or if, on translation to dock, the lateral miss distance appears to be unsatisfactory.

The sequence of the piloting procedure is important in that attitude alignment is accomplished before docking system spinup. If the system is spun up first, the gyro-dynamics of the spinning mass would cross-couple vehicle attitudes in a direction $90°$ to rotational commands required during alignment.

4.3.6 Pilot Proficiency

The simulation report in Appendix C provides a detailed description of a nominal docking setup and gives statistical results of various pilot runs. As indicated, pilots were able to dock consistently with lateral miss distances less than 2 inches and angular misalignments less than $3°$ including the effects of $1.6°$ ATS-V wobble.

4.3.7 Docking Duration

Both the electrical power and thermal condition of the spacecraft are affected by the duration of the docking phase and the relative sun attitude. From the simulation runs, docking was completed in essentially all cases in less than 15 minutes though a 1 hour duration was used (conservatively) to size the power and thermal subsystems.

4.3.8 Fuel Requirements

The simulation runs described in Appendix C showed a maximum fuel utilization of 1.5 lbs. This included the requirement for basic translation and angular and lateral maneuvering.

4.4 CONCLUSIONS AND RECOMMENDATIONS

The required docking accuracies can be met after a reasonable training period by the average pilot. From analysis of the errors obtained in the simulation and the realization that additional improvements can be anticipated, docking control errors can confidently be expected to be kept safely within the allowable region. The duration of the docking phase was consistently under 15 minutes, thereby assuring essentially negligible power drain and equipment temperature rise during docking.

5.0 POST CONTACT DOCKING, DESPIN, SEPARATION AND OBSERVATION

THE RMU/ATS-V DOCKING MANEUVER CAN BE ACCOMPLISHED WITHOUT STRUCTURAL OR COMPONENT DAMAGE UTILIZING MECHANICAL LATCHING. THE ATS-V CAN BE DESPUN IN A PERIOD OF 6.5 MINUTES WITHOUT DESTABILIZING NUTATION BUILD UP. THE VEHICLES CAN THEN BE EASILY SEPARATED FOR THE OBSERVATION PHASE.

5.1 DOCKING, DESPIN, AND SEPARATION

5.1.1 Requirements

The requirements, alternatives, and selected approach are defined in the following subsection. The first requirement for this phase is that the latching mechanism be capable of forming a suitable attachment between the two vehicles with minimum structural loading during the latching operation. Also, the latch must have the capability of tolerating contact misalignments of at least 2 inches of lateral miss distance and at least 3° in angular misalignment (see Piloted Docking Simulation Study, Appendix C).

Next, the RMU must provide adequate control stability to compensate for the normally destabilizing effect of a dual spin vehicle configuration which possesses a transverse moment of inertia greater than its spin moment of inertia. The RMU must also provide a smooth decelerating torque to successfully reduce the ATS-V spin velocity to zero without undue vibrational excitation. Finally, the RMU system must be capable of separating completely from the ATS-V without colliding during the separation sequence.

5.1.2 Technical Approaches/Considerations

a. Latch Design

A number of techniques have been considered for latching the two vehicles together. These include exterior hooks with a central indexing cone, two-sided claws (or tongs), and pneumatically expanded devices; magnetic coupling was also investigated. Various ATS-V docking interfaces were also investigated including the apogee motor thrust flange and the inner and outer surfaces of the solar panels. All concepts were considered in light of overall system requirements to determine the optimum design approach. At this time, three equispaced "tongs" mounted on a rotatable truss structure constitute the baseline latching design concept, and the ATS-V apogee motor thrust flange is the selected docking interface. (See Section 7 for a further discussion of latching alternatives and the selected approach.)

b. Latch Closure

The three latches must all capture the ATS-V thrust flange quickly and positively before initial contact induced vehicle motions cause loss of acceptable latching geometry (latch miss). The technique selected to insure capture is to: (a) rotate the latches at a speed synchronized to ATS-V's spin rate, (b) limit closure velocities to about 0.2 fps to prevent excessive rebound at contact, and (c) automatically trigger all three latches simultaneously when suitable latching geometry is achieved. Following the capture operation, the two vehicles must be pulled together in a manner which will avoid excessive structural loads. Techniques for this drawdown include spring-driven and pneumatic-powered mechanisms. At this time pneumatic-powered drawdown is preferred because of weight considerations and operational advantages. These advantages include: (a) essentially a constant force is available throughout the drawdown process including the full drawdown position where full force is desirable to prevent chatter (this is contrasted with springs where force decays through the drawdown process to a minimum at the full drawdown position), (b) damping is readily provided by flow metering, and (c) simple, sure recycling is accomplished by venting and spring-powered recocking (with light springs).

A digital analysis of the forces involved in the latching process was performed during the study. Results are presented in Appendix D and indicate that the following design values should be used in latch design.

1. Tongs with 4 inches between inner and outer jaws
2. Preloaded to 200 lbs. each to hold RMU if flat spin occurs.
3. Spring constant of 500 lbs./ft. both lateral and axial.
4. Basic structural spring constant 50,000 lbs./ft.
5. Triggers located 2.01 inches inside tongs.

c. Energy Dissipation and Stability

Stability problems were encountered in the ATS-V launch because of the high level of heat pipe energy dissipation. When coupled with ATS-V's particularly unfavorable inertia ratio following apogee motor burn it caused rapidly divergent nutation and ultimate tumbling into a flat spin. Accordingly, some technique for providing offsetting energy dissipation in the unspun vehicle (RMU) must be provided to assure overall stability. Sources of such stabilizing energy dissipation include reaction jets (active nutation control), and various passive nutation dampers. For the baseline design concept, this stabilizing energy dissipation is

available from the Attitude Control System DPG's. The DPG's are passive and provide the required energy dissipation via their damping fluid. Although the reaction jets could be controlled to oppose vehicular rates (and this possibility provides a good back-up capability) the passive DPG's are preferred and provide much more than adequate energy dissipation capability as indicated below. Three basic factors influence the discussion of stability of energy-dissipating rotating bodies. These are:

1. Text books have related increase or decrease of nutation angle θ (stability) to energy dissipation rate $\dot{E}$. In effect, $\dot{E}$ is proportional to the product $\theta \ \dot{\theta}$ for a given flight condition defining spin angular velocity (ω_s) and inertia ratio $\sigma = \dfrac{I_S}{I_T}$

   where $\quad I_S$ = moment of inertia about spin axis, and

   $\qquad I_T$ = moment of inertia about transverse axis

   Energy dissipation in a spun section (with angular momentum conserved) is destabilizing, for σ less than one, and energy dissipation in the unspun section is stabilizing for all σ. This can be shown by considering, for a dual spinner, a momentum relationship

$$H^2 = (I_T \ \omega_T + \omega_S)^2 + (I_T + \omega_T)^2 \qquad (1)$$

and an energy relationship

$$E = 1/2 \ I_T \ \omega_T^2 + 1/2 \ I_S \ \omega_S^2 \qquad (2)$$

where $\quad H$ = total angular momentum

$\qquad \omega_T$ = transverse angular velocity

For energy dissipation in the unspun section (assuming a frictionless bearing between the two sections), ω_S stays constant, while external torques are applied to the unspun section to maintain it at zero spin so that from Equation (2),

$$\dot{E}_u = I_T \ \omega_T \ \dot{\omega}_T \qquad (3)$$

Since $\dot{E}_u < 0$ (dissipation), $\dot{\omega}_T < 0$ which represents stability.

For energy dissipation in the spun section, no external torques are applied because of the frictionless bearing. Accordingly, momentum is conserved, so that the derivative of Equation (1) can be set to zero and combined with Equation (2), eliminating ω_S. There results

$$\dot{E}_S = I_T \left(1 - \frac{I_T}{I_S}\right) \omega_T \dot{\omega}_T$$

or

$$\dot{E}_S = I_T \left(\frac{\sigma - 1}{\sigma}\right) \omega_T \dot{\omega}_T \tag{4}$$

By contrast, this expression indicates stability only when $(\sigma - 1) > 0$.

2. From observation of ATS-V telemetry data, the ATS-V nutation system appears to be linear; i.e., the nutation angle builds up (or decreases) exponentially, so that

$$\dot{\theta} = \frac{1}{\tau} \theta$$

also

$$\theta = \theta_o e^{t/\tau}$$

where τ = time constant

and t = time

3. Physical considerations suggest that for small angles the energy dissipation rate in a given vehicular configuration varies as θ^2. This is because the transverse angular velocity varies as θ, and hence the power might be expected to vary as θ^2.

The preceding three factors interrelate compatibility. This is, if

$$\dot{\theta} = \frac{1}{\tau} \theta \qquad \text{(point \#2)} \tag{5}$$

and also Equations (3) and (4) are of the form

$$\dot{E} \sim \omega_T \cdot \omega_T$$

and

$$\theta \approx \frac{I_T \omega_T}{I_S \omega_S} = \frac{\omega_T}{\sigma \omega_S}$$

- 114 -

so that, approximately,

$$\dot{E} \sim \sigma^2 \omega^2 \theta \dot{\theta}$$

or $\quad\quad \dot{\theta} \sim \dfrac{E}{\theta} \quad\quad$ (point #1) $\quad\quad\quad\quad$ (6)

Then

$$\frac{\dot{E}}{\theta} \sim \frac{1}{\tau} \; \theta$$

or

$$\dot{E} \sim \frac{1}{\tau} \; \theta^2 \quad\quad \text{(point #3)} \quad\quad\quad\quad (7)$$

Equations (3) and (4) provide the proportionality indicated in Equation (6), so that Equation (7) can be formulated in terms of the effective time constants for divergence (or convergence) as

$$\tau_s = -\frac{I_T \, \omega_s^2 \, \sigma \; (\sigma - 1)}{(\dot{E}/\theta^2)} \quad\quad\quad\quad (8)$$

$$\tau_u = -\frac{I_T \, \omega_s^2 \, \sigma^2}{(\dot{E}/\theta^2)} \quad\quad\quad\quad (9)$$

where

$\tau_S \quad =$ time constant for energy dissipation occurring in the spun section, and

$\tau_U \quad =$ time constant for energy dissipation occurring in the unspun section.

By comparison of the time constants for convergence and divergence associated with the energy dissipation sources (described in the above equations) for a dual spin configuration such as ATS-V + RMU, net stability requires that:

$$\left| \dot{E}_U \right| > \frac{I_S}{I_T - I_S} \; \left| \dot{E}_S \right| \quad\quad\quad\quad (10)$$

which for the case of the baseline RMU implies that for
stability the energy dissipation in the unspun section (RMU)
must exceed only .210 times the energy dissipation present
in the spun section (ATS-V heat pipes).

The relative magnitudes of heat pipe and DPG energy dis-
sipation observed or projected can now be examined. In
Figure 5-1 the power dissipation is plotted on log-log paper
against the nutation angle θ. ATS-V observation data is
shown, realizing that the quadratic form is valid primarily
for small angles of θ (say, less than 10°). For the ATS-V
after apogee boost case, the data from the portion of the
post flight report showing the effect of large nutation angles
is also shown to illustrate the reduction in projected power
at the larger angles (compared to the quadratic law).

The major uncertainty is the energy dissipation of the heat
pipes anticipated in the dual spin configuration (ATS-V
and RMU attached). One attempt at making such a pro-
jection has been made by applying the heat pipe model
established by Hughes to emperically match observed flight
and experimental data. This model shows the dependence
upon various fixed parameters of the system such as fluid
density, viscosity, geometrical constants, etc.; and upon
flight conditions such as spin frequency and nutational
frequency. This model with appropriate numerical constants
introduced reduces to

$$\frac{\dot{E}}{\theta^2} = 1.44 \times 10^{-6} \frac{\sigma^2 \omega_S^4}{1 - 0.219 (\omega_S)^{1/2}} \frac{\text{Watts}}{\text{Deg}^2} \qquad (11)$$

showing that energy dissipation increases with increasing spin
speed and increasing inertia ratio. For the dual spin con-
figuration (compared with the sensitive ATS-V post apogee boost
condition) both spin speed and inertia ratio are reduced so that
the anticipated energy dissipation as shown in Figure 5-1 is
extremely low (0.004 watts/deg^2).

Also shown in the figure is a computation of the equivalent
energy dissipation rate for the RMU DPG's. This rate is based
upon the DPG viscous resistance torque

$$T = b \dot{\alpha}$$

where b = DPG damping constant, 0.06 lb ft sec   (12)

$\dot{\alpha}$ = DPG gimbal angle rate in rad/sec

$$= \frac{h}{b} (\cos \alpha) \, \omega_b$$

h = DPG per axis momentum, 1.2 lb ft sec

ω_b = RMU body axis angular velocity in rad/sec

Since $\omega_b = \omega_n \, \theta$

where

ω_n = nutational frequency relative to inertial reference, 1.33 rad/sec for ATS-V/RMU combination,

the dissipation rate can be computed as a function of nutation angle θ as follows:

$$\dot{E} = \frac{1}{2} b \, (\alpha^2) \, max$$

$$\dot{E} = \frac{1}{2} b \, (\frac{h}{b})^2 \, \cos^2 \alpha \, \omega_n^2 \, \theta^2 \qquad (13)$$

Since two transverse axes are equally effected by the nutation, this equation must be doubled for total dissipation. Also, to present an effective comparison of stability margin, values must be divided by 0.210 (from Equation (10)). These adjusted values were then converted to watts and plotted on Figure 5-1. The curve shown includes the gimbal deflection (cos α) effect as well.

This stabilizing energy dissipation is well above any dissipation rate thus far observed and two orders of magnitude above that computed for the dual spin configuration on the basis of the Hughes model. As a matter of interest, the equivalent energy dissipation capability of the RMU reaction jets, if mechanized to oppose nutation rates, is also shown on the figure. Although two pairs of jets could be simultaneously employed per axis, only one pair is shown. The power capability would simply double for two pairs.

- 117 -
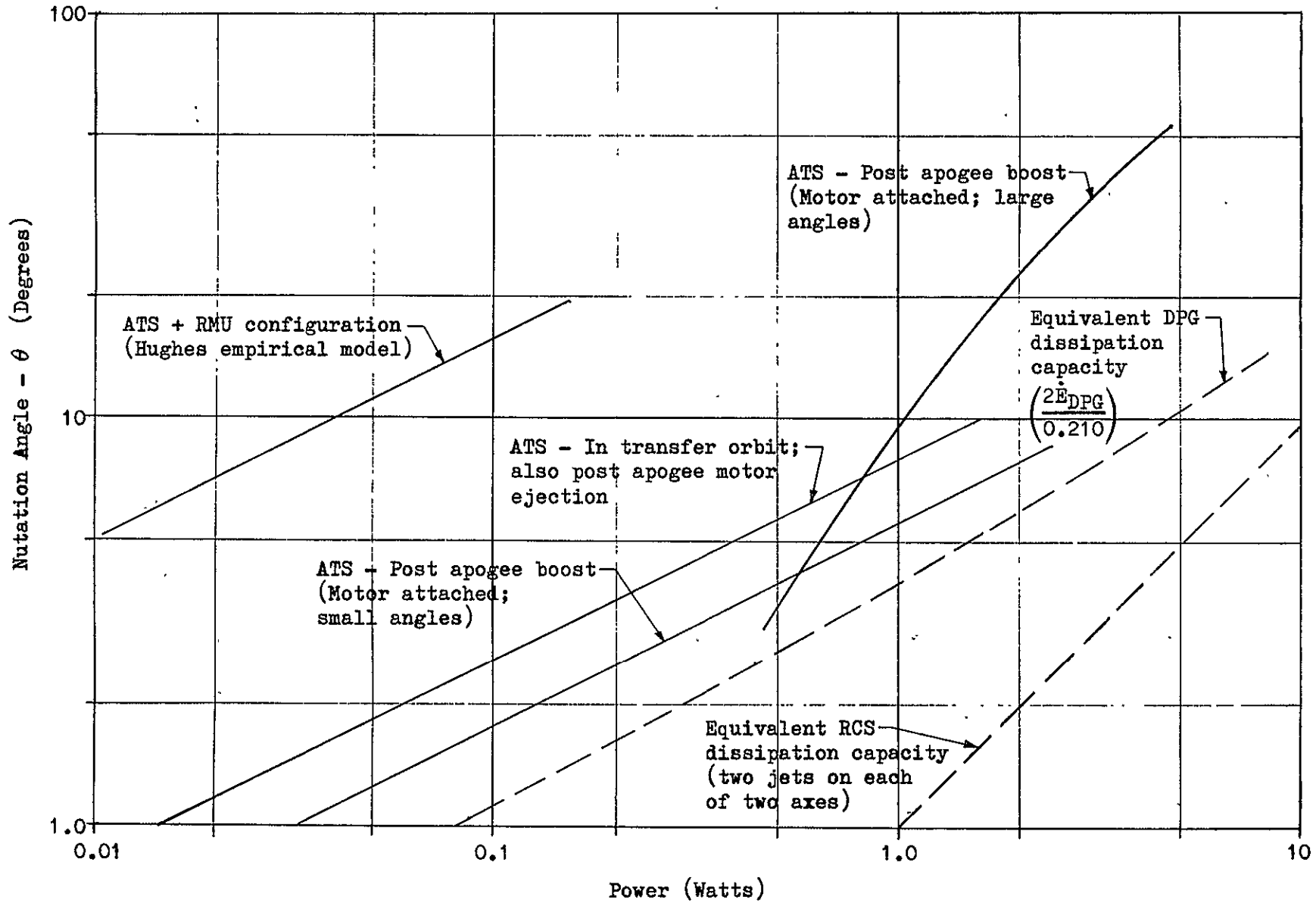
Figure 5-1 Energy Dissipation

From this analysis of the energy dissipation considerations, the RMU can be confidently expected to have ample capability to control the despin operation of the ATS-V. Additionally, the energy dissipation of the heat pipes will essentially be eliminated once the despin torque has been applied because the fluid in the circular pipes will be forced to one end (in effect, caged) and not have the opportunity to dissipate significant amounts of energy through sloshing.

A digital study was made to confirm the validity of the above assessment of energy dissipation requirements. The study used a mathematical model of the heat pipe energy dissipation phenomena, and constants were checked against ATS-V flight data. The results, presented in Appendix D, substantiate that DPG damping is ample to stabilize the dual spin bodies. The excellent agreement of the simulated dynamic model with both the ATS-V flight data and the analytically predicted ATS-V/RMU performance substantiates the model's validity for dual-spin (ATS-V/RMU) predictions. The close agreement of the simulation results with the flight data and with the analytically predicted values is also shown in Table 5-1. The table compares the values of the divergence time constants obtained from these sources.

d. Despin

Following the latching of the RMU spin cage to the ATS-V docking ring, spin deceleration can be provided by applying electrical torque to the spin cage motor. One possibility is to command the roll reaction jets full on and modulate the spin motor torque to maintain RMU attitude control, thus causing ATS-V spin deceleration. Alternately, a constant spin motor torque can be applied to the ATS-V and the RMU attitude control system (including reaction jets) can be used to control RMU roll attitude. Although either of these approaches is workable, the latter approach has been selected because it permits a lower spin motor torque level and minimizes control system complexity.

e. Vehicle Separation

Two concepts have been advanced for the separation maneuver. One is to very slowly and carefully release the latches, observe relative positions and velocities of the vehicles, and slowly maneuver the RMU away from inside the ATS-V shroud. Another possibility is to release the latches and place the RMU translational X-direction reaction jets full on to clear the ATS-V shroud before any lateral velocities have opportunity to cause physical interference. Either

Table 5-1. Comparison of Analytical, Simulated and Flight Data on Heat Pipes

| | Nutation Divergence Time Constant (Sec.) | | | | |
| | ATS-V | | | ATS-V and RMU | |
	In Transfer Orbit	Post Apogee Burn	Post Motor Ejection	Without DPG Control System	With DPG Control System
ATS-V FLIGHT DATA	120	11	-19 (Conv.)		
ANALYTICALLY PREDICTED (RMU/ATS-V)				5000	-24.5 (Conv.)
DYNAMIC MODEL SIMULATION	140	≈10	-20 (Conv.)	Several Thousand	-26 (Conv.)

approach should work because relative velocities will be small
in both cases since jet impingement forces are small and latches
can be designed to assure negligible tip-off at release. The
following shows how a "fast" exit would be achieved without
colliding.

The RMU must translate 22 in. in the X-direction without
experiencing pitch or yaw which would cause a 6 in. lateral shift
at the outboard end of the spin cage and result in collision between
the RMU and ATS-V. This is the equivalent of 5 1/2° of RMU pitch
or yaw. The RMU translational jets will provide this required separation
by a 3-second burn (approximately .5 ft/sec) and coast. Since the RMU
Attitude Control System will be operating, the DPG's will resist any
disturbance torque, and the moment producing reaction jets will be
energized should the transverse angular error exceed 2 1/4°. Accor-
dingly, the angular excursion of the RMU will also be small. The
impingement force from the jets on the ATS-V has been calculated to
be approximately 10% of the jet thrust, and is symmetrical. Thus,
ATS-V angular rates and excursion and clearance without collision
seems assured. Even in the absence of control, calculations indicate
that an assumed 3σ unbalance of reaction jet force (4% deviation each
jet) with the jets left on the entire time would cause less than half the
RMU angular allowance before the RMU cleared the shroud (4.9 sec).

Separation without collision is, then, readily provided. Also, ATS-V
attitude excursions should not be severe and rates should be low enough
that gravity gradient deployment is not impaired. ATS-V attitude
requirements should, however, be further assessed in the next phase to
verify that in its separated rate, the gravity gradient experiment can be
initiated.

5.1.3 Nominal Post Contact Docking, Despin and Separation Sequences

The following is the baseline sequence for this mission phase. Total time should
not exceed 15 minutes, though one hour has been used as a conservative design guide
in sizing power and thermal requirements.

a. Latching

When the latch "tongs" have extended over apogee motor mounting
flange of ATS-V to a sufficient depth to insure capture, they will
automatically be triggered to close simultaneously. Closure of the
tongs will occur in a damped manner to minimize impact loading;
the tongs will first close in the lateral direction to effect capture
and then pull the two spacecraft together in an axial rigidizing
action.

Once latching is accomplished, the coupled RMU/ATS-V system will constitute a "dual-spin" spacecraft. As indicated previously, nutational stability of the system will be assured by providing more damping energy dissipation within the pitch and yaw DPG's of the RMU than in the heat pipes of ATS-V. Active control is also available from the RMU's RCS system. The favorable ratio of energy dissipation will be further improved after ATS-V despin is initiated approximately 5 - 10 seconds after the docking clamps have closed (the despin torque exerted on ATS-V by the RMU despin-drive's torque motor will force the coolant fluid against one end of the heat pipes and essentially eliminate that source of damping). The latching process including subsequent damping of transient vehicle motions is expected to be completed within 3 to 4 seconds (see Appendix D).

b. Despin

When a stable spin mode for the coupled configuration has been reached as sensed by accelerometers or DPG gimbal angle data, the pilot will initiate despin by commanding a constant despin voltage on the torque motor. Despinning ATS-V will take approximately 7 minutes. During this period, roll stability of the RMU will be maintained by the roll DPG of the RMU which will automatically energize the RCS thrusters as needed for desaturation of its momentum wheels. The pilot will monitor the spin rate of ATS-V on the TV monitor and will reduce the despin torque as the rate approaches zero as required for stopping ATS-V in its desired orientation.

c. Separation

When ATS-V is despun, the RMU docking latches will be commanded to open, and a delta-V will be commanded to translate the RMU in the X-direction thus separating from ATS-V and concluding this phase of the mission. Lateral and rotational motions will be sufficiently small that collision between the two spacecraft is precluded.

5.1.4 Conclusions and Recommendations

An acceptable latching technique has been developed to provide suitable coupling of the two vehicles while not exceeding reasonable loads (see Appendix D). Stability of the dual-spin ATS-V/RMU combination is provided by the Attitude Control System DPG's, and control of the ATS-V spin speed down to zero angular velocity can be easily provided (see Appendix D). Separation of the two vehicles following the despin operation can be accomplished without danger of physical interference between them.

5.2 OBSERVATION PHASE

Having successfully despun the ATS-V vehicle and separated the RMU from its latched position, the RMU can be readily positioned for good camera coverage of the gravity and damper boom deployment and subsequent ATS-V operations.

5.2.1 Observation Phase Requirements

The observation phase is initiated when the RMU is detached from the ATS-V and begins to move away. For the baseline mission, this is the final phase which terminates when the ATS-V observation is no longer possible or required and the RMU is inserted into a non-interfering terminal orbit. The duration of this phase is defined by the period consumed by the ATS-V in reorienting and extending the gravity gradient booms. One hour of observation following separation is considered a minimum requirement. Additional equipment or equipment capability beyond that required for the despin mission is to be kept to a minimum for the observation phase.

5.2.2 Technique Considerations

In the development of the approach for this phase, several basic considerations affecting the technique employed have been examined and are briefly discussed here.

5.2.2.1 High-Gain Antenna Pointing Constraints

Since a high-quality TV picture must be transmitted to earth throughout this phase, the high-gain antenna must be continuously pointed to the earth. In the baseline RMU design, this constrains the RMU to move with its fixed TV axis pointing toward the ATS-V and the fixed antenna axis (normal to the TV viewing axis) pointing toward the earth. Section 7 discusses the possible addition of a steerable TV axis or steerable antenna axis to remove the constraint, but the selected baseline does not include these provisions. The constraint, in any event, is not a difficult one to accommodate for the observation phase.

5.2.2.2 Power

A possible time-limiting factor is the draining of the on-board batteries. The charge remaining on the batteries for this phase is a function of the time duration of the prior phases, the solar power generation during those phases, and the utilization of power by on-board equipment. Accordingly, vehicle attitude and electrical power utilization during the observation phase should be controlled to minimize battery drain.

5.2.2.3 Thermal Balance

The temperature rise or fall of the equipment on board the RMU is critically dependent upon relative sun attitude and power utilization. In general, the equipment cools when the sun is along the RMU spin axis and warms when the sun is in a plane normal to the spin axis. Accordingly, this mission phase must be planned with the consideration of limiting, or at least delaying, temperature extremes at the RMU subsystem equipment locations.

5.2.3 Nominal Trajectory

5.2.3.1 Trajectory

The RMU trajectory during this mode can be very simple. It consists simply of a small lateral translation as depicted in Figure 5-2 to move the ATS-V into a better sun angle for observation while maintaining the required attitude constraints as previously discussed to insure a good picture. Figure 5-2 diagrammatically views the trajectory as seen from the earth depicting the vehicle attitude orientation. The RMU is constrained to move such that the TV LOS is a spoke of a "wheel" with the earth/ATS-V line of sight as the "axle" and the ATS—V the "hub." Figure 5-3 similarly shows the required reorientation of the vehicle as the ATS-V orbits the earth. The solar aspect sensors and POLANG data support the attitude control efforts along with video cues. Since the nominal RMU attitude maneuver is a rotation about the high-gain antenna axis, commands to only one DPG are required, except for long-term orbital geometry shifts (Figure 5-3).

Because the gravity-gradient booms are of the order of 120 feet and a 64° field of view is available in the camera, a viewing position some 200 feet away from the ATS-V should provide full coverage. The operator will maneuver the vehicle using techniques previously discussed in the rendezvous phase for optimizing viewing aspects and range for best illumination, particular points of interest (e.g., close-up), etc.

Inasmuch as a velocity of one foot per second can be imparted to the RMU with an expenditure of approximately .075 pounds of fuel, negligible reaction fuel is required for conduct of anticipated observation trajectories. The allocated time of one hour for the observation phase is considered adequate to support desired observation requirements. However, a delayed observation period could require an RMU spin/despin cycle as discussed in Section 6.

5.2.4 Conclusions and Recommendations

A brief investigation of the observation phase reveals that the ATS-V vehicle can be observed from a very good vantage point during its boom deployment operations. The ground operator will be able to exercise considerable latitude with observation
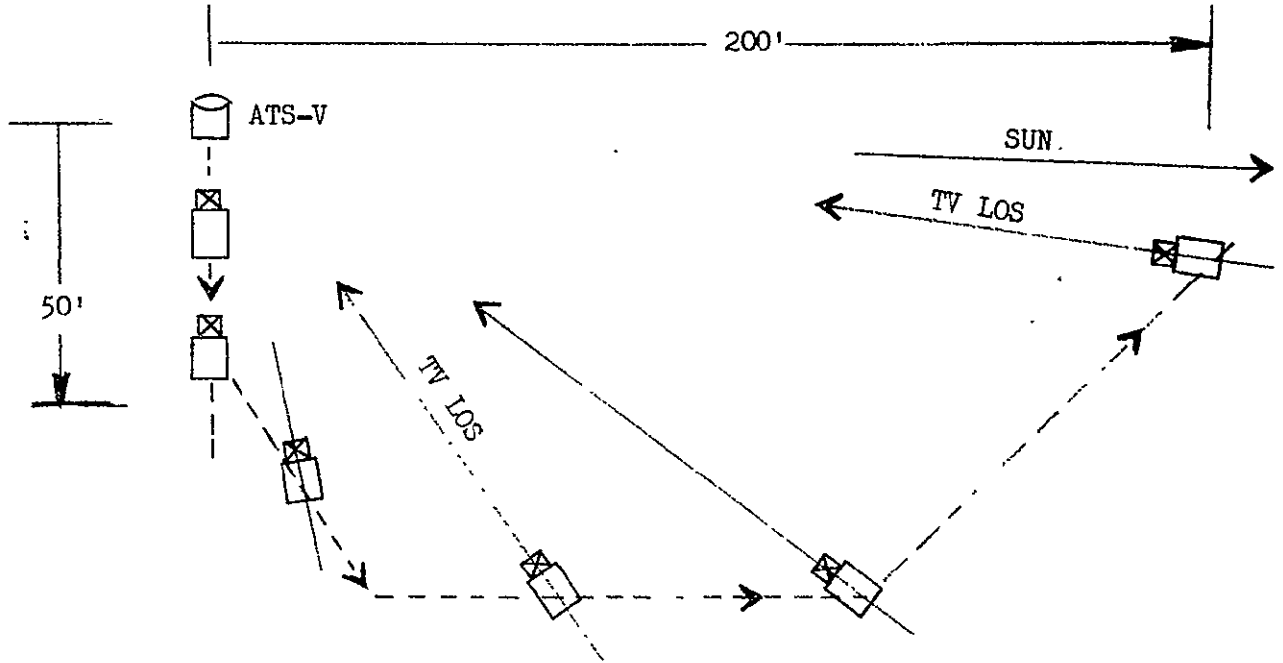
FIGURE 5-2

REPRESENTATIVE RMU OBSERVATION PHASE TRAJECTORY
VIEWED FROM EARTH
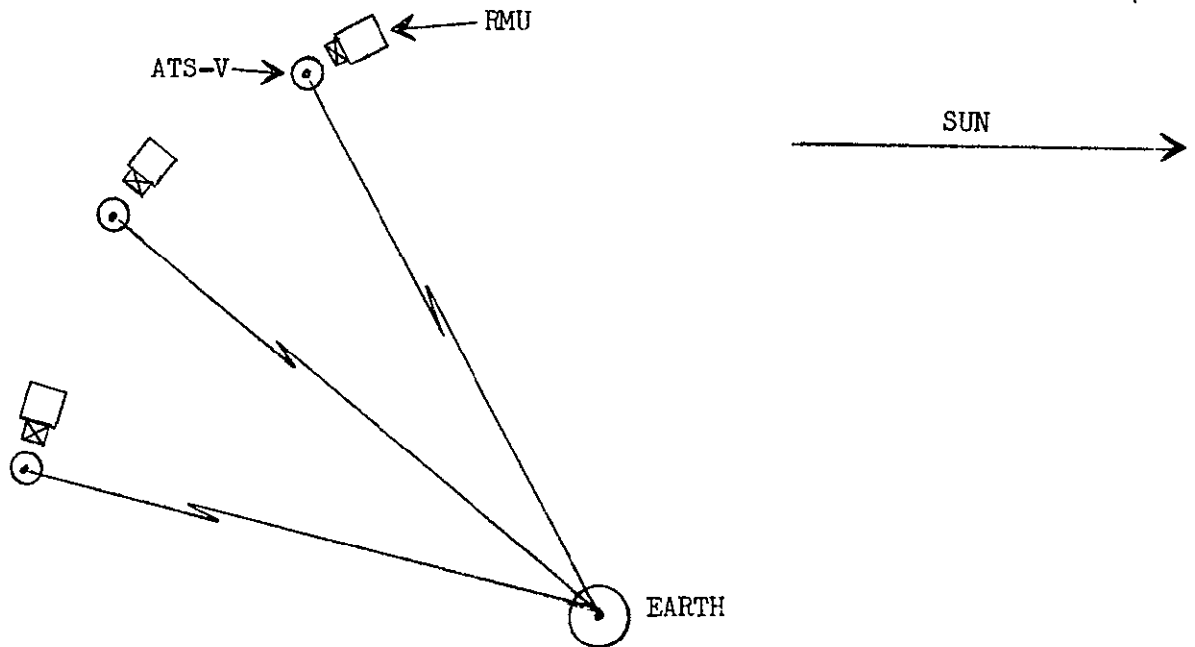
FIGURE 5-3

RMU GEOMETRY IN OBSERVATION PHASE
VIEWED FROM NORTH

ranges and aspect angles. Only minute quantities of fuel are required for this phase. such that no additional imposition of fuel loading requirements is necessary. Since this operation is essentially no different from the rendezvous operation, no additional equipment is required and no significant power or thermal penalties are imposed on the vehicle for performing the observation task.

6.0 ALTERNATIVE MISSION CAPABILITY

SUBSEQUENT TO DESPINNING ATS-V, ADDITIONAL TASKS AND EXPERIMENTS CAN BE PERFORMED BY THE RMU WHICH WILL ENHANCE PROGRAM COST EFFEC-TIVITY.

The bulk of this report deals with the functional and physical definition of a baseline system capable of accomplishing the ATS-V despin mission. During the course of the study, an investigation was made of the ability of the RMU, with at most minor design modifications, to accomplish additional mission functions to further demonstrate and obtain data on orbital maintenance operations. The following paragraphs present brief discussions of such optional mission capabilities consisting of communication experiments, long-term ATS-V observation following despin, rendezvous with ATS F/G, and orbital fuel transfer.

The intent is to assess the impact of such mission requirements by considering possible implementations, and no optimization is suggested. In all cases, further NASA/NR discussions are required prior to introducing certain of these alternate capabilities as system mission requirements.

6.1 COMMUNICATION EXPERIMENTS

As shown in the following, the RMU can, with the inclusion of a defined set of modifications, provide ranging to the ATS-V and/or implementation of the L-band Air Traffic Control experiment.

6.1.1 Communication Experiment Requirements

In general terms, the objectives and requirements of the three communication experiments considered are given below:

a. Ring-Around Ranging

   In this experiment, the range from the RMU to the ATS-V is determined by measuring the tuned frequency of an oscillator formed by an RF patch of varying length including ATS-V and RMU transponders. Because the ATS-V transmitter and receiver frequencies are already established, the RMU must provide the inverse capability; i.e., receive at the ATS-V transmit frequency and vice versa. Since the ATS-V L-band system operates only through the high-gain antenna, this experiment can be more readily performed at C-band. However, it could be performed at L-band after the ATS-V vehicle is despun or before with an intermittent or a sampled data approach.

b. **ATS-V Ranging Through RMU**

In this experiment, the ground station compares the RMU range with the combined range obtained in the loop comprised of ground to RMU to ATS-V to RMU to ground links. In this case, the RMU must communicate with the ground and with the ATS-V on different frequencies to avoid interference and must, therefore, provide the necessary transmitter and receiver capabilities. Again, for the RMU/ATS-V link the RMU must provide the inverse of the ATS-V transmit and receive frequencies, and if the experiment is to be performed prior to despin, C-band must be employed unless the aforementioned sampling technique is employed. If long range measurements (ATS-V/RMU) are required, a high-gain antenna capability must be provided on the RMU for the RMU/ATS-V link.

c. **Air Traffic Control**

For this experiment to represent the proposed ATS-V air traffic control (ATC) experiment implementation, it must be operated at L-band. Communication with both ground and airplanes is provided simultaneously by employing different portions of the L-band spectrum, and the same high-gain antenna can be employed for both. The high-gain antenna is required in order that the aircraft need not provide high-gain antennas and thus operate in accordance with the intended dimensional.implementation.

6.1.2 Mechanization Alternates

Considering these several experiment possibilities, various implementation alternatives can be considered for each of the experiments. In Table 6-1, various frequency and antenna configuration alternatives are listed to support discussion of mechanizations of the three experiments. The table does not reflect the communication requirements of the baseline mission. The alternate mechanizations and their impact on the baseline design are discussed in the following paragraphs.

Ring-Around Ranging

Since this experiment involves transmission between spacecraft, the RMU must have a transponder with inverse frequencies relative to ATS-V. If implemented at C-band, the RMU would have to receive at 4 GHz and transmit at 6 GHz. Subassemblies from the basic transponder may be able to be switched to form the inverse transponder if the C-band system is used. However, to be conservative approximately one-half the components for the inverse transponder should be assumed additional components. Redundancy is not considered necessary for this experiment. When in this mode, the basic RMU-to-ground transponder will not be in use. Therefore, this experiment does not place an additional

- 128 -

TABLE 6-1
FREQUENCY ALTERNATIVES FOR RMU COMMUNICATION EXPERIMENTS

Experiment	ATS-V			RMU			GROUND STATION		
	Recv. Freq. (ghz)	Xmit Freq. (ghz)	Antenna Type	Recv. Freq. (ghz)	Xmit Freq. (ghz)	Antenna Type	Recv. Freq. (ghz)	Xmit Freq. (ghz)	Antenna Diam.(FT)
A. Ring-around, ATS-V Ranging									
(1) C-Band	6	4	Hi-gain or Omni	4	6	Hi-gain or Omni	4	--	85 or 40
(2) C & L Bands	6	1.55	Hi-gain	1.55	6	Hi-gain or Omni	1.55	--	15
(3) L-Band	1.65	1.55	Hi-gain	1.55	1.65	Hi-gain or Omni	1.55	--	15
B. ATS-V Ranging through RMU									
(1) C-Band to ATS, L-Band to Ground	6	4	Hi-gain or Omni	4 & 1.65	6 & 1.55	Hi-gain or Omni	1.55	1.65	15
(2) C & L Bands to ATS, C & L Bands to Ground	6	1.55	Hi-gain	1.55 & 1.65	6 & 4	Hi-gain or Omni	4	1.65	85 or 40 &15
(3) L-Band to ATS, C-Band to Ground	1.65	1.55	Hi-gain	1.55 & 6	1.65 & 4	Hi-gain or Omni	4	6	85 or 40
C. Air Traffic Control									
(1) L-Band, dual satellites	1.65	1.55	Hi-gain	1.65	1.55	Hi-gain	1.55	1.65	15
(2) L-Band, single satellite	--	--	--	1.65	1.55	Hi-gain	1.55	1.65	15

load on the spacecraft power bus. Thus, the impact on satellite design
of adding the experiment would be no additional power requirement, approxi-
mately 7 lbs. additional weight and no change in the antenna subsystem. The
impact on the ground terminal would be essentially an inexpensive frequency
meter calibrated to read out directly in range.

As noted in Table 6-1, the second method of implementation requires an
RMU receiver at 1.55 GHz and a transmitter at 6 GHz. The basic C-band
transmitter normally used for the RMU-to-ground link could be switched to
operate at 6 GHz for the RMU-to-ATS-V link. The L-band ATS-to-RMU
function would require an additional antenna and receiver front end with
the IF and master oscillator portions of the basic transponder being used. The
impact upon spacecraft design would be approximately the same as the first
method except for the additional antenna. The ground station would require
the use of the 15 foot L-band terminal with the special frequency meter added.

The third method uses all L-band and requires the addition of a complete L-
band transponder and antenna to the RMU. Since redundancy is not required,
the weight addition to the spacecraft would be approximately 18 lbs. with no
significant increase in power requirement. The ground station would be the
same as with the second method.

ATS-V Ranging Through RMU

For any of the three alternatives listed in Table 6-1, two complete transponders
are required on the RMU with both operating simultaneously. This would add
approximately 18 lbs. weight to the spacecraft with an additional power
requirement of at least 30 watts. Referring to Table 6-1, only the first of the
three alternatives uses C-band on the ATS-V for both the receive and transmit
functions. Since the ATS-V L-band system cannot operate through the
ATS-V omni antenna, either an
intermittent or a pulsed measurement technique must be used with the other
two alternatives if the measurements are to be made prior to despinning the
ATS-V. It would also require that the RMU to ATS-V line of sight be normal
to the spin axis of the ATS-V within 15°.

For the second and third alternatives (Table 6-1) the impact on the ground
station to implement this experiment is very small since all the major equip-
ment required already exists. For the first alternative, however, the L-band
ground terminal would have to use a larger antenna (40-foot minimum) to
allow transmission of the RMU video signals (the C-band RMU transponder has
inverted frequencies for this case).

This experiment would give very accurate range and range-rate measurements between the RMU and ATS-V which would be a valuable aid during rendezvous and docking maneuvers. This could also yield valuable experimental data for use in the design of the Tracking and Data Relay Satellite Program.

Air Traffic Control

Two alternatives are listed in Table 6-1 for this experiment. They require the same equipment and the only difference is in the type of data that can be obtained with two satellites (RMU and ATS-V) instead of one. To implement this experiment, a complete L-band transponder is required and the spacecraft power drain is heavy.

If the L-band transponder were also used for transmitting the video signals, then no additional transponder weight would be necessary as the L-band subsystem weight is approximately the same as the C-band subsystem. To duplicate the L-band system that ATS-V has, 110 watts of bus power would be used, which represents an increase of 92 watts relative to the baseline design. If the L-band antenna beam were made smaller than an ATS-V, then the delta power requirement could be reduced to 42 watts. In addition, the L-band ground station antenna would have to be at least a 40-foot dish instead of the existing 15-foot unit.

If the L-band transponder is carried in addition to the baseline C-band system, no ground station modification is needed; a weight increase of 20 pounds would, however, be incurred on the RMU.

6.1.3 Selected Mechanizations

A review of the alternate possible mechanizations has resulted in the selection of two candidates which offer particularly good cost-effectiveness. The first mechanization is limited to performing only the ring-around ranging experiment, while the second is capable of performing all three experiments. These two mechanizations are described in the following paragraphs.

Ring-Around Ranging Experiment Only

This is similar to the experiment suggested by Mr. R. J. Darcy of NASA and which has been conducted by NASA from a ground terminal to ATS-V; the concept is shown in Figure 6-1. The main difference in the method is that NASA used an amplitude modulator instead of a frequency modulator. A voltage-controlled oscillator (VCO) in the RMU is modulated by noise spikes from the audio amplifier and is transmitted to the ATS-V at 6 GHz. When the range is sufficiently reduced, approximately 40 n.m., the ATS-V will receive the signal, translate in frequency, amplify and retransmit at 4 GHz back to the RMU. In the RMU the receiver amplifies and converts the
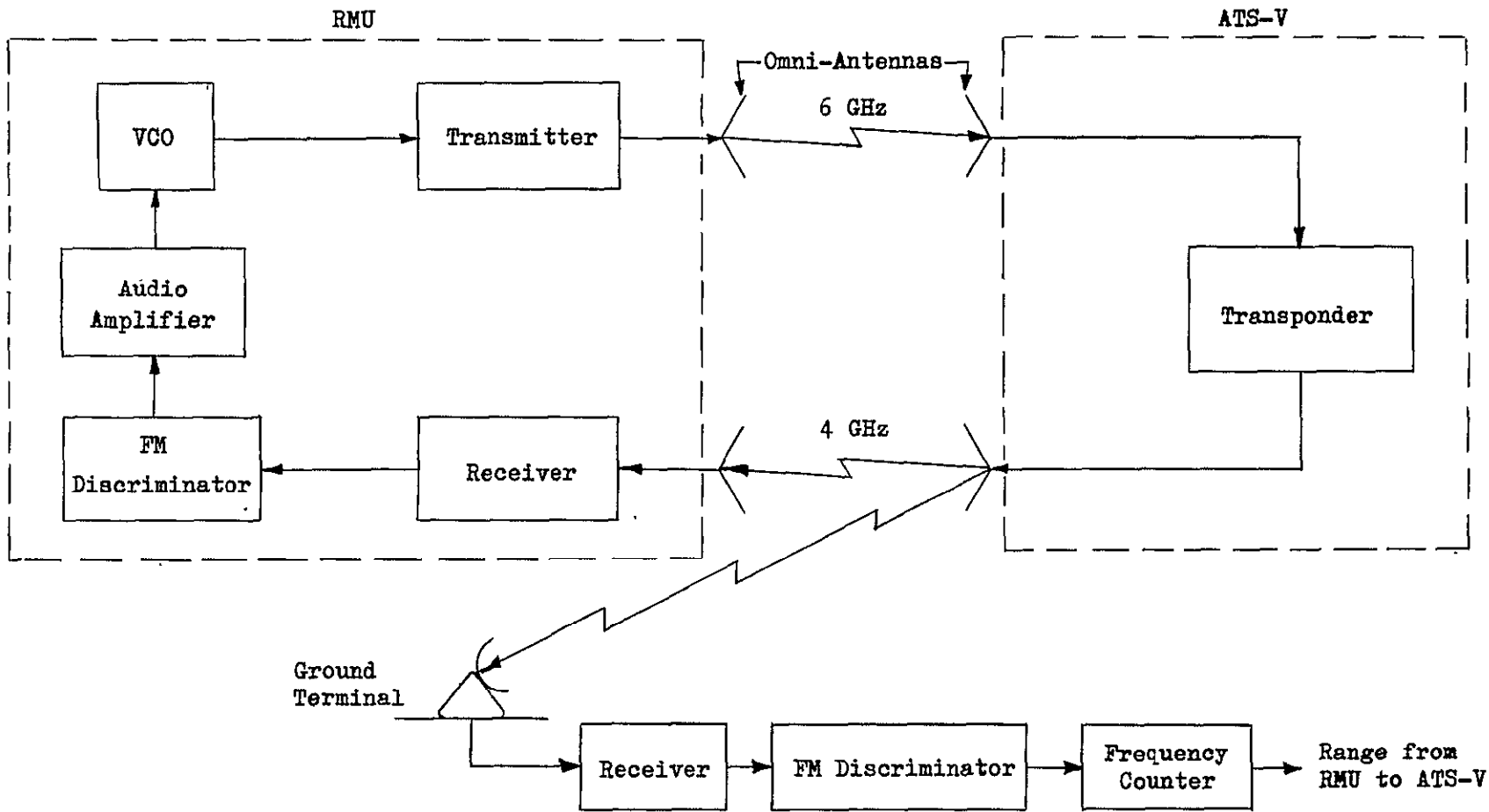
Figure 6-1 Ring-Around Experiment Configuration

signal to the nominal VCO frequency (approximately 65 MHz) and feeds this to a frequency discriminator. The output of the discriminator is amplified and fed back to the VCO to complete the ring-around. After a steady state condition has been achieved, the loop will oscillate at a frequency which is a function of the distance between the RMU and the ATS-V spacecraft.

Since the signal that is transmitted by the ATS-V is at 4 GHz and from an omni-antenna, it can also be received by a ground terminal. With an FM discriminator in the ground terminal, similar to the one on the RMU space-craft, the ring-around frequency can be determined and thus the spacecraft-spacecraft range can be measured on the ground. The relationship between range and frequency is:

$$R = \frac{5 \times 10^8}{f}$$

where:

R = RMU to ATS-V range in feet

f = ring-around frequency in HZ.

Thus for the maximum range of 40 n.m., the frequency would be 1 KHz and would increase as the range decreases. The accuracy depends upon the level of sophistication, but could easily be ± 0.1 percent of the range down to about 100 feet. To obtain a minimum range of approximately 100 feet would require two or three range modes in the RMU with commandable filters and attenuators, but this would not be too complex.

Three Experiment Capability

This capability requires a low power C-band transponder on the RMU for the RMU/ATS-V link which has the receive and transmit frequencies inverted with respect to ATS-V. An L-band transponder is also required on the RMU for the RMU/ground and RMU/aircraft links. The choice of making the inverse frequency transponder C-band will also allow the RMU to operate with other satellites having C-band transponders, such as the ATS series and Intelsat series of satellites. Referring to Table 6-1, ring-around ranging between the satellites would be at C-band as in Experiment A-1. Experiment B would be mechanized as Experiment B-1 with ranging between RMU and ATS-V accom-plished as shown in Figure 6-2. The ranging signal is sent from the ground through the RMU to the ATS-V which amplifies the signal, translates it in
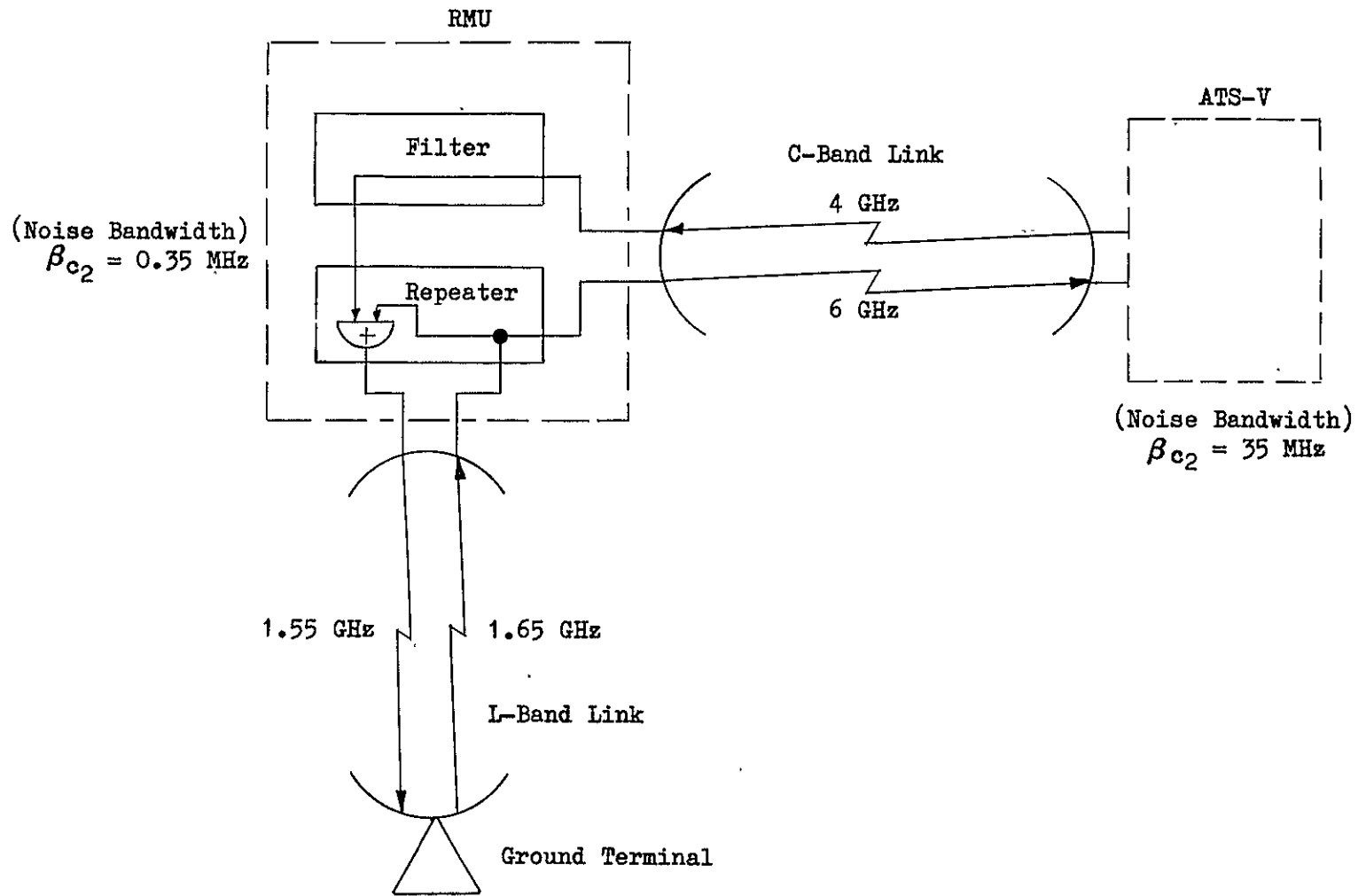
Figure 6-2 Remote Tracking Configuration

frequency, and retransmits to the RMU where the signal is translated again and retransmitted to the ground terminal. The ground terminal measures the time delay of the ranging tones to derive the range to the RMU plus the RMU to the ATS-V range. The ground terminal then measures the range to the RMU and subtracts it from the previous measurement to obtain the distance from the RMU to the ATS-V. As shown in Figure 6-2, the ranging signal is received by the RMU at 1.65 GHz and is translated to 6 GHz for transmission to the ATS-V, which retransmits at 4 GHz to the RMU. The 4 GHz signal is translated and filtered in the RMU and retransmitted at 1.55 GHz along with the signal received from the ground.

Assuming omni C-band antennas on both vehicles, and narrow-band filtering, ATS-V/RMU ranges to about 35 miles and an accuracy of at least 10 ft. can be predicted. The minimum useful range of this system depends primarily upon the saturation characteristic of the C-band transponders, in particular, the level at which either receiver blocking or parasitic oscillations take place. To derive the minimum range, saturation measure-ments would have to be made of a transponder which is essentially identical to the ATS-V transponder. In any event, the minimum useful range is less than 100 feet and may be as low as 10 feet.

The ATS-V Air Traffic Control experiment can also be performed with essentially the same equipment complement as on ATS-V. The primary dif-ference is the use of higher gain L-band RMU and ground antennas which are needed for the RMU video transmission. The increased RMU antenna gain makes it possible to conduct the experiment using low gain antennas on the aircraft, thus more nearly simulating future operational conditions. The experiments planned with ATS-V required a tracking antenna on the aircraft because of the lower gain. The consequence of this is to preclude the proper evaluation of aircraft antenna designs for operational systems and the proper evaluation of the multipath problem since multipath is insignificant with tracking antennas.

The other important advantage gained by including the ATC experiment on RMU is the possibility of conducting a two-satellite system test following ATS-V despin. The most likely operational ATC system will be the two-satellite per area system. By obtaining the range from the aircraft to both satellites (spaced a few thousand miles apart) and the aircraft altimeter reading, the coordinate position of the aircraft can be computed.

The ATC experiment configuration is shown by the frequency plan in Figure 6-3. The L-band ground terminal transmits two ranging signals, one is relayed through the RMU to the aircraft and the other through ATS-V. In the aircraft both signals are received and are multiplexed along with the

L-Band

C-Band

ATS-V

RMU

A/C

GROUND

Ranging System
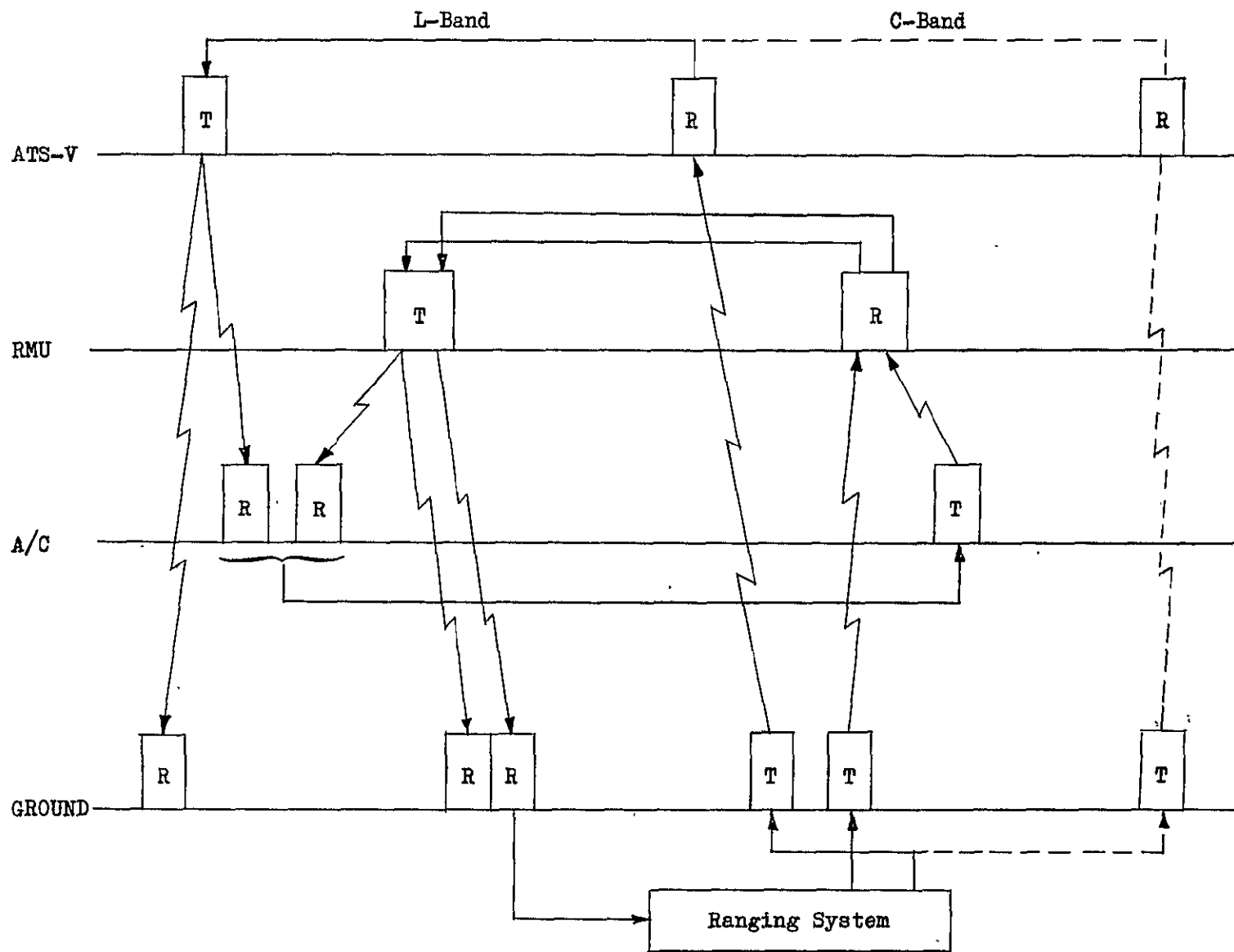
Figure 6-3 Frequency Plan - ATC Experiment

aircraft altimeter reading and retransmitted through the RMU to the ground terminal. The signals received from the satellite by the aircraft are also received by the ground terminal which can compute the ground-satellite-aircraft range and the range from ground to the satellite; by subtracting the two, the range from satellite to aircraft can be derived.

The ground terminal computes and catalogs the aircraft position, thus accomplishing the surveillance part of the experiment. The operator then uses the L-band link with voice communication to relay this information to the aircraft. This accomplishes the position navigation and voice communication part of the experiment.

One variation of the experiment is shown in Figure 6-3 by the dotted lines. In this case the ranging signal, which is relayed through ATS-V, is sent on a C-band uplink and in ATS-V is cross-strapped over to the L-band transponder. By completing a measurement in this mode, a direct comparison can be made of the propagation delay between C-band and L-band.

6.1.4 Conclusions and Recommendations

The three suggested communications experiments can be accomplished in a variety of ways, as shown. Although a number of experiment combinations are possible, the ring-around ranging experiment can be accomplished relatively simply with an RMU weight impact of approximately 7 lbs. and minor ground instrumentation. A configuration which permits all three experiments (requiring L-band implementation) reflects an RMU weight increase of approximately 20 lbs. for communication equipment, an RMU communication system power requirement increase of approximately 60 watts, and generates the requirement for a 40-foot ground antenna operating at L-band.

6.2 LONG TERM OBSERVATION

As shown in the following, the RMU has the capability of performing periodic observations of the ATS-V over a period of one year with the expenditure of very little additional fuel.

6.2.1 Long-Term Observation Requirements

A capability for periodically observing the ATS-V at close range over a period of one year is required. This capability must be provided with minimum design impact upon the RMU equipments and fuel requirement. The following specific considerations apply:

    a.   Trajectory Selection

        A trajectory must be provided for stationing the RMU at a safe distance from the ATS-V during quiescent periods (in between observation periods)

for perhaps several months without requiring frequent tracking and
orbital correction. A trade-off of distance between vehicle stations
(for orbit interference avoidance), fuel minimization, and response
to observation needs, is inherent.

b. Attitude and Spin Control

For the selected baseline design the RMU must be despun for rendez-
vous and observation, and spun for temperature stabilization and solar
power generation during interim periods. This approach must be
retained if significant design impact is to be avoided.

c. Component Life

Similarly, for minimum design impact, the approach to providing the
long-term observation capability must minimize the operating life
requirements for components which are sensitive in this regard.

d. Thermal Control

The baseline RMU design is based on leaving the spacecraft in its
quiescent (spinning) mode during equinox-related eclipse periods.
Also, thermal control is based on a 6-hour duration in the despun
mode. Again, if design impact is to be minimized, these constraints
must also apply to the long-term observation mission.

6.2.2 Selected Approach

Long-term observation of ATS-V can be accomplished with a number of techniques;
a representative approach is discussed to establish feasibility for this added capability.

With the RMU in the normal observation phase as briefly described in Section 5.0,
a sequence of deactivating the RMU on station might consist of the following:

1. With the TV camera constantly viewing the ATS-V, rotate the unspun
    RMU around the ATS-V/earth LOS to the position corresponding to the
    original pre-docking RMU orientation; i.e., RMU TV pointing North
    toward the ATS-V.

2. After reducing the relative translational velocity to zero, impart to
    the RMU a velocity increment (ΔV) of 0.935 ft/sec in the direction
    opposite orbital velocity which puts the RMU into a transfer orbit
    having a slightly smaller period than that of the ATS-V.

- 138 -

3. After the impulse has been applied, orient the RMU X-axis normal to the orbit plane, spin up the RMU to approximately 20 rpm and turn off the dual purpose gyros. This spin-up activity should require approximately .28 pounds fuel.

4. Twelve hours later, circularize the orbit with another 0.935 ft/sec impulse opposing orbital velocity. This reduced orbit corresponds to an orbital displacement of .2° lead per revolution (80 n.m.) relative to ATS-V.

5. After a period of two days, reverse the two-impulse procedure to re-establish the RMU period equal to that of the ATS-V, thus stationing it in synchronous orbit 240 n.m. ahead of the ATS-V (two-full circular orbit revolutions at 80 n.m./revolution plus two half revolutions each at 40 n.m./revolution).

The total fuel required for these translation maneuvers is approximately 0.3 lb. Ground tracking will be accomplished during this period of orbital transfer in order to provide more accurately the final small orbital adjustments.

To activate the RMU for the next observation period, the following sequence might be accomplished:

1. Give the RMU a 0.935 ft. per second ΔV impulse in the direction of orbital velocity.

2. Circularize the orbit by applying a like ΔV twelve hours later. This enables the ATS-V to catch up at the rate of .2° per revolution (80 n.m.).

3. Again, two days later (RMU 40 n.m. ahead of ATS-V), apply a 0.935 ft/sec ΔV opposite orbital velocity to cause orbital interception.

4. During the final hours the RMU approaches the ATS-V in a manner similar to the baseline mission and the original baseline rendezvous technique can again be performed as explained in Section 3. Reaction fuel is minimized by despinning the RMU prior to rotating the unspun RMU into the acquisition configuration (i.e., spin axis/ TV axis pointing roughly toward the ATS-V). Again, the orbital phasing and attitude control techniques are essentially identical to those of the baseline rendezvous phase.

The required fuel for each deactivation/activation cycle is estimated as less than three pounds based upon .56 pounds for the spin/despin operation, .6 pounds for the orbital transfers, and the remainder for rendezvous and observation maneuvers. The fuel requirements will logically dictate the number of observation periods that can be accom-

plished, and clearly the fuel quantity available is primarily dependent upon that used during the RMU baseline ATS-V despin mission.

The electrical power subsystem of the baseline RMU design is presently sized for supporting 6 hours of operation in the despin mode. During this period, however, the most significant power requirement is that associated with the light source for illuminating the shaded ATS-V docking interface. A considerable reduction in this energy requirement is expected during the observation periods where docking is not required since sunlite illumination can be used. Thus, longer observation periods may be possible from a power standpoint. Variations in the solar incidence angle during observation will also impact the power budget as well as the thermal considerations. Accordingly, the observation periods should be adjusted on the basis of telemetered equipment temperature and power data. Longer observation periods may also be possible by interim periods of RMU spin up and despin predicated upon close tracking scrutiny and careful vehicle control. The limitation of not conducting an observation during the equinox-related eclipse periods appears to be acceptable at this point.

The life of the components selected for the baseline design is adequate for this optional mission capability. In this regard the baseline batteries are the most sensitive element of the system. However, by utilizing discharge accumulation techniques during equinox periods, the number of recharge cycles can be minimized to where the cycle-life is within the range of the selected batteries.

6.2.3 Conclusions and Recommendations

A brief study of the requirements for a long-term observation capability indicates that the nominal planned baseline system and subsystems can provide this capability with no modification except for the possible addition of a minor amount of fuel. The fuel remaining by virtue of baseline design margins (essentially 3 sigma launch errors) can be expected to provide substantial capability for many observations.

6.3 ATS-F/G RENDEZVOUS

The RMU has the capability of performing a rendezvous with the ATS-F or -G following its observation of the ATS-V with the expenditure of a small amount of additional fuel.

6.3.1 ATS-F/G Rendezvous Requirements

A capability for the RMU to rendezvous with and observe the ATS-F/G is required. This implies a transfer from the ATS-V orbit to that of the newly launched ATS-F/G. The final rendezvous and observation phases should be essentially similar to those provided for the baseline ATS-V mission. Inasmuch as ATS-F/G will probably be launched one or more years after the RMU launch, the RMU equipment must exhibit a long life capability in excess of one year. Again, functional capability of the RMU must be provided with minimum design impact upon the RMU equipment. Some of the basic considerations in providing this ATS-F/G rendezvous capability are as follows:

a. Transfer Trajectory/Fuel Requirements

    A trajectory must be provided which will accomplish the rendezvous
    in time for the observation of the early ATS-F/G orbital operations,
    while at the same time minimizing required reaction jet fuel. The
    fuel required to accomplish the orbital inclination change will depend
    directly upon the difference in the inclination angles; the fuel require-
    ment for in-plane corrections, however, depends upon the time per-
    mitted for completion of rendezvous. Accordingly, a technique
    allowing maximum time must be utilized.

b. Electrical Power/Thermal Considerations

    As previously discussed for the long-term observation capability
    (Section 6.2) on-board power requirements must be compatible with
    power generation and conservation capability for long-term operation.
    Similarly, a successful thermal balance is required so that equipment
    temperatures are maintained within satisfactory bounds for long-term
    system operation. These considerations must be faced exactly as for
    the long-term observation mission.

c. Attitude Control - Deactivation/Activation

    Again, as discussed in the previous sections, the technique for changing
    from the spinning to non-spinning configuration must preserve fuel and
    provide for proper application of the attitude control subsystem.

d. Component Life

    Inasmuch as the requirement for this mission implies an extension of vehicle
    utility of at least one year, on-board subsystems must be reviewed relative
    to possible impact experienced in assuring this long duration useful life.

6.3.2 Selected Approach

    To achieve operational objectives with a minimum expenditure of fuel, the
RMU should be placed in synchronous orbit at the intended ATS-F/G operational
longitude prior to ATS-F/G launch. This means a very slow shift of RMU longitude
from the ATS-V longitude of 107° West to the assumed ATS-F/G longitude target of
100° West. If, for example, a transfer time of one month were allowed, the longitude
change would be accomplished at the rate of .233° per day, and would require a
total ΔV impulse of 4.4 feet per second (.34 lb. fuel). In this way, the RMU must
provide additional minor orbital corrections following the ATS-F/G launch to
compensate for the injection dispersion of that launch. Relative to the possibility of
orbital interference on the basis of purely geometrical considerations, the probability
of actual physical interference of the two vehicles is less than one in 10^9 without con-
sidering any tracking/maneuvering technique of interference avoidance.

The ensuing fuel requirements depend very little upon the in-plane orbital correction required unless a large longitude correction is required to be made extremely early. Accordingly, the RMU orbital correction would be made during the ATS-F/G orbital correction period and coordinated so that an RMU 2° per day correction capability should be fully adequate. This would require approximately 38 ft./sec.

ΔV or 3 lb. fuel. The actual rendezvous can be provided exactly as outlined in the baseline, with acquisition occurring at either 6:00 p.m. or 6:00 a.m. in orbital sun time, depending upon whether the RMU is initially leading or lagging the ATS-V vehicle, respectively.

By far, the most significant portion of additional fuel requirement is dictated by the inclination correction required. The ATS-F/G may be placed in orbit with an inclination angle of up to 1.5°. Assuming that the ATS-V inclination is, at that time, essentially 0°, required impulse and associated reaction fuel can be simple expressed as approximately 175 feet per second of ΔV per degree of inclination (corresponding to 13.5 lbs. fuel). The amount of fuel required for this mission will, in most cases, be left over from the baseline mission simply because a nearly 3 sigma statistical allowance is made for assurance of adequate baseline fuel. Considering that in 67% of the baseline missions only 1/3 of the provided fuel will be expended, the rendezvous mission can normally be accomplished with the reserve. In short, the optimum amount of fuel to be carried is a result of a statistical analysis based upon baseline reserve requirements, ATS-F/G orbital correction philosophy, and the priority assigned to this alternate mission capability.

The sequence with which the RMU is spun up and later despun and pointed is identical to that previously explained in Section 6.2 (Long-Term Observation).

The power generation/utilization treatment provided in Section 6.2 is applicable here; in short, adequate power is generated in the spinning mode and the power drain during the despun mode is such that no serious compromise of ATS-F/G observation is anticipated.

The RMU equipment thermal considerations are exactly as they were for the long-term observation mission (6.2) in the comparable spinning, rendezvous, and observation phases; i.e., no significant mission compromise is expected.

A review of the various RMU vehicle subsystems confirms (as indicated in Section 6.2) that the planned baseline equipments experience no anticipated difficulty in realizing a useful life well in excess of one year. If the ATS-F/G rendezvous occurs significantly more than one year after RMU launch, the life limitation of the baseline silver-zinc batteries will have to be reviewed.

6.3.4 Conclusions and Recommendations

A brief review of the requirements for an ATS-F/G rendezvous and observation capability indicates that the planned baseline system and subsystems are capable of accomplishing this mission with no modification. Thermal and electrical power constraints are no more demanding than for the baseline mission and/or the previously discussed long-term observation mission. The subsystem equipment operating life is adequate to meet the requirements for at least a year of orbital parking; longer periods may require a shift to NiCad batteries at extra weight. The primary impact is the possible additional fuel required for the orbital transfer inherent in the rendezvous. The principal parameter for consideration is the recognized requirement for approximately 13.5 lbs. fuel per degree change in orbital inclination. The determination of the statistically optimum fuel reserve increase to properly provide for this additional mission must be further evaluated.

6.4 FUEL TRANSFER

Utilization of the RMU system for fuel transfer is feasible but requires a number of design modifications which appear relatively simple.

6.4.1 Fuel Transfer Requirements

The basic requirement is for the RMU system to provide the capability of transferring hydrazine from an ATS-F/G spacecraft into the RMU tanks. A more general requirement for such a maintenance spacecraft might be to provide capability to transfer fuel in either direction. The aspect of proper rendezvous with a target spacecraft has been treated elsewhere in this report, so will not be discussed further here. Additional requirements associated with this operation include the minimization of fuel leakage prior to, during, and after the transfer operation to avoid chemical damage and/or disastrous fuel loss. Implied in the operation is the protection of the probe-associated equipment from temperature extremes. To accomplish fuel transfer, a pressure difference must exist between the two fuel systems and each system must subsequently revert to its normal reaction control system operating pressure. Lastly, this additional capability must be provided with minimum impact on the baseline system and on the ATS-F/G despin.

6.4.2 Technical Approaches/Considerations

To provide the required capability, a number of approaches have been considered. Some of these are discussed below:

a. Fuel Line Exit Provisions

A basic determination is how the fuel line leaves the envelope of the RMU. Primary candidate approaches include side exit and front exit. The latter approach appears to be simpler, although provisions for *

operating in the presence of the spin cage must be accomplished. Also, the centerline cannot be conveniently utilized because of the camera location. Nevertheless, this configuration provides the most promise.

b. Probe Alignment and Engagement

Two general categories of probe engagement exist. One category involves securing the vehicles together and then inserting the probe into the receptacle. The other maneuvers the probe into position relative to the receptacle prior to latching and securing the vehicles. Both approaches present some mechanical design problems, and both require some degree of probe alignment prior to latching unless the probe is on the centerline. At this time, the approach which offers the most promise with the selected RMU configuration is that of latching the vehicles as in the baseline mission and controlling angular position carefully with the aid of index marks around the docking ring, thus enhancing probe/receptacle pre-alignment.

c. Disconnect Valves and Mechanisms

Another important consideration is the design of the mechanism whereby engagement is made and proper flow control accomplished without leakage. Redundant leakage protection is required, and accommodation of reasonable misalignments must be anticipated.

6.4.3 Nominal Fuel Transfer System Design

As previously suggested, the RMU system offers the capability of accomplishing fuel transfer in several ways. A representative concept is outlined below to permit assessment of anticipated RMU system impact.

a. Fuel System Modifications

Figure 6-4 shows the baseline reaction control subsystem (described in Section 7), modified to provide the propellant transfer capability. Two principal system additions are involved. One is the probe connection into the RMU N_2H_4 line with a series valve which provides the on-off link to the other spacecraft. Secondly, a nitrogen bottle is provided with its related regulator and valve so the system can be repressurized following the pressure reduction required to enable the flow of fuel to the RMU from the ATS-F/ G system. This pressurization capability can also be used to support the transfer of fuel from the RMU to another satellite.

- 144 -
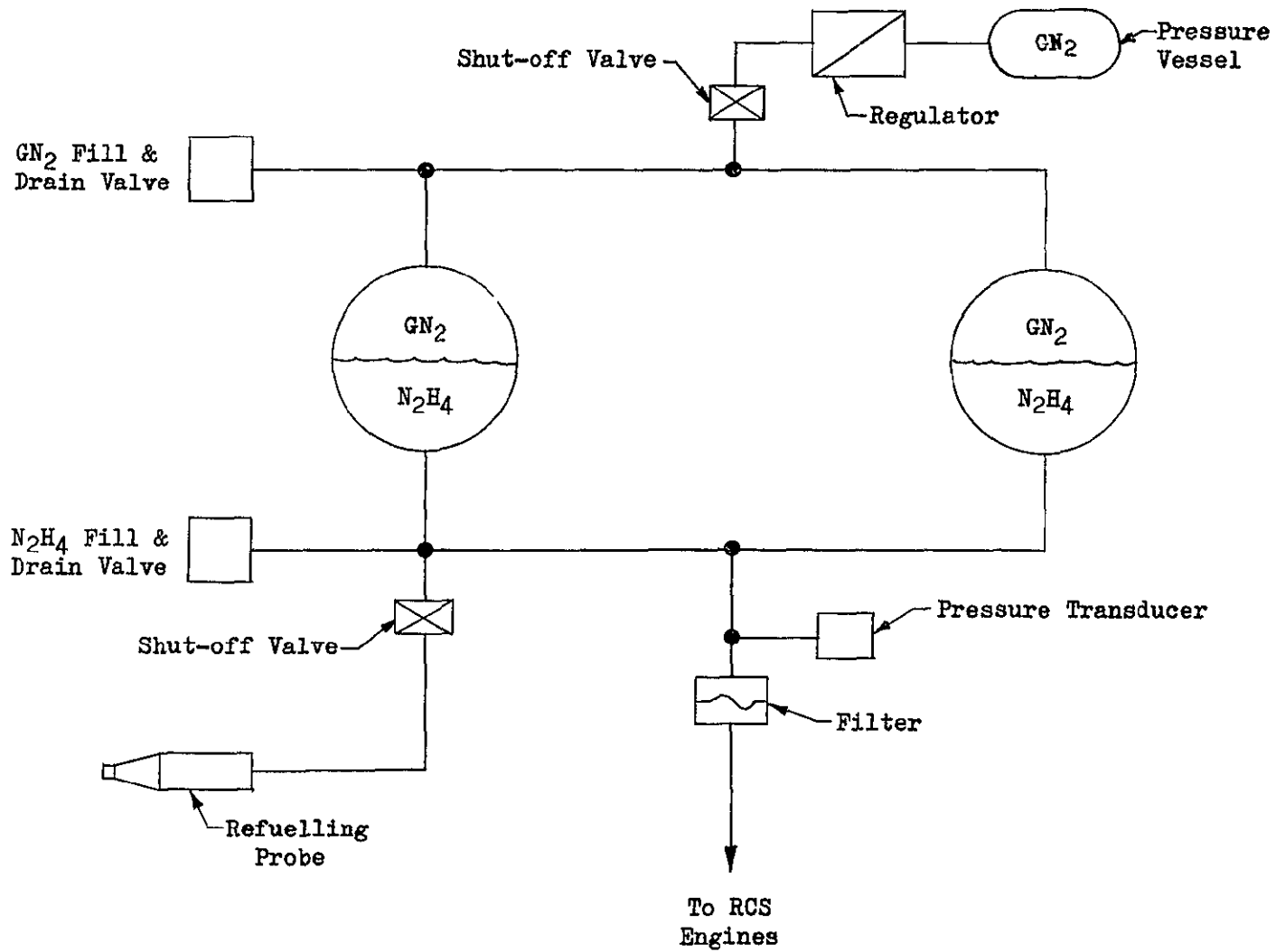
Figure 6-4 Reaction Control Subsystem Modified to Support Fuel Transfer

To provide such a two-way fuel transfer capability, the N_2 regulator is set at a pressure which is above the operating pressure of the reaction control system (RCS). This excess pressure will force the fuel into the ATS-F/G RCS; after the transfer is completed, the RMU N_2 shut-off valve is closed and the N_2 fill/drain valve would be used to bleed off any excess pressure on the basis of the pressure transducer output. Fuel transfer from ATS-F/G to the RMU is accomplished in much the same manner: the pressure is reduced by N_2 bleed-off to allow propellant flow, next the pressure is raised to the regulated pressure, and finally pressure is reduced to operating level by N_2 bleed-off.

b. Vehicle Design Concepts

A general layout depicting a concept enabling the linking of the two fuel systems is shown in Figure 6-5. This system provides for a transfer tube carried during the early mission phases by the spin cage and thus disconnected at each end. During the fuel transfer operation, the spin cage is stopped at a predetermined index position, permitting receptacle engagement at the in-board end. Following latching to the ATS-F/G docking ring, properly marked to control roll angle, the outboard end of the tube will be aligned within, say, one inch of the ATS-F/G receptacle. The same mechanism driving the elements together at the in-board tube end continues to drive to assure engagement at the ATS-F/G end (wherein provision is made to accept the misalignment tolerances). Following appropriate valving, transfer and tube closure operations, the tube is retracted from the ATS-F/G receptacle. This general approach provides for a minimum weight and complexity in the spin cage, and a minimum number of drive mechanisms.

c. System Modifications

The changes to the RMU system to furnish a fuel transfer capability are as follows:

Additional weight of the added spin cage sleeve, actuator drive mechanism, N_2 bottle, and system valving is estimated at 10 lbs. Inasmuch as only the transfer sleeve tubing, weighing under one pound (including counterweight), is mounted on the spin cage and the heavier equipment is in-board near the axial c.g. location, the moment of inertia ratio is not affected significantly.

Although the system is more complex because of the addition of remote control valves and an actuator drive mechanism, the design of these devices is considered to be straightforward and does not significantly

- 146 -

complicate the RMU system. The overall vehicle reliability will be negligibly affected because of the fail-safe (series valves) design approach.

Unless two-way fuel transfer is required, special thermal protection is not anticipated for the sleeve itself because of the absence of complex mechanisms and fluids prior to the refueling operation; if multiple transfers are required, protection and possibly heating would be anticipated. The actuator drive mechanism, located near the body of the RMU, can be included inside the thermal protection cover of the equipment compartment.

In addition, appropriate qualification, checkout and test of added design elements must be anticipated.

6.4.4 Conclusions and Recommendations

The RMU can support a fuel transfer operation with modest system design additions/modifications.

7.0 INTEGRATED SPACECRAFT DESIGN

THE BASELINE SYSTEM WILL DESPIN ATS-V AS THE PRIMARY MISSION TASK.
IT MAKES MAXIMUM USE OF EXISTING TECHNOLOGY AND ATS HARDWARE AND
IS WELL SUITED TO A PROTO-FLIGHT APPROACH. IT CAN BE LAUNCHED ON A
THOR DELTA AND IS COMPATIBLE WITH A LOW-COST, SHORT SCHEDULE PROGRAM.

7.1 SPACECRAFT SYSTEM

The baseline spacecraft configuration is a conventional design which can be produced
primarily from developed components. The requirements, alternatives, and selected
approach relating to the overall spacecraft configuration are discussed below.

7.1.1 Requirements

Several basic objectives have been established which dictate design philosophy.
This spacecraft, constrained by a short schedule, must be low cost yet highly reliable.
This, in turn, requires a state-of-the-art, straightforward approach to the spacecraft with
weight optimization secondary to use of developed hardware. Total weight, however,
must be within the capabilities of the Thor Delta.

A major physical constraint imposed on the RMU configuration is that it be stable in
the long-term, spin-mode of the drift orbit; i.e., the moment of inertia about the spin
axis must exceed the moment of inertia about the transverse axes. In general, this
involves maximizing the vehicle diameter and minimizing its length. The maximum
diameter is constrained by the 57-inch inside diameter of the standard Thor Delta boost
fairing. Minimum length is limited by the necessity of axially locating some of the major
spacecraft elements. The contribution of these elements to overall vehicle length is 98
inches as follows: 28 inches for apogee motor, 6 inches for apogee motor ejection mech-
anism, 10 inches for despin mechanism, 18 inches for TV camera subsystem, and 36 inches
from TV camera to docking latches at the required field-of-view. In view of these two
dimensional constraints, judicious placement of subsystem elements is requisite to attain-
ing the desired moment of inertia relationship. The overall length of 98 inches can be
accommodated by the Thor Delta payload envelope since the available length from the
attach interface of the third stage motor to the forward end of the boost fairing (at a
diameter required for the docking latches) is approximately 106 inches.

The RMU configuration must also provide for appropriate location of 12 reaction control
system (RCS) thrusters needed for 6 degree-of-freedom (DOF) maneuverability. Thrusters
should be located symmetrically about the vehicle center of mass (c.m.), and RCS tanks
must be located so that propellant depletion does not shift the c.m. beyond acceptable
limits.

PRECEDING PAGE BLANK NOT FILMED

7.1.2 Alternatives

Early in the study, a consideration of mission and operational requirements and dimensional constraints of the launch vehicle payload fairing suggested that a vehicle concept featuring a cylindrical body similar to Pioneer, Intelsat III, and ATS-V (among others), would offer many potential advantages. A cylindrical body approach provides a large surface area for the solar array and maximizes the internal volume for placement of the subsystems and the apogee motor. This configuration has been adopted for the RMU baseline.

Initial configurational studies of the RMU considered placement of the subsystems on a primary platform and possibly one other equipment shelf parallel to the first but separated to provide adequate access. Assessment of vehicle moment of inertia in pitch and yaw compared to roll indicated this internal packaging arrangement would not be suitable. As previously discussed, the length of the spacecraft and the relative positions of the despin cage, despin mechanism, and apogee motor are fixed, which leaves subsystem arrangement as the only variable configuration parameter. Therefore, the feasibility of supplementing a primary equipment platform with secondary surfaces near the periphery was examined to permit moving a maximum of subsystem mass outboard relative to the spin axis. This approach resulted in favorable inertia ratios and was selected for the baseline concept.

Since all of the subsystem boxes have flat mounting surfaces, the more efficient secondary shelf configuration was an octagonal shape rather than circular. An eight-sided shelf configuration, compared to six, provided a near-optimum surface area for subsystem mounting and a greater remaining usable surface area on the primary platform. Those items on the secondary shelves, which also adjoin the primary platform, could theoretically be mounted on either. In the final design, the basis for choice in this respect would probably relate to access and ease of installation.

7.1.3 Selected Configuration

Figures 7-1 and 7-2 provide three types of design definition of the selected baseline RMU configuration: an external view of the launch vehicle with payload; a minimum detail view illustrating the general arrangement of all major elements of the launch vehicle above the attach interface at the forward end of the second stage; and the detailed general arrangement/inboard profile views of the RMU.

Configurationally, the RMU spacecraft features a cylindrical body 55.4 inches in diameter and 55.5 inches in length, with a multi-element tubular truss cage structure incorporating docking and latching mechanisms used for the ATS-V despin operations mounted at the forward end. The cage assembly is structurally attached to the RMU body by the despin mechanism. A tapered cylindrical inner structure provides a mounting and separation plane near the aft end of the RMU body for the apogee motor. The same plane serves as the mounting interface for a short conical adapter which mates with the forward end of the standard third stage interstage structure. The periphery of the cylindrical

body, consisting of four removable panels, provides a gross surface area of 67 square feet for the solar cells. Openings are provided to accommodate various spacecraft attitude control system optical sensors, propellant tank servicing connections, the C-band omni antenna horns, and the planar array antenna. The satellite subsystems are mounted within the cylindrical body on a single transverse and eight longitudinal platforms.

The apogee motor is attached to the inner cylindrical structure by a "V"-band ring. Release of the band permits longitudinal jettisoning of the motor after burnout; ejection force is provided by the spring-type ejection mechanism located at the forward end of the motor. Insulation blankets, attached to the RMU structure, are placed over the outer surfaces of the motor case to satisfy flight and post burnout thermal conditions. A thermal shield is positioned over the nozzle of the motor to satisfy the thermal requirements during the transfer orbit. The shield will be jettisoned at motor ignition by the exhaust.

The attitude control system hydrazine tanks are mounted on the forward surface of the primary equipment shelf. The two tanks shown are Apollo Command Module RCS fuel tanks with a short cylindrical boss on one end and a bolt flange to provide mounting interface to the equipment shelf on the other end. The propellant tanks are on one side of the shelf and the major portion of the subsystems are on the opposite side; the space-craft c.m. shift from full to empty tanks is approximately 0.6 inches. The propellant subsystem components, such as valves, filter, and pressure transducer, are all mounted on the aft surface of the equipment platform. Cutouts are provided for the propellant lines from the two tanks to pass through the platform. The propellant tanks are connected in parallel to the RCS engine clusters. Fill and drain servicing fittings are located on the aft surface of the equipment platform on the -Z axis.

The RCS engine system consists of 4 clusters of 3 engines each. A pair of the engine clusters are located at the aft end of the vehicle in the 45° and 225° radial positions. The other two clusters are positioned at the forward end of the body and located in the 135° and 315° radial positions. The three engines which comprise a cluster are mounted to a machined interface pad which assures maintenance of alignment and rigidity of the subassembly as shown in Section B of Figure 7-2. The orientation of the clusters is such that pairs of engine nozzles point both forward and aft, and in the +Z and +Y directions. All translation, pitch, yaw and roll maneuvers can be accomplished by firing the thrusters in pairs. The fore and aft mounting planes of the thrusters, basically the ends of the spacecraft body, have been positioned to be equidistant relative to the c.m. of the RMU to minimize cross coupling of reactions when pairs of thrusters are operated.

The principal elements of the electrical power subsystem include the solar cell panels, batteries, and associated control electronics. Four removable solar array panels form the cylindrical outer surface of the RMU body. Each solar array panel is removable without affecting the adjacent panels. The electrical power subsystem components are located on the upper surface of the primary equipment platform and on several of the secondary equipment shelves, as shown in Sections E and C, and view H (Figures 7-1 and 7-2).

-157-

The forward surface of the primary platform accommodates the propellant tanks, the three Dual Purpose Gyros (DPG's), portions of the electrical power and communication subsystems in addition to the 20 C-band omni antenna horns. No equipment, other than the propellant tank manifolding and interconnect lines to the servicing fittings, are mounted on the aft surface of the platform as presently configured. All other subsystem modules are mounted on the eight secondary shelves as shown in Section C, and in view H which illustrates the flat pattern arrangement (Figures 7-1 and 7-2).

The TV camera subsystem general arrangement is shown on the inboard profile and view G. This subsystem consists of a pair of identical cameras mounted in a gear motor driven structural frame to permit positioning either camera behind either the wide angle lens or the telephoto lens. The lenses are fixed mounted in front of the cameras, with the wide angle lens positioned on the vehicle centerline. The complete TV camera support assembly is attached to the forward end of the despin mechanism, which is spacecraft body mounted. Electrical cabling from the camera control components mounted on the equipment shelves pass through the hollow center of the despin mechanism to the TV cameras. The illumination source to light the ATS-V during the docking maneuver is a ring-shaped cold cathode tube assembly approximately 22 inches in diameter supported by bracketry from the TV camera mounting.

The remaining principal element of the RMU spacecraft is the forward mounted mechanical-structural assembly, termed the despin cage, which provides the docking interface with the target ATS-V vehicle. The configurational approach selected for the baseline RMU is the result of extensive study of the problem of docking and despinning the ATS-V vehicle. The despin cage is comprised of two major assemblies, the despin cage structure and the docking latch mechanisms. Major parameters involved include: the geometry and physical relationship between the two vehicles at final closure, the docking interface provided by the apogee motor thrust ring of the ATS-V, boost fairing payload envelope constraints of the RMU launch vehicle, the field-of-view requirements for the TV subsystem, the structural loading and dynamic requirements for the cage structure, fabrication, and assembly considerations. The length of the despin cage assembly is established by the optical field of view of the wide angle TV camera lens (to permit seeing the docking interface), the length of the TV cameras, and the support structure which interfaces with the forward end of the despin mechanism. Axial misalignment of the docking interface within the ATS-V skirt does not influence the despin cage length but impacts upon the latch design.

As a result of extensive docking and despin conceptual studies, performed prior to and during the contract, the selected general approach embodies the following features. The docking interface on the ATS-V is the body mounted half of the ATS-V apogee motor "V"-band clamp ring located approximately 19 inches forward of the aft end of the vehicle. Although a few items such as connectors are near the ring, it is considered to provide a satisfactory structural and configurational surface for docking. A three-point docking and latching subsystem was selected as the best conceptual approach considering the potential initial contact misalignments and the known coning of ATS-V about its spin axis. A combination spring and pneumatic actuation system is utilized for automatically

closing the latches upon initial contact and for opening them after despin of ATS-V is accomplished. The design provides for three close/open cycles. The despin cage consists of a truss structure configured to provide the minimum weight capable of providing support for the three docking latches and satisfying the structural loads and dynamics requirements during docking and despin operations. As noted on Figure 7-1, the forward portion of the despin cage is covered with an opaque plastic shroud to serve as a stray light glint-shield for the TV camera.

7.1.4 Mass Properties

Detailed mass properties analyses of the baseline RMU were performed establishing weight, center of gravity and moment of inertia about 3-axes. Vehicle arrangement studies were performed to obtain desired center of gravity and stability. Despin cage mass properties characteristics were generated and utilized, in conjunction with the mass effects of the expendable propellant on the RMU spacecraft center of gravity and dynamic balance throughout the mission.

The baseline configuration, as shown in Figures 7-1 and 7-2, results in an RMU launch weight of 1140 pounds and a weight of 500 pounds after apogee motor jettison. The nominal weight of the spacecraft includes a contingency weight allowance of 20 pounds. The spacecraft longitudinal (X) center of gravity is 24.6 inches forward of the spacecraft/ TEM 442-1 apogee motor separation plane, the lateral (Y) and vertical (Z) centers of gravity are located on the centerline of the spacecraft. The moment of inertia of the spacecraft after apogee motor jettison for roll (I_{xx}), pitch (I_{yy}), and yaw (I_{zz}) are respectively 49.1, 44.5, and 43.8 slug ft.^{2} and result in a ratio of $I_r/I_p = 1.10$. The moment of inertia of the spacecraft with propellant expended for roll (I_{xx}), pitch (I_{yy}), and yaw (I_{zz}) are respectively 44.1, 42.1, and 41.4 slug ft.^{2} and result in a ratio of $I_r/I_p = 1.05$.

The baseline configuration mass properties are as shown in Tables 7-1 and 7-2. Sequenced mass properties of the combined ATS-V and RMU are shown in Table 7-3. A detailed weight statement for all subsystems and components is provided in Table 7-4.

7.2 SUBSYSTEMS

Subsystems comprising the baseline RMU configuration are: structure and mechanisms, electrical power, attitude control, reaction control, communications, telemetry and command, video and illumination, docking, propulsion, and thermal control. Each subsystem is discussed separately in the paragraphs that follow.

7.2.1 Structure and Mechanisms

The characteristics of the RMU baseline configuration structure are provided in a general manner in Section 7.1 where many features of the various mechanisms have also been treated briefly. Additional detail is included below to fill in the picture to the level of definition presently established. No detailed structural analysis has been performed, but preliminary calculations have been completed which indicate that the structural concept is adequate for the mission.

SD 71-286

TABLE 7-1

RMU WEIGHT SUMMARY

ITEM	WEIGHT (LBS)
Structure	71.0
Cage & Docking	19.0
Video & Illumination	41.0
Thermal	9.0
Electrical Power	94.0
Telemetry & Command	49.0
Communication	57.0
Attitude Control	63.0
Reaction Control	33.0
Contingency	20.0
Weight Empty	456.0
Propellant - N_2H_4	53.0
Pressurant - GN_2	1.0
Gross Weight-Full Propellant	510.0
Less: Apogee Mtr. Mount & Cone Apogee Mtr. Ejection Prov.	-8.0 -2.0
Gross Weight - Full Propellant in Orbit	500.0

TABLE 7-2
RMU SEQUENCED MASS PROPERTIES

Condition	Weight (Lbs)	C. G. (IN)			Inertia (SLUG Ft^2)			Minimum Inertia Ratio I_{roll} to I_{pitch} (or I_{yaw})
		X	Y	Z	ROLL	PITCH	YAW	
LAUNCH	1140.0	19.8	0.0	0.0	63.1	94.9	94.2	0.66
Less Adapter-Third Stage	-54.0							
APOGEE MOTOR IGNITION	1086.0	21.7	0.0	0.0	59.0	74.6	73.9	0.79
Less Apogee Mtr. Propellant	-524.0							
APOGEE MOTOR BURNOUT	562.0	28.8	0.0	0.0	50.9	54.1	53.4	0.94
Less-Apogee Mtr. Case	-52.0							
-Apogee Mtr. Mnt. & Cone	-8.0							
-Apogee Mtr. Eject. Prov.	-2.0							
RMU FULL PROPELLANT	500.0	31.6	0.0	0.0	49.1	44.5	43.8	1.10
Less: 3/4 Fuel N_2H_4	-39.0							
RMU OFF-LOADED	461.0	31.2	0.0	0.0	45.4	42.3	41.6	1.07
Less: Remaining Fuel N_2H_4	-14.0							
RMU PROPELLANT EXPENDED	447.0	31.0	0.0	0.0	44.1	42.1	41.4	1.05
DE-SPIN CAGE & MECH.	27.0	59.1	0.0	0.0	0.6	3.8	3.8	

TABLE 7-3

COMBINED
RMU & ATS-V

SEQUENCED MASS PROPERTIES

CONDITION	WEIGHT (LBS)	C.G. (IN)			INERTIA (SLUG FT. ^{2})		
		X	Y	Z	ROLL	PITCH	YAW
ATS-V*	982.8	112.1	0.0	0.0	98.6	85.0	82.8
RMU	500.0	31.6	0.0	0.0	49.1	44.5	43.8
TOTAL - Combined ATS-V & RMU	1482.8	85.0	0.0	0.0	147.7	593.0	596.1
LESS: 3/4 Fuel N_2H_4 (RMU)	-39.0						
TOTAL - Combined ATS-V & RMU Offloaded	1443.8	86.3	0.0	0.0	144.0	570.6	573.7
LESS: Remaining Fuel N_2H_4 (RMU)	-14.0						
TOTAL - Combined ATS-V RMU (Fuel Expended)	1429.8	86.8	0.0	0.0	142.7	563.3	566.4

NOTE: *ATS-V Mass Properties Data: Telecon F. H. Gardiner (NR) and J. Phenix (NASA/GSFC) 29 Oct. 1970

TABLE 7-4

REMOTE MANEUVERING UNIT
(RMU)
DETAIL WEIGHT STATEMENT

ITEM	WEIGHT (LBS)	CENTER OF GRAVITY		
		X	Y	X
Structure Subsystem				
Inner Cylinder & Cone Assy.	23.0	22.0	0.0	0.0
Despin Support Cone	4.4	30.0	0.0	0.0
Apogee Motor Mount & Cone	7.0	1.5	0.0	0.0
Apogee Motor Ejection Prov.	3.0	29.5	0.0	0.0
Propellant Platform	14.0	27.0	0.0	0.0
Equipment Platform	13.0	21.2	0.0	0.0
T.V. Camera Turret & Cover	5.0	48.5	0.0	0.0
Miscellaneous	1.6	23.5	0.0	0.0
TOTAL STRUCTURE	71.0	23.5	0.0	0.0
Cage and Docking Subsystem				
Cage Structure	(10.9)	(53.3)	(0.0)	(0.0)
Sprockets – Aft End	2.4	35.3	0.0	0.0
– Fwd End	1.4	41.7	0.0	0.0
– Structs & Misc.	1.0	38.0	0.0	0.0
Frame – Sta 41.5	0.4	41.5	0.0	0.0
– Sta 57.5	0.4	57.5	0.0	0.0
– Sta 72.5	0.4	72.5	0.0	0.0
– Sta 95.3	0.5	95.3	0.0	0.0
Struts – Aft Section	1.6	49.5	0.0	0.0
– Interm Section	1.6	65.0	0.0	0.0
– Fwd Section	1.2	84.0	0.0	0.0
Docking Mech.	(6.3)	(94.3)	(0.0)	(0.0)
Latches #1	1.5	94.5	0.0	-15.0
#2	1.5	94.5	13.5	7.5
#3	1.5	94.5	-13.5	7.5
Gas Lines & Generators	1.8	94.0	0.0	0.0
Wiring & Misc.	(1.8)	(68.0)	(0.0)	(0.0)
TOTAL – CAGE & DOCKING	19.0	68.3	0.0	0.0

TABLE 7-4 Continued

REMOTE MANEUVERING UNIT
(RMU)
DETAIL WEIGHT STATEMENT

ITEM	WEIGHT (LBS)	CENTER OF GRAVITY		
		X	Y	X
Video & Illumination Subsystem				
T. V. Camera				
T. V. Camera – #1	3.0	51.0	0.0	-5.8
– #2	3.0	51.0	0.0	0.0
T. V. Camera Lens – 10 MM	1.0	57.5	0.0	0.0
– 50 MM	1.5	57.5	0.0	-5.8
T. V. Camera Control Unit – #1	6.5	21.7	23.0	0.8
– #2	6.5	21.7	-23.5	2.5
T. V. Camera Cable – #1	0.5	33.0	0.0	0.0
– #2	0.5	33.0	0.0	0.0
Light Assembly				
Cold Cathode Light	2.5	56.5	0.0	0.0
Power Supply	10.0	16.5	0.0	-22.8
Cables & Miscellaneous	0.5	36.0	0.0	-5.0
T.V. Camera Motor	4.0	53.0	0.0	-3.0
Miscellaneous	1.5	33.0	0.0	-6.3
TOTAL – VIDEO & ILLUMINATION	41.0	33.0	-0.1	-6.3
Thermal Subsystem				
Insulation	6.5	34.0	0.0	0.0
Covers and End Seals	1.0	16.0	0.0	0.0
Covers – Apogee Motor	1.0	-5.5	0.0	0.0
Paint & Miscellaneous	0.5	36.0	0.0	0.0
TOTAL – THERMAL	9.0	27.7	0.0	0.0

-164-

TABLE 7-4 Continued

REMOTE MANEUVERING UNIT
(RMU)
DETAIL WEIGHT STATEMENT

ITEM	WEIGHT (LBS)	CENTER OF GRAVITY		
		X	Y	X
Electrical Power Subsystem				
Solar Cells	20.0	30.9	0.0	-0.3
Solar Cells Substrate	20.0	30.9	0.0	-0.3
Batteries - #1	20.0	33.1	-16.5	16.5
- #2	20.0	33.1	16.5	-16.5
Regulator	2.0	29.5	11.0	22.7
Battery Charger	2.0	23.3	-11.2	21.2
Power Distribution Box	3.0	23.0	21.6	-5.7
Inverter	3.5	22.0	10.8	20.8
Wiring Connectors & Misc.	3.5	29.0	0.0	0.0
TOTAL - ELECTRICAL POWER	94.0	31.0	1.1	1.4
Telemetry and Command Subsystem				
Telemetry	(26.0)	(23.7)	(-0.6)	(1.2)
Encoder - #1	7.0	20.9	-7.0	19.0
- #2	7.0	22.3	7.0	-20.2
Transmitter - #1	1.0	17.7	-19.0	13.3
- #2	1.0	18.0	-14.8	-20.0
Diplexer - #1	0.3	18.0	19.2	-16.2
- #2	0.3	17.4	-19.2	16.2
Signal Conditioner - #1	1.5	17.3	15.0	-18.7
- #2	1.5	16.7	-15.0	18.7
Encoder Regulator - #1	1.0	16.3	11.5	21.5
- #2	1.0	23.3	7.3	23.0
Antenna – Whip (8 req.)	1.0	60.0	0.0	0.0
Hybrid Balum Assy.	1.0	57.0	0.0	0.0
Wiring, Connectors & Misc.	1.9	25.0	0.0	0.0
Supports & Misc.	0.5	23.6	0.0	-1.2

TABLE 7-4 Continued

REMOTE MANEUVERING UNIT
(RMU)
DETAIL WEIGHT STATEMENT

ITEM	WEIGHT (LBS)	CENTER OF GRAVITY		
		X	Y	Z
Telemetry and Command (continued)				
Command	(23.0)	(21.3)	(0.8)	(-0.9)
Decoder - #1	6.2	22.5	19.8	5.3
- #2	6.2	22.3	-5.5	-21.2
Receiver - #1	1.0	21.6	6.8	23.0
- #2	1.0	23.7	-2.0	23.0
Clock	3.8	17.2	-19.8	8.2
Regulator - #1	1.0	16.4	6.2	23.8
- #2	1.0	16.8	-8.2	-23.0
Wiring, Connectors & Misc.	2.0	24.5	0.0	0.0
Supports & Misc.	0.8	21.2	0.8	-0.9
TOTAL - TELEMETRY AND COMMAND	49.0	22.5	0.1	0.2
Communication Subsystem				
Antenna Electronics	3.8	19.2	-21.4	-3.2
Repeater - #1	9.3	33.0	-1.5	17.4
- #2	9.2	33.0	1.5	-17.4
Transmitter	10.0	32.5	12.5	-12.5
Switch - Receiver	0.1	26.0	-1.1	18.5
- Transmitting	0.1	26.0	1.3	18.5
Antenna Switch Driver	0.2	16.3	19.3	16.2
Planar Array Antenna	1.1	18.0	-0.5	25.5
Omni Antenna System	(20.0)	(28.4)	(-0.9)	(-0.3)
Radiating Elements (20 Req.)	6.0	28.5	0.0	0.0
Divider - 5 Way	0.6	28.0	18.5	2.0
- 5 Way	0.6	28.0	-18.5	2.0
- 5 Way	0.6	28.0	18.5	-2.0
- 5 Way	0.6	28.0	-18.5	-2.0
- 4 Way	1.0	28.0	-16.6	-5.5
Co-ax Cable, Guides & Misc.	10.6	28.5	0.0	0.0
Wiring, Cables, Connectors & Misc.	3.2	26.0	0.0	0.0
TOTAL - COMMUNICATION	57.0	29.6	0.5	-1.9

TABLE 7-4 Continued

REMOTE MANEUVERING UNIT
(RMU)
DETAIL WEIGHT STATEMENT

ITME	WEIGHT (LBS)	CENTER OF GRAVITY		
		X	Y	Z
Attitude Control Subsystem				
Sun Sensor - #1	0.5	59.5	0.0	-26.0
- #2	0.5	2.0	0.0	26.0
Solar Aspect Sensor - D1	0.4	58.7	-18.0	18.0
-D2	0.4	33.2	0.0	27.5
- D3	0.4	30.0	-24.5	-12.5
- D4	0.4	30.0	24.5	-12.5
Attitude Control Logic Electronics	5.0	23.1	19.3	11.4
Nutation Accelerometer - #1	1.5	23.5	20.5	-12.2
- #2	1.5	24.0	-20.5	12.2
Dual Purpose Gyro - #1 Yaw	9.0	29.0	-21.0	4.6
- #2 Pitch	9.0	29.0	21.0	-4.6
- #3 Roll	9.0	32.5	-11.0	20.5
Despin Mechanism	17.0	37.2	0.0	0.0
Despin Mech. Controller	4.0	23.3	-21.4	8.1
Wiring, Connectors & Misc.	4.0	30.0	-6.0	1.5
TOTAL - ATTITUDE CONTROL	63.0	30.8	-1.8	4.4
Reaction Control Subsystem				
Thruster Module (3 Jet) - #1	3.5	4.0	17.5	-17.5
- #2	3.5	4.0	-17.5	17.5
- #3	3.5	57.5	17.5	17.5
- #4	3.5	57.5	-17.5	-17.5
Tank & Support (Apollo CSM) - #1	7.4	36.0	14.5	14.5
- #2	7.4	36.0	-14.5	-14.5
Distribution & Misc.				
Pressurization	0.5	30.9	-3.3	0.0
Supply	1.5	26.5	-0.5	-1.5
Brackets & Misc	0.6	27.5	-1.2	-1.0
Fill & Drain Valves	0.4	21.5	0.0	-27.0

TABLE 7-4 Continued

REMOTE MANEUVERING UNIT
(RMU)
DETAIL WEIGHT STATEMENT

ITEM	WEIGHT (LBS)	CENTER OF GRAVITY		
		X	Y	Z
Reaction Control Subsystem (continued)				
Pressure Transducer	0.3	25.0	-3.0	-17.5
Filter	0.4	25.0	0.5	-20.0
Miscellaneous	0.5	32.6	0.0	0.0
TOTAL - REACTION CONTROL	33.0	32.6	-0.2	-0.2
Contingency				
Contingency	20.0	30.5	-0.5	-1.5
TOTAL - CONTINGENCY	20.0	30.5	-0.5	-1.5
WEIGHT EMPTY - RMU	456.0	30.5	0.0	0.0
Propellant - N_2H_4	53.0	36.0	0.0	0.0
Pressurant - GN_2	1.0	36.0	0.0	0.0
GROSS WEIGHT - FULL PROPELLANT RMU	510.0	31.1	0.0	0.0

7.2.1.1 Primary Structure

The major elements of the spacecraft structure are identified on the inboard profile shown in Figure 7-1. The primary load distribution structure of the satellite is an inner cylindrical assembly with diameters of 13 and 15 inches at the forward and aft ends respectively. This 20.5 inch long section incorporates a machined ring at the aft end which is the spacecraft half of the "V"-band attach ring joining the spacecraft and the intermediate adapter to the third stage motor. Separation at this plane permits jettisoning of the apogee motor. The primary equipment mounting platform is attached to the forward end of the inner tapered cylinder. Interfacing at the same juncture is a shallow conical adapter which supports the despin drive mechanism. The despin cage is attached to the outer rotor member and the TV camera assembly is attached to the non-rotating body-mounted, inner shaft of the despin mechanism.

The structural concept adopted is considered conventional and is typical of that which has been employed on various spin stabilized satellites which have flown. The structure is to be fabricated from aluminum alloy, and possibly magnesium, each used optimally to provide minimum weight, minimum cost, ease of fabrication, and conservative design margins. Preliminary evaluation of the basic structure indicates that in several cases, material thicknesses will be minimum gages resulting from fabrication requirements, which exceed those thicknesses required to satisfy the structural load requirements.

7.2.1.2 Secondary Structure

A planar shelf assembly, positioned at the forward end of the tapered cylindrical primary structure section, provides for mounting a portion of the vehicle subsystems and the secondary peripherial subsystem mounting shelves, which support the remainder of the subsystems. This primary equipment platform is to be fabricated from 1 inch thick aluminum alloy honeycomb with integral inserts provided to permit attachment of the subsystems. To distribute more of the mass of the subsystems near the periphery of the spacecraft body (for stability reasons) a series of flat equipment mounting surfaces normal to the primary shelf were added. An octagonal configuration was selected as a reasonable compromise between usable surface area/number of panels. These secondary equipment mounting platforms are positioned on the aft surface of the primary platform; the two propellant tanks are placed on the forward side.

To provide mounting surfaces for the attitude control nozzle assemblies, sun sensors, and whip antennas, formed ring frames are used at the ends of the spacecraft body. These 6-inch wide frames, beaded and perforated by lightening holes, are supported by four extrusions attached to the primary equipment shelf at the outer surface of the vehicle, and by a series of tubular struts which tie into the inside diameter of the primary equipment shelf. The four longitudinal extrusions serve as edge attach members for the solar array panels.

Fittings which permit attachment for vertical hoisting of the completely assembled spacecraft will be provided on the forward end of the spacecraft body where the four longitudinal extrusions intersect the upper ring frame.

The solar cell array consists of four removable panel sections which are attached to the spacecraft body along the four longitudinal extrusions and along the flanges of the forward and aft ring frames. The substrate is fabricated from 1/4 inch thick honeycomb panels consisting of aluminum core and fiberglass facing sheets. Although the panels are not primary load carrying structure, they do provide some positioning and stabilizing of end ring frames after installation.

A flat pattern layout of the four panels is shown in Figure 7-3. This drawing defines all of the cutouts necessary to accommodate the various elements which penetrate the solar panels, including: the propellant tank servicing connections, twenty C-band omni-antenna horns, four solar aspect sensors, the L-band planar array antenna and eight of the attitude control nozzles.

An alternative concept for the solar array panels considered two cylindrical sections which would be attached around the periphery to the primary equipment platform. This "belly band" approach has been used on several satellite configurations. The study design investigation concluded that this approach was not favorable for the RMU primarily because of the requirement for the end ring frames to provide a mounting surface for the VHF whip-antennas, RCS engine clusters and the sun sensors. Attachment of solar panels to the end frames would be difficult because of the physical clearance required to permit the cylindrical sections to slide over these equipment items mounted on the end frames. These protrusions dictate that the panels be installed and removed in a radial direction relative to the spacecraft body.

7.2.1.3 Despin Cage Structure

For the despin cage structure a truss system has been configured to provide a structural transition from the 3 docking latches through a 9-point attach interface with the cage support structure on the despin mechanism. A detailed stress analysis will be performed on the cage structure to verify the basic concept. The truss assembly could be either welded or pinned socket type of construction, both of which will be investigated during the design phase of the flight hardware contract. The cage assembly is bolted to a conical adapter assembly which is attached to two surfaces on the outer rotating portion of the despin mechanism. The attach interface with the cage is large enough in diameter to permit installation and removal without disturbing the TV camera/light subsystem.

7.2.1.4 Mechanisms

The general category of mechanisms on the RMU includes the following devices: the spin-despin drive unit for the docking cage, the docking latches, the TV camera gimbal mechanism, the apogee motor "V"-band clamp release device, the apogee motor ejection mechanism, and the VHF whip antenna deployment mechanism. A discussion

of the spin/despin drive unit is provided in Section 7.2.3 of this study report, while that of the docking latch system is provided in Section 7.2.8. A description of all other devices is provided in the following text.

The TV camera subsystem includes two vidicon cameras attached to the non-spinning (spacecraft body mounted) portion of the spin/despin mechanism located near the base of the despin cage (see Figure 7-1). The cameras are supported by a structural turret which aligns one camera with the spin axis of the vehicle. The turret is capable of being rotated 180° which permits either camera to be moved to the centerline position. A wide angle lens on the spin axis and a telephoto lens offset to be in line with the adjacent camera are fixed in position. Thus, the wide angle view is always obtained along the cage spin axis in the critical final docking closure phase. In normal operation the camera turret will not be rotated since either a wide angle or a telephoto image can be obtained by transmitting the output signal of the appropriate camera. Should one of the cameras fail, however, the turret arrangement allows the remaining camera to be utilized for either purpose. The camera turret is driven by a d-c gear motor. For the baseline, a Globe 28 volt gear motor, Model 102A199, was selected. This gear motor will rotate the cameras through 180° in approximately 2 seconds. Other gear ratios could be selected depending upon the rotation period desired. The pivot bearings for the turret may be either a ball bearing configuration or a sleeve type utilizing teflon filled material. Either approach is available state of the art.

A "V"-band clamp release mechanism is used to secure the apogee motor and third stage intermediate adapter to the RMU inner cylinder structure at spacecraft station 7.5 (see Figure 7-1). The formed "V" segment is attached to an outer steel band, the ends of which terminate in a pair of machined fittings. These fittings, 180° apart, are held together by a pair of squib actuated separation bolts, each with dual bridge wires to provide redundancy. The third stage intermediate adapter retains the "V"-band clamp after separation through a series of tether springs. This will insure non-reengagement of the band to the mating surfaces, preclude spacecraft damage, and insure that the band is jettisoned with the motor. This technique is normally used at the attach interface between solid propellant motors and satellites of this type. The "V"-band clamp will be configured to satisfy the dimensional and dynamic constraints determined for the attach interface.

Separation force for jettisoning the apogee motor and adapter is provided by a simple coil spring compressed between the forward end of the motor case and the despin mechanism support cone. The spring is tethered to the motor case, and concentric cylindrical elements provide guided support for the first 6 inches of motor case movement.

Eight VHF whip antennas are mounted on the forward end-ring frame of the body as shown in Figure 7-1. As a result of the physical incompatibility of the whips in their operational position with the boost shroud payload clearance envelope, the antennas will be mounted in a manner which permits folding each whip aft along the outer surface of the RMU. The hinged joints will be spring loaded to rotate the whips to the operational position when the payload fairing is jettisoned. The whips will be folded aft along the

body and constrained by a circumferential cord while the boost 'fairing is being installed. Subsequently the cord will be removed and the whips will bear against the boost fairing structure. Concurrence of the feasibility of this approach was obtained from the payload fairing manufacturer, McDonnell-Douglas.

7.2.1.5 Conclusions and Recommendations

In the stowed configuration, the RMU is entirely compatible with the payload clearance envelope defined for the boost fairing. The cylindrical body has been sized at 55.4 inches which will permit certain items, such as propellant servicing connections, the solar aspect sensors, and the attitude control nozzles which extend beyond the basic body mold line, to remain within the allowable 57-inch payload diameter.

The design studies performed during the course of the study contract demonstrate that the RMU subsystems can be integrated into the baseline configuration defined herein. While minor changes in form factor and mass of subsystem elements may occur, the favorable spin stability margin, following apogee motor separation, should not be affected significantly. The required structural elements and mechanisms are simple in nature, do not require the use of exotic materials or manufacturing techniques, and are therefore well suited to a low-cost/high confidence program approach.

7.2.2 Electrical Power

In the initial phases of the study a number of alternate power subsystem concepts were considered. These are illustrated by the tradeoff-tree shown in Figure 7-4. Selection of the baseline approach, which is indicated on the tradeoff-tree, was based on a thorough examination of baseline mission requirements, program ground rules as well as requirements and constraints imposed by baseline RMU subsystem mechanizations and spacecraft configurations. Some of these considerations relate to the entire power subsystem concept and are discussed in the following text; requirements which impact individual subsystem elements only are covered in subsequent subsections.

Solar cell arrays were selected as the primary power source over-RTG's on the basis of the inherent size, weight and cost advantages. The desire for simplicity, low cost and high reliability made the use of oriented solar panels undesirable; thus, body mounted panels were selected as a baseline.

The power demands of the RMU subsystems were reviewed in detail as a function of mission phase; the results of these investigations are summarized in Table 7-5. Based on this data, a power profile was defined as a function of mission phase as shown in Figure 7-5 which also illustrates the power output of the body mounted solar panels. The method utilized to determine the power output of the panels, as well as a discussion of the related parameters is given in detail in Section 7.2.2.1.
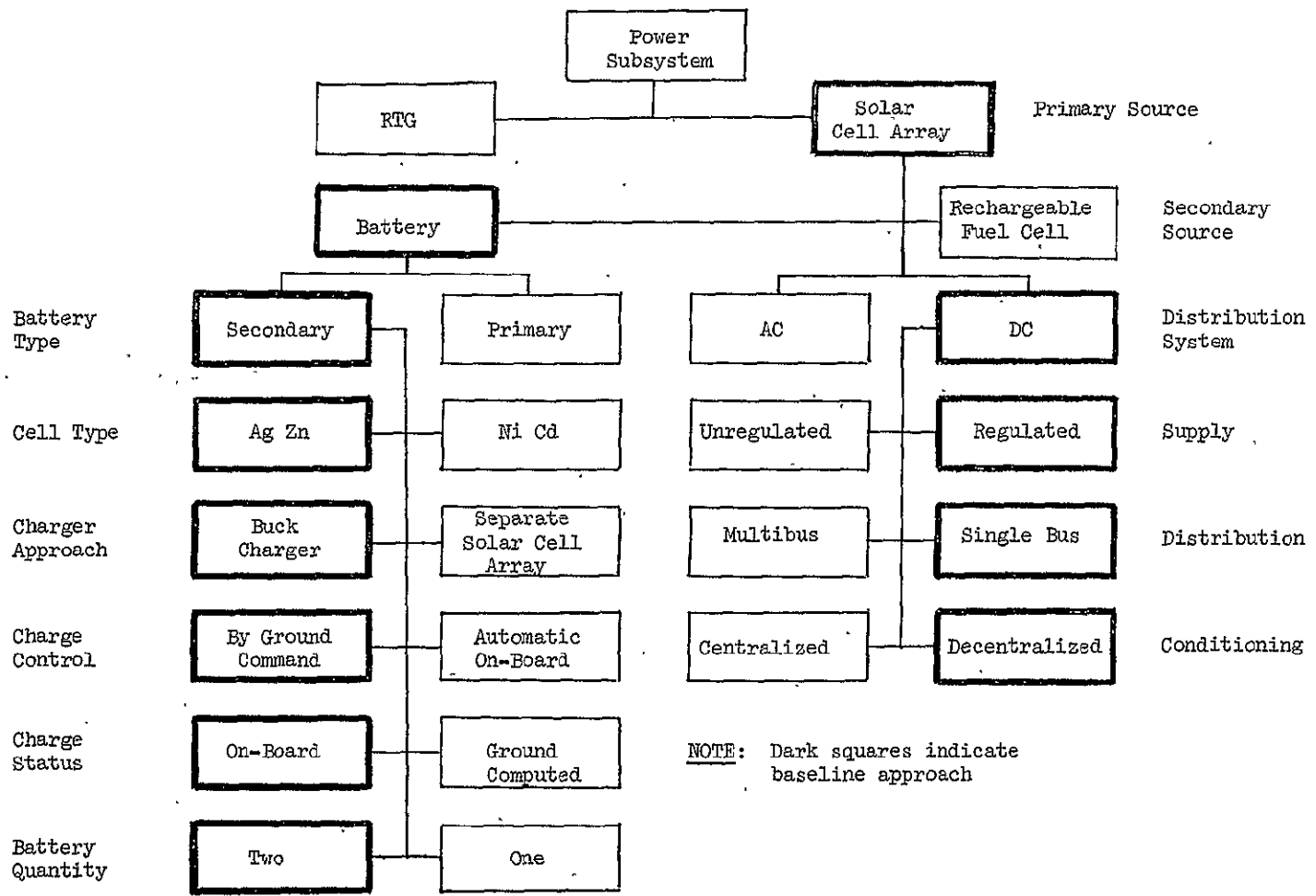
Figure 7-4. Alternative Power Subsystem Mechanization Concepts

TABLE 7-5. RMU POWER DEMANDS

SUBSYSTEM	COMPONENT	POWER (WATTS)	DUTY CYCLE PER MISSION PHASE (%)				
			LAUNCH	RENDEZVOUS	PRE-CONTACT DOCKING	POST-CONTACT DOCKING	OBSERVATION
TELEMETRY & COMMAND	RECEIVER	1.0	100	100	100	100	100
	CLOCK	4.8	↑	↑	↑	↕	↑
	ENCODER	3.1					
	DECODER	2.0					
	TRANSMITTER	5.6	↓	↓	↓	↓	
	SIGNAL CONDITIONER	0.7	100	100	100	100	100
COMMUNICATIONS	TRANSMITTER	18.0	50	50	50	50	50
	REPEATER	5.0	↕	↕	↕	↕	↕
	ANTENNA ELEC.	2.0	50	50	50	50	.50
ATTITUDE CONTROL	ELECTR. & SENSORS	18.5	100	100	100	100	100
	DPG MOTORS						
	START	60.0		10 Min.			
	RUN	36.0		100	100	100	100
	DPG TORQUERS	8.0		20	1	40	1
	DPG RESOLVERS	5.0		100	100	100	100
	DESPIN MOTOR	5.0-40.0				8 Min.	
	VALVE DRIVERS	5.0	INTERMITTENT				
VIDEO & ILLUMINATION	LIGHT ASSEMBLY	100.0			70	30	50
	TV CAMERAS	12.0		100	100	100	100
	STEPPER MOTOR	28.0	EMERGENCY ONLY				
REACTION CONTROL	PRESS. TRANSDUCER	0.3	100	100	100	100	100
	VALVES	15.0	INTERMITTENT				
PROPULSION	INITIATORS	140.0	One Pulse				
ELECTRICAL POWER	DPG INVERTER LOSSES						
	START	33.0		10 Min.			
	RUN	9.0		100	100	100	100
	BATTERY CHARGER	78.0	24 Hrs.				
	BATT. STATUS MONITORS	0.2	100	100	100	100	100
	REGULATION / DISTRIBUTION	5%	100	100	100	100	100
MISCELLANEOUS	CONTINGENCY	10%	100	100	100	100	100

-176-
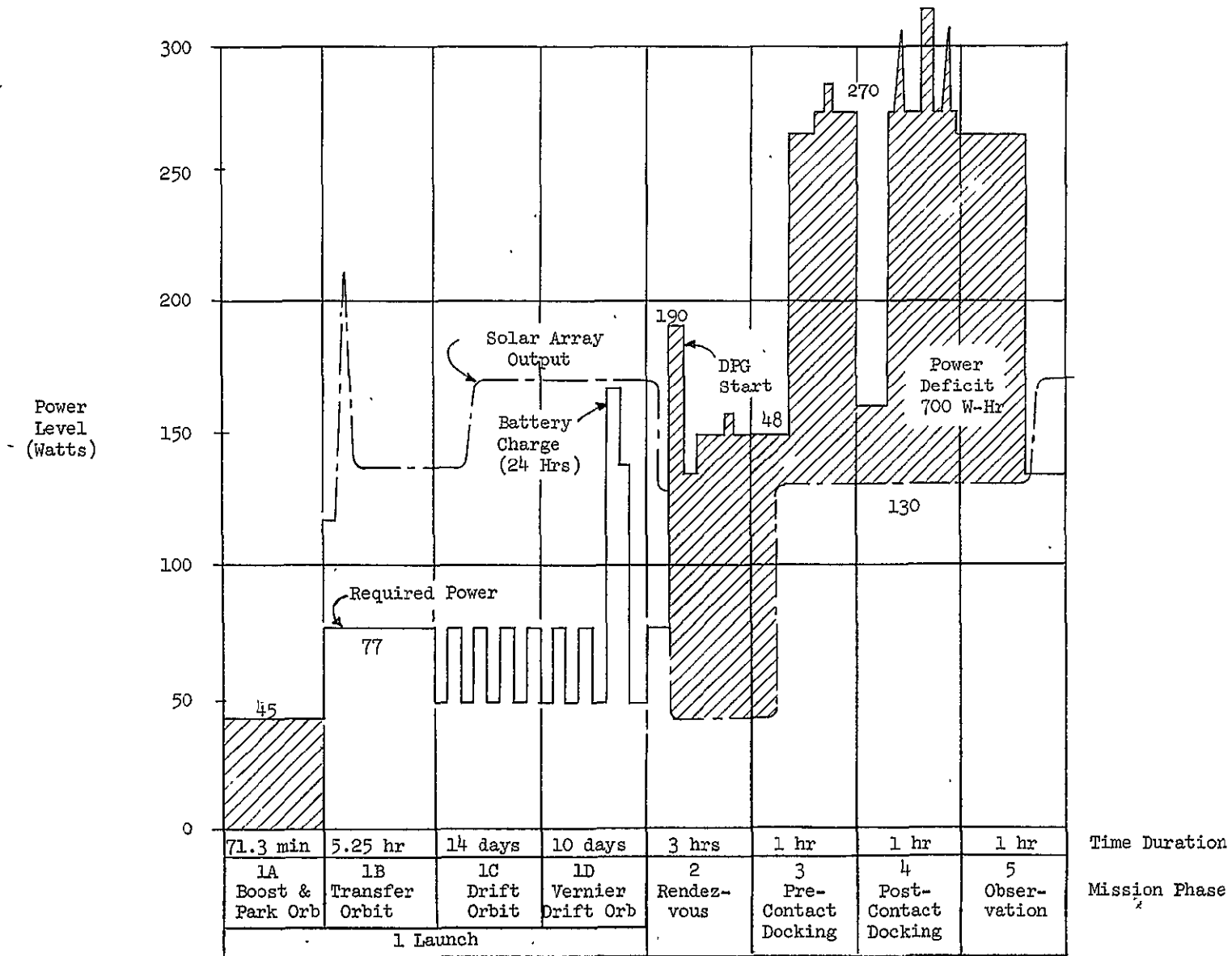
Figure 7-5. RMU Power Profiles

As shown in Figure 7-5, the power demand significantly exceeds the solar panel output during those mission phases where the RMU is not spinning. The power deficit of approximately 700 watt-hours defines the requirement for a secondary power source of significant magnitude. Batteries were chosen for this purpose over rechargeable fuel cells due to the lack of available space-proven hardware in fuel cells.

Selection of the specific baseline battery as well as that of the battery charger, charge control and status monitor are discussed in Section 7.2.2.2. Considerations related to selection of the baseline distribution and conditioning concept are given in Section 7.2.2.3. Figure 7-6 shows the block diagram of the baseline power subsystem.

7.2.2.1 Solar Panels

The RMU solar array design must develop maximum power output in order to minimize required battery capacity. Maximum power capability is determined by spacecraft design considerations which limit the array to a cylindrical configuration of 67 square feet total area. Area allowance for equipment clearances and assembly fasteners is established as follows:

C-band omni antenna horns (20)	180 in^2
C-band high-gain antenna assembly (1)	120 in^2
Solar aspect sensors (3)	39 in^2
RCS thrusters (8)	47 in^2
Miscellaneous umbilicals	24 in^2
Rim borders	86 in^2
Panel borders	224 in^2
TOTAL	$720 \text{ in}^2 = 5.0 \text{ ft}^2$

Thus, the usable body area is 62 square feet; assuming a 10 percent loss factor for intercell and cell connector clearances and application losses, the net cell area is approximately 56 square feet. Based on this the average projected cell area which can be illuminated by the sun at any given time is approximately 18 square feet.

The spatial attitudes of the RMU influence sun aspect angles which impact the power available at any instant. The principal aspect angles are diagrammatically shown in Figure 7-7 where, for convenience in presentation, the time base is non-uniform (equal space per mission phase). Sun angles are in degrees off normal and the zero ordinate is arranged such that the plot provides an indication of relative affect on power output. Since, for the baseline mission, RMU launch and ATS despin is assumed to occur just prior to Autumnal equinox, the solar aspect angle approaches zero degrees as the mission progresses.

Solar Panels

λ_1 λ_2 λ_3 λ_4

-43/-32 VDC

Battery
Charger

-37/-39 V

Charge-
Discharge
Control ← Command

Regulator

-28 + 0.1 VDC
Regulated Bus

400 Hz
Inverter

1 ∅   3 ∅   To S/C
              Sub-
              Systems

115 V to DPG's

Battery
Status
Monitor

Battery
Status
Monitor

-29/-37.1 V

Battery
#1

Battery
#2
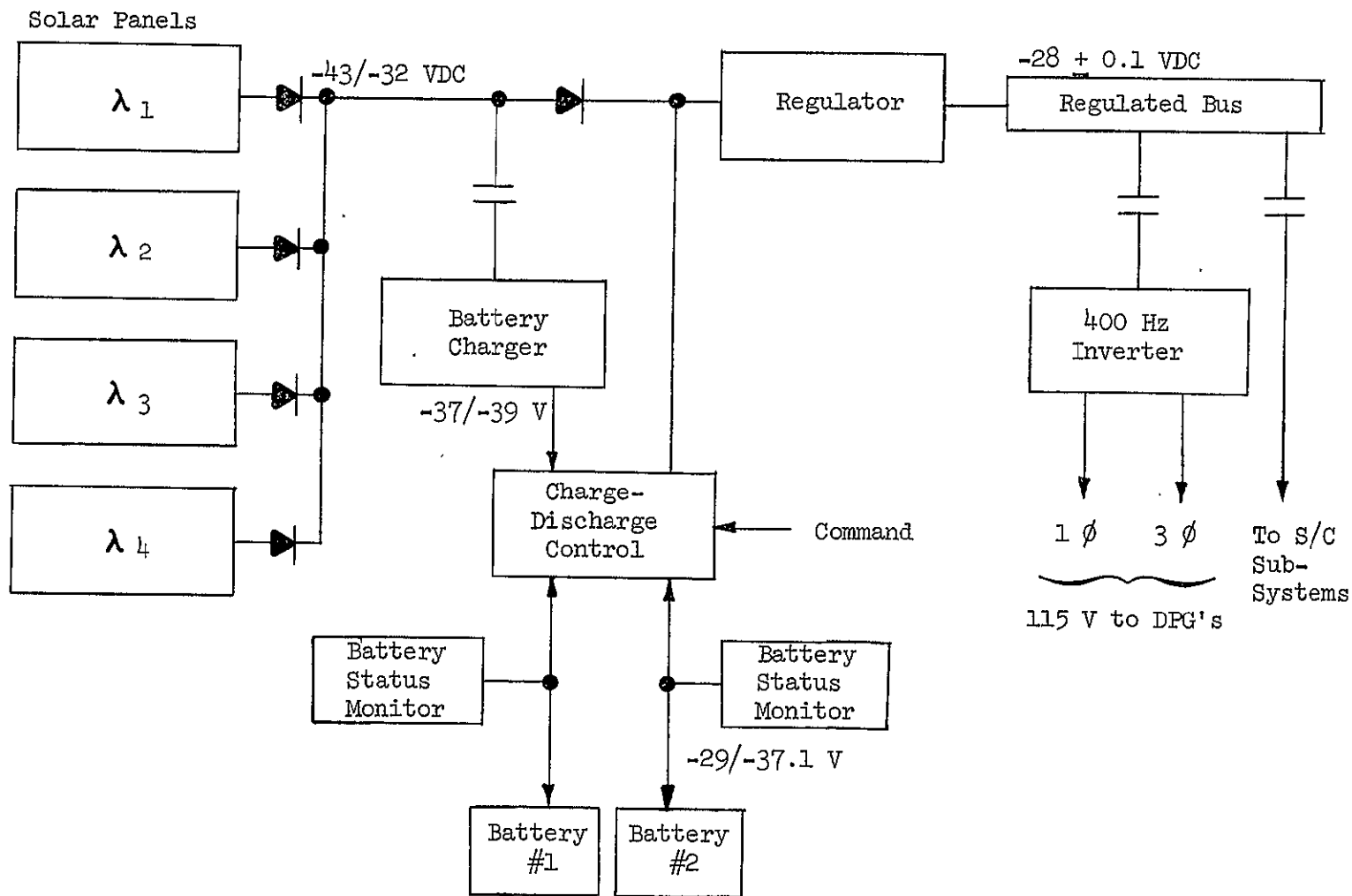
Figure 7-6.   RMU Power Subsystem

Sun Aspect Angle
(Degrees off Normal)

Umbra

RMU Spinning

RMU Despun

RMU Spinning

0
10
20
30
40
50
60
70
80
90

71.3 Min	5.25 Hr.	14 Days	10 Days	3 Hrs.	1 Hr.	1 Hr.	1 Hr.	Long	Duration
1A Boost & Park Orb.	1B Transfer Orbit	1C Drift Orbit	1D Vernier Drift Orb.	2 Rendez-vous	3 Pre-Contact Docking	4 Post-Contact Docking	5 Obser-vation	In-Parking Orbit	Mission Phase

1 Launch
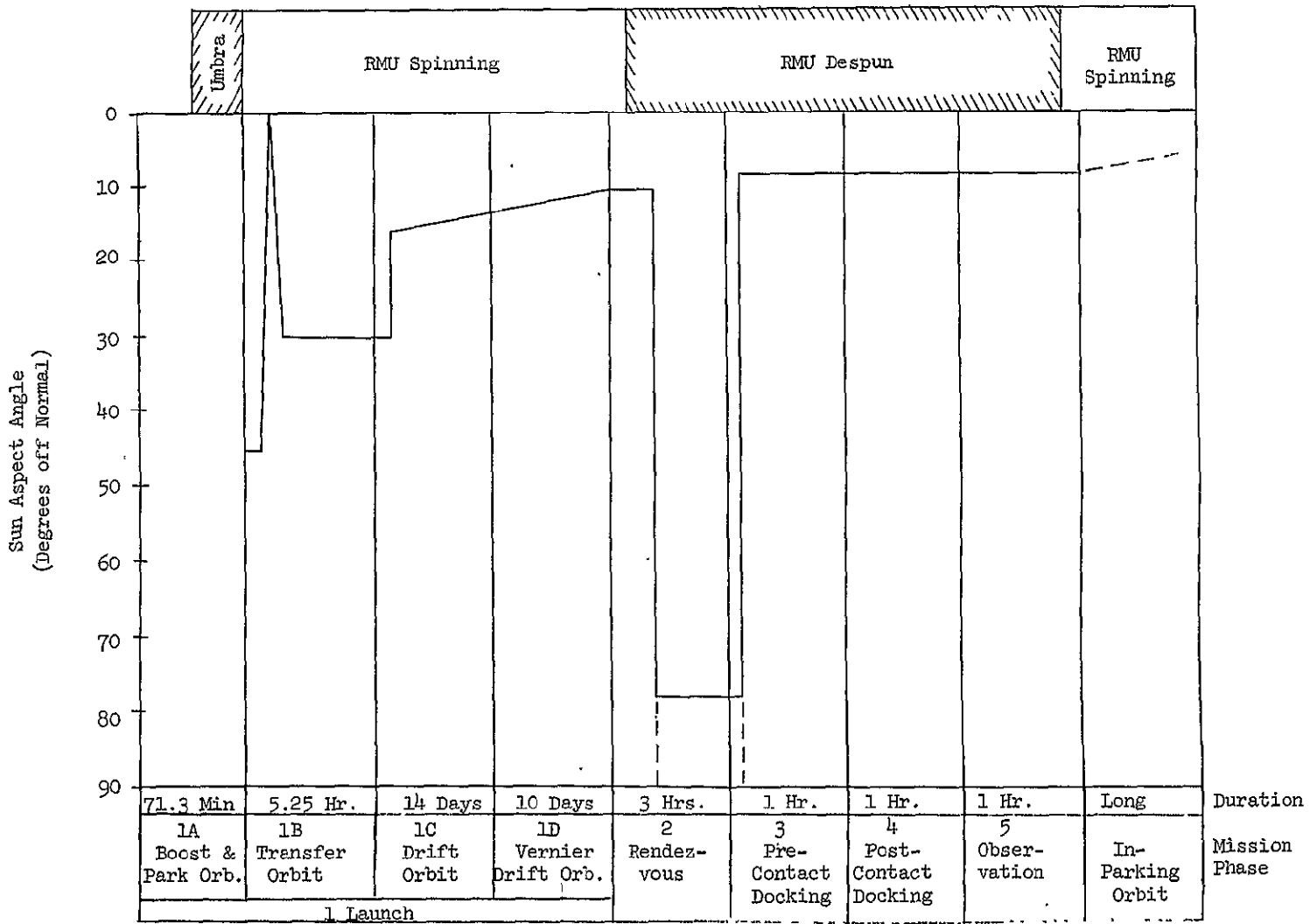
Figure 7-7. Sun Aspect Angle on
RMU Solar Panels

Space Division
North American Rockwell

The only umbra passage encountered occurs during the latter stage of the boost phase in the 100 n.m. parking orbit. All power during this umbra will be provided by the RMU batteries. Spacecraft attitude is altered twice during Phase I operations: the first time to attain proper attitude for apogee motor firing, and the second time to align the spin axis normal to the orbit plane after jettisoning of the apogee motor. In-Phase 2 the RMU is reoriented for visual acquisition of and closure to the ATS-V. Next, during Phase 3, the RMU is turned to face the aft end of ATS-V.

Solar array output is also significantly affected by the temperature of the array. The "barbecue" affect attained when the RMU is spinning results in favorable low temperatures and increased power output over that attained in the despun mode. Figure 7-7 indicates the spinning and despun modes as a function of mission phase. Array temperature is also a function of solar aspect angle.

An NR-developed computer program was used to compute panel temperatures as a function of these parameters. The cylindrical array was simulated as consisting of 12 appropriately oriented one square foot panels, either spinning or despun as a function of mission phase. The computer program produces CRT printouts of which Figures 7-8 and 7-9 are typical examples for the spinning and despun phases, respectively. Operating temperatures of the array were computed to be as follows:

Sun Angle (Degrees Off Normal)	Temperature (C^o)	
	Spinning	Despun
0	17.0	70.6
10	15.8	63.1
16	14.5	57.4
23.5	12.7	48.8
30	10.8	--
78.5	--	17.7

Characteristics of the cell/coverslide system selected as most cost effective and appropriate for the RMU design are as follows:

Cell type	N/P Silicon
Cell size	2 x 2 cm
Cell thickness	14 mils
Bulk resistivity	2 ohm-cm
Coverslide material	Microsheet
Coverslide thickness	6 mil
Anti-reflective coating	SiO_x (or TiO_x)

PANEL TEMPERATURES, DEGREES C

0627-01-01
0020 0000

30.0
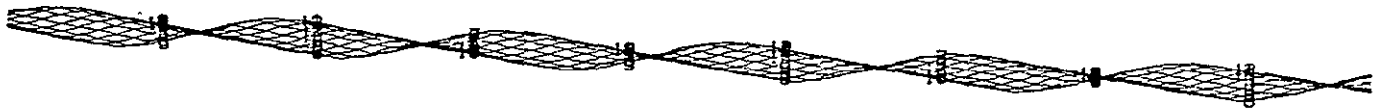
20.0

MISSION HOURS

Figure 7-8. Typical CRT Printout of
Panel Temperature -- Spinning Mode

-182-

SD 71-286
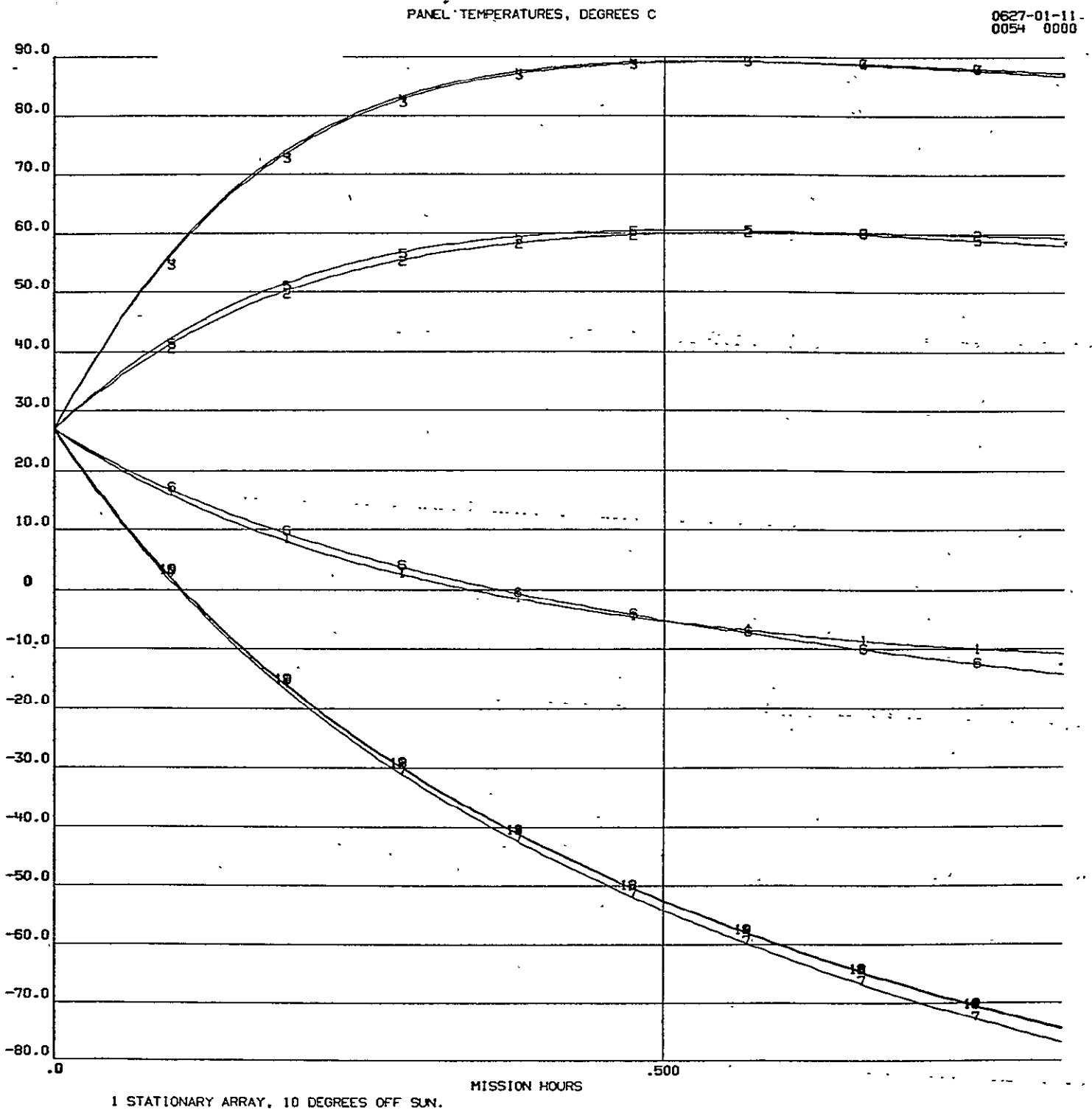
Figure 7-9. Typical CRT Printout of
Panel Temperature -- Despin Mode

SD 71-286

The 2 x 2 cm N/P silicon cells were selected since, per information provided by Centralab and Spectrolab (Heliatek), they are the most cost effective for this application. The low resistivity 2 ohm-cm cells were chosen as a baseline since they offer a voltage advantage (fewer cells in series) over high resistivity cells; this is illustrated in the following comparison of representative cells (at 25°C):

	2 ohm-cm cell	10 ohm-cm cell
Nominal volts	485 mv @ 60.1 mw	430 mv @ 56.8 mw
Open circuit volts	585 mv	550 mv
Short circuit current	142 ma	145 ma

On the basis of the above data the RMU solar array requires approximately 150 strings of 92 cells each in series, arranged in parallel groups for higher reliability. This arrangement will require approximately 13,700 cells.

Degradation influences on this array should not be severe considering the short parking orbit with majority time at synchronous orbit. Degradation factors are estimated to apply as follows:

Ultraviolet	4%
Series Resistance	3%
Standard Cell Errors	2%
Penetrating Radiation	1%
Micrometeoroids	0.5%

Based on the above parameters of the baseline RMU solar array design, the total specific power output (watts per square foot) of the array was computed for each mission phase as a function of solar aspect angle in the spinning and despun modes. Typical CRT printouts of the NR-developed computer program are shown in Figures 7-10 and 7-11 for the spinning and despun modes, respectively. The array power output profile is shown in Figure 7-5.

7.2.2.2 Battery and Battery Charging

The baseline mission profile calls for RMU launch and completion of ATS-V despin prior to the onset of the once-per-orbit eclipse periods caused by the Autumnal equinox. Nevertheless, prudent engineering practice requires that provisions be made for survival of at least one such equinox period thus permitting the despin operation to be performed after the eclipse season has passed. This consideration calls for a battery which can be recharged a number of times. Thus, referring to the tradeoff tree of Figure 7-4, the approach chosen for the baseline concept utilizes a secondary battery.

INDIVIDUAL PANEL POWER OUTPUTS, WATTS/SQ.FT

0627-01
0019 0
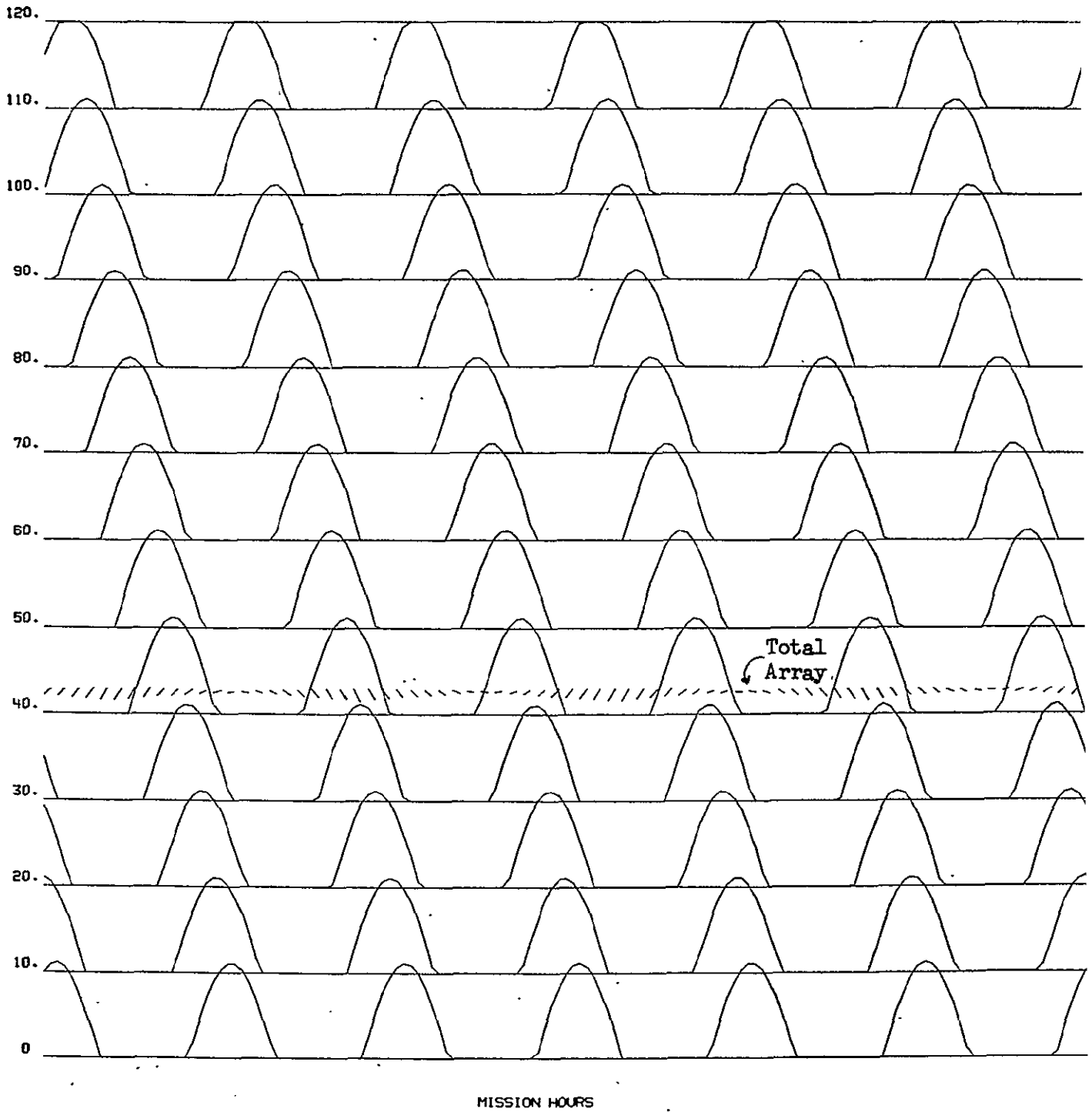
Figure 7-10. Typical CRT Printout of
Panel Power Output -- Spinning Mode

-185-   SD 71-286

INDIVIDUAL PANEL POWER OUTPUTS, WATTS/SQ.FT
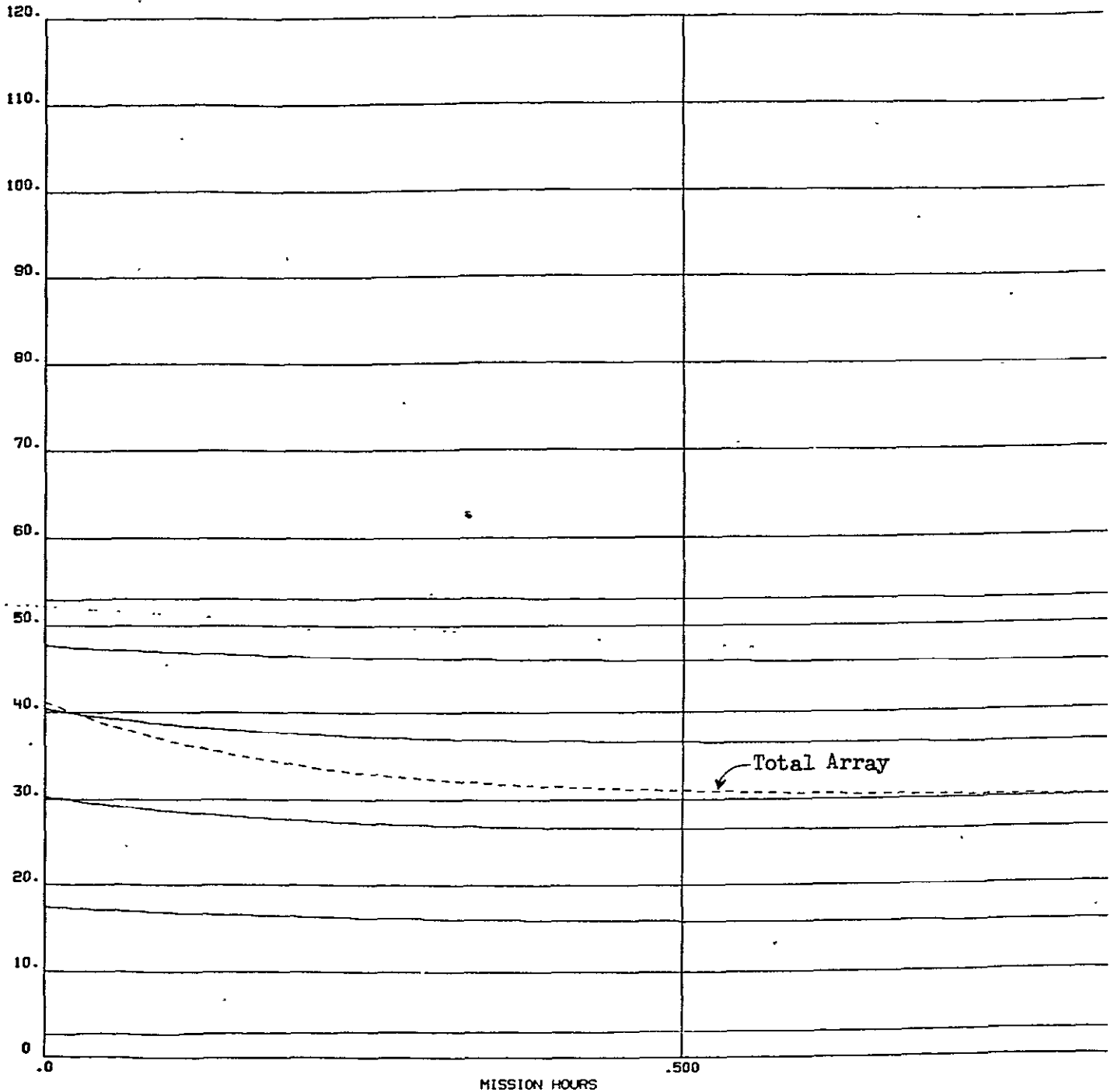
1 STATIONARY ARRAY, 10 DEGREES OFF SUN.

Figure 7-11. Typical CRT Printout of
Panel Power Output -- Despun Mode

The battery must supply all power requirements of the spacecraft in excess of solar array capabilities during the despun phases of the mission. As shown in Figure 7-5, approximately 700 watt hours of energy is required from the battery. This 700 watt hour demand requires a 1400 watt hour battery, operating at 50 percent depth of discharge. Assuming nominal 30 volt batteries, this requirement is the equivalent of a 47 ampere hour battery.

Despite heavy recent R&D efforts, batteries more than any other power subsystem component have generally poor failure records. Although described as the auxiliary (secondary) power source, full battery performance is, in the selected concept, requisite to mission success. Thus, for the baseline concept the approach of utilizing two batteries, rather than one, has been selected. The utilization of two batteries allows one of them to remain on the line at all times while the other is being charged; the desired reliability through parallel redundancy can also be attained by this approach if each battery has adequate capacity.

Weight optimization is, in general, not the primary consideration on this program. The relatively large battery capacity requirement coupled with the desire to provide battery redundancy, makes weight nonetheless a major selection criteria for batteries. Flight proven AgZn batteries in the 40-65 ampere hour range weigh on the order of 28 to 35 pounds. Thus a redundant set of AgZn batteries weighs 56 pounds at a minimum, and the approximate weight penalty of 100% resulting from the use of NiCd batteries is a major weight factor.

As shown in Figure 7-12, however, discharge/charge cycle considerations are heavily in favor of NiCd batteries over AgZn units. Silver-cadmium batteries offer a compromise solution in this respect but are very sensitive to thermal control and charge control conditions. Assuming discharge accumulations (postponement of recharge) to approximately 50 percent depth of discharge during the eclipse season, a minimum of six discharge/charge cycles are necessary for the baseline mission. A review has revealed that space proven AgZn batteries with 6, 10, 30 and even 250 discharge/charge cycle capabilities are available.

On the basis of these factors the selected baseline approach utilizes two AgZn batteries. The specific battery chosen is the Eagle-Picher Industries Model MAR4265-5; this unit is fully qualified and in current use on Apollo. The battery characteristics are as follows:

Rated Capacity: 40 amp-hr
    (at low rate)

Number of cells: 20
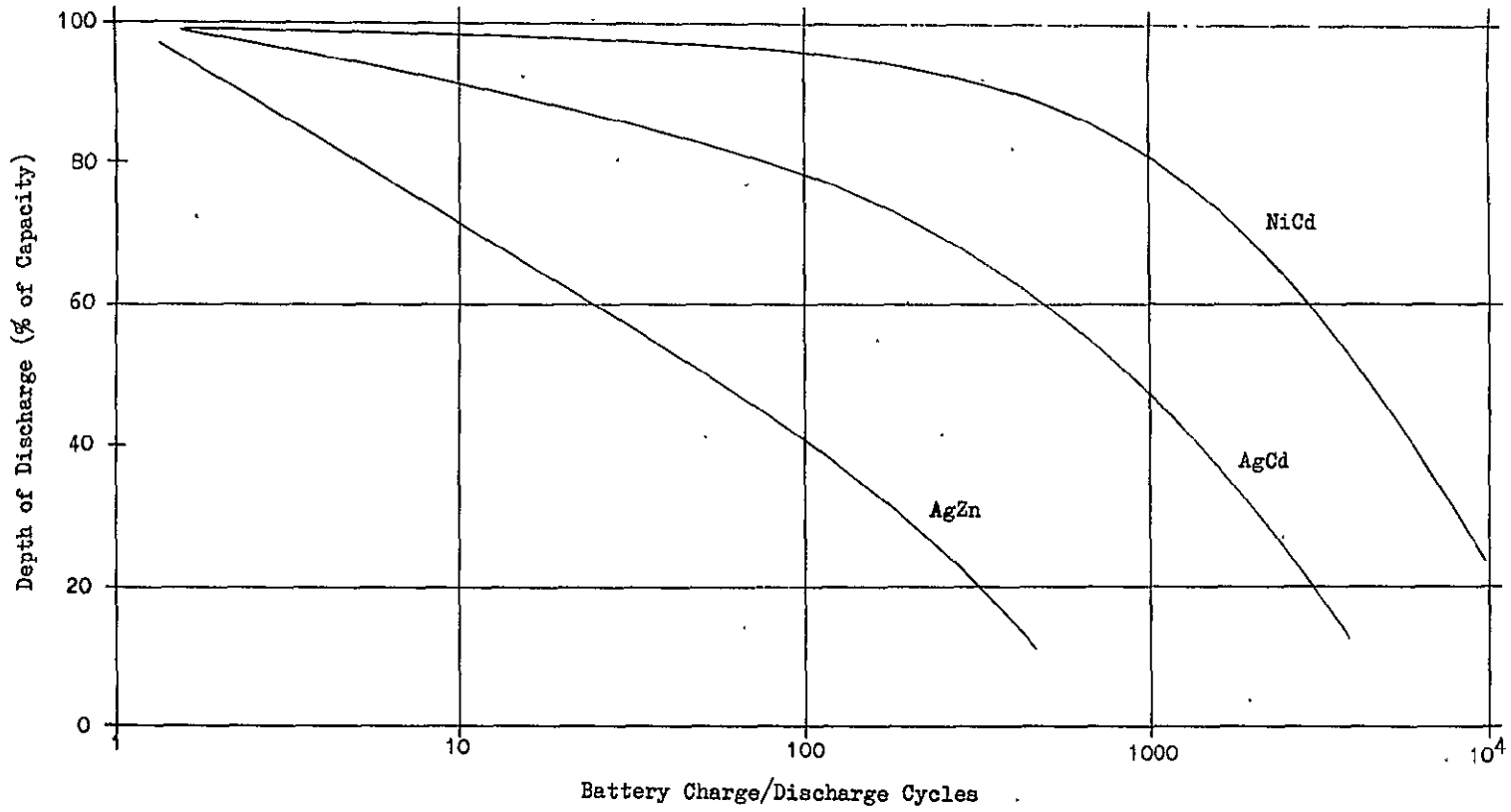
Figure 7-12. Battery Cycle Life

Voltage:
Maximum:	39.1 volts
Open circuit:	37.1 volts
Nominal operating:	30.0 volts
Final:	28.6 volts

Wet Life:	1 year

Cycle Life:
Specified:	9 @ 50% discharge
Lab. Tested:	30 @ 100% discharge

One of the approaches considered for battery recharge is similar to that utilized in ATS-V: since the solar array produces power excess during spin-mode operations, the array can be arranged in two sections so that one portion can be shorted out to reduce voltage and power available when battery charging is not desired. This approach does not eliminate the need for limiting of charging current, while it increases array complexity. Thus, this approach was discarded in favor of utilizing a space qualified combination series (buck) regulator/current limiter device which does not require rearrangement of the solar array. The selected series regulator designed and qualified for the Airlock Vehicle will be utilized as a constant potential battery charger without modification. The current limit point can be set in the range 0 to 1.5 amperes, and voltage regulation within ± 1% is provided with input voltage, load and temperature variations. External resistance may be added to effect two level current limit control should low level float or trickle charging prove desirable.

Since the AgZn batteries have a relatively limited cycle-life, discharge of each battery will proceed to the 50 percent level before recharging will be accomplished. Automatic on-board recharge control is not well suited to this mode of operation. Thus the selected approach utilizes ground commands for initiation and termination of charging either battery. To supplement and enhance the accuracy of ground computation for determination of charge status, separate on-board status monitors are utilized for each battery. For the baseline concept the Model 925 LRV-2 monitors, made by Curtis Instruments, have been selected. These units were qualified for the Lunar Rover Vehicle. The selected concept allows both batteries to be recharged from a 50% discharged state in less than 24 hours.

7.2.2.3 Power Distribution, Conditioning and Regulation

The ATS-V communications and telemetry/command gear utilized on the RMU contains its own power conditioning and regulation equipment and is designed to operate from a DC bus at -24.5 to -32.5 volts. All other RMU subsystems, with the exception of the motors and pickoffs of the DPG's, are compatible with a negative DC supply.

Thus, referring to Figure 7-4, for the baseline design a DC primary distribution system was selected nominally operating at -28 volts; separate AC power is supplied to the DPG's. Also, for uniformity of approach with the ATS-V equipment, the baseline design utilizes a decentralized voltage conditioning concept: where individual components of RMU subsystems require conditioning beyond that provided by the DC bus, such conditioning is provided on the subsystem level.

By utilizing appropriate current limiting and fusing at the loads, a single DC bus should provide adequate mission success probability and this concept is therefore used in the baseline design. Wide voltage swings (0-75v) of the array and battery supply circuit dictate some degree of regulation for the main supply bus. A simple voltage limiter circuit is essentially all that is required for this application (as in the ATS-V). However, thermal control problems and power losses can be minimized by utilizing a non-dissipative regulating method which retains the power within the source. In view of the availability of such a non-dissipative space qualified regulator, this approach of voltage control was selected for the DC bus in the baseline design.

The baseline regulator is Model EMVR 161, made by the Electro-Magnetics Division (EMD) of Gulton Industries for the Skylab program. This regulator consists of a free-running switching mode (PWM) regulator module that is supplemented with power supply and drive converter modules. Nominal rated input from solar array or battery is in the range of 33 to 48 volts; maximum rated array voltage is 125 volts. Load voltage must be lower than input voltage, but can be set over a range of 24 to 30 volts with $\pm$ 0.1 regulation regardless of load resistance. Should a detailed load analysis show the desirability of regulating the DC bus at other than -28 volts, the selected regulator can readily provide this flexibility.

The inverter selected for providing AC power to the DPG's is Model EMIR 200A made by the EMD of Gulton Industries. This solid state inverter provides 400 Hz three-phase quasi-square-wave power to the DPG motors and 400 Hz single phase excitation to the DPG gimbal angle pickoffs; overall inverter efficiency is 80% (excluding motor runup). The inverter, although not space qualified as a unit, utilizes previously space proven modules and has been built and laboratory tested in a flight-packaged form for a prior NR project involving DPG's.

7.2.2.4 Conclusions and Recommendations

The preceding power subsystem discussions were based on an early and very conservative assumption that a total of 6 hours will be needed to complete mission phases 2 through 5; on this basis a battery capacity of 700 watt-hours was indicated. More current results of pilot-in-the-loop simulations and updated tracking accuracy calculations indicate a definite probability of a significant reduction in the required time duration for these mission phases. Indications are that a 50% reduction in required battery capacity may be realized. This would possibly make the use of NiCd rather than AgZn batteries a more advantageous choice, thus gaining extended mission and cycle life within present weight estimates.

7.2.3 Attitude Control

This section presents a description of the baseline RMU attitude control subsystem (ACS) and some of the rationale for the subsystem concept selection. Mission requirements, control mode definitions and descriptions, system performance data, mechanization considerations, and component data are included.

The RMU is a fully maneuverable spacecraft and, as such, requires three degrees-of-freedom (DOF) in attitude and three DOF in translation. The thrusters of the reaction control subsystem produce some of the related control torques and all of the necessary translational forces. The required thruster select logic is an integral part of the attitude control subsystem; thus the ACS is involved in control of attitude as well as control of translation. In the following text both of these ACS functions are discussed.

The primary requirements and constraints which govern the basic nature of the baseline ACS are a direct derivative of the type of stabilization technique selected for the various RMU mission phases. Choice of stabilization technique was based on a thorough examination of program ground rules, mission requirements, and analytical/developmental data available from prior NR efforts related to RMU type vehicles. A summary of the selected concept as a function of mission phase is given in Table 7-6; the rationale for the choices made is discussed below.

A spin stabilization technique was selected for all phases from launch through the drift orbit phase for the following reasons:

1. Spin is already provided by the Thor Delta spin table of the second stage.

2. System mechanization costs can be minimized through the use of existing hardware and familiar well-developed techniques. Hardware and software changes for the ground station will also be minimized.

3. The spin stabilization technique provides a simple passive method for thrust vector control during apogee burn, whereas three axis stabilization techniques would require a more complex active thrust vector control system. This approach facilitates the use of an inexpensive existing solid rocket apogee motor without thrust vector control.

For the remaining mission phases three axis stabilization of the RMU has been chosen as the baseline concept. Spinning or "dual spin" RMU configuration was rejected for these mission phases for the following reasons:

1. With contemporary spinning or "dual spin" spacecraft, wobble angles can be stabilized only to the order of 0.1 degrees due to mass balancing limitations. The resultant wobbling TV picture is not considered to be adequately stable to provide the necessary data for the visual acquisition, visually guided rendezvous closure, pre-docking alignment, etc., operations.

TABLE 7-6   STABILIZATION BY MISSION PHASE

MISSION PHASE		INERTIA RATIO ($I_{SPIN}/I_{TRANSVERSE}$)	STABILIZATION TECHNIQUE
Transfer Orbit		0.79	Spin
Apogee Motor Burn		0.79 (Initial) 0.94 (Final)	Spin
Drift Orbit		1.10 (Initial) 1.07 (Final	Spin
Rendezvous		---------	3 Axis Stabilization
Pre-Contact Docking		---------	3 Axis Stabilization
Post Contact Docking	ATS Spinning	0.1733	Energy dissipation in de-spun section (RMU) of dual spin vehicle.
	ATS Despun	---------	3 Axis Stabilization
Observation			

2. On spinning or "dual spin" spacecraft, attitude maneuvering produces nutation which cannot be damped rapidly without the use of relatively large nutation damping mechanisms. During periods with significant nutation, the wobbling TV picture would again be of questionable value in the above critical operations.

3. During the final phases of the docking closure the pilot must have a rapid-response, essentially real-time command capability. This is difficult to attain on spinning or "dual spin" spacecraft due to the nutational coning which follows each attitude control torque application. For this reason, in the baseline concept all attitude maneuvering is done prior to cage spinup. After cage spinup, the RMU becomes a "dual spin" configuration even though cage angular momentum is relatively small. Thus, in the final closure, with the cage spinning, only translational maneuvers are planned, and the "dual spin" effects do not adversely impact this critical docking phase. Similarly, when the RMU is docked with the ATS-V, the three axis stabilized RMU and the spinning ATS-V form a "dual spin" system. During this period the above shortcomings of "dual spin" type vehicles are again not of consequence and the "dual spin" approach provides a convenient method for stabilizing the system without additional hardware.

For implementation of the three axis stabilization and control concept utilization of reaction jets as the only effectors was rejected on the basis that (a) they would not provide sufficient attitude stability for the television camera, and (b) would be lacking in sufficient attitude hold capability for the final docking closure operation and/or for ready pilot identification of relative rotation versus relative translation.

Thus, the use of a momentum exchange type three axis stabilization system was indicated as the most appropriate for this application. The proprietary DPG system developed by NR was found to be an excellent candidate for implementing this approach. The DPG system also eliminates the need for a separate energy dissipation device for stabilizing the coupled RMU/ATS-V "dual spin" configuration in the docked mode. The DPG is a form of control moment gyro capable of stabilizing the RMU to angular rates that are more than an order of magnitude smaller than is available from a pure reaction jet stabilization system. The DPG's are automatically desaturated by reaction jet firings.

As noted in Table 7-6, during the early part of the mission, prior to apogee motor ejection, the ratio of RMU spin-axis/transverse-axis inertia is less than unity indicating the need for active nutation control. The concept adopted for this requirement is the same as that utilized on ATS-V thus providing full compatibility with ground equipment; the same accelerometers are utilized as were used on ATS-V.

-193-

This motivation also prompted selection of the same attitude sensing method and attitude sensors for the baseline RMU design as those utilized on ATS-V; the approach uses POLANG information in conjunction with sun sensors (spinning mode) and solar aspect sensors (three axis stabilized mode) for ground-based computation of RMU attitude.

The concept described above results in the subsystem mechanization given in Figure 7-13. The thrusters of the reaction control subsystem are located and oriented as shown in Figure 7-14 which also defines a basic jet select logic for producing torques and translational forces. Detailed descriptions of each control mode and of the mechanization of the major subsystem elements are given in the following subsections.

7.2.3.1 Control in the Spinning Mode

Active nutation control (ANC) is required during the transfer orbit, apogee burn and post apogee burn phases prior to apogee motor ejection to correct nutation angle buildup. Nutation angle buildup can be expected to occur since the spin axis is the minor axis of inertia and will be unstable in the presence of energy dissipation sources. However, the rate of nutation angle divergence can be minimized through careful design of the RMU subsystems to keep energy dissipation at low levels. Less than 0.6 lb of RCS propellant is estimated for nutation damping requirements.

During the drift orbit phase, following apogee motor ejection, the RMU is spinning about a major axis of inertia and hence is stable without ANC. The ANC can, if desired, be employed to reduce the convergence-time of any nutation excited by precessional or translational thrusting maneuvers.

A functional block diagram of the ANC system is given in Figure 7-15. Nutation is sensed by a pair of linear accelerometers which are located near the outer periphery of the RMU and have sensitive axes parallel to the desired spin axis. Mounted in this fashion, the accelerometers provide outputs proportional to the angular acceleration about the two transverse axes of the S/C. For given vehicle spin rates and inertia ratios, the nutation angle is proportional to the accelerometer outputs. As depicted in Figure 7-15 automatic ANC operation is initiated and cut off by a level detector operating on the accelerometer signals. The jet pulses are phased at the proper place in the spin cycle by detecting the descending zero crossing of the accelerometer output. The descending zero crossing is an easily detectable signal and defines the time at which the transverse body rate is a maximum about the sensed axis. The optimum time to apply jet pulses for rate damping is when the jet torque is parallel but opposed to the body rate.

When enabled, the system provides for automatic initiation of pulsing when the nutation angle exceeds approximately one degree and ceases operation when the nutation angle becomes smaller than 0.5 degree. A manual over-ride of the cut off level detector permits the pulsing to continue until the manual command is removed. With proper calibration, this mode is capable of reducing the nutation angle to less than 0.1 degree.
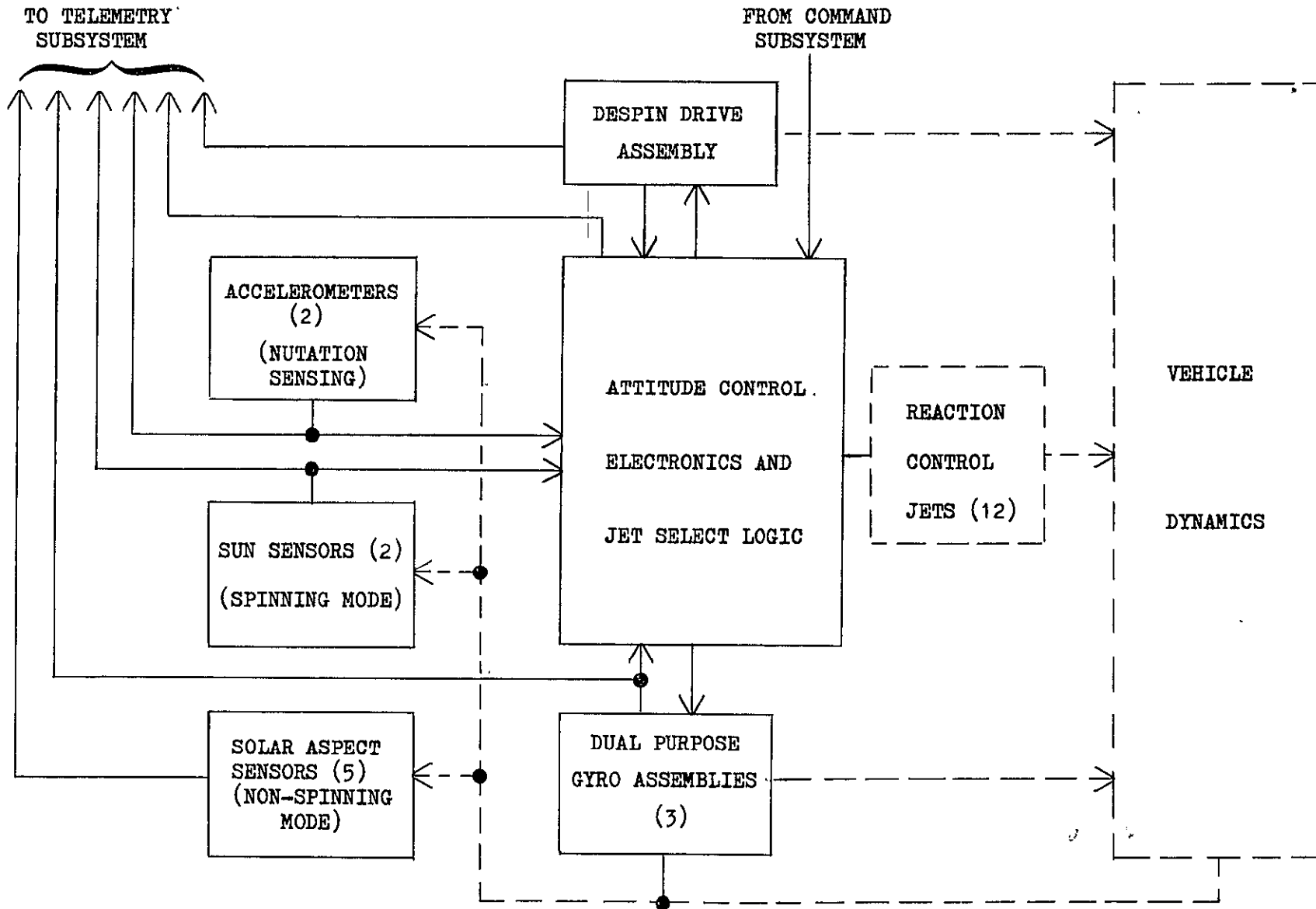
Figure 7-13. Attitude Control Subsystem

19.0" Typ — 18.25" Typ — 26.5" Typ

Front Jets ② ①

Rear Jets ⑦ ⑧

45° 45°

19.0" Typ

18.25" Typ

+Y +X

Despin Cage

⑫ Rear Jets ⑤ Front Jets

⑥

High-Gain Antenna

⑨ ③

⑪ ④

High-Gain C-Band Antenna

+Z
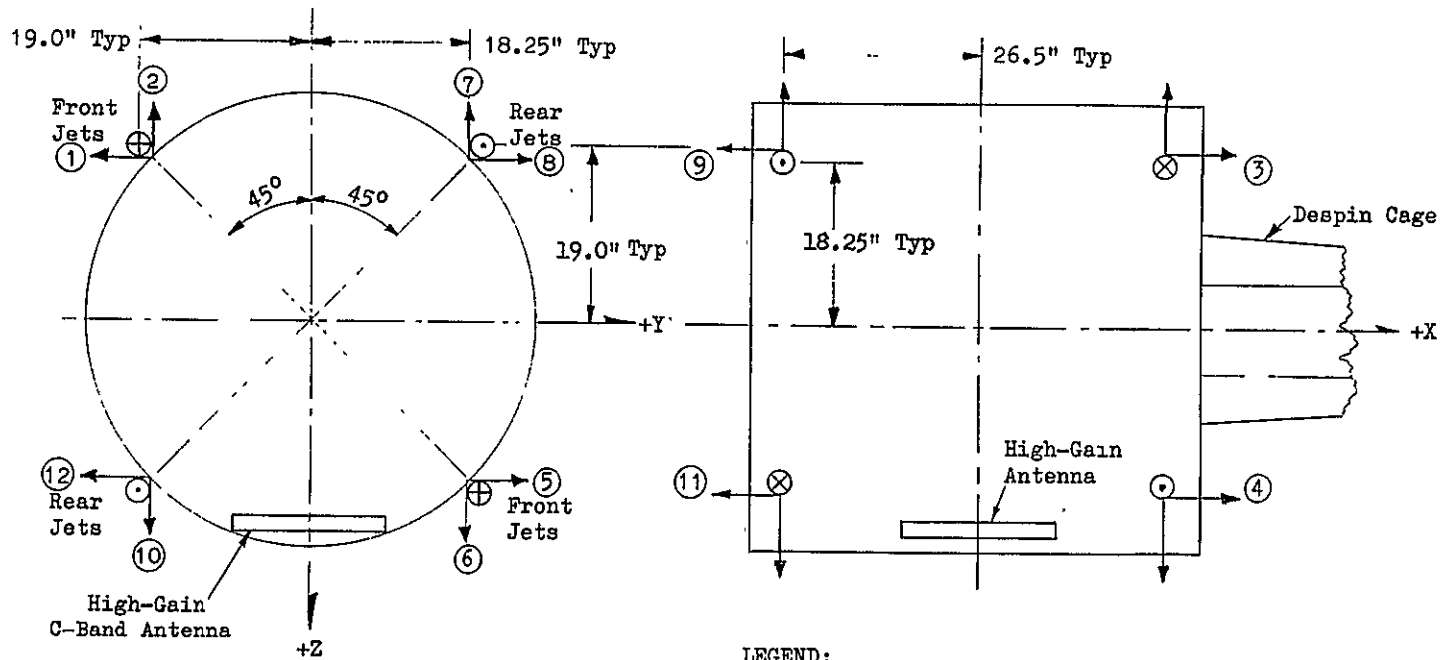
View Toward Aft End of RMU

DIRECTION	JET NUMBER	
	Translation*	Rotation*
+X	9-11	1-5
-X	3-4	2-6
+Y	1-12	3-11
-Y	5-8	4-9
+Z	2-7	1-8
-Z	6-10	5-12

LEGEND:

—→① Nozzle Direction & Jet Identification

⊙ Nozzle Facing Out of Paper

⊗ Nozzle Facing Into Paper

* In case of conflict, rotation has precedence over translation

Figure 7-14. Reaction Jet Configuration and Jet Select Logic

TO TELEMETRY

```
                                          ┌─────────────────────┐
                                          │   LEVEL DETECTION   │
                                          └─────────────────────┘
┌──────────────────┐                      ┌─────────────────────┐    ┌──────────────┐
│  ACCELEROMETER   │                      │       PULSE         │    │ TO JET SELECT│
│ UNITED CONTROL   │                      │    GENERATION       │───▶│ LOGIC AND RCS│
│   (PAL-5706)     │                      │       LOGIC         │    │VALVE AMPLIFIERS│
└──────────────────┘                      └─────────────────────┘    └──────────────┘
                                          ┌─────────────────────┐
                                          │   ZERO CROSSING     │
                                          │    DETECTION        │
                                          └─────────────────────┘
```
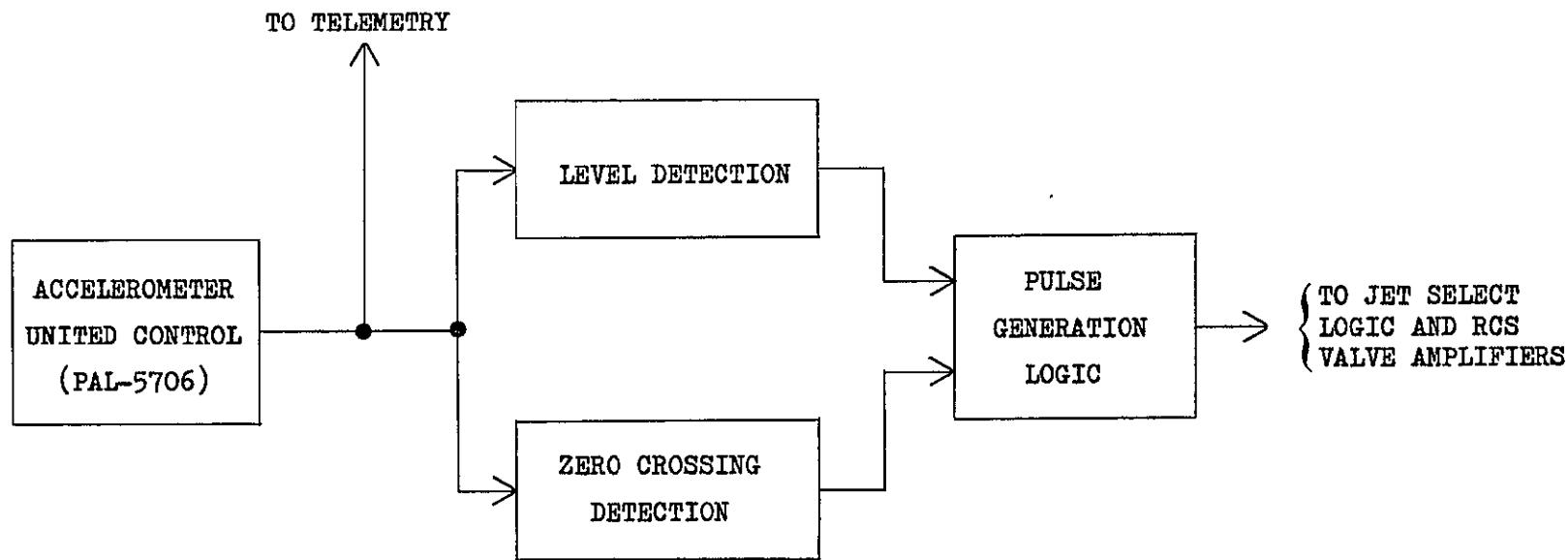
Figure 7-15. Active Nutation Control (Per Axis)

Space Division
North American Rockwell

Re-orienting the spinning RMU to new attitudes requires precessional control. This is achieved by commanding reaction jet torque pulses for approximately 90 degrees of each spin cycle such that the time averaged torque produces precession in the desired inertial direction (see Figure 7-16). The proper direction of the torque pulses during the spin cycle is achieved by phasing them with respect to the sun sensor pulses.

The radial translational thrusting pulses are also phased with respect to the sun sensor pulses to yield the time averaged velocity change in the desired direction (see Figure 7-16). The precession and radial thrusting is achieved with the same control logic by selecting jet pairs which produce either torque or translational forces. As shown in Figure 7-16, the sun pulse triggers the pulse phasing counter which initiates the force or torque command when the count goes through zero. The pulse duration counter commands the thrust off when it goes through zero. Axial translational thrusting does not involve phasing relative to the sun; thus the related ground command is fed directly to the jet select logic.

RMU attitude is determined by ground computation based on (a) data transmitted from the two RMU sun sensors in real-time analog form, and (b) data provided from the tracking stations relative to polarization angle of the C-band spacecraft beacon (POLANG). This technique is identical to that employed on the ATS-V spacecraft.

7.2.3.2 Control in the Three Axis Stabilized Mode (Including "Dual Spin" Mode)

In the three axis stabilized mode of operation pitch and roll maneuvers of the RMU are restricted to approximately $\pm$ 5 degrees relative to the RMU-to-ground station line-of-sight (LOS). This requirement stems from the need to maintain the video transmission link via the high gain C-band antenna array. First-order attitude sensing in pitch and roll will be provided by observation of received C-band signal strength. This LOS will rotate in inertial space as the RMU progresses in its orbit; depending on RMU orientation in specific mission phases (X-axis in orbit plane or normal to it), this rotation of the LOS will necessitate a 15 degree per hour rate to be commanded either about the pitch or the roll RMU axis. The baseline concept calls for this rate to be ground commanded. Additional pitch maneuvers of small magnitude will be required to align the RMU X-axis with the ATS-V spin axis prior to docking. The TV sensor will be the primary sensor in this operation.

In yaw the RMU maneuvers are limited only by a desire of not pointing the TV camera at the sun (even though automatic sun shutters are provided). The primary yaw maneuvers will be made relative to the ATS-V rather than relative to inertial space. The primary yaw attitude data will again be derived from the video image.

As a backup to these attitude references, ground-computed RMU attitude information will be available from telemetered solar aspect sensor data and from POLANG measurements made by the ground stations. This approach and the related hardware selected is essentially identical to those employed on the ATS-V thus affording total compatibility with current ground station hardware and software.
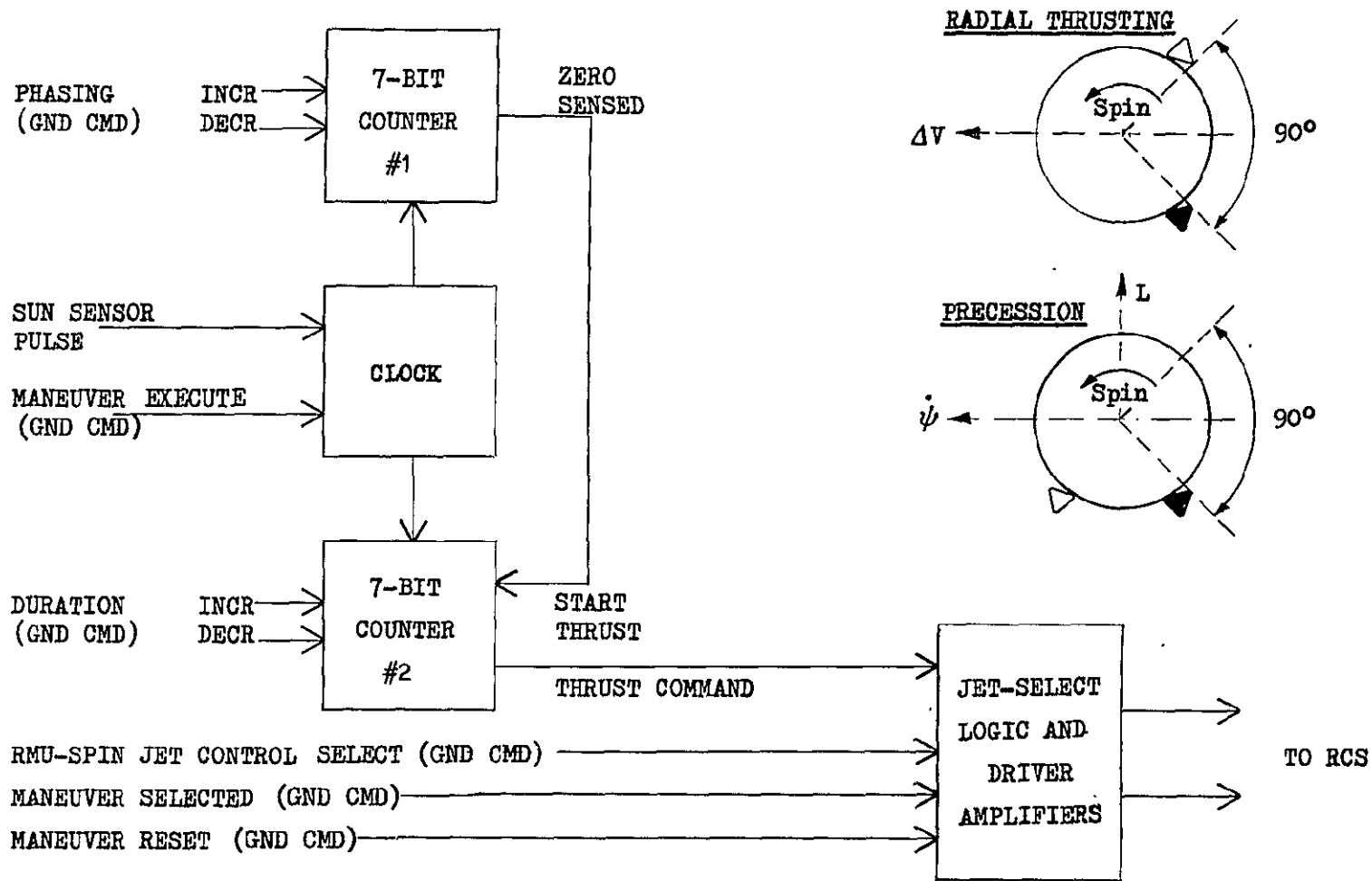
Figure 7-16. Spinning RMU Precession and Translation Control

Translational forces are available along all three of the spacecraft axes. These are manually commanded at the ground station and no control circuitry other than jet select logic is provided onboard the spacecraft. A minimum impulse command capability has been found to be desirable in order to achieve the small translational velocity changes required for precise docking. Minimum thrust pulse durations of 60 milliseconds have been found to be desirable in the RMU piloted docking simulation. In the baseline concept these minimum impulse circuits will be mechanized at the ground station. This capability requires a minimum impulse control mode switch and one shot circuits in the control console capable of producing the 60 millisecond pulse width commands.

The primary attitude control requirements imposed by the 3-axis stabilized operational mode consist of the following:

1. An inertially stable base must be provided for the TV sensor. To distinguish ATS-V transverse relative velocities from apparent velocity due to the attitude motions of the RMU, the attitude drift rates must be an order of magnitude lower than the angular rotation rates of the line of sight.

2. Precise attitude holding capability must be provided for docking (order of tenths of degrees).

3. Attitude maneuver rates and response time constants must be consistent with good pilot control.

4. Roll attitude drift in the presence of reaction torques caused by pre-docking spinup of the docking cage must be minimized to prevent loss of high gain antenna lock-on causing loss of TV image.

5. Following the docking of the RMU with the ATS-V, the RMU must stabilize the "dual spin" vehicle. Without RMU stabilization, the configuration is unstable due to the presence of energy dissipation sources in the ATS-V.

The manner in which the DPG system satisfies the above requirements can best be established by examining some of its basic dynamic properties.

Dual Purpose Gyro (DPG) Description - A DPG is a form of control moment gyro which, due to its configuration, also provides attitude information and automatic (passive) stabilization capability. The manner in which these operational features are achieved is described below. A functional diagram of a single DPG is given in Figure 7-17. Two single-degree-of-freedom gyros are connected by trunnion gears. A brushless d-c torque motor rotates the gimbals in a scissoring fashion so as to produce a vector change in angular momentum along the control axis. The change in angular momentum of the spacecraft body is equal and opposite to the momentum change in the DPG. A viscous fluid is sealed between the gyro gimbal assembly and the gyro case. The viscous fluid provides a torque which opposes the gimbal motion and is proportional to gimbal rate. A resolver is mounted on the gimbal to provide a measurement of the gimbal angle. The electrical gimbal angle signal feeds a solid state switching circuit which in turn commands reaction jet torques about the control axis to desaturate the DPG's.
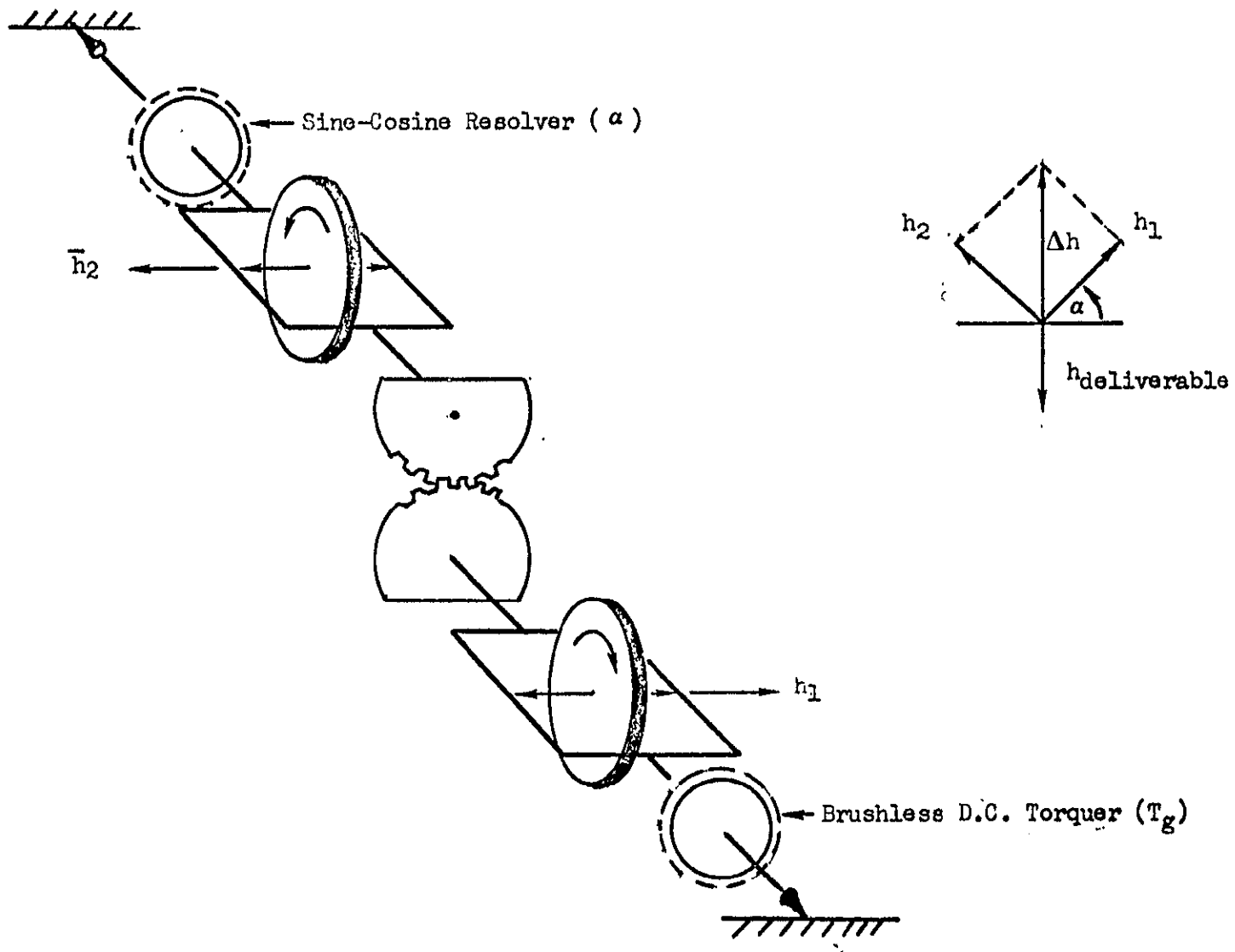
Figure 7-17. Dual-Purpose Gyro

A single axis dynamic model of the DPG is presented in Figure 7-18. The following nomenclature applies:

T_G – torque applied to gimbal by torque motor

I_G – gimbal inertia about gimbal axis of a single rotor assembly (2 rotors per DPG)

b – damping coefficient provided by viscous fluid on a single rotor (2 rotors per DPG)

α – DPG gimbal angle

h – angular momentum of one gyro rotor (2 rotors per DPG)

T_v – torque imposed on vehicle by DPG

T_{rcs} – reaction jet torque on the vehicle

T_e – external torque on the vehicle

I_v – moment of inertia of the RMU

r – RMU attitude rate

The block diagram with its rate feedback loop demonstrates that the system is basically a rate command system and, in the absence of T_G commands, will stabilize the vehicle body rates to zero. This is also evident from the following relationship:

$$T_v = \frac{h \, \text{Cos} \, \alpha}{b} \, (T_G - 2h \, \text{Cos} \, \alpha \, r) \qquad (1)$$

where T_G can be scaled directly in rate command units.

For small α, the system is linear. For reasonable ranges of values I_G may generally be neglected. The resulting system is a linear first order system with a transfer function of:

$$\frac{r}{T_G} = \frac{\frac{1}{2h}}{\tau_s + 1} \qquad \text{or} \qquad \frac{r}{r_c} = \frac{1}{\tau_s + 1} \qquad (2)$$

The system response time constant (τ) is $\dfrac{bI_v}{2h^2}$.

The "scissored" configuration of the DPG's essentially eliminates the cross coupling torques which are inherent in many other control moment gyro configurations. Therefore, a complex control logic to minimize cross coupling is not required.

The following approximate relationship may be derived for the single axis DPG:

$$\phi = \phi_0 + \int_0^t \phi_c \, dt - \left(\frac{b}{h \, \text{Cos} \, \alpha}\right) \alpha \qquad (3)$$
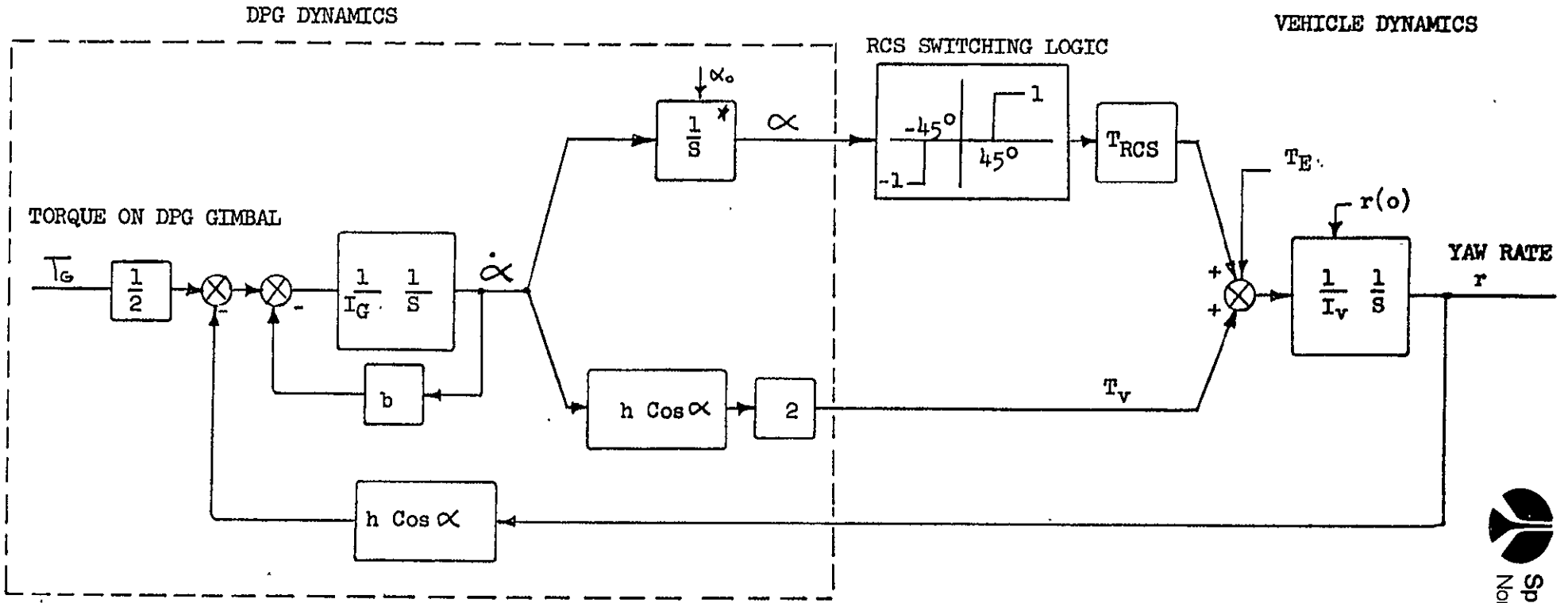
Figure 7-18. Dual Purpose Gyro (DPG), Single Axis Dynamic Model

This relationship demonstrates that attitude information can be computed on the ground using telemetered gimbal angle data (α), rate command data ($\emptyset_c$), and an initial attitude estimate ($\emptyset_o$) from sun sensor and "POLANG" data. The use of this DPG attitude reference algorithm will be particularly beneficial during rendezvous and docking to prevent roll attitude excursions beyond the limits of the high gain antenna with the resultant loss of the TV picture.

The DPG's also provide torques for stabilization of the RMU docked with the ATS-V. From equation (1) above, the torques applied to the vehicle are proportional and in the opposite sense from the body rate. This provides ideal phasing for the stabilization of this "dual spin" configuration. The primary contribution of the DPG's toward stabilizing this "dual spin" configuration, is their inherent capability to dissipate significant energy ·in the despun portion of the configuration. The energy dissipation rate in the two transverse-axis DPG's is given by

$$\dot{E}_{DPG} = -h(\frac{h}{b})\, W_n^{\,2}\, (\cos\alpha)^2\, \theta^2 \tag{4}$$

where W_n is the nutation frequency (frequency of the angular motion observed in the RMU body coordinates) and θ is the magnitude of the nutation angle. For small gimbal angles (α) equation (4) reduces to

$$\dot{E}_{DPG} = -h(\frac{h}{b})\, W_n^{\,2}\, \theta^2 \tag{5}$$

<u>DPG Sizing and Performance Characteristics</u> – The primary DPG design parameters are the angular momentum per gyro wheel (h), the damping constant (b), and the maximum torque load bearing capability that the gimbal and bearing assemblies must be capable of sustaining. The RMU performance requirements which must be considered in determining these parameters are:

1. The RMU attitude maneuver rates must be consistent with good pilot control during rendezvous and docking. RMU docking simulation results indicate that a single discrete level command capability is acceptable and that the pilots prefer rates of approximately 0.6 to 1.0 degrees per second.

2. The attitude maneuver settling time constant must be consistent with good pilot control; pilot-in-the-loop simulations indicate that a time constant on the order of 2.0 seconds maximum is satisfactory.

3. Roll attitude drift during spinup of the docking cage must be limited to less than $\pm 5^\circ$ to prevent loss of high-gain antenna lock-on.

4. The energy dissipation available from the DPG's must be adequate to stabilize the RMU/ATS dual spin configuration. A stability margin must be provided as an allowance for uncertainties in the predicted energy dissipation levels in the ATS-V vehicle.

The fourth requirement has been quantitatively assessed in Section 5.0 where the required energy dissipation rate (in the DPG's) for stabilizing the RMU/ATS-V "dual spin" configuration is shown to be:

$$\dot{E}_u > 0.210 \, \dot{E}_s$$

where E_u is the rate at which energy is to be dissipated in the unspun section (RMU) by the DPG's, while E_s is the rate at which energy is dissipated in the spinning section (ATS plus docking cage of RMU) by the heat pipes. As shown in Section 5.0, the expected magnitude of energy dissipation rate in the heat pipes, as a function of the nutation angle (θ), is given by

$$\frac{\dot{E}_s}{\theta^2} = 4(10)^{-4} \, \frac{watts}{degree^2} . \tag{6}$$

Thus, as a minimum requirement for neutral stability (zero margin), the rate of energy dissipation to be provided by the two transverse-axis DPG's, as a function of nutation angle, is

$$\frac{\dot{E}_u}{\theta^2} = 4(0.210)(10)^{-4} = 0.84(10)^{-4} \, \frac{watts}{degree^2} . \tag{7}$$

Equations (6) and (7) are plotted in Figure 7-19.

A summary of the DPG parameters selected on the basis of the above requirements and the resulting system performance characteristics are given in Table 7-7. The DPG deliverable momentum provides a commanded angular rate capability of approximately $\pm 1°$ per second in each axis without the use of RCS propellants. The attitude response settling time constant is approximately 1.8 seconds. Roll attitude drift during spinup of the docking cage is held to less than ± 3 degrees.

Using the selected DPG parameters, equation (5) gives the energy dissipation rate provided by the two DPG's (for small gimbal angles) as

$$\frac{E_{DPG}}{\theta^2} = 0.0175 \, \frac{watts}{degree^2} \tag{8}$$

which is approximately 200 times the minimum dissipation rate required for neutral stability per equation (6). The DPG energy dissipation rate plotted in Figure 7-20 is based on equation (4) and is, therefore, not restricted to small gimbal angles; to illustrate the very substantial stability margin provided by the DPG's, Figure 7-20 also shows a plot of the minimum energy dissipation rate required for neutral stability per equation (7).

-205-
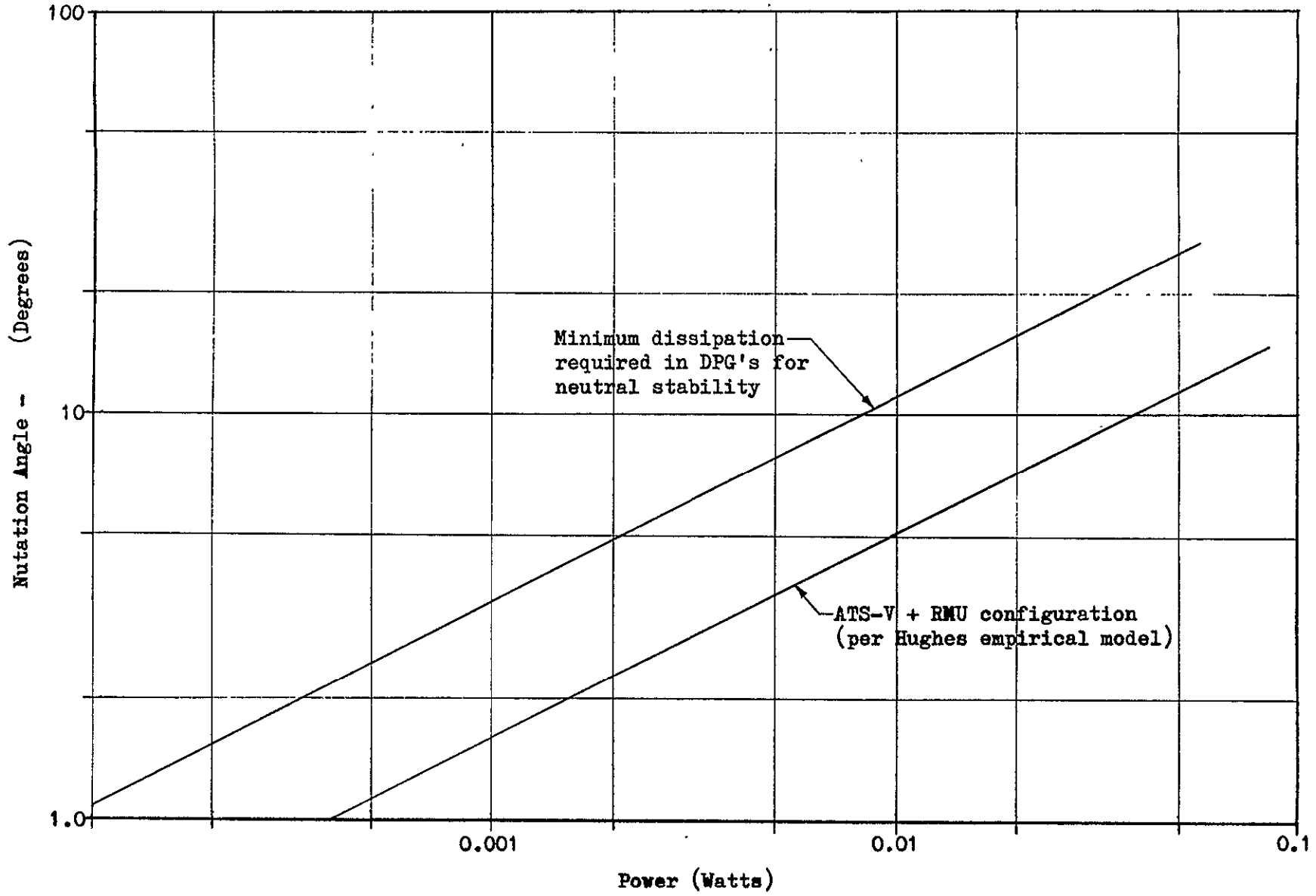
Figure 7-19 Minimum Required DPG Energy Dissipation

Table 7-7. SUMMARY OF DPG PARAMETERS AND SYSTEM PERFORMANCE CHARACTERISTICS

	PARAMETER	BASELINE VALUE
DPG Parameters	Angular Momentum Per Rotor (h)	0.6 Ft-Lb-Sec.
	Damping Constant (b)	0.03 Ft-Lb/Rad/Sec
	Torque Gain (h/b)	20
	Gimbal Travel to Physical Stops (α_m)	$\pm$ 85 Deg.
	Gimbal Travel for Desaturate Switches (α_D)	$\pm$ 45 Deg.
	Maximum Gimbal Rate (Load Limit) ($\dot{\alpha}_m$)	365 Deg/Sec.
DPG/RMU System Performance Parameters	Attitude Maneuver Rates (DPG Transferable Momentum) (ω_v)	$\pm$ 1.1 Deg/Sec.
	Attitude Response Time Constant (τ)	1.8 Sec.
	Rate Damping Gain	24 Ft-Lb/Rad/Sec
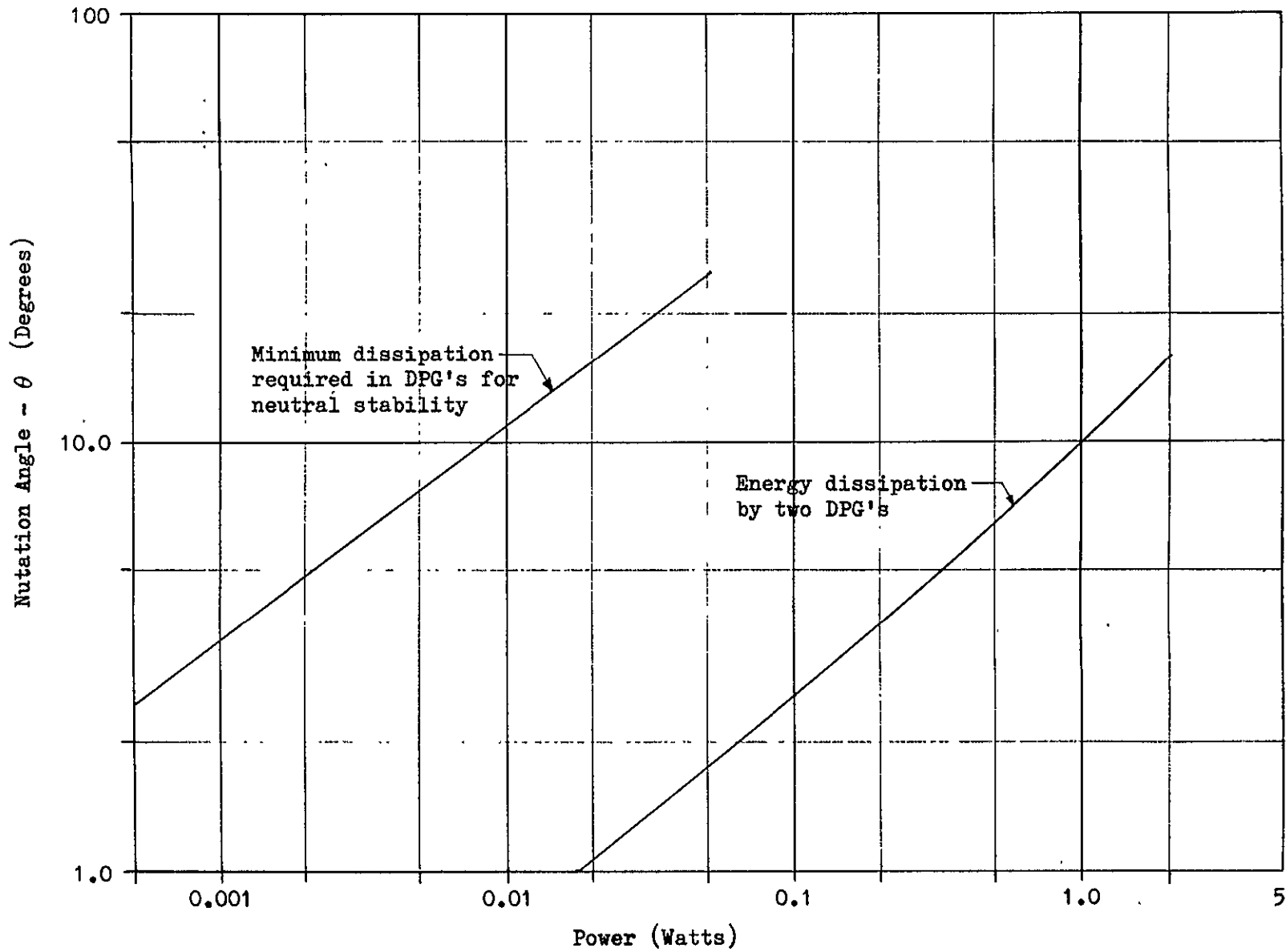
Figure 7-20 DPG Energy Dissipation

The DPG maximum gimbal rate capability is approximately 18 times that induced by normal maneuvering at $1°$ per second vehicle rates, and is capable of sustaining the gimbal rates associated with nutation angles of up to 13.7 degrees in the "dual spin" mode. This capability far exceeds the expected nutation angles, thus indicating that further reductions in the DPG damping constant (b) could be made. Further reductions in b would decrease the attitude response settling time constant and would increase the energy dissipation rate for the dual spin stabilization. The present margins are, however, felt to be adequate and no further reduction in b appears warranted at this time.

Further stabilization of the dual spin configuration could also be provided by the reaction jets. The DPG gimbal pick-off could be fed into a lead filter to provide a signal proportional to the body rate which in turn would be used to command the reaction jets. Also the active nutation control logic could be modified so as to provide nutation damping during this phase. In addition, the active nutation control system within the ATS could be enabled to provide further stabilizing torques. However, the DPG's alone appear to provide a satisfactory margin of stability.

As described in Section 4.0 and Appendices B and C, analog pilot-in-the-loop precontact docking simulations were performed using the DPG parameters selected for the baseline design. Similarly, as described in Section 5.0 and in Appendix D, the dynamics of the ATS-V/RMU "dual spin" system were analyzed in a digital simulation of the post contact docking phase. A math model of the ATS-V heat pipes was included in the "dual spin" simulation. It was found to very closely duplicate the ATS-V nutational instability characteristics determined from flight data. Both the analog and the digital simulations have shown good correlation with the preceding analytical results and have indicated that the performance of the baseline DPG design meets or exceeds the requirements.

7.2.3.3 Mechanization

The primary hardware elements of the RMU attitude control subsystem are the DPG's, the despin/docking cage drive assembly, the control system sensors and the control system electronics. The baseline implementation of these elements is briefly discussed in the following.

A preliminary layout of a single DPG is given in Figure 7-21. The hysteresis synchronous gyro rotor assemblies, each in its hermetically sealed gimbal, will be provided by the Kearfott Division of the Singer-General Precision Company; these units have a long history of successful flight applications. The torquer is a standard brushless DC torque motor provided by Aeroflex Laboratories. The gimbal resolver is a proven sin-cosine resolver and again will be provided by Kearfott.

These elements plus the gimbal bearings and trunnion gears are mounted in the sealed housing to be provided by NR. The DPG case is filled with silicone fluid to provide the desired level of viscous damping torque about the gimbal axis. Several similar DPG units have been built and laboratory tested by NR in their flight packaged configuration.

-209-
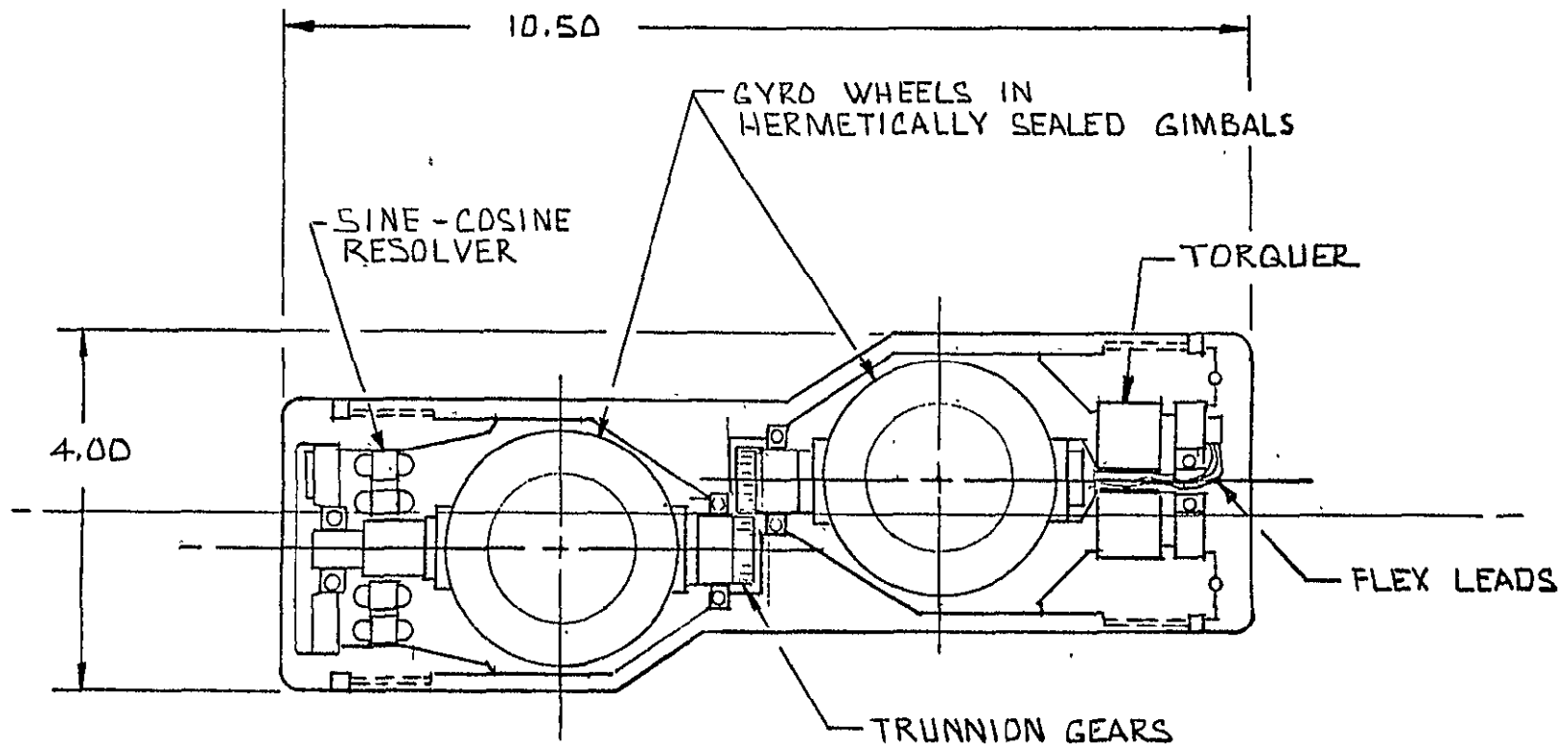
FIGURE 7-21. DPG CONFIGURATION

Space Division
North American Rockwell

A layout of the selected Ball Brothers despin drive assembly is presented in Figure 7-22. The torque motor is a DC brush type torque motor presently being qualified for the OSO-H program. Thirteen slip rings are provided of which three are required for operation of the torque motor. The design is an adaptation of the principles utilized in the highly successful OSO vehicles and utilizes several of the flight proven components.

The sensors are all identical to the units utilized on ATS-V; the sun sensors are made by the Hughes Aircraft Company, the solar aspect sensors are provided by Adcole and the ANC accelerometers are a product of United Controls.

The attitude control electronics assembly, made by NR, will utilize space proven solid state components. The functional elements of the electronic assembly will include all the logic elements previously described in conjunction with the various control modes. In addition it will also include the electronics related to control of the Ball Brothers despin cage drive assembly; a functional block diagram of the related logic elements is given in Figure 7-23. The rotational rate is sensed with a magnetic pick-off providing 30 pulses per revolution. A pulse standardizer generates square wave pulses of uniform shape. A filter is employed to smooth these square wave pulses and provide a d-c spin rate signal to the summing amplifier. Since the command system is only capable of providing discrete rather than analog commands, two 7-bit counters and a digital-to-analog converter are utilized to generate a d-c spin rate command to the summing amplifier. Pulses are commanded from the ground station into the coarse and fine counters to increment and decrement the counters. The magnetic pick-off spin rate sensing technique does not provide "clean" data at low spin rates. Therefore, to despin the ATS-V to zero rate, open-loop braking torque commands are provided. These commands will be initiated at the ground station and will be removed when the spin speed approaches zero. The bearing and brush friction of the spin motor will provide the necessary braking torque to reduce the residual spin speed to zero.

7.2.4 Reaction Control

The reaction control subsystem (RCS) of the RMU must be capable of producing the vehicle torques and forces needed for performing the following functions and operations:

1. Precession of the RMU spin axis for attitude orientation during the spinning mode of operation;

2. Active nutation control (ANC) during the transfer orbit through ejection of the apogee motor;

3. Delta-V's for in-plane and out-of-plane orbit parameter adjustments in the spinning mode;

4. Torques for despinning the RMU;
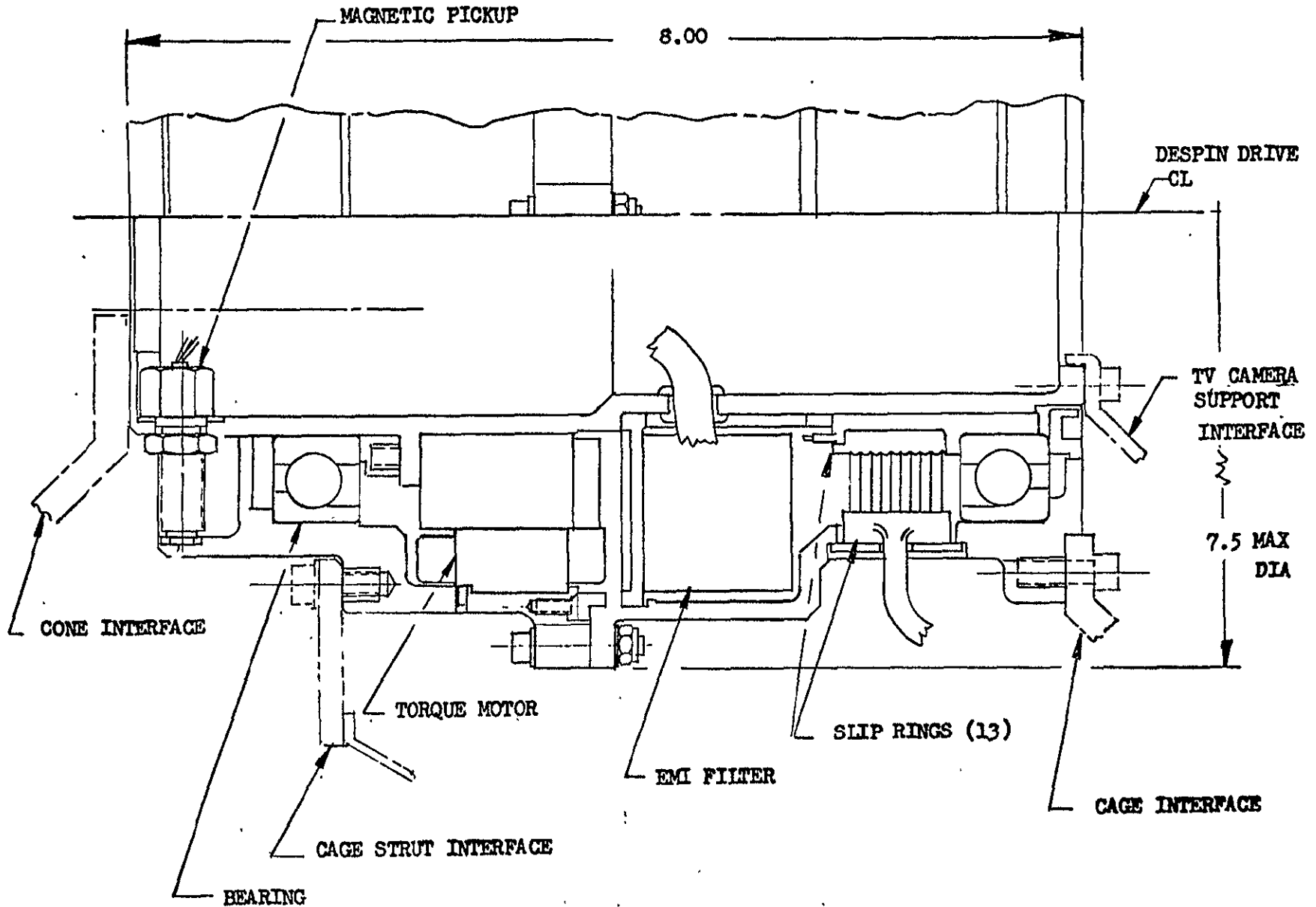
FIGURE 7-22. DESPIN DRIVE ASSEMBLY
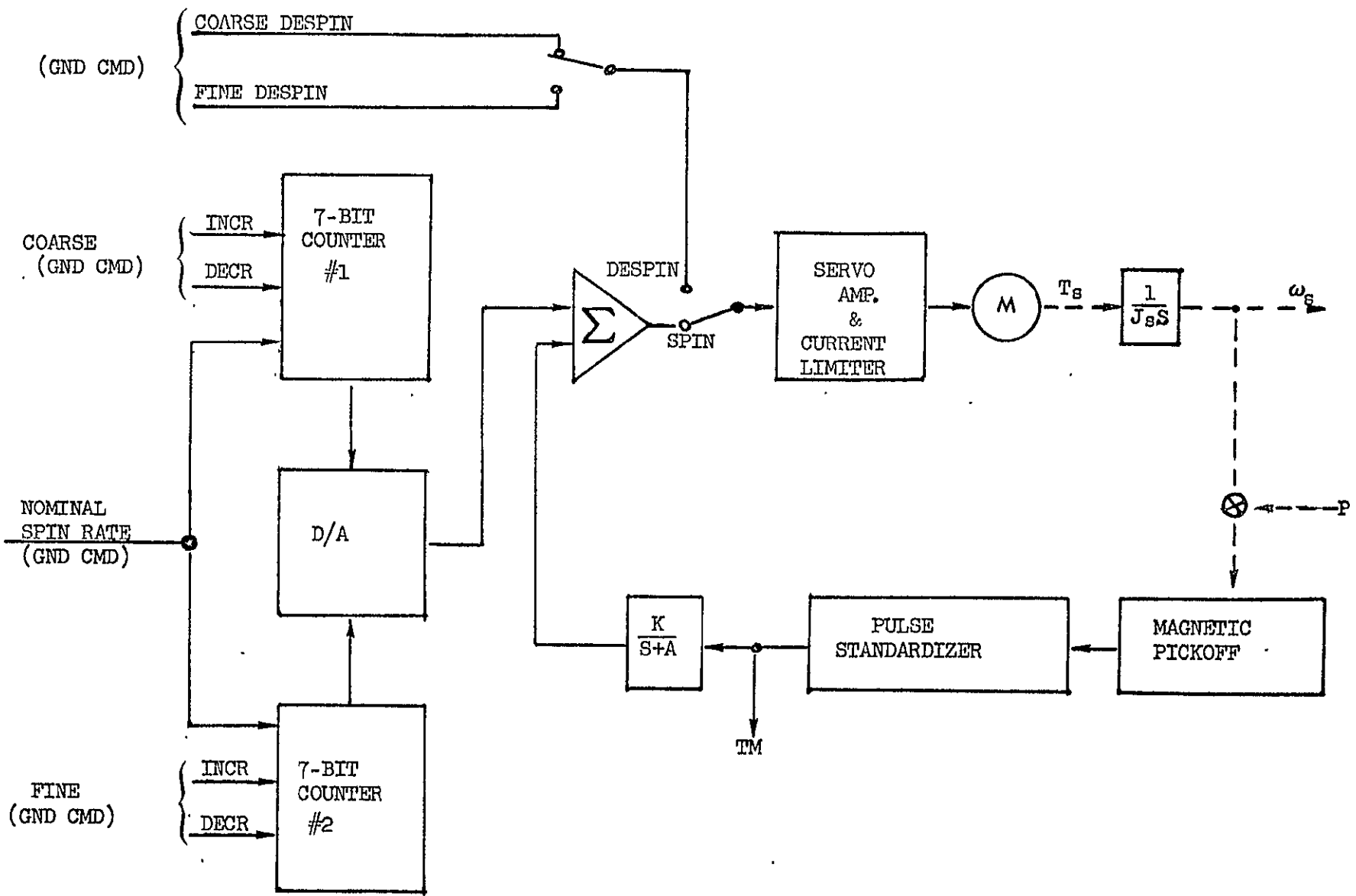
Figure 7-23. Docking Cage Spin Control

5. Delta-V maneuvers in the 3-axis stabilized mode;

6. Vehicle torques for desaturation of DPG's in the 3-axis stabilized mode (including despin of ATS-V).

To provide these capabilities, the RCS must provide bi-directional translational forces along three axes as well as bi-directional torques about those axes. As described in previous subsections, a concept utilizing 12 thrusters, arranged in 4 clusters of 3 thrusters each, was selected for the baseline design. Locations and orientation of the thrusters provide the desired bi-directional 6 DOF control capability while producing essentially pure torque couples as well as nearly eliminating thrust vector misalignment when translational forces are applied.

The translational delta-V maneuvers related to precontact docking operations, as well as those related to final drift orbit trimming, were found to require very low minimum impulse-bit capabilities on the order of 0.03 lb-sec. The remaining operations require thrust levels of 1.0 lb minimum per thruster. To limit control authority variations, the ratio of initial to final thrust for the blow-down type mechanization was held to 3:1 maximum. Required total impulse was established as 8,422 lb-sec as shown in Table 7-8. Impulse requirements were computed conservatively assuming constant vehicle mass for all translational maneuvers.

Initially, three mechanization concepts were considered for these requirements.

1. A hybrid approach utilizing cold gas thrusters for the low impulse maneuvers with mono-propellant hydrazine engines providing the higher thrust capabilities;

2. A pure mono-propellant hydrazine system operating with a regulated pressurant supply;

3. A pure mono-propellant hydrazine system operating in a blow-down mode.

A review of space proven hardware revealed that the simplest third concept can be mechanized with readily available thrusters and propellant tanks. Thus, this concept was selected for the baseline design.

Selection of subsystem components, mechanization of the baseline subsystem as well as its characteristics, are discussed in the following subsections.

7.2.4.1 Propellant Tanks

A survey was made of qualified hydrazine tankage to determine their applicability to the RMU application. A summary of candidate space qualified tankage and their size, capacity, and status are shown in Table 7-9.

Table 7-8. RCS Impulse Requirements

Function	Required Capability	Impulse (lb-sec)
Precession of RMU	231 degrees	621
(Pre-Apogee Burn)	(148)	
(Post-Apogee Burn)	(68)	
(Corrections)	(15)	
Active Nutation Control		120
Correction of In-plane Drift Orbit Errors	210 ft./sec.	3340
Correction of Out-of-plane Drift Orbit Errors	185 ft./sec.	2940
Reducing Orbital Drift (→0)	18 ft./sec.	286
Despin of RMU	60-0 RPM	180
Closure, and Docking with ATS-V	14 ft./sec.	218
DPG Desaturation		490
(Primarily during ATS-V Despin)		
Separation, Observation and Parking Orbit Injection	21 ft./sec.	227
TOTAL		8,422

Table 7-9. Candidate RCS Tankage

Application	Number of Tanks Required; Size; Volume* & Propellant Capacity**	Comment
European COMSAT	4~9.5" Sphere: 450 Cu. In. each 16.8 Lb. per tank	Tanks and butyl rubber diaphragms are under development by Pressure Systems, Inc. Tank is modified Intelsat II design. Qualification scheduled for early '71. Deliveries start in March '71.
Apollo	2~12.6" x 17.3"; 1490 Cu. In. each; 54.0 Lb. per tank.	Tank and expulsion system is the Apollo command module reaction control system fuel container.
Surveyor	3~10.0" x 15.0"; 805 Cu. In. each; 29.0 Lb. per tank.	Developed, qualified and flown for the Surveyor program. Out of production but potentially available. Tankage may require new bladders.
Gemini RCS	4~5.0" x 24"; 440 Cu. In. each 15.7 Lb. per tank.	Developed, qualified and flown on the Gemini program. Out of production and may be difficult to locate and refurbish. May have length problem.
Mariner 69	3~11.2" sphere; 695 Cu. In. each: 24.9 Lb. per tank.	Developed, qualified and flown under Mariner 69 program. Procurement of butyl bladder may be a problem.

* Max. internal volume. No allowance for ullage, expulsion device, etc.

** Corresponds to max. internal volume.

The European Comsat spacecraft tanks are being made by Pressure System Incorporated (PSI) under contract for a West German firm. The dimensions and capacity are the same as used on the Intelsat III program; however, a butyl rubber diaphragm is installed to provide positive expulsion capabilities. The tank has a capacity for 16.8 pounds of propellant. Four tanks would be required to meet the RMU propellant loading requirements. Qualification of the tank is scheduled for early 1971.

The Surveyor and Gemini RCS are potential sources of tanks which have been qualified and space proven during their respective programs. Although they are out of production, tanks which are remaining from the programs may be potentially available and refurbished for use in the RMU program.

The Mariner 69 tank shell is manufactured by PSI but the company that made the butyl rubber expulsion diaphragm is no longer active in the area. However, the Mariner 69 tanks have been specified by JPL for Mariner 73, which would indicate that a source would be sought for supplying the expulsion diaphragms. The 11.2 inch diameter tank has a total capacity of 24.9 pounds. Three tanks are required to satisfy RMU propellant loading.

The Apollo Command Module fuel tank is the largest tank considered for the RMU application. It has a diameter of 12.6 inches and a length of 17.3 inches with a volume of 1490 cubic inches. The tank, furnished by Bell Aerospace, utilizes a titanium shell and a teflon expulsion bladder (made by Dielectric Corporation). Although the tank is not presently in production, a potential source is available from RCS systems previously flown on the Apollo Command Modules. The tanks require refurbishing by Bell Aerospace including the installation of a new teflon bladder. An advantage in using two of these tanks is that they offer potential RCS growth capability since less than fifty percent of their capacity is used for the baseline design (two tanks are required to allow symmetrical mounting about the RMU center of mass).

The Apollo Command Module tanks were selected for the baseline design. The selection was based primarily on availability, cost, and growth potential considerations. Also, due to the 50% loading factor, they offer a very favorable 2.5:1 ratio of initial to final propellant pressure in the blow-down mode.

7.2.4.2 Thrusters

In the initial phase of the study, contacts were made with manufacturers of hydrazine mono-propellant thrusters to determine the status of engines within the required thrust regime. A summary of engine status is shown in Table 7-10.

Hamilton Standard makes the Intelsat IV engines which operate in a blow-down mode with thrust decay of 5.7 to 2.8 pounds and corresponding inlet pressures of 250 to 100 psia, respectively. The IDCSP engine is a blow-down type with a thrust range of 5.0 to 2.2 pounds at corresponding inlet pressures of 250 to 75 psia. The lowest level at which the qualified five pound engine has been operated is 1.5 pounds, but it is not qualified at this thrust level.

TABLE 7-10   CANDIDATE HYDRAZINE THRUSTERS

MANUFACTURER & MODEL NO.	QUALIFIED THRUST RANGE, LBS	STATUS
TRW	4.1 to 0.80	Developed and flown on the Intelsat III satellite.
HAMILTON STANDARD REA 16-5 and REA 23-4	5.0 to 2.2	Developed and flown on IDCSP, NATO Communication Satellite and ATS C, D & E. Will be used on Intelsat IV & a classified program. Not qualified at the 1.0-lb. thrust level.
ROCKET RESEARCH MR-6A	5.0 to 2.57	Developed to support the LMSC P95 Program. Will be flown in 1970. Not qualified at the 1.0-lb. thrust level.
MARQUARDT & AEROJET	5.0	Both companies have developed 5-lb thrust systems - none qualified or flown.

Rocket Research has developed and qualified a five pound thruster for an LMSC program scheduled to fly in the near future. Although no problem is foreseen in operating at the one pound thrust level, it is not qualified below 2.57 pounds.

The TRW engine applicable to these requirements is a modification of the engine flown on the Intelsat III program. The original engine is qualified in a blow-down mode from 4.0 to 0.8 pounds thrust. Modification would consist of installing a 90° canted nozzle so that the thrusters can be installed with the longitudinal axis of the catalyst bed normal to the boost acceleration vector. This is required to eliminate migration of small particles of catalyst into the injector (caused by vibration and loads associated with the boost phase), which could create problems during engine start. This thruster has been qualified with a 45 degree canted nozzle configuration, and no problems are anticipated with the 90° canted version.

In view of its known and proven performance in the low (1.0 to 2.5 lb) thrust range, the TRW engine was selected for the baseline design.

7.2.4.3 Baseline RCS Concept

A schematic of the subsystem selected for the baseline RMU RCS is shown in Figure 7-24. It consists of four rocket engine modules with each module containing three engine assemblies, two propellant tanks with positive expulsion bladders, a propellant filter, a pressure transducer, two propellant tank vent valves, a propellant fill valve, and a pressurant fill valve.

The baseline concept uses the thrusters that were developed, qualified, and flown on the Intelsat III program, modified to provide a 90 degree canted nozzle. The thrusters use a spontaneous catalyst (Shell 405) and are capable of operating over a thrust range of 4.1 to 0.8 pounds thrust at inlet pressures of 600 to 75 psia, respectively, in either a steady state or pulse mode. In the RMU baseline design, they will be used in the range of 2.5 to 1.0 lb. The nominal steady state thrust characteristic, as a function of propellant tank pressure, is shown in Figure 7-25 for the pressure range applicable to the RMU. The steady state specific impulse and pulse mode specific impulse are presented in Figure 7-26. Pulse mode operation is shown for duty cycles of 117 ms ON and 883 ms OFF, and for 1 to 5 second firings; both are representative of duty cycles which will be used on the RMU. The engine is capable of providing a minimum impulse bit of 0.03 lb.-sec. at engine inlet pressures of 100-110 psia.

The propellant valve consists of a dual coil, dual seat, solenoid valve developed for the Intelsat program by Stratos Western Division of Fairchild-Hiller. The configuration provides a redundant elastomeric seal against internal leakage in the closed position. If one poppet fails to seal properly, the other poppet will still seal, thereby increasing reliability. An integral filter provides 25 micron absolute filtration. The valve requires 5 watts of power operating with a single coil.
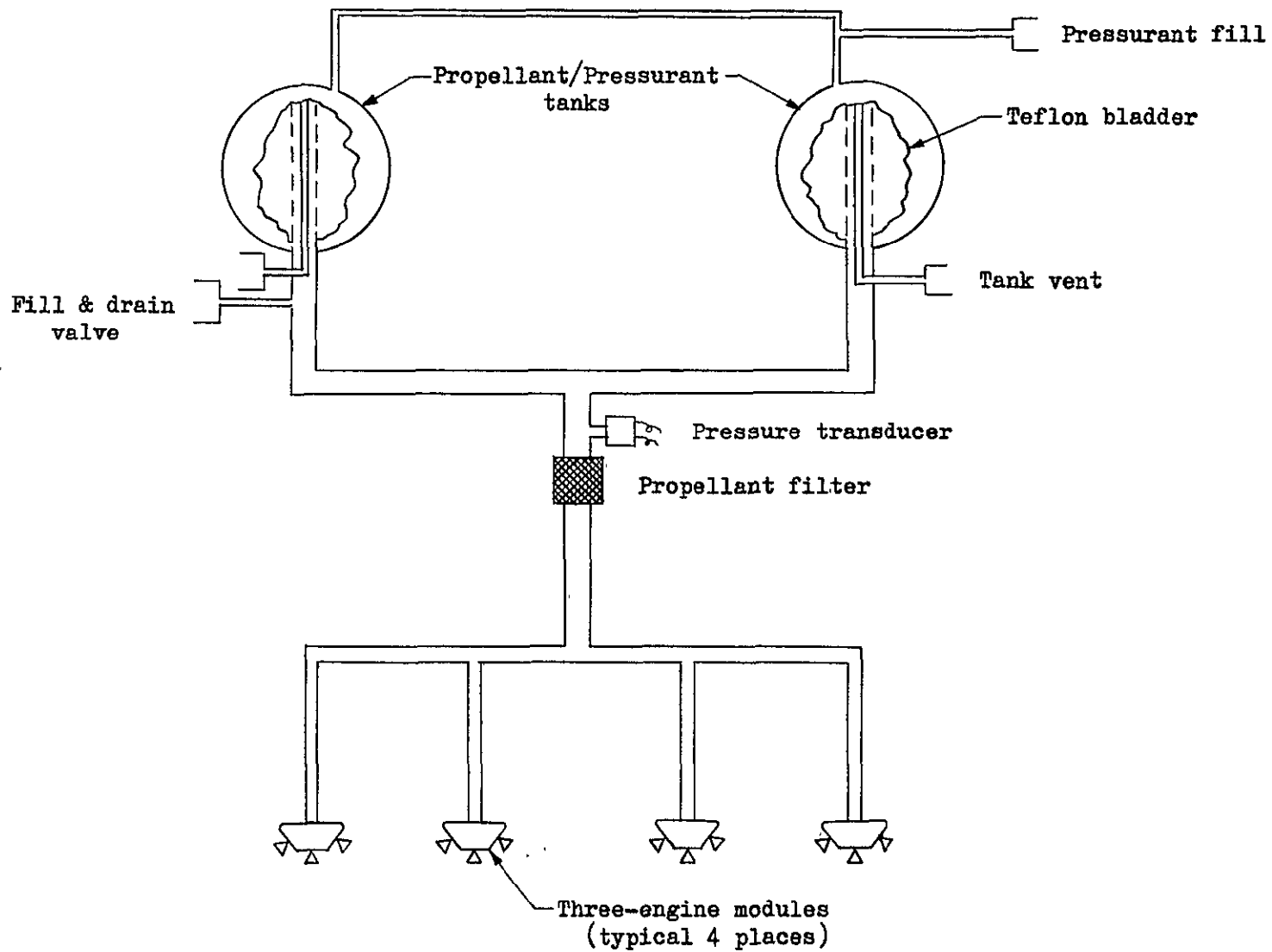
Figure 7-24. RMU Propulsion Subsystem Schematic

Space Division
North American Rockwell
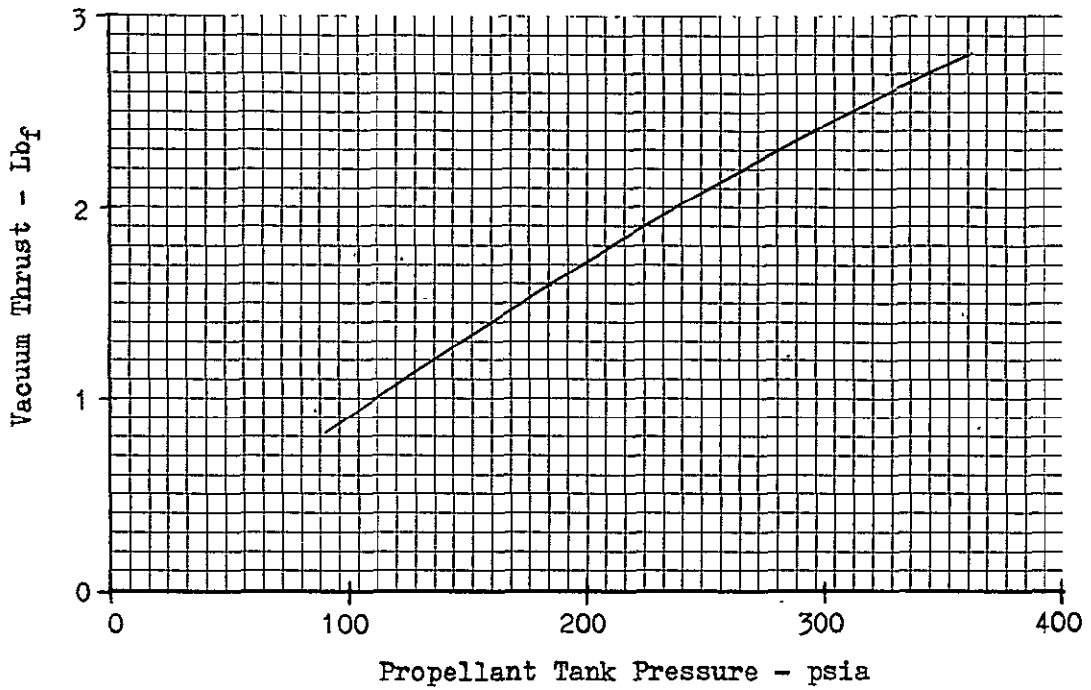
Figure 7-25. Steady State Thrust versus Tank Pressure
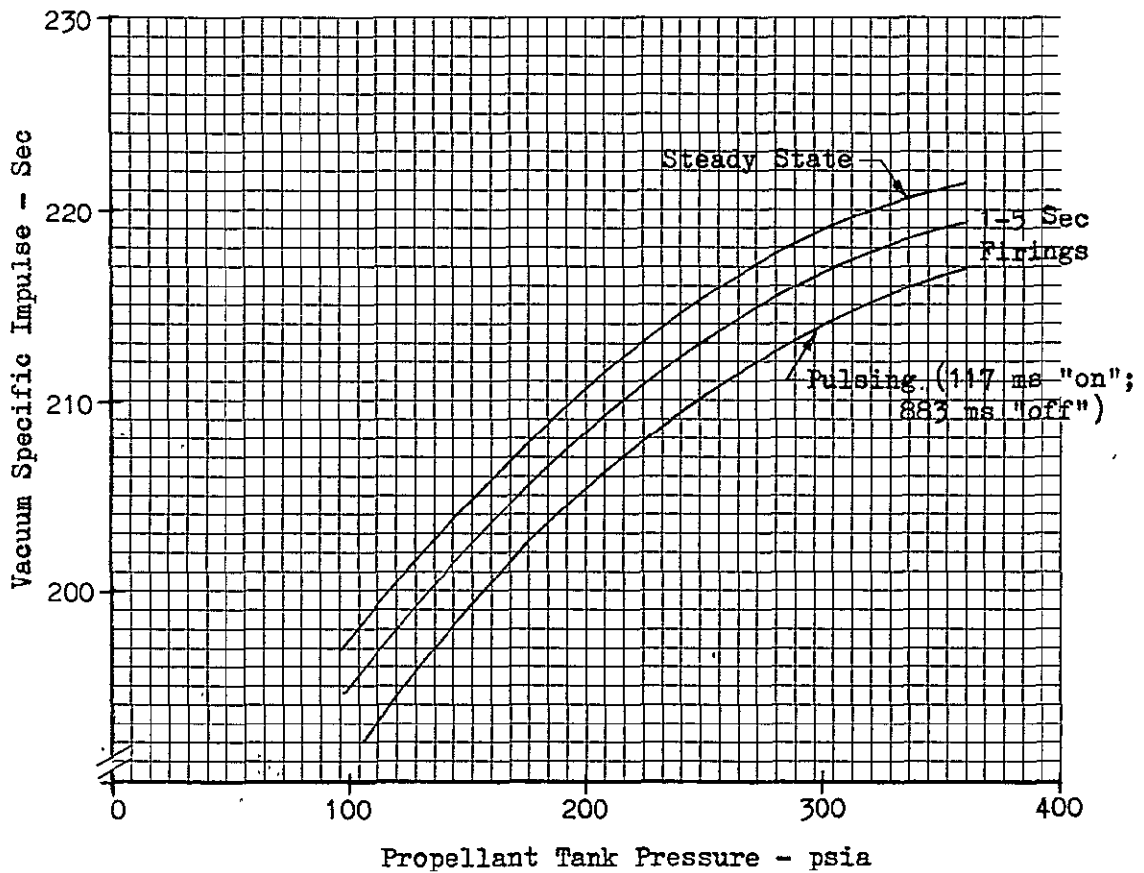
Figure 7-26. Specific Impulse versus Tank Pressure

The Apollo command module RCS fuel tanks have a usable capacity of approximately 1473 cubic inches. The tanks use a teflon expulsion bladder to provide zero gravity expulsion capabilities. Tank design pressure is 291 psia with a design burst pressure of 710 psia. For the RMU application, the tanks are loaded to approximately fifty percent of their capacity, and require an initial pressure of approximately 210 psia. The tank pressure, as a function of the propellant remaining, is shown in Figure 7-27 for tank blow-down at a constant temperature. The tanks are mounted 180 degrees apart to minimize spacecraft center of gravity variations during propellant expulsion. Each tank contains one-half of the required propellant and the outlets are manifolded together. A pressure balance line is connected between the two ullages to ensure equal pressure and equal propellant quantity within each tank.

An inline filter, manufactured by Wintex Corporation, is installed in the propellant feed line. This filter was qualified for use on the Program 777 spacecraft and has a 15 micron absolute rating. It has sufficient capacity to accommodate ten times the amount of contaminate anticipated based on total propellant load required for actual mission requirements.

The pressure transducer, used for monitoring propellant feed pressures, is being used on the USAF Program 777 spacecraft. The unit is manufactured by Statham Instruments. It requires 0.3 watts and provides a 0 to 5.0 VDC output proportional to propellant pressures from 0 to 500 psia with an error band of $\pm$ 1.8 percent of full scale over the required temperature range, and $\pm$ 0.8 percent at a selected temperature.

Fill and drain valves are provided for tank venting, propellant fill and drain operations, and propellant tank-ressurizing. The same type of manually operated valve is used for all these applications. The valve was developed by TRW for use on the Mariner 69 spacecraft and has redundant seal features which are capable of maintaining leakage rates of less than 1×10^{-7} scc/sec. of helium at temperatures of -150 degrees.

Based on the performance characteristics of the thrusters, the tankage parameters and the impulse requirements of Table 7-8, a propellant budget was computed as shown in Table 7-11. The computations allowed for performance variations resulting from gradual decrease of pressure in the blow-down mode. The very conservative propellant margin of 8.6 lb. was included to allow for potential follow-on missions after ATS-V despin. Should weight limitations so dictate, this quantity could be reduced.

7.2.5 Communications

The RMU communications subsystem has three functional requirements:

1. It provides the downlink for transmission of the video signals from the RMU TV camera; this requirement applies only in the 3-axis stabilized mode of RMU operation;
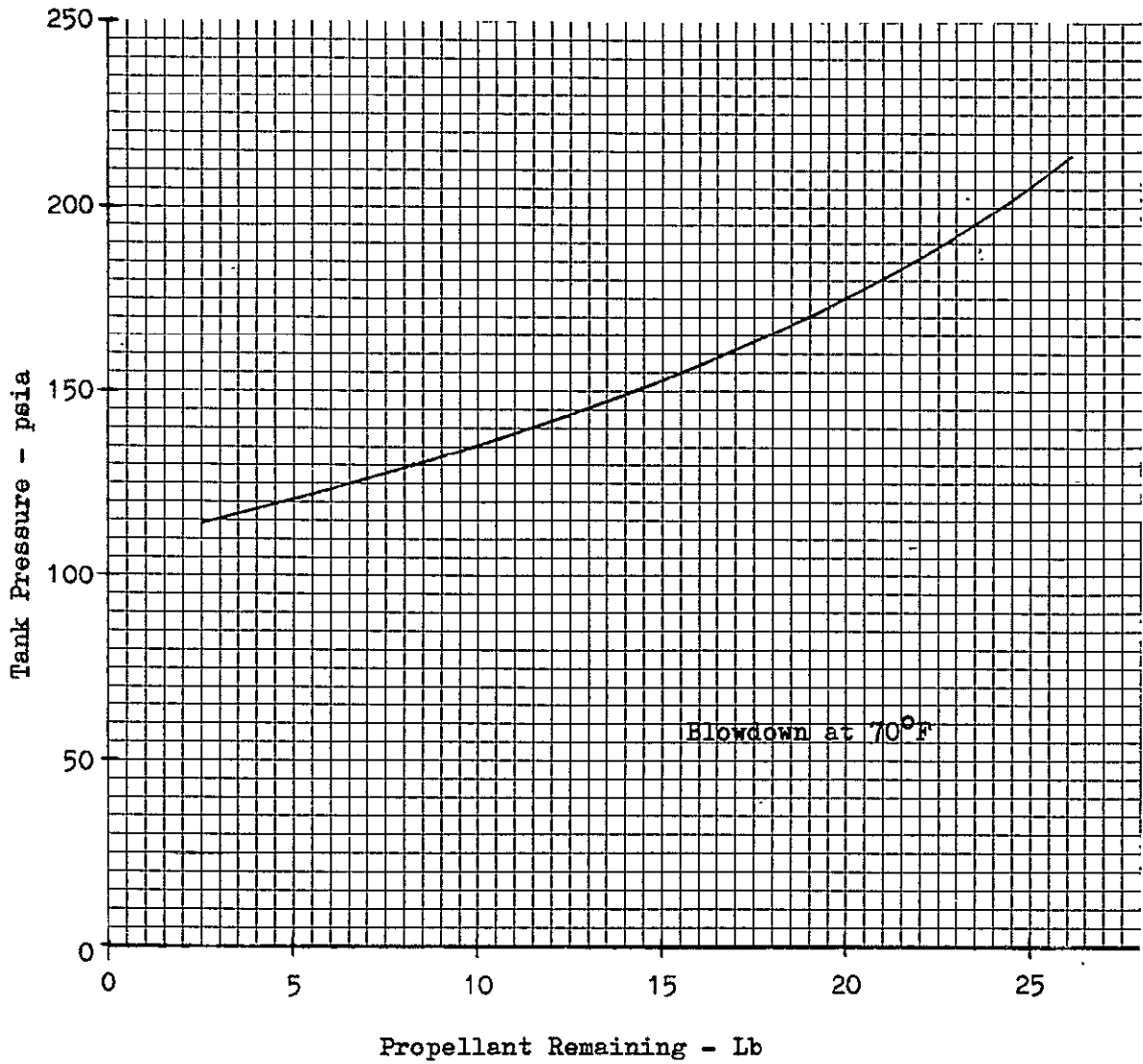
Figure 7-27. Tank Pressure versus Propellant Remaining

Table 7-11. RCS Propellant Requirements

Function	Total Impulse (lb-sec)	Average Isp (sec)	Propellant Weight (lb)
Precession	621	204	3.0
Nutation Damping	120	.200	0.6
In-Plane Error Correction	3340	203	16.4
Out-of-Plane Error Correction	2940	196	15.0
Reducing Orbital Drift	286	195	1.5
Despin of RMU	180	200	0.9
Closure & Docking	218	200	1.1
Gyro Desaturation	490	200	2.4
Separation, Observation and Parking Orbit Injection	227	200	1.6
Propellant Margin			8.6
Residual			2.1
TOTAL			53.0

2. It acts as a transponder for ground based tracking of the RMU;

3. Its linearly polarized downlink beacon is utilized for measurement of POLANG data by the ground stations; the POLANG data is required to allow computation of RMU attitude.

At an early stage of the study a programmatic ground rule was established to utilize the ATS C-band communications gear on the RMU. The baseline RMU communications subsystem depicted in Figure 7-28 is in full accord with this ground rule; the illustration identifies each functional element of the subsystem by its part number as assigned on the ATS program by the Hughes Aircraft Company. The only exception is the omni antenna; a new antenna is utilized since the ATS unit could physically not be accommodated on the RMU.

The subsystem will operate at the same frequencies as the C-band system of ATS-V to assure ground equipment compatibility. The C-band transmitter of only one of the two spacecraft will be energized at any one time.

Although the elements of the subsystem are those utilized on ATS, the RMU mechanization and operational use of the equipment differ somewhat from that on the ATS-V spacecraft. This is because a parallel L-band system was utilized on ATS-V for an Air Traffic Control (ATC) experiment and provided functional redundancy to the non-redundant C-band system. Since the RMU does not carry the L-band gear, the redundancy is provided by (a) utilizing two parallel antenna electronics units as well as two parallel repeater modules, and (b) utilizing only one of the two TWT's of the transmitter at any one time; thus the second TWT is used as a backup redundant element.

The following subsections (a) show that the use of only one 4 watt TWT provides satisfactory margins in all modes, and (b) provide a description of the new C-band omni antenna baseline design.

7.2.5.1 Link Calculations

The link calculations reflecting the use of only one TWT at a time are given in Tables 7-12 and 7-13; the resultant carrier/noise power density values derived in these link calculations are then compared in Table 7-14 with the carrier/noise power density values required for adequate performance of tracking, POLANG and video image transmitting functions.

As shown in Table 7-14 the modest link performance required for range and range-rate tracking is easily attained: a margin of more than 30 db exists, with either the Mojave 40' or the Rosman 85' dish even when the omni antenna of the spacecraft is used.
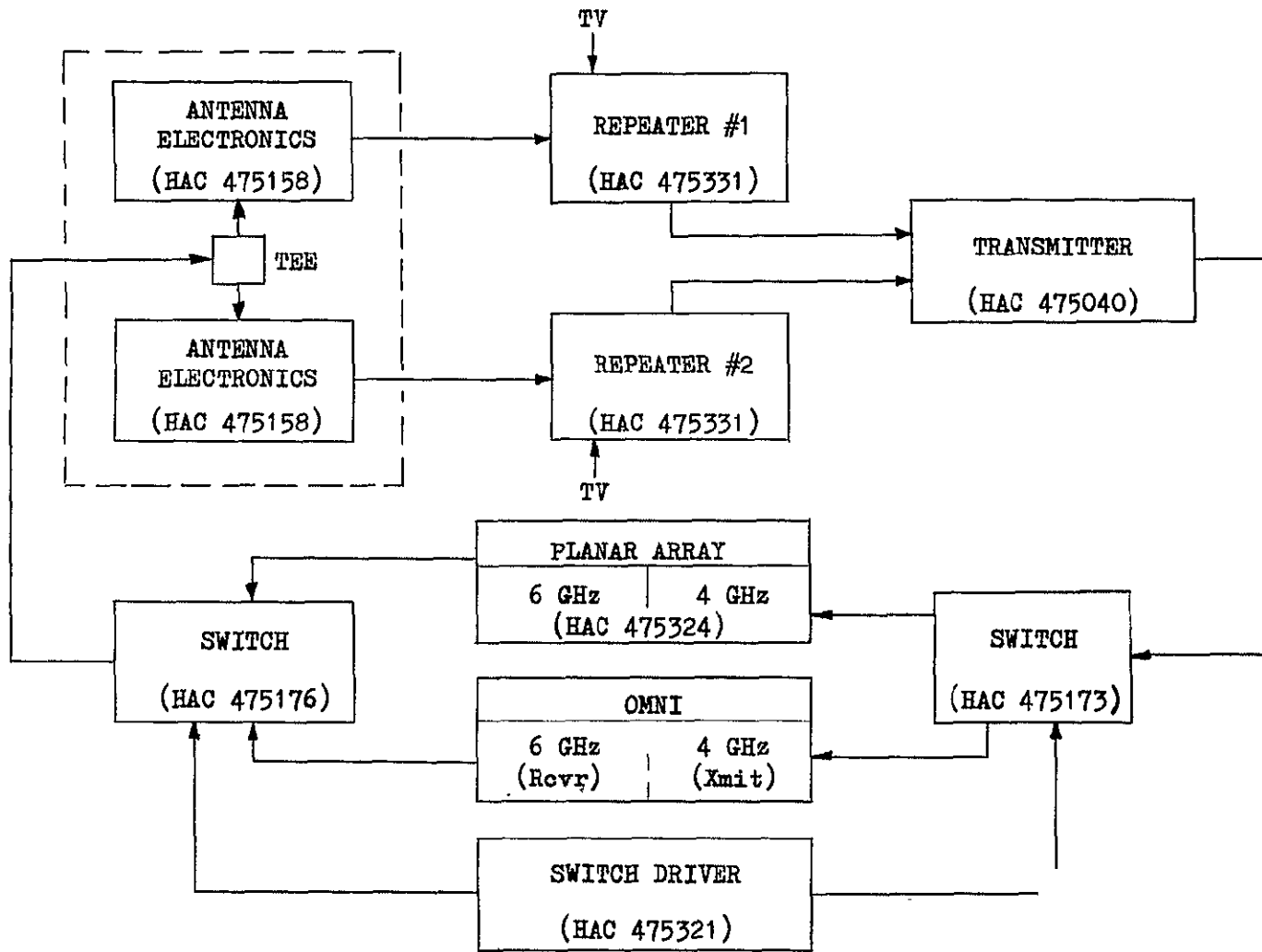
Figure 7-28. Communications Subsystem

Table 7-12. RMU to Ground Link (C-band 4.1 GHz)
Performance Using Omni Antenna

Ground Station / Link Parameter	Rosman (85' Dish)	Rosman (40' Dish)
Transmitter Power, dbw	6.0	6.0
Line Losses, db	-2.3	-2.3
RMU Antenna Gain, db	0.0	0.0
Effective Radiated Power, dbw	3.7	3.7
Off-Beam Center Allowance, db	-0.0	-0.0
Space Attenuation, db	-197.1	-197.1
Ground Antenna Gain, db	58.0	51.0
Received Carrier Power, dbw	-135.5	-142.5
Receiver System Nois Temp., db-°K	17.8	17.8
Receiver Noise Power Density, dbw/Hz	-210.8	-210.8
Carrier/Noise Power Density, db	75.3	68.3

Table 7-13. RMU to Ground Link (C-band 4.1 GHz)
Performance Using High Gain Antenna

Ground Station / Link Parameter	Rosman (85' Dish)	Rosman (40' Dish)
Transmitter Power, dbw	6.0	6.0
Line Losses, db	-2.3	-2.3
RMU Antenna Gain, db	16.7	16.7
Effective Radiated Power, dbw	20.4	20.4
Off-Beam Center Allowance, db	-1.0	-1.0
Space Attenuation, db	-197.2	-197.2
Ground Antenna Gain, db	58.0	51.0
Received Carrier Power, dbw	-119.8	-126.8
Receiver System Noise Temp., db-°K	17.8	17.8
Receiver Noise Power Density, dbw/Hz	-210.8	-210.8
Carrier/Noise Power Density, db	91.0	84.0

TABLE 7-14

C-BAND DOWNLINK MARGINS

RMU ANTENNA	GROUND STATION ITEM	ROSMAN (85' DISH)	MOJAVE (40' DISH)
OMNI	Carrier/Noise Power Density, db/Hz	75.3	68.3
	Required for Range & Range Rate, db/Hz	36.5	36.5
	MARGIN, db	38.8	31.8
	Carrier/Noise Power Density, db/Hz	75.3	68.3
	Required for Polarization Angle Tracking, db/Hz	48.0	48.0
	MARGIN, db	27.3	20.3
HIGH GAIN	Carrier/Noise Power Density, db/Hz	91.0	84.0
	Required for Television Transmission, db/Hz	88.0	88.0
	MARGIN, db	3.0	-4.0

For a received signal-power-to-noise-power density ratio of 48 db, the POLANG system will resolve the plane of polarization of the incident energy radiated by a slowly moving satellite to within one degree. As shown in Table 7-14 this requirement is readily met: a margin of more than 20 db is indicated with either the Mojave or the Rosman station using the omni antenna of the spacecraft. For signal levels greater than 48 db, the accuracy improves, reaching a limit of ± 0.15 degrees at a signal level of 85 db.

A high quality (CCIR standard) TV picture is considered a necessity due to its importance to the overall RMU mission. Therefore, a requirement of S/N = 50 db (peak-to-peak signal to weighted rms noise) was chosen. Using the same spectrum bandwidth of 25 MHz as was used with the ATS satellites, this requires a carrier-power-to-noise-power density ratio of 88 db. As shown in Table 7-14, this requirement is met with a satisfactory margin when the high-gain spacecraft antenna is used in conjunction with the 85' dish at Rosman. Performance with the Mojave 40' dish is marginal. This is, however, not considered a severe handicap since the baseline concept utilizes only Rosman as a control station in the visually guided mission phases. In the absence of a Mojave/Rosman TV-data link, video received at Mojave could not be utilized for real time pilot-in-the-loop control of the RMU.

7.2.5.2 Omni Antenna Baseline

Full definition of requirements for the RMU C-band omni antenna is best based on a detailed analysis of the ground equipment's characteristics and/or on tests conducted with the ground equipment. Efforts to obtain data during the study have shown that it is not readily available, and generation of such data was not within the scope of the study. Therefore, in cooperation with NASA and Westinghouse (ATS) personnel, tentative antenna requirements were established as a guide to defining a baseline design concept. By necessity very conservative assumptions were made in defining these tentative requirements as follows:

1. The antenna, using a 4 watt transmitter, must deliver at the output terminals of a 40 foot parabolic antenna, a minimum signal level of -125 dbm;

2. Requirement 1 must be met with all attitude orientations planned for the RMU, from approximately 30 minutes after injection into the transfer orbit and through the remainder of the mission;

3. Antenna pattern null depth (amplitude modulation) shall not exceed 10 db;

4. Phase modulation due to antenna phasing shall not exceed one radian single amplitude;

5. The antenna shall be linearly polarized with the polarization vector parallel to the RMU spin axis.

To assess requirement 2 above, the RMU spin axis attitude relative to the RMU – Mojave line-of-sight was computed for the transfer orbit phase; the results are shown in Figure 7-29 which also indicates the RMU altitude during that phase.

. Although a folded annular horn was considered as a candidate concept, it was rejected in favor of an array of wave guide horns on the basis of cost. A 20-element array of wave guide horns was chosen as a candidate system in light of the conservative preliminary system requirements. A preliminary analysis of this system indicates patterns with null depths on the order of 9 db with phase modulation on the order of + 0.6 radians and an approximate signal margin of 13 db over mission requirements. Although the system is not composed of off-the-shelf hardware, its design and performance characteristics are well known, and development cost and lead time are not critical.

At present the ground station equipment is believed to tolerate considerably higher phase and amplitude modulation than the limits set for the antenna design would indicate. Thus, a thorough analysis of ground station characteristics should allow a significant future reduction in antenna complexity.

7.2.6 Telemetry and Command

To assure total compatibility with the existing ATS ground equipment and software, and in the interest of minimizing program costs, a decision was made early in the study to utilize ATS-V telemetry and command (T&C) gear on the RMU. Accordingly, the study effort was directed at reviewing the ATS-V equipment in light of RMU requirements.

7.2.6.1 Telemetry

A preliminary RMU telemetry list was prepared to establish telemetry requirements; the list is given in Table 7-15. Examination of this list indicated that the ATS-V equipment is adequate for handling the RMU telemetry load. A functional block diagram of the baseline telemetry subsystem is given in Figure 7-30; the diagram identifies each element by its ATS part number as assigned by the Hughes Aircraft Company (HAC). Although the baseline concept utilizes two signal conditioning units (SCU), preliminary indications are a future detailed review of telemetry requirements may allow only one SCU to be used. In such a case the SCU output will be cross-strapped to the encoders providing total redundancy.

The two telemetry transmitters utilize the same two VHF frequencies as those allocated to ATS-V. Since the RMU encoders are cross-strapped to the transmitters, sufficient versatility is provided to allow simultaneous transmission from the ATS-V and the RMU (on a different frequency per vehicle).
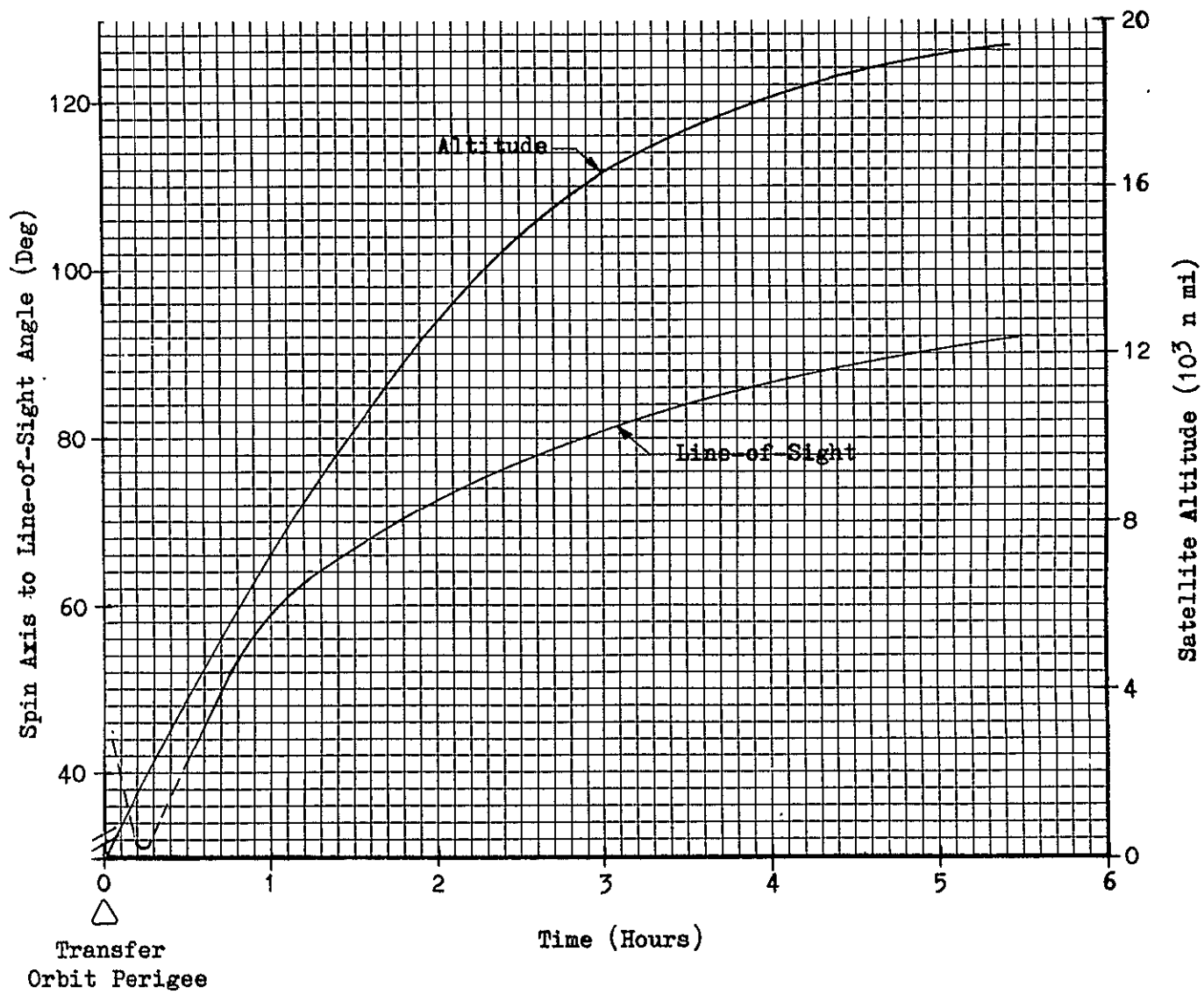
Figure 7-29. Altitude and Spin Axis Angle versus Time
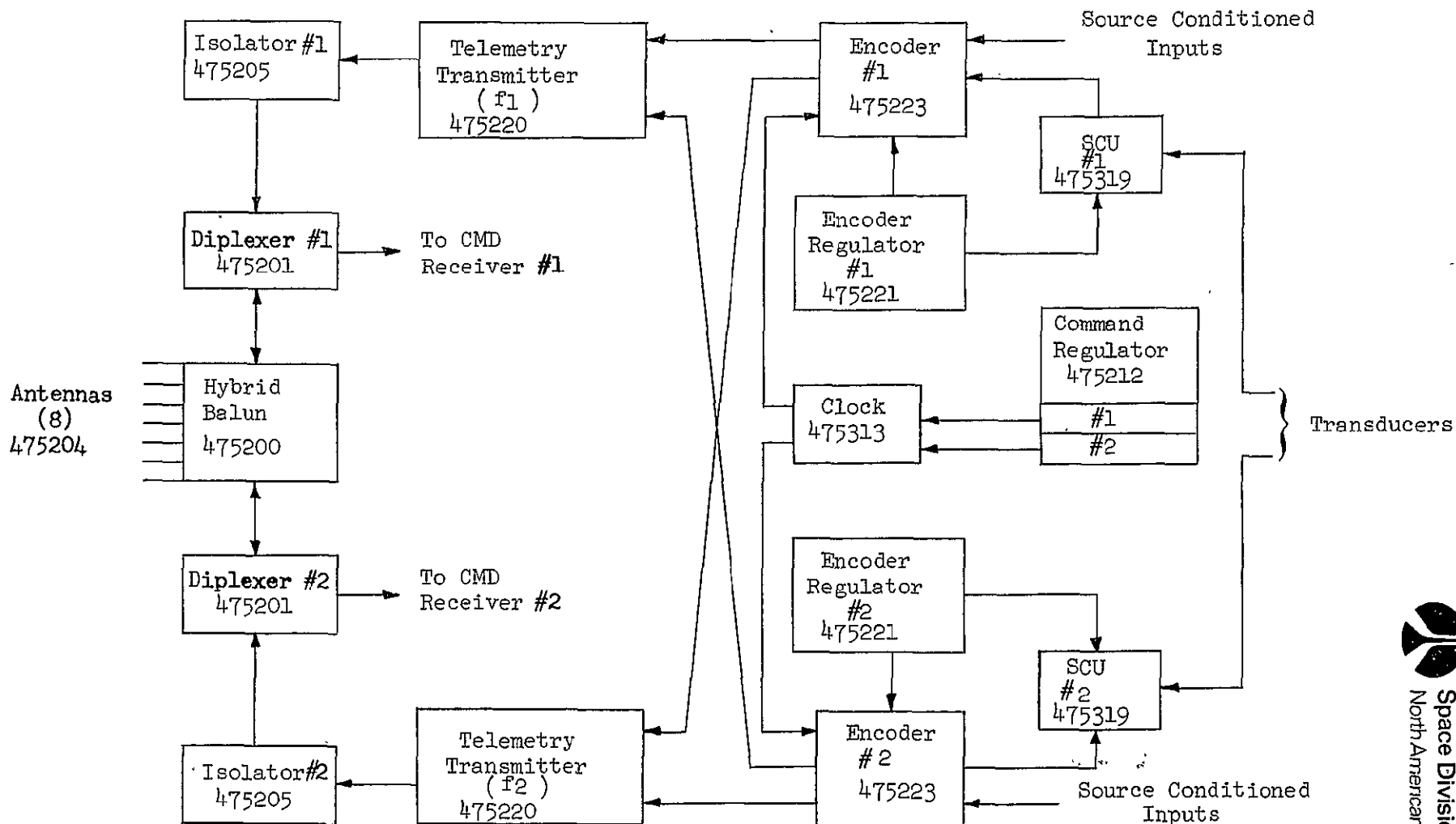
Figure 7-30.   Telemetry Subsystem

TABLE 7-15 TELEMETRY MEASUREMENT LIST

NO.	FUNCTION	UNITS	FUNCTION RANGE	DATA FORM
	POWER SUBSYSTEM			
1	Main Bus Voltage	Volts	27-29	Analog
2	Regulator Output Current	Amperes	0-15	Analog
3	Battery Charge Current	Amperes	0-2	Analog
4	Battery Discharge Current	Amperes	0-10	Analog
5	Solar Bus Voltage	Volts	20-60	Analog
6	Solar Array Current	Amperes	0-10	Analog
7	Test Cell Voltage	Millivolts	0-700	Analog
8	Test Cell Current	Milliamps	0-160	Analog
9	Test Cell Current	Milliamps	0-160	Analog
10	Solar Panel Temperature	°F	-200 – +250	Analog
11	Solar Panel Temperature	°F	-200 – +250	Analog
12	Solar Panel Temperature	°F	-200 – +250	Analog
13	Solar Panel Temperature	°F	-200 – +250	Analog
14	Inverter Input Current	Amperes	0.2.2	Analog
15	Battery #1 Temperature	°F	0-120	Analog
16	Battery #2 Temperature	°F	0-120	Analog
17	Battery #1 Charge State	Percent	0-100	Analog
18	Battery #2 Charge State	Percent	0-100	Analog

TABLE 7-15 TELEMETRY MEASUREMENT LIST - Continued

NO.	FUNCTION	UNITS	FUNCTION RANGE	DATA FORM
	TELEMETRY & COMMAND SUBSYSTEM			
1	TM Transmitter #1 ON, #2 OFF	***	***	Discrete
2	TM Transmitter #2 ON, #1 OFF			Discrete
3	TM Transmitter #1 & #2 OFF			Discrete
4	TM Frame Sync			Digital
5	Spacecraft TM, I.D., Encoder #1	TBD	TBD	Analog
6	Spacecraft TM, I.E., Encoder #2	TBD	TBD	Analog
7	TM Encoder Subcom Position			Digital
8	TM SCO. ON/OFF			Discrete
9	Calibration Reference	-4.855	-4.855	Analog
10	Encoder Mode, Normal/Dwell			Discrete
11	Command Register #1 Contents			Digital
12	Command Register #2 Contents			Digital
13	Command Decoder Execute Env.			SCO
14	Command Enable ON/OFF #1			Discrete
15	Command Enable ON/OFF #2			Discrete
16	Command Decoder, Rec. #1 Select			Discrete
17	Command Decoder, Rec. #2 Select			Discrete
18	Command Mode (FSK/Count)#1			Discrete
19	Command Mode (GSK/Count)#2			Discrete
20	Command Decoder Pwr #1 ON/OFF			Discrete
21	Command Decoder Pwr #2 ON/OFF			Discrete
22	TM Transmitter #1 Output Power	Watts	1.6 - 2.5	Analog
23	TM Transmitter #2 Output Power	Watts	1.6 - 2.5	Analog

***Discrete-Digital inputs 0 to -24V in Function range and 0 to -5V in TM range.

TABLE 7-15 TELEMETRY MEASUREMENT LIST — Continued

NO.	FUNCTION	UNITS	FUNCTION RANGE	DATA FORM
	COMMUNICATIONS SYSTEM			
1	C-band Rptr #1 Ft Mode ON/OFF	***	***	Discrete
2	C-band Rptr #2 Ft Mode ON/OFF			Discrete
3	C-band Rptr #1 WBD Mode ON/OFF			Discrete
4	C-band Rptr #2 WBD Mode ON/OFF			Discrete
5	Rec.Signal Strength Rptr #1	Watts		Analog
6	Rec.Signal Strength Rptr.#2	Watts		Analog
7	C-band Xmtr Power Output	Watts		Analog
8	TWT #1 Filament ON/OFF			Discrete
9	TWT #2 Filament ON/OFF			Discrete
10	Xmtr Regulator #1 ON/OFF			Discrete
11	Xmtr Regulator #2 ON/Off			Discrete
	DOCKING SYSTEM			
1	Docking Latch #1 Open/Closed	***	***	Discrete
2	Docking Latch #2 Open/Closed			Discrete
3	Docking Latch #2 Open/Closed			Discrete
4	Gas Gen.Cartridge #1 Continuity			Discrete
5	Gas Gen.Cartridge #2 Continuity			Discrete
6	Gas Gen.Cartridge #3 Continuity			Discrete
7	Gas Gen.Cartridge #1 FIRED			Discrete
8	Gas Gen.Cartridge #2 FIRED			Discrete
9	Gas Gen.Cartridge #3 FIRED			Discrete

***Discrete — Digital inputs 0 to -24V in Function range and 0 to -5V in TM range.

TABLE 7-15 TELEMETRY MEASUREMENT LIST – Continued

NO.	FUNCTION	UNITS	FUNCTION RANGE	DATA FORM
	ATTITUDE CONTROL SUBSYSTEM			
1	Roll DPG Sine	Volts	-1 to +1	Analog
2	Roll DPG Cosine	Volts	-1 to +1	Analog
3	Pitch DPG Sine	Volts	-1 to +1	Analog
4	Pitch DPG Cosine	Volts	-1 to +1	Analog
5	Yaw DPG Sine	Volts	-1 to +1	Analog
6	Yaw DPG Cosine	Volts	-1 to +1	Analog
7	Roll DPG Torque Motor (-, OFF, +)	Volts	-1, 0, +1	Discretes
8	Pitch DPG Torque Motor (-, OFF, +)	Volts	-1, 0, +1	Discretes
9	Yaw DPG Torque Motor (-, OFF, +)	Volts	-1, 0, +1	Discrete
10	RCS Jet #1 Firing ON/OFF			Discrete
11	RCS Jet #2 Firing ON/OFF			Discrete
12	RCS Jet #3 Firing ON/OFF			Discrete
13	RCS Jet #4 Firing ON/OFF			Discrete
14	RCS Jet #5 Firing ON/OFF			Discrete
15	RCS Jet #6 Firing ON/OFF			Discrete
16	RCS Jet #7 Firing ON/OFF			Discrete
17	RCS Jet #8 Firing ON/OFF			Discrete
18	RCS Jet #9 Firing ON/OFF			Discrete
19	RCS Jet #10 Firing ON/OFF			Discrete
20	RCS Jet #11 Firing ON/OFF			Discrete

TABLE 7-15 TELEMETRY MEASUREMENT LIST – Continued

NO.	FUNCTION	UNITS	FUNCTION RANGE	DATA FORM
	ATTITUDE CONTROL			
	SUBSYSTEM – Continued			
21	RCS Jet #12 Firing ON/OFF			Discrete
22	Spinning Sun Sensor #1 pulse ON/OFF			Discrete
23	Spinning Sun Sensor #2 pulse ON/OFF			Discrete
24	Docking Cage Rotation Rate			Pulse Train
25	Nutation–Accel #1 Waveform	g's		Analog
26	Nutation–Accel #2 Waveform	g's		Analog
27	Spinning Sun–Sensor #1 Angle	degrees	$-50°$ to $+50°$	Digital
28	Spinning Sun–Sensor #2 Angle	degrees	$-50°$ to $+50°$	Digital
29	Solar Aspect Angle A	degrees	$0°$ to $128°$	Digital
30	Solar Aspect Angle B	degrees	$0°$ to $128°$	Digital
31	Sensir ID	Units	1 to 5	Digital
32	ACS Counter #1 Setting	Units	0 to 128	Digital
33	ACS Counter #2 Setting	Units	0 to 128	Digital
34	RMU–Spin Jet Control ON/OFF			Discrete
35	Minimum Inpulse Mode ON/OFF			Discrete
36	Docking–Cage Spin Control ON/OFF			Discrete
37	Docking–Cage Nominal Rate ON/OFF			Discrete
38	Docking–Cage Despin High ON/OFF			Discrete
39	Docking–Cage Despin Low ON/OFF			Discrete
40	Solar Aspect System ON/OFF			Discrete
41	Reaction Jet #1 Enable ON/OFF			Discrete
42	Reaction Jet #2 Enable ON/OFF			Discrete
43	Reaction Jet #3 Enable ON/OFF			Discrete
44	Reaction Jet #4 Enable ON/OFF			Discrete

TABLE 7-15 TELEMETRY MEASUREMENT LIST - Continued

NO.	FUNCTION	UNITS	FUNCTION RANGE	DATA FORM
	ATTITUDE CONTROL SUBSYSTEM - Continued			
45	Reaction Jet #5 Enable ON/OFF			Discrete
46	Reaction Jet #6 Enable ON/OFF			Discrete
47	Reaction Jet #7 Enable ON/OFF			Discrete
48	Reaction Jet #8 Enable ON/OFF			Discrete
49	Reaction Jet #9 Enable ON/OFF			Discrete
50	Reaction Jet #10 Enable ON/OFF			Discrete
51	Reaction Jet #11 Enable ON/OFF			Discrete
52	Reaction Jet #12 Enable ON/OFF			Discrete
53	Roll DPG Motor A ON/OFF			Discrete
54	Roll DPG Motor B ON/OFF			Discrete
55	Pitch DPG Motor A ON/OFF			Discrete
56	Pitch DPG Motor B ON/OFF			Discrete
57	Yaw DPG Motor A ON/OFF			Discrete
58	Yaw DPG Motor B ON/OFF			Discrete
59	Roll Resolver Excit ON/OFF			Discrete
60	Pitch Resolver Excit ON/OFF			Discrete
61	Yaw Resolver Excit ON/OFF			Discrete
62	Roll DPG Desat Sw. Enable ON/OFF			Discrete
63	Pitch-Yaw DPG Desat Sw. Enable ON/OFF			Discrete
64	Solar Aspect Sensor Monitor A ON/OFF			Discrete

TABLE 7-15 TELEMETRY MEASUREMENT LIST – Continued

NO.	FUNCTION	UNITS	FUNCTION RANGE	DATA FORM
	ATTITUDE CONTROL SUBSYSTEM – Continued			
65	Solar Aspect Sensor Monitor B ON/OFF			Discrete
66	Solar Aspect Sensor #1 Temp	Degrees	-160°F to 185°F	Analog
67	Solar Aspect Sensor #2 Temp	Degrees	-160°F to 185°F	Analog
68	Solar Aspect Sensor #3 Temp	Degrees	-160°F to 185°F	Analog
69	Solar Aspect Sensor #4 Temp	Degrees	-160°F to 185°F	Analog
70	Solar Aspect Sensor #5 Temp	Degrees	-160°F to 185°F	Analog
71	SAS Electronics Temp	Degrees	0°F to 100°F	Analog
72	Nutation Accel. #1 ON/OFF			Discrete
73	Nutation Accel. #2 ON/OFF			Discrete
74	Spinning Sun Sensor #1 ON/OFF			Discrete
75	Spinning Sun Sensor #2 ON/OFF			Discrete
76	Autonutation Control #1 ON/OFF			Discrete
77	Autonutation Control #2 ON/OFF			Discrete
78	Autonutation #1 Activate ON/OFF			Discrete
79	Autonutation #2 Activate ON/OFF			Discrete
80	Manual Nutation Control #1 ON/OFF			Discrete
81	Manual Nutation Control #2 ON/OFF			Discrete

Discretes – Digital Inputs 0 to -24V in function range and 0 to -5V in TM range.

7.2.6.2 Command

The preliminary RMU command list given in Table 7-16 indicates that the capabilities of the ATS command equipment are adequate for the RMU application. Figure 7-31 is the block diagram of the baseline command subsystem; again, the ATS-V part numbers of each element are given as assigned by HAC. The command subsystem is identical to that of ATS-V; driver electronics were added for actuation of squibs utilized in RMU subsystems.

The RMU command system will utilize the same frequency as that allocated to ATS-V; appropriate vehicle address codes will permit independent command/control of the ATS-V and the RMU. In some of the mission phases, when the RMU is under "pilot" control, real-time, fast response command execution is essential to assure accurate and timely maneuvering. When commands of this nature are transmitted to the RMU, the "execute" tone will also be transmitted without prior "verification" of command receipt via the telemetry link.

7.2.7 Video and Illumination

The video and illumination subsystem is a key subsystem providing the primary source of information upon which the docking operation will be based. It is primarily composed of developed components, though the selected vidicon tube has not yet flown and the light source must be fabricated and qualified specifically to the requirements of this mission. The subsystem is, however, essentially available state-of-the-art as indicated subsequently.

The video and illumination subsystem must satisfy three basic functional requirements: (a) it must provide the capability of visually acquiring the ATS-V from a reasonably long range without imposing severe requirements on the ground tracking capability, (b) it must provide visual cues needed for guiding the RMU to the ATS-V, and (c) it must facilitate precontact alignment and docking closure operations. After the primary mission objective of despinning the ATS-V is attained, the subsystem must provide visual data during separation and observation operations.

During the acquisition and rendezvous phases, the ATS-V will be illuminated by sunlight. During the docking operations, however, the recessed docking interface area on the aft end of ATS-V will be in total shadow (the piloted simulation, Appendix C, indicated that sunlight reflections on the ATS-V aft end during autumn and winter were undesirable and a spring or summer despin is anticipated). Sufficient indirect scattered sunlight is not considered to be available in that area for obtaining images even if a low light level TV camera was used. Thus, the video and illumination subsystem must provide a suitable light source.

Additional significant requirements result from reliability considerations. The TV camera is the primary sensor of the RMU in the 3-axis stabilized mode of operation. Failure of this sensor would be tantamount to mission abort. Thus, at an early stage, two decisions were made to safeguard against such a situation: (a) redundancy must be provided by using two TV cameras, and (b) the cameras must be protected from direct sunlight impinging on the sensing elements of the cameras.

TABLE 7-16 RMU COMMAND LIST

POWER SUBSYSTEM

1.	Battery charger ON
2.	Battery charger OFF
3.	Inverter ON
4.	Inverter OFF
5.	Load Control #1 ON

| 53. | Load Control #49 ON |
| 54. | Load Control #1 OFF |

| 102. | Load Control #49 OFF |

TELEMETRY COMMAND SUBSYSTEM

1.	TM Transmitter #1 ON, #2 OFF
2.	TM Transmitter #2 ON, #1 OFF
3.	TM Transmitter #1 and #2 OFF
4.	TM Transmitter #1, Encoder Select
5.	TM Transmitter #2, Encoder Select
6.	PCM Encoder #1 ON
7.	PCM Encoder #1 OFF
8.	PCM Encoder #2 ON
9.	PCM Encoder #2 OFF
10.	SCO #1 ON
11.	SCO #2 ON
12.	SCO #1 and #2 OFF
13.	Encoder #1 Dwell Mode Select
14.	Encoder #2 Dwell Mode Select
15.	Dwell Channel Select
16.	Waveform Switch #1 ON/OFF
17.	Waveform Switch #2 ON/OFF

TABLE 7-16 RMU COMMAND LIST – Continued

COMMUNICATIONS

1. C-Band Transmitter TWT #1 Filament ON
2. C-Band Transmitter TWT #2 Filament ON
3. C-Band Transmitter TWT HV ON
4. C-Band Transmitter Repeater #1 Select
5. C-Band Transmitter Repeater #2 Select
6. Select Planar Array Antenna
7. Select Omni Antenna
8. C-Band Repeater #1 FT Mode ON, WBD Mode OFF
9. C-Band Repeater #2 FT Mode ON, WBD Mode OFF
10. C-Band Repeater #1 WBD Mode ON, FT Mode OFF
11. C-Band Repeater #2 WBD Mode ON, FT Mode OFF
12. C-Band Repeater #1 OFF
13. C-Band Repeater #2 OFF

DOCKING SYSTEM

1. Fire Gas Generator Cartridge #1
1. Fire Gas Generator Cartridge #2
3. Fire Gas Generator Cartridge #3

PROPULSION SYSTEM

1. Solid Motor Ignition
2. Solid Motor Jettison
3. Solid Motor Ignition Circuit Severance

TV AND ILLUMINATION SUBSYSTEM

1. Light #1 ON
2. Light #2 ON
3. Light #1 OFF
4. Light #2 OFF
5. TV Camera #1 ON
6. TV Camera #2 ON
7. White Clipper Low
8. White Clipper High
9. TV Camera #1 OFF
10. TV Camera #2 OFF

TABLE 7-16 RMU COMMAND LIST - Continued

11. Camera Turret CW
12. Camera Turret CCW
13. Shutter Overide #1 ON
14. Shutter Overide #2 ON
15. Shutter Overide #1 OFF
16. Shutter Overide #2 OFF
17. Iris #1 Step-up
18. Iris #2 Step-up
19. Iris #1 Step-down
20. Iris #2 Step-down
21. Video Camera #1 Select
22. Video Camera #2 Select
23. Camera Target Voltage Increase
24. Camera Target Voltage Decrease

ATTITUDE CONTROL SUBSYSTEM

1. RCS + Roll
2. RCS - Roll
3. RCS + Pitch
4. RCS - Pitch
5. RCS + Yaw
6. RCS - Yaw
7. RCS + X Translation
8. RCS - X Translation
9. RCS + Y Translation
10. RCS - Y Translation
11. RCS + Z Translation
12. RCS - Z Translation
13. DPG + Roll
14. DPG - Roll
15. DPG + Pitch
16. DPG - Pitch
17. DPG + Yaw
18. DPG - Yaw
19. RMU - Spin Jet Control ON/OFF
20. RMU - Spin Jet Phasing Increment
21. RMU - Spin Jet Phasing Decrement
22. RMU - Spin Jet Duration Increment
23. RMU - Spin Jet Duration Decrement
24. Minimum Impulse Mode ON/Off
25. Docking - Cage Spin Control ON/OFF

TABLE 7-16 RMU COMMAND LIST – Continued

ATTITUDE CONTROL SUBSYSTEM – continued

26. Docking – Cage Nominal Rate
27. Docking – Cage Coarse Increment
28. Docking – Cage Coarse Decrement
29. Docking – Cage Fine Increment
30. Docking – Cage Fine Decrement
31. Docking – Cage Despin High Torque
32. Docking – Cage Despin Low Torque
33. ACS Counter #1 Reset
34. ACS Counter #2 Reset
35. Solar Aspect System ON/OFF
36. Reaction Jet #1 Enable ON/OFF
37. Reaction Jet #2 Enable ON/OFF
38. Reaction Jet #3 Enable ON/OFF
39. Reaction Jet #4 Enable ON/OFF
40. Reaction Jet #5 Enable ON/OFF
41. Reaction Jet #6 Enable ON/OFF
42. Reaction Jet #7 Enable ON/OFF
43. Reaction Jet #8 Enable ON/OFF
44. Reaction Jet #9 Enable ON/OFF
45. Reaction Jet #10 Enable ON/OFF
46. Reaction Jet #11 Enable ON/OFF
47. Reaction Jet #12 Enable ON/OFF
48. Roll DPG Motor A ON/OFF
49. Roll DPG Motor B ON/OFF
50. Pitch DPG Motor A ON/OFF
51. Pitch DPG Motor B ON/OFF
52. Yaw DPG Motor A ON/OFF
53. Yaw DPG Motor B ON/OFF
54. Roll Resolve Excitation ON/OFF
55. Pitch Resolve Excitation ON/OFF
56. Yaw Resolve Excitation ON/OFF
57. Roll, DPG Desaturate Switch Enable ON/OFF
58. Pitch-Yaw DPG Desaturate Switch Enable ON/OFF
59. Nutation – Sensing Accelerometer #1 ON/OFF
60. Nutation – Sensing Accelerometer #2 ON/OFF
61. Spinning Sun-Sensor #1 ON/OFF
62. Spinning Sun-Sensor #2 ON/OFF
63. Autonutation Control System #1 ON/OFF
64. Autonutation Control System #2 ON/OFF
65. Autonutation Control System #1 Activate ON/OFF
66. Autonutation Control System #2 Activate ON/OFF
67. Manual Nutation Control #1 ON/OFF

TABLE 7-16 RMU COMMAND LIST - Continued

ATTITUDE CONTROL SUBSYSTEM - continued

68.   Manual Nutation Control #2 ON/OFF
69.   Solar Aspect Sensor and Angle Detector CMDA
70.   Solar Aspect Sensor and Angle Detector CMDB
71.   Solar Aspect Sensor and Angle Detector CMDC
72.   Solar Aspect Sensor and Angle Detector CMDD
73.   RMU - Spin Maneuver Reset

| Diplexer #1 475215 | → | Command Receiver #1 475210 |

Power Bus

| Command Decoder 475211 | #1 | #2 | | #2 | #1 | Command Regulator 475212 |

| Diplexer #2 475215 | → | Command Receiver #2 475210 |

Outputs

| Squib Drivers (New) | →
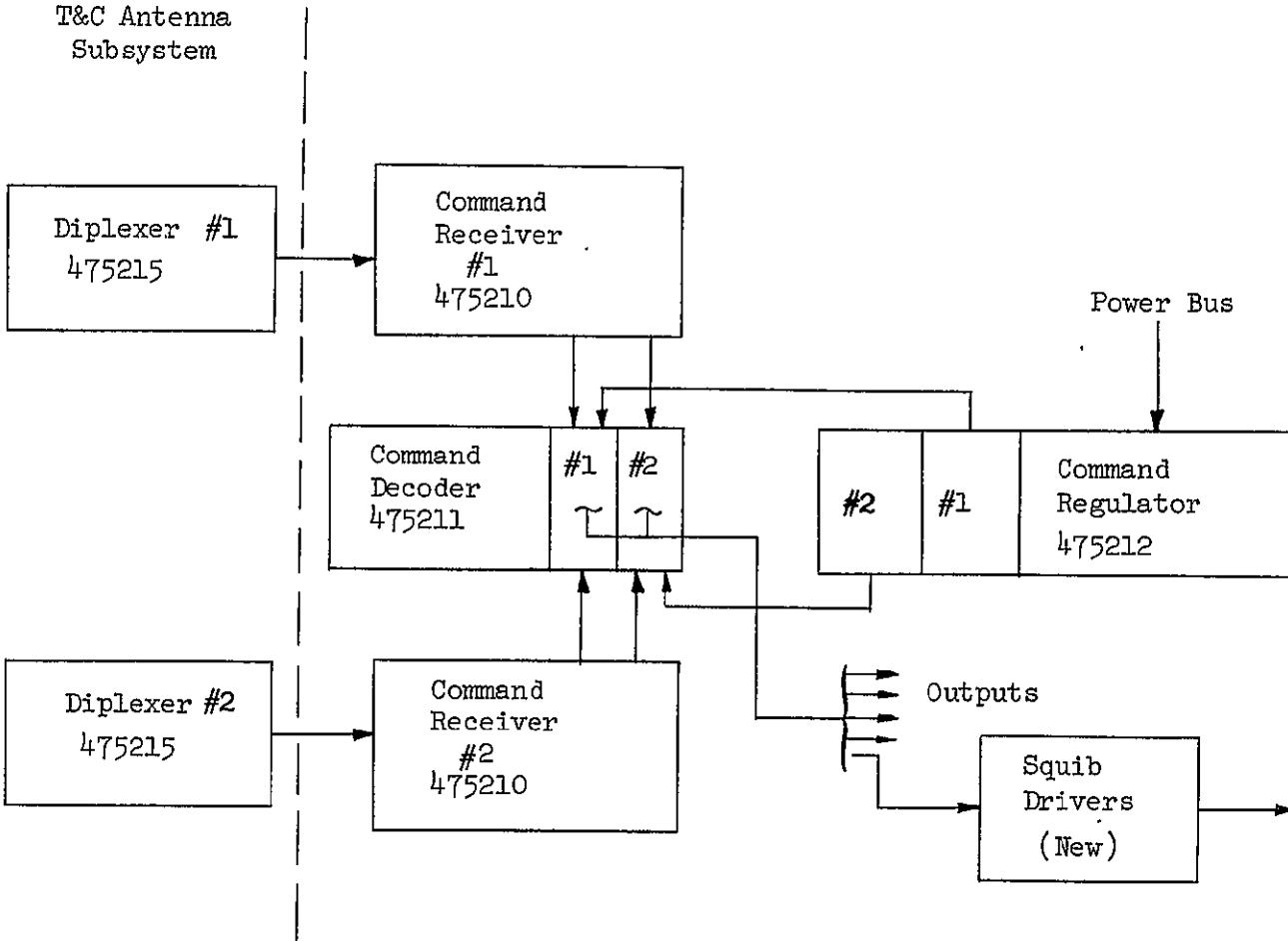
Figure 7-31.   Command Subsystem

Examination of the viewing geometry as a function of mission phase results in two somewhat contradictory requirements:

1. The use of a narrow field-of-view (FOV) lens is indicated to provide a recognizable image of ATS-V (i.e., larger than a star) from as long a range as possible. A narrow FOV lens, however, tends to reduce the probability of including the ATS-V in the small image field without a search maneuver. A satisfactory compromise was found in using a 50 mm lens which provides a 14° vertical FOV. Boresight of the lens, if fixed, must·be parallel to the RMU X-axis, but does not necessarily have to be on the vehicle centerline. Steering of the camera LOS would facilitate acquisition if suitable acquisition geometry were not provided by ground guidance.

2. During the docking operations a wide FOV lens is needed to allow coverage of the entire ATS-V docking interface area from a very close range. A 10 mm lens, which provides a 64° vertical FOV, was found to satisfy this requirement. This lens, if fixed, must be boresighted on the X-axis of the RMU to facilitate accurate pre-docking alignment. Steering of the camera LOS would permit 4 steradian observation of ATS-V after despin but is not a requirement in the baseline mission.

Various methods were considered for providing the necessary camera redundancy in light of the lens requirements. One approach considered utilized two turret-mounted lenses for each camera, with one camera located on the RMU centerline while the other slightly offset from the axis. This approach provided only partial redundancy; if the centerline-mounted camera failed the other camera could not provide the critical center-line view for docking operations. Due to this shortcoming, as well as due to its complexity, this approach was rejected.

A second concept involved the use of a 5:1 zoom lens (50 to 10 mm) mounted on the vehicle centerline; two cameras, mounted in a common gimbal were located in such a manner that either could be positioned behind the zoom lens by rotating the gimbal. This concept satisfied all the requirements but would have involved a special lens design to meet the requirements. The zoom-drive motor also involved added complexity. Thus this concept was rejected in favor of a similar yet less complex arrangement. This third concept, which was selected for the baseline design, retains the gimbal-mounted camera principle, but uses two fixed lenses in place of a single zoom lens. The wide FOV lens is mounted in a fixed position on the RMU centerline; the narrow FOV lens off the center-line. With this arrangement the desired FOV is obtained by switching between cameras or, in the case of a camera failure, by rotating the remaining camera to the desired lens position.

Camera LOS steering was considered as a means of providing added flexibility to RMU operations. It could be accomplished in various ways. If an omni antenna or steerable antenna were provided, the camera LOS could be steered by maneuvering the RMU. In the baseline concept, however, a high gain antenna is employed because of availability and to minimize prime power requirements. This antenna must be pointed to Earth within narrow angular limits and the RMU can, therefore, steer the camera LOS only in a narrow band about the yaw plane. In the baseline mission this steering is sufficient to accommodate both the acquisition and docking phases; i.e., (a) ground tracking capability is more than adequate to provide acquisition geometry which obviates the need for any steering or, at most, requires only limited steering in the yaw plane, and (b) the docking operation does not require steering. Therefore, to avoid unnecessary complexity, no steering capability for the camera LOS, other than RMU steering in the yaw plane, is provided in the baseline RMU. During the ATS-V observation phase and for subsequent missions, 4π steradian steering capability would permit full coverage of observed satellites, a possible advantage. The steering could be accomplished by various means, such as providing an omni or steerable antenna, incorporating pitch steering provisions for the camera, adding a rotatable mirror for steering the camera LOS in the pitch plane, or adding cameras for viewing in the pitch plane. All involve considerable additional complexity, the least impact probably resulting from adding cameras. Steering the cameras or a mirror would usually not be too difficult, but in the baseline concept, the cage and its shroud obstruct the view and appear to preclude this approach. A steerable antenna is the most complex of the options and is considered unsuited to the baseline concept. As indicated previously, the possible uses of a steered camera LOS subsequent to ATS-V despin are not considered to warrant inclusion of the capability at this time.

The baseline video and illumination subsystem concept selected for this application on the basis of the above requirements and considerations is schematically illustrated in Figure 7-32. Details pertaining to the primary subsystem elements are given in the following subsections.

7.2.7.1 TV Cameras

Consideration was given to utilizing a stereo camera system. Pilot-in-the-loop simulations have, however, shown no need for this added complexity. The pilots were able to judge range and range-rate very adequately on the basis of stadia without the aid of a stereo image.

During recent pilot-in-the-loop simulations, a severely blurred image was produced when the rotating ATS-V was viewed by means of an ordinary Vidicon type TV camera; this presented a considerable handicap in accurate performance of docking maneuvers. The blurring was traced to the long retention characteristics of ordinary Vidicon tubes.
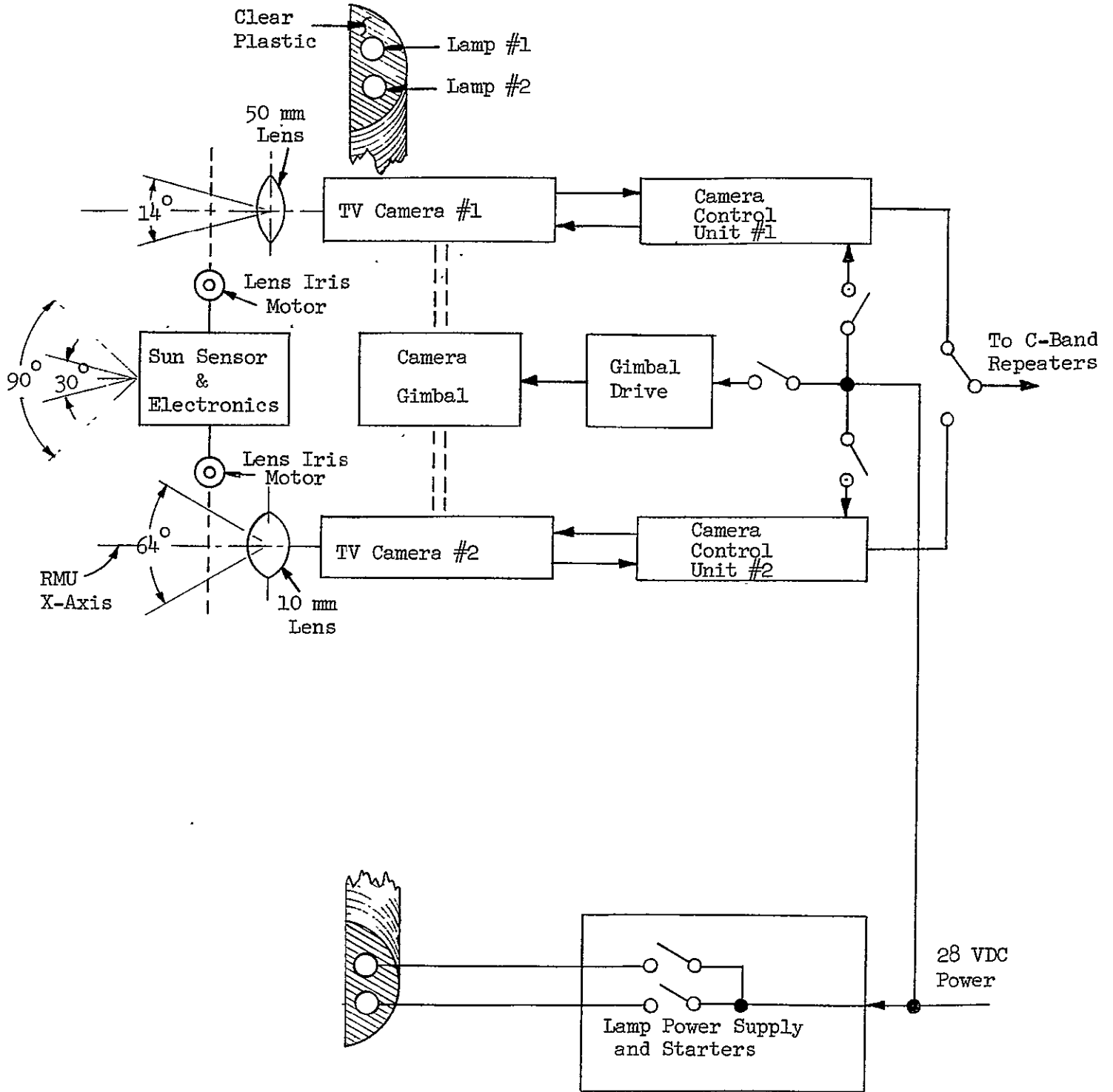
Figure 7-32. Video and Illumination Subsystem

Two solutions were tried in the simulations and both were found satisfactory from an image quality standpoint. One method involved the use of an image orthicon camera while the other consisted of merely changing from a conventional Vidicon tube to a lead-oxide (PbO) Vidicon tube. Since image orthicon cameras are not considered practical for space applications, the lead-oxide Vidicon approach was selected for the baseline concept. Although these tubes have not been space qualified, no particular difficulties are expected in this regard since the lead-oxide tubes use the same gun structure and mechanical design features as the ordinary Vidicon tubes; thus the lead-oxide tube can be readily provided in the ruggedized configuration commonly used in space applications of Vidicons. An added advantage of lead-oxide tubes is that their sensitivity peaks at around 5200 Angstroms which exactly coincides with the principal frequency of light produced by the cold-cathode tubes utilized for illumination. This fortunate match is anticipated to result in considerable reduction of electrical power required for illumination.

The TV camera selected for the baseline design is the Lear Siegler Model 0791 which is an updated solid state version of the camera used on ATS-V; the updated camera has been space qualified. Modifications required to accommodate the lead-oxide tube are expected to be minimal.

Two cameras are provided. One is positioned behind a fixed wide FOV lens on the RMU centerline, the other behind a fixed narrow FOV lens off the centerline. The cameras are gimbal mounted and can be rotated to exchange lens positions. The gimbal would not be rotated at all unless one of the cameras should fail. If such a failure should occur, the remaining camera can be rotated into position behind either of the two lenses thus providing full operational capability. In the absence of a failure, wide FOV or narrow FOV images can be obtained by merely switching the video output of the appropriate camera to the C-band communication system.

7.2.7.2 Lens Assembly

The lens assembly contains a 50 mm (14° vertical FOV) lens and a 10 mm (64° vertical FOV) lens; the F/numbers of the two lenses are 2.0 and 1.8 respectively. Each lens has a motor driven iris capable of completely closing thus eliminating the need for separate sun shutters. The basic lenses, without the motor driven iris, have been space qualified; although the version equipped with a motor driven iris has not been space qualified; no difficulties are expected.

A sun sensor assembly is provided as part of the lens assembly for the purpose of triggering the iris of each lens to the fully closed position whenever the sun approaches the field of view of the cameras. The sun sensor assembly, schematically illustrated in Figure 7-33, consists of a dual photodiode sensor, a low resolution wide angle lens to project an image on the photodiode, and suitable electronics. The center portion of the dual diode has a FOV of 30°; any indication of direct sunlight in this FOV activates the stepping motor on the 50 mm lens to fully close its iris. Surrounding this inner diode is a toroidal shaped diode whose FOV extends from 30° to 80°; any indication of direct sunlight on the toroidal or on the inner diode will actuate the closing of the iris on the 10 mm lens. An override capability is provided in the electronics to allow opening of the iris by ground command in case a sunglint has accidentally closed it.
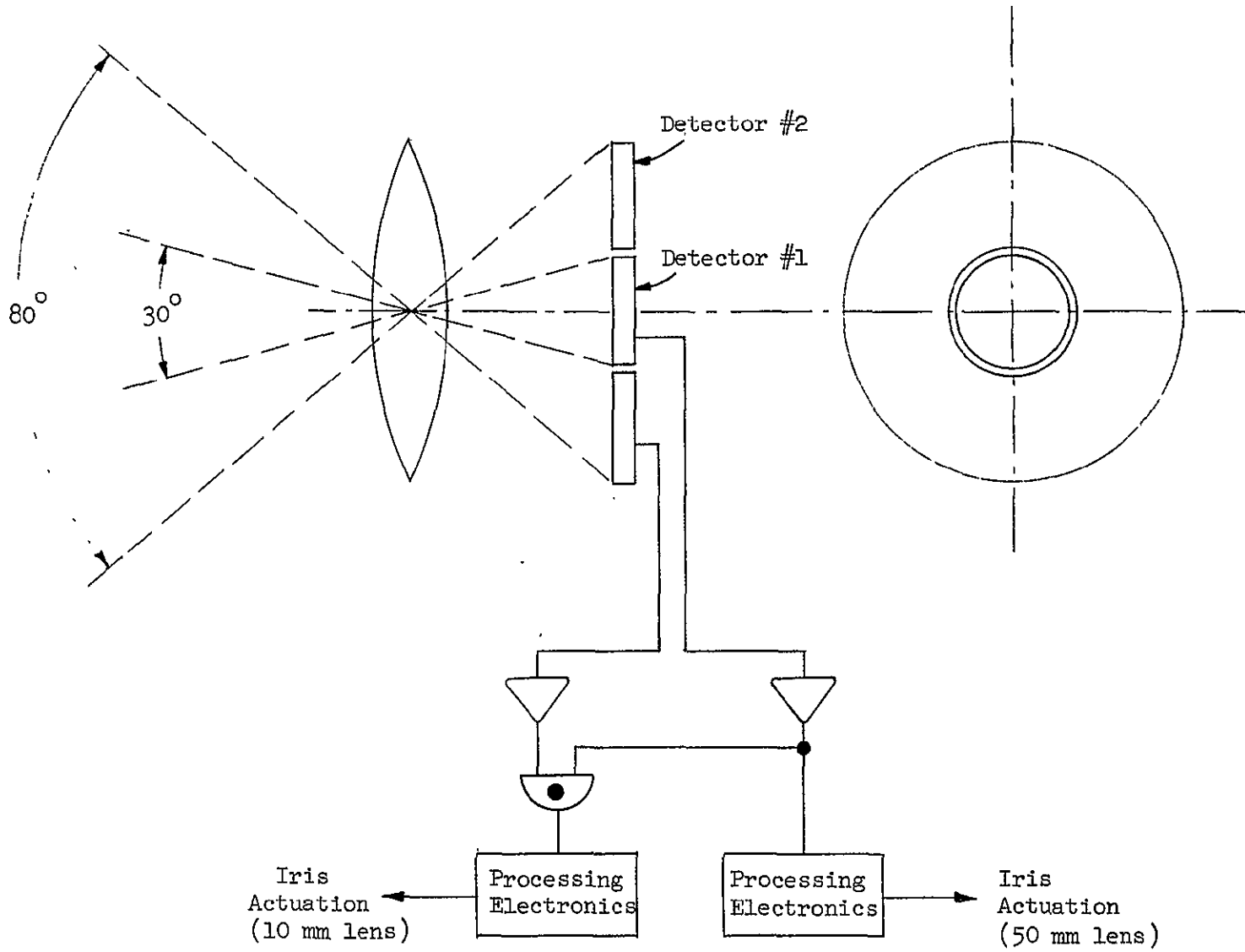
Figure 7-33. Sun Sensor

7.2.7.3 Illumination

Several methods of providing the required illumination have been considered. One of the concepts involved the use of a space qualified pulsed Xenon light source; in the RMU application the pulsing had to be synchronized with the television camera. However, when a Xenon light source flashes at TV rates (60 times per second) its efficiency is extremely poor requiring excessive electrical power. Due to this reason as well as due to size and weight penalties this approach has been rejected.

The use of a small reflector on the RMU was also considered as a means of directing sunlight into the aft end of the ATS-V. During the last critical phase of the docking operation the close proximity of the two vehicles leaves very little access for sunlight. This approach could probably not produce sufficient light energy and was rejected as impractical.

The selected light assembly concept utilizes two concentric cold-cathode type lamps. A separate power supply is provided to furnish the starting and operating power to the lamps. Power switching circuitry allows either or both lamps to be energized. Recent simulation tests indicated that a light intensity of 200 foot-candles is needed for appropriate illumination when the distance is 5 feet between the docking interfaces. The cold-cathode lamps produce 100-120 lumens/watt so that, with both lamps operating at 75 watts total lamp power, this light level requirement can be met. Allowing for losses in the power supply a total power requirement of 100 watts is anticipated when both lights are operating.

Preliminary indications are that appropriate trimming of TV camera target voltages, white clipping levels and video gains will allow significant reduction in light level requirements with a resultant saving in power. Similarly, a power reduction is expected to result from full utilization of the excellent spectral match of the cold-cathode light source and the lead-oxide Vidicon tube.

The lamps are potted using a clear selastic into an appropriately shaped reflector; the reflector configuration is designed to direct the light energy mainly on the peripheral area around the apogee motor thrust ring of the ATS-V which is of low reflectance while keeping the light level low at the highly reflective center portion of the ATS-V thermal control louvers.

7.2.8 Docking and Despin

The docking subsystem consists of a docking mechanism supported by a cage structure which can be spun up and synchronized with the ATS-V spin rate. The docking mechanism consists of 3 latches with recycling provisions. The ground rules established in the study for the design of the docking subsystem are that it must:

1. Meet the general environmental condition of the mission,

2. Facilitate alignment and synchronization procedures,

3. Tolerate ATS-V wobble and pilot alignment error,

4. Provide capture to the extent necessary to accomplish despin, and

5. Accomplish despin and separation without changing ATS-V's configuration.

The first ground rule impacts the design significantly, particularly the docking mechanism since it must operate mechanically and/or pneumatically in space; thermal and vacuum environments will be particularly pertinent. This consideration led to the eventual discarding of an approach to expand inflatable materials against ATS-V surfaces as a means of effecting capture because of the lengthy development time anticipated to insure proper performance in the space environment as well as for certain operational disadvantages. Also, since the docking subsystem is at the extremity of the spacecraft, the launch environment (particularly lateral vibration) will be significant.

The second requirement necessitates that the docking mechanism must not block the field of view of the video and illumination subsystem. This, in turn, suggests that the docking mechanism and its support structure should be arranged to leave the centerline area of the RMU free for viewing and lighting.

As discussed in greater detail in Section 4.0 and Appendix C, the third ground rule requires that the latching mechanism tolerate an angular misalignment of at least 3° and, at the same time, a lateral miss distance of 2". The lateral miss distance tolerance and the angular misalignment allowance will accommodate the ATS-V wobble combined with pilot error.

The fourth requirement suggests positive coupling. Magnetic coupling was considered since it would eliminate impact forces involved in an actual docking. Magnetic coupling and despin is considered impractical, however, because of excessive power demands and extreme precision station-keeping requirements. Positive coupling or docking is, then, a requirement, and the docking subsystem must accommodate the loads associated with initial impact, capture and subsequent despin. A despin torque of about 2.0 ft-lb must be transmitted through the latches to ATS-V during the despin operation.

The last ground rule eliminates permanent attachment schemes and strongly suggests use of the apogee motor thrust flange as the structural interface. Thus, methods of attaching yo-yo despin devices or spin rockets through use of explosively or mechanically expanded penetrating devices were eliminated. Also, attaching to or expanding onto the solar panels was discarded in favor of the more structurally suitable apogee motor thrust flange. The last ground rule also demands that the latching scheme provide sufficient clearance to accommodate the wobble of the spacecraft and that it be synchronized with

the ATS-V spin rate to avoid collision with the "black boxes" and the Cannon plugs which surround the thrust flange. Finally, the last ground rule also necessitates that the attachment device be completely separable from ATS-V when despin is complete.

Based on the above general requirements, a baseline docking subsystem concept was developed consisting of a cage structure supporting three mechanical latching mechanisms, with spring powered capture and pneumatically powered release. The concept was analyzed in a digital simulation and showed that docking could be accomplished without generating severe loads (see Appendix D, Post Contact Docking Analysis). The baseline concept is discussed in detail in the following subsections.

7.2.8.1 Cage

The baseline docking cage structure as shown in Figure 7-34 is an aluminum truss cage that supports the docking mechanism and transmits docking loads to the main load carrying structure of the spacecraft through the despin drive assembly. The base of the cage is separable from the despin drive assembly to provide ready access to the video and illumination subsystem located inside the cage. The cage is cylindrical in cross section at its base and sized to provide ample clearance between the spinning cage structure and the stationary video and illumination equipment. At its forward end the cage is triangular in cross section to provide rigid support between the three latches with maximum clearance relative to the ATS-V. The minimum length of the cage is established by clearance consideration between ATS-V and the RMU and by the need to contain the latches and the apogee motor thrust flange within the 64° field-of-view of the selected video optics. The length, in any event, must be as short as possible for mass properties and structural dynamics reasons.

7.2.8.2 Baseline Latching Mechanism

The latching device shown on Figures 7-2 and 7-34 was developed early in the study to permit design of the spacecraft to be finalized, mass properties calculated, digital studies to proceed, and pricing to be completed. Subsequent to its development, variations on the baseline mechanical latching concept were investigated to determine if greater misalignments could be tolerated and operating characteristics improved.

Studies by the Apollo Docking Design Group concluded that the miss distance could be increased substantially by use of an "expanding cone" which articulates with the hooks to achieve the required clearance inside the apogee motor thrust ring. Conical expansion would be controlled by 3-point contact to coordinate centering while latching. The first kinematic studies of the hooking motion were pursued using various 4-bar linkages which would first close for capture then permit translation for draw down. The steps in development of an expanding cone considered (1) tilting ramps, (2) hinged bars, (3) rotating eccentric cones, and (4) fixed-end, slotted links. The studies were based on allowing for an angular misalignment of at least 3° and a miss distance of at least 2 inches, greater tolerances if possible. This suggested that the hooking and expanding portions of the mechanism should be designed as thin as possible. Thus, a "tong" became

a likely concept for development. The tong employs a hooking jaw externally on the thrust ring and a "pressure jaw" internally centering the thrust ring with simultaneous action. The "pressure jaw" of the tong is, in essence, the expandable centering cone of the baseline concept.

The obvious closing of the tong first appeared as a 2-bar strut, holding the tong open, with the spring actuator folding the linkage and drawing it into a draw down/translational slot. This first attempt showed promise, but the force effectiveness was reversed. It had over-center, infinite force to hold it in the open position and something less than spring force to snap it closed and effect draw down translation.

The next study produced a tong that was bell crank actuated by the closing spring so that the first half of the spring retraction snapped the tongs securely closed with an over-center lock and the last half translated the locked tong for draw down. Finally, the actuation energy source was reversed as a means of saving weight; i.e., maximum work (capture) is performed by expanding gas and the minimum (release and reset) by venting and springs. Figure 7-35 illustrates the concept. The latch is cocked prior to final docking operations by pressurizing the retract piston with high pressure from a gas-generator cartridge. The manifolding system is shown in views $^\#$H and $^\#$K (Figure 7-34). Three gas-generator cartridges are equally spaced around the despin cage and are integrated into the manifold system by "T" fittings. They supply the energy for three separate latching operations.

The latching sequence starts automatically when a trigger in any of the three latches is tripped by the ATS-V thrust flange. This energizes a solenoid in the trigger mechanism of each of the other 2 latches, producing a nearly simultaneous closing of the three tongs. After the tongs have securely closed, capturing and centering the ring, the time for draw down will be dependent upon the degree of misalignment and the dynamic product of those forces opposing the springs. Time becomes of little consequence in this portion of the cycle, in that capture is secure and substantial force is being applied to zero the interface gap. The grip forces are ample to meet the design requirement of 2.0 ft-lbs for despin. Latch release after despin would be accomplished by venting the gas and applying opening force with the extend spring. Discussions with the vendor indicate that firing of one cartridge would not affect the remaining cartridges, and that by proper selection of the grain material contamination of the cylinder assemblies would not be a problem relative to subsequent recycling. Each cylinder assembly would be provided with a vent line routed aft along the spin cage to a position that would not impart any reaction to the ATS-V. Venting of the high pressure gas from the cylinders would be accomplished by actuating a vent valve.

In the interest of minimizing weight, the tongs would be designed on a load sharing basis; i.e., a hook element will carry 50% of the applied radial load, while each of the other 2 tong sets carry 25% of the radial load on their cone elements.

ATS APOGEE
MOTOR RING

CAPTURE TONGS

HOLDING PAWL

TRIP SOLENOID

INLET
PRESS
FOR
RETRACT

EXTEND SPRING

RETRACT PISTON

TRIGGER
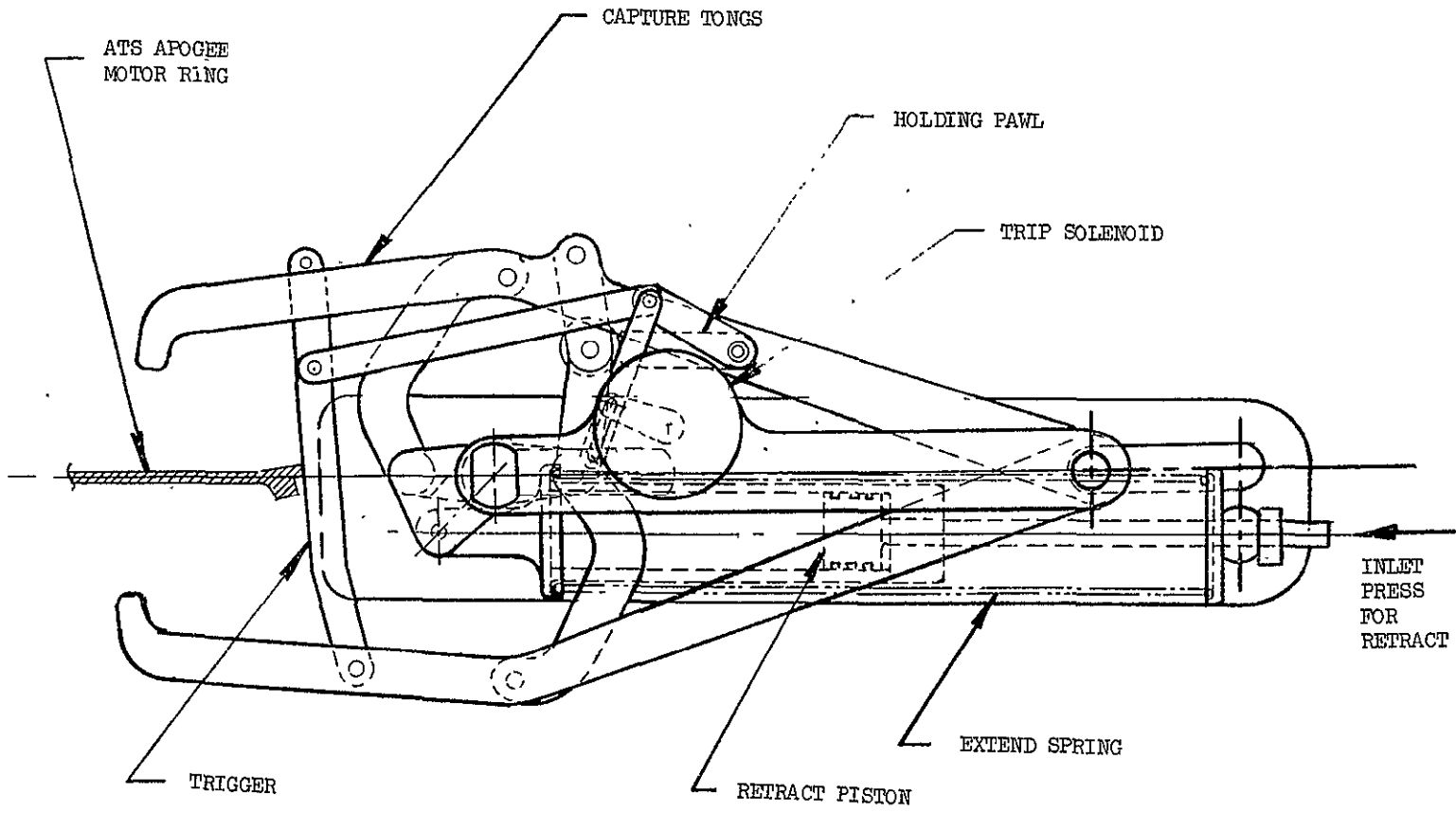
FIGURE 7-35.   ALTERNATE LATCH CONCEPT

The present design appears satisfactory from a mechanism standpoint and provides wide misalignment tolerance through the simple means of properly locating the tong hinge point for the required jaw opening. Suitable damping and spring constants can be built into this concept at suitable weights, though the latch will require stringent weight reduction effort because of its location at the extremity of the spacecraft.

Another possibility in the latch approach is the use of cold gas in lieu of gas cartridges. This is the approach utilized in the Apollo docking system and eliminates any possibility of problem due to contamination from exhaust products. Time has not yet been available for accomplishing the search and design aspects for the pyro/gas system but it is visualized as a central, 3-pyro breech, connected by stainless plumbing to the 3 latch cocking cylinders. This arrangement would undoubtedly be heavier than gas cartridges but would locate the heaviest portion of the system closest to the RMU CG.

The latch described above was modeled in a digital study and effected capture, draw down, and despin for maximum misalignment docking conditions. Forces generated were not large and this latch concept appears satisfactory. (See Appendix D.)

7.2.9 Propulsion

As described previously in Section 2.0 of this report, a survey was made of existing apogee motors and the TEM 442-1 solid propellant motor manufactured by the Thiokol Chemical Corporation was selected for the RMU application. The TEM 442-1 motor is a modified version of the TEM 442 motor developed for and flown by the Sandia Corporation. The modified motor was developed for the Burner IIA program. The modifications were aimed primarily at decreasing inert weight, and consisted of changing the case from D6AC steel to titanium and reducing the internal insulation. The motor configuration, nozzle design, and propellant remain virtually unchanged from the original motor.

The TEM 442-1 motor has been test fired and qualified but it has not as yet flown. At least 3 motors will have been flown on the Burner IIA program by the time the RMU is scheduled to be launched.

Although the motor was designed for spin rates in excess of RMU applications, it was tested only in a non-spinning condition. Thus, Thiokol recommends that a test firing be conducted in the spinning mode. The expended motor casing will then be used for the inert motor on the program.

The motor consists of a 6AL-4V titanium spherical case with internal insulation and a nozzle constructed of vitreous silica phenolic with a graphite throat insert. The load weight is 576 pounds with a burnout weight of 50.1 pounds. The specific impulse is 272 seconds and it delivers a total impulse of 142,725 lb-sec with an impulse reproducibility of ± 1.0 percent. Maximum thrust is 8,710 pounds. The motor has a burn time of 17.8 seconds and an action time of 19.0 seconds. Overall length is 33.04 inches with a maximum diameter of 26 inches. It has a nozzle expansion ratio of 17.3:1.

The safe-arm technique to be utilized on the RMU has not been fully resolved. Mechanical interlocking systems and electronic devices have both been successfully employed on many types of space vehicles. Skynet, Radio Astronomy, Explorer, and Anchored Interplanetary Monitoring Platform are examples of unmanned spacecraft, all launched from the Eastern Test Range, which do not use a mechanical interlocking safe-arm system. The launch escape, tower jettison and pitch motors used on the Apollo spacecraft also employ an electronic safe-arm system. The TEM 442-1 motor is configured for an electronic system. Using this motor in its current configuration would offer both economic and schedule advantages and, based upon the precedents set by successful launching of related spacecraft from ETR, action should be initiated to obtain the necessary waivers to permit its use with the current ignition systems.

Discussions have, nevertheless, been held with Thiokol relative to the modifications required to install a mechanical device on the TEM 442-1. The location of the present igniter on the motor may be seen in Figure 7-1. Sufficient clearance exists to install the mechanical interlock system but a weight penalty of between four and six pounds would result. Because the motor is required to function in the spin mode for the RMU application, counterbalance weights would be required and should be placed opposite the igniter system. An alternate approach would be to locate the igniter on the head-end of the motor. This location would simplify the spin balance problem and reduce the weight penalty but would require an increase in motor length. A static firing would be required irrespective of the location selected.

7.2.10 Thermal Control

The thermal design of most spin-stabilized synchronous satellites is basically passive, while non-spinning synchronous satellites often require active thermal control systems. Spinning satellites can use a simple passive temperature control system based upon the temperature averaging that results from the "barbecue" effect of the spin mode. Non-spinning vehicles do not have this advantage and therefore usually employ an active type of temperature control such as shutters or louvers. The RMU has both spin-stabilized and non-spinning phases in its mission with a period of up to six hours in the despun mode including rendezvous and docking with the ATS-V. A preliminary study has been made to determine the type of temperature control system needed for this mission. The study showed that the RMU can be controlled essentially by passive means with a combination of insulation and thermal control coatings, with only a small amount of heating required in certain areas.

The basic approach utilized in the baseline concept consists of insulating the equipment shelf area and apogee motor compartment as shown in Figure 7-36. This will protect the equipment compartment from the extreme temperatures ($\pm 250^\circ$F) reached by the solar panels during the despun attitude prior to docking. A well insulated equipment compartment will also minimize temperature changes caused by transient conditions encountered during parking orbit, transfer orbit, and drift orbit eclipses during an equinox.
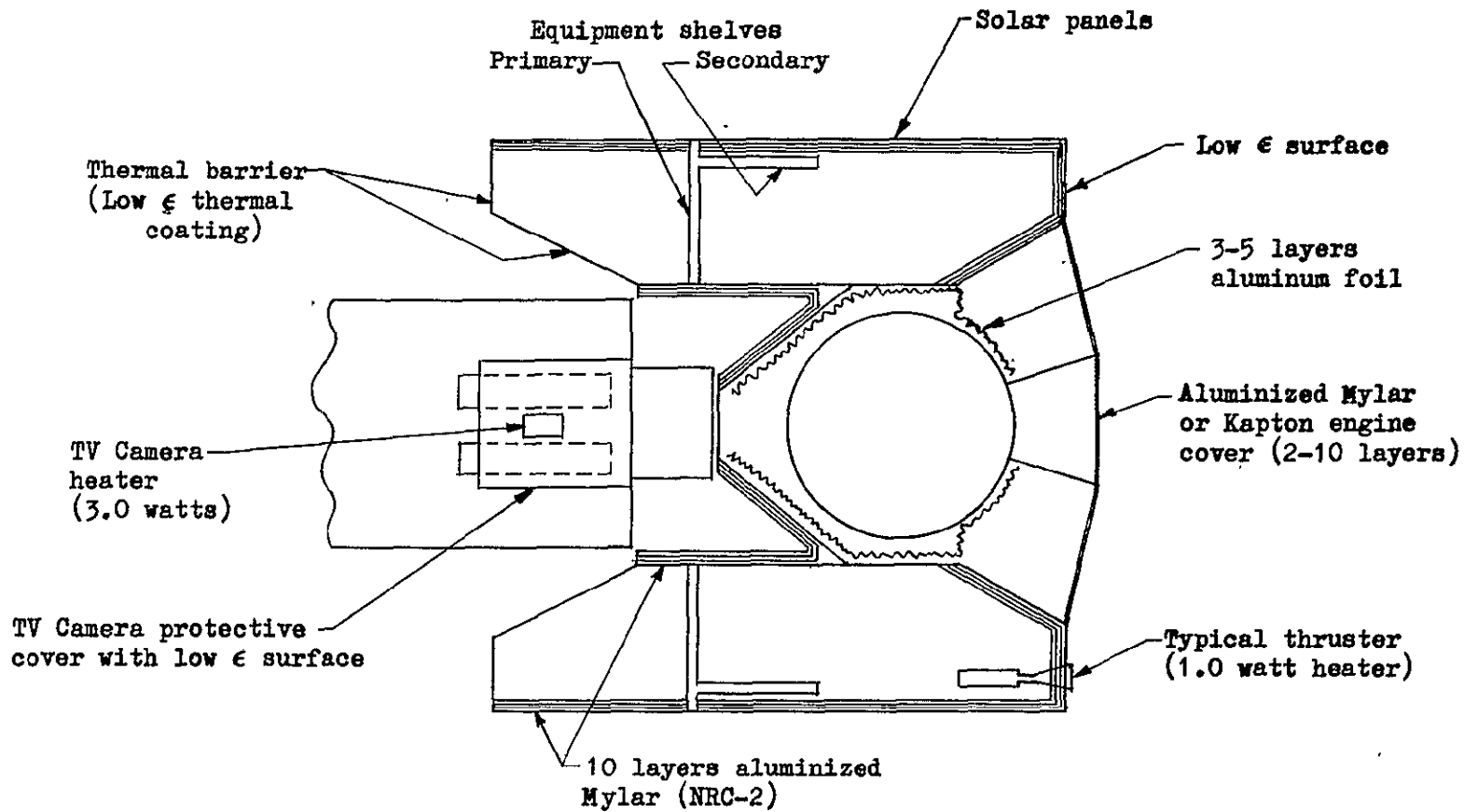
Figure 7-36 RMU Thermal Control

For equipment mounted outside the insulated shelf area, individual thermal control is utilized. The TV cameras are housed in a temperature control "can" with approximately 3 watts of continuous heating. The propulsion system thrusters are insulated and utilize one watt per thruster to stay within temperature limits. The baseline design utilizes radioisotope heaters for both applications. These units are now being space qualified by TRW on the Pioneer Program.

Table 7-17 presents a tabulation of estimated RMU component temperatures for the various phases of the mission. Pre-launch and boost environments are based upon data obtained from McDonnell Douglas indicating that (1) the interior of the launch vehicle will be conditioned to $77 \pm 5^\circ$ F prior to launch, and (2) during boost, the interior of the boost fairing will reach a maximum temperature of 250° F approximately two minutes before fairing jettison.

For analytical purposes, the attitude of the RMU vehicle was assumed to be randomly oriented during parking orbit. For the 6 hour transfer orbit, the vehicle is in the spin mode with the normal to spin axis at an angle of 30° with the vehicle-sun line. During drift orbit, the vehicle is spin-stabilized with its X-axis perpendicular to the orbit plane (the equatorial plane). In the rendezvous and docking phases, the vehicle is 3-axis stabilized with an initial 3-hour "tail-to-sun" attitude followed by a final 3-hour period when its X-axis is perpendicular to the sun. The following subsections provide some of the detail considerations related to the thermal control aspects of the primary RMU spacecraft elements.

7.2.10.1 Solar Panels

The temeprature of a cylindrical spinning solar array perpendicular to the sun and with adiabatic ends can be approximated as follows:

Energy Radiated to Space = Absorbed Solar Energy

$$\sigma \epsilon A T^4 = \alpha A_p S$$

$$T = \left(\frac{\alpha}{\epsilon} \cdot \frac{S}{\sigma \pi} \right)^{1/4} \tag{1}$$

where T = average solar cell temperature, $^\circ$R

α = solar absorptivity

ϵ = infrared emissivity

S = solar constant, 443 Btu/(hr) (ft^2)

σ = Stefan-Boltzmann constant, 0.1713 Btu/(hr) (ft^2) ($^\circ$R^4)

Table 7-17. Estimated RMU Component Temperatures (°F)

	Pre-Launch	Boost (Maximum Temperature)	Parking Orbit	Transfer Orbit	Apogee Motor Firing (including Soak-Back)	Drift Orbit	Drift Orbit Eclipse	Rendezvous & Docking (Despun) Aft To Sun (3 Hour Max)	Rendezvous & Docking (Despun) ⊥ To Sun (3 Hour Max)
Solar Cells	77 ± 5	200	± 250	40 ± 20	40 ± 20	60 ± 10	-250 (Min)	-250	± 250
Equipment Compartment*	77 ± 5	85	75 ± 10	60 ± 20	70 ± 40	60 ± 20	50 ± 20	50 ± 20	70 ± 20
Apogee Motor	77 ± 5	85	75 ± 10	60 ± 10	N/A	N/A	N/A	N/A	N/A
Cameras	77 ± 5	100	90 ± 10	Decreasing (A)	0 ± 10	0 ± 10	0 ± 10	120 ± 20 (Operating)	120 ± 20 (Operating)
Docking Cage	77 ± 5	150	TBD	TBD	TBD	76 ± 20	-200 (Min)	-200 (Min)	76 ± 20
Docking Latches	77 ± 5	85	75 ± 10	TBD	TBD	76 ± 20	56 ± 20	30 ± 20	76 ± 20
RCS Thrusters*	77 ± 5	120	TBD	40 ± 40	TBD	60 ± 40	50 ± 40	50 ± 40	60 ± 40
"C" Band Omni & High Gain Antennas and Sun Sensors	77 ± 5	200	±200	40 ± 20	40 ± 20	60 ± 20	-200 (Min)	-200 (Min)	±200
Despin Mechanism	77 ± 5	100	TBD	50 ± 20	50 ± 20	50 ± 20	40 ± 20	40 ± 20	100 ± 20

(A) Decreases from +100 to -10 min

* Components containing N_2H_4 will be insulated to preclude temperature dropping below 40°F.

$$A = \text{cylindrical radiating area, } \pi d \ell$$

$$A_p = \text{solar projected area, } d \ell$$

The temperature based upon the above relationship usually is between 50 and 70°F depending upon packing density, solar cell energy conversion efficiency, and the properties of the cells used. (Equation (1) does not account for solar cell conversion efficiency, which is approximately 9 – 10 percent.)

Based upon the above discussion, and the fact that the sun line will be maintained within ± 23.5 degrees of the orbit plane, the predicted solar panel temperature for drift orbit (synchronous orbit) is 60 ± 10°F. During transfer orbit, the predicted temperatures will be somewhat lower at 40 ∓ 20°F due to the face that the sun line will be at an angle of 30 degrees with the normal to the spin axis.

Maximum solar panel temperatures will occur when the spacecraft is in the despun phase perpendicular to the sun prior to docking. Solar cells directly under the sun may reach local temperatures as high as 250°F, depending upon solar cell thermal properties and the degree of internal heat leakage.

Minimum solar panel temperatures will occur during the cold soak conditions of a possible drift orbit eclipse and during the tail-to-sun attitude of the rendezvous approach. Temperatures can go as low as –200 to –250°F during these periods.

7.2.10.2 Equipment Shelves

The inner compartment containing the equipment shelves must be insulated from the solar panels because of the extreme temperatures (± 250°F) reached by the solar panels during the rendezvous and docking phases of the mission and possibly during drift orbit eclipse conditions. The basic approach will consist of insulating the equipment shelf area and apogee motor compartment as shown in Figure 7-36. Approximately 5 – 10 layers of aluminized Mylar insulation (NRC-2 type) will be applied to the inside surface of the solar cell panels. At least ten layers of aluminized Mylar or Kapton will be applied to the aft end of the vehicle. The forward end of the vehicle can be used to reject pre-rendezvous (spinning mode) heat loads generated in the equipment compartment, which are on the order of 55 w. A combination of thermal coatings and/or insulation will be used here, dependent upon actual heat loads.

With the forward end of the vehicle designed to reject spinning mode heat loads as stated above, the insulation on the solar panels can be sized to reject the additional heat loads generated internally during rendezvous and docking, when the average solar panel temperature is considerably colder than during drift orbit. Although the solar panels can also be used to reject a portion of the heat during drift orbit, a detailed thermal analysis will be required to determine the extent of this capability (if any) based upon such factors as solar panel temperatures during cold soak, insulation performance, etc.

That a passive system is a feasible concept for the despun stages of the mission can be demonstrated by utilizing a version of the well-known "billet-heating" equation:

$$t' - t_{sp} = (t_o - t_{sp}) e^K + \frac{q}{hA} (1-e^K) \tag{2}$$

where $K = \dfrac{-hA \, \Delta\theta}{WC_p}$

t_o = initial average equipment temperature, ^oF

t' = final average equipment temperature, ^oF

t_{sp} = average solar panel temperature, ^oF

$\Delta\theta$ = total time, hr

W = mass of equipment, lb

C_p = specific heat of equipment, $Btu/(lb)(^oF)$

A = area of solar panels, ft^2

h = effective average heat transfer coefficient across insulation, $Btu/(hr)(ft^2)(^oF/Ft)$

q = internally generated heat load, Btu/hr

During the initial three-hour despun attitude, the average solar panel temperature will be very low, perhaps -150 to -200^oF. With a total internal heat load of 120w, of which 50w are rejected by the forward end of the vehicle, the required heat rejection through the solar panels will be 70w, plus approximately 10w from the sunlit aft end for a total of 80w. If the effective emissivity of the solar panel Mylar insulation is assumed to be 0.04, a conservative value, then the average equipment compartment temperature will show approximately a 13^oF temperature drop as shown in Figure 7-37 for a three-hour tail-to-sun attitude with an initial temperature of 60^oF.

During the final three-hour despun attitude, the RMU will be perpendicular to the sun. Solar panel temperatures at this time will range from $+250$ to -250^oF, with perhaps an average temperature of -30^oF. Again, using equation (2), it was determined that the average temperature in the equipment compartment will rise approximately 20^oF from an initial temperature of 50^oF.

SD 71-286
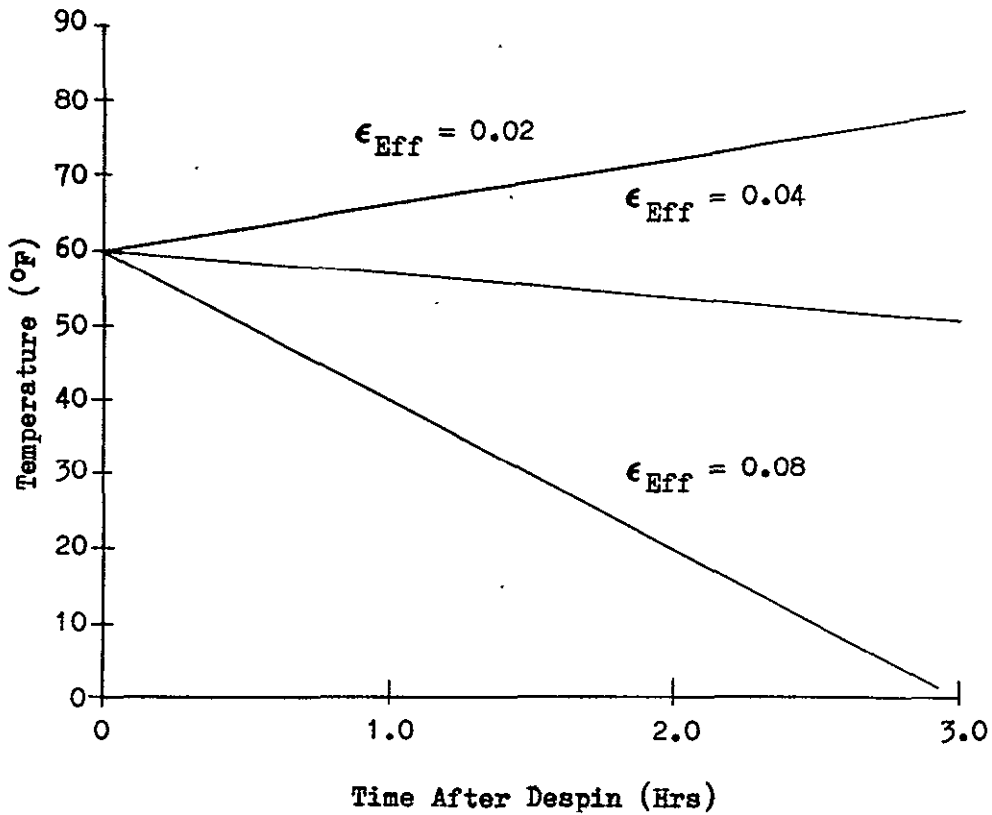
Figure 7-37. Average Equipment Compartment Temperature
as a Function of Insulation Effectiveness

The general conclusion that can be reached from the above discussion is that temperature control during the despun phase of the mission can be achieved by relying upon the thermal mass of the equipment inside the insulated compartment to hold temperatures within limits. For the same reasons, eclipse cold soaks encountered during the equinox period will not be a problem. Additionally, any unusual thermal environmental conditions encountered during parking and transfer orbits will not cause drastic temperature changes.

Regarding the equipment shelves themselves, the general rule will be to closely couple heat producing equipment to the shelves. Conversely, non-heat producing items, particularly the propellant tanks, will be de-coupled to improve their thermal lag characteristics. Heat producing items will not be concentrated together but dispersed to produce an even internal temperature distribution.

7.2.10.3 Apogee Motor

The apogee motor presents three thermal problems: (1) engine cold soak in the transfer orbit prior to motor separation; (2) plume heating effects on the aft end of the vehicle; and (3) spacecraft structure heating caused by heat soak-back from the engine during and after firing.

Problems encountered in the transfer orbit can be solved by depending upon the thermal mass of the engine to provide adequate pre-ignition temperatures. The engine propellant is qualified to 50-90°F, but Thiokol representatives have stated that the actual propellant temperature range is between 20 and 100°F and nozzle temperatures can range considerably lower and higher than that. However, a certain amount of doubt exists concerning the allowable temperature excursions of the nozzle, particularly with regard to temperature gradients between the nozzle and propellant. In view of this, a safe approach will be to insulate the engine compartment from the environment (using ten layers of aluminized Mylar or Kapton) with an outer thermal coating having an α/ϵ ratio around 0.6. This will result in an outer surface temperature of approximately 70°F based on a 60 degree angle between the surface normal and sun line.

Plume heating problems will be avoided with the proper combination of insulation and thermal coating properties. On previous open-ended vehicle designs, aluminized Kapton has been used (single layer) with the inner emissivity equal to 0.8 and outer emissivity equal to 0.05 to prevent overheating from the apogee engine plume. Multiple layer insulation cannot be used with this arrangement, however, as the Kapton would probably exceed its 800°F limit. For the RMU, the aft end will be enclosed with an aluminum skin which will provide a convenient mounting area for the required insulation. In this case, a low emissivity coating with an α/ϵ of less than one is expected to be sufficient for both plume heating and the direct solar heating that will be encountered during rendezvous.

Heat soak-back will be prevented by providing from three to five layers of aluminum foil in the engine compartment and by reducing mounting lug areas to a minimum. The aluminum foil is required because apogee motor case temperatures measured in JPL test firings peaked near 700°F within a few seconds after the motor burn. The foil insulation will be mounted on the structure instead of the motor so that it will provide protection against cold-soak after motor ejection.

7.2.10.4 Reaction Control Subsystem

The thrusters will be mounted inside the thermally controlled equipment compartment. This will aid thruster thermal control, although conditions encountered during rendezvous and docking will probably cause some of the thrusters to be cold-biased. Thus, subject to future detailed thermal analyses the baseline design utilizes a single 1.0 watt isotope heater per thruster.

The RCS propellant tanks and lines will be thermally isolated from the spacecraft structure by means of Mylar insulation and non-metallic spacers at the mounting points. This will provide maximum thermal lag protection in the transient phases of the mission.

7.2.10.5 TV Cameras

The TV cameras are mounted outboard of the main spacecraft structure and are shadowed from the sun so they are in a very cold-biased environment. Camera temperature limits are -40°F to 160°F non-operating, and 0°F to 140°F operating. Preliminary studies indicate that non-operating camera temperatures will be above the minimum if they are provided with 3 watts of heating and are enclosed in a can with insulation or a low outer surface emissivity (0.05). Constant wattage isotope heaters will be used for this application.

7.2.10.6 Docking Cage and Latches

The docking cage has a wide range of permissible temperatures. However, the temperature of the docking cage will greatly influence the temperature of the TV cameras and despin mechanism during drift orbit, when both of these components are shadowed from the sun. Thus, the sun-shield of the spin cage will use a thermal coating with α/ϵ close to unity; as a result cage temperatures will be in the region of 70 to 80° during the drift orbit.

7.2.10.7 Antennas

The C-band high-gain antenna will probably experience very low temperatures during rendezvous. For this reason, the antenna will be thermally insulated from the inner compartment so that it will not adversely affect internal temperature.

The omni antenna is distributed around the periphery of the RMU, and consequently will experience a wide range of temperatures during the despun phases of the mission. Here again, the antenna will be thermally insulated from the interior of the spacecraft to minimize the affect on internal temperatures.

7.2.10.8 Despin Mechanism

The thermal environment of the despin mechanism can only be estimated at this time. Minimum environmental temperature will occur when the despin mechanism is inactive and will be in the region of +50°F. When the despin mechanism is activated, temperatures will depend in part on the heat generated by the mechanism and could possibly go as high as 120°F.

7.3 GSE BASELINE

The equipment to support checkout, integrated system testing, launch activities, and mission support makes maximum use of equipment presently provisioned for the ATS or other NASA programs and test equipment presently in NR tool cribs or available from commercial sources. Preliminary selection of the RMU GSE has been performed in the following order of preference:

1. Existing ATS-V equipment items that are usable "as-is".

2. Existing equipment available and usable "as-is" from other NASA programs.

3. Existing ATS equipment that requires minor modification for RMU usage.

4. Existing equipment from other programs that require minor modification for RMU usage.

5. Additional fabrication of items to existing designs.

6. Fabrication of equipment to a modification of existing designs.

7. New design and fabrication of items unique to the RMU program.

Maximum site usage of all RMU GSE items will be scheduled to minimize duplication of design and equipment items (i.e., the same GSE item will be used for final assembly checkout, system functional tests, system performance tests, integrated systems tests, pre-flight tests and mission control activities). All RMU GSE designs are within the present "state-of-the-art" and the only major innovation is the optical despin unit which will be an adaption of the design of an existing "breadboard" assembly developed for the RMU/ATS-V precontact docking simulation operations at the North American Rockwell plant in Downey during October and November 1970.

7.3.1 Mission Control Console

The pilot control console will provide sufficient information and command access to the RMU subsystem for the pilot to:

1. Manually command maneuvers and operations.

2. Monitor RMU status.

The pilot control console includes triple bays for three-man operation. The "pilot's" section contains those control and monitoring functions associated with translation, rotation, and docking and despin. The co-pilot's bay contains those control and monitoring functions associated with spin synchronization and phasing and latch operation. The status engineer's bay contains those monitoring functions associated with status of critical spacecraft items, such as fuel, power, jets, DPG's, etc.

Visual real time displays are provided for the pilot and co-pilot by a video screen in each bay. A spinning image is supplied to the pilot; a despun image to the co-pilot. Ranging aids in the form of concentric circles for stadia measurements are superimposed upon the video image of both screens. Digital displays and status indicators are provided for display of all other data. The displays are engineered to avoid ambiguity and interference with the video image. Digital displays are in engineering units, properly scaled.

The command instructions are generated by the actuation of hand controllers on switches. For these discrete switches and hand controllers, the address and instruction codes are generated automatically. Commands generated at the console will not utilize the verification sequence normally followed in the ATS system. The console is shown in Figure 7-38 and a list of equipment is presented below. Both were extracted from the Simulation Report, Appendix C. As indicated by the list the Mission Control Console is supported by a visual system engineer's console. The visual system engineer's function will be to insure the proper operation of the video system during the piloted phase of the mission.

RMU CONSOLE EQUIPMENT

Pilot Bay

1. 1 TV monitor 17-inch 525 line
2. RMU light switch (three position switch, off, single, dual)
3. 1 rotational controller
4. ATS despin initiate switch
5. 1 translational controller
6. 1 minimum impulse switch
7. Roll attitude display $\pm$ 20 degrees

1. Pilot's Monitor
2. Pilot Displays and Controls
3. Co-Pilot's Controls
4. Rotation Hand Control
5. Translation Hand Control
6. Co-Pilot's Monitor
7. Indexing Pulse Display
8. Engineer's Monitor
9. Engineer's Control Panel
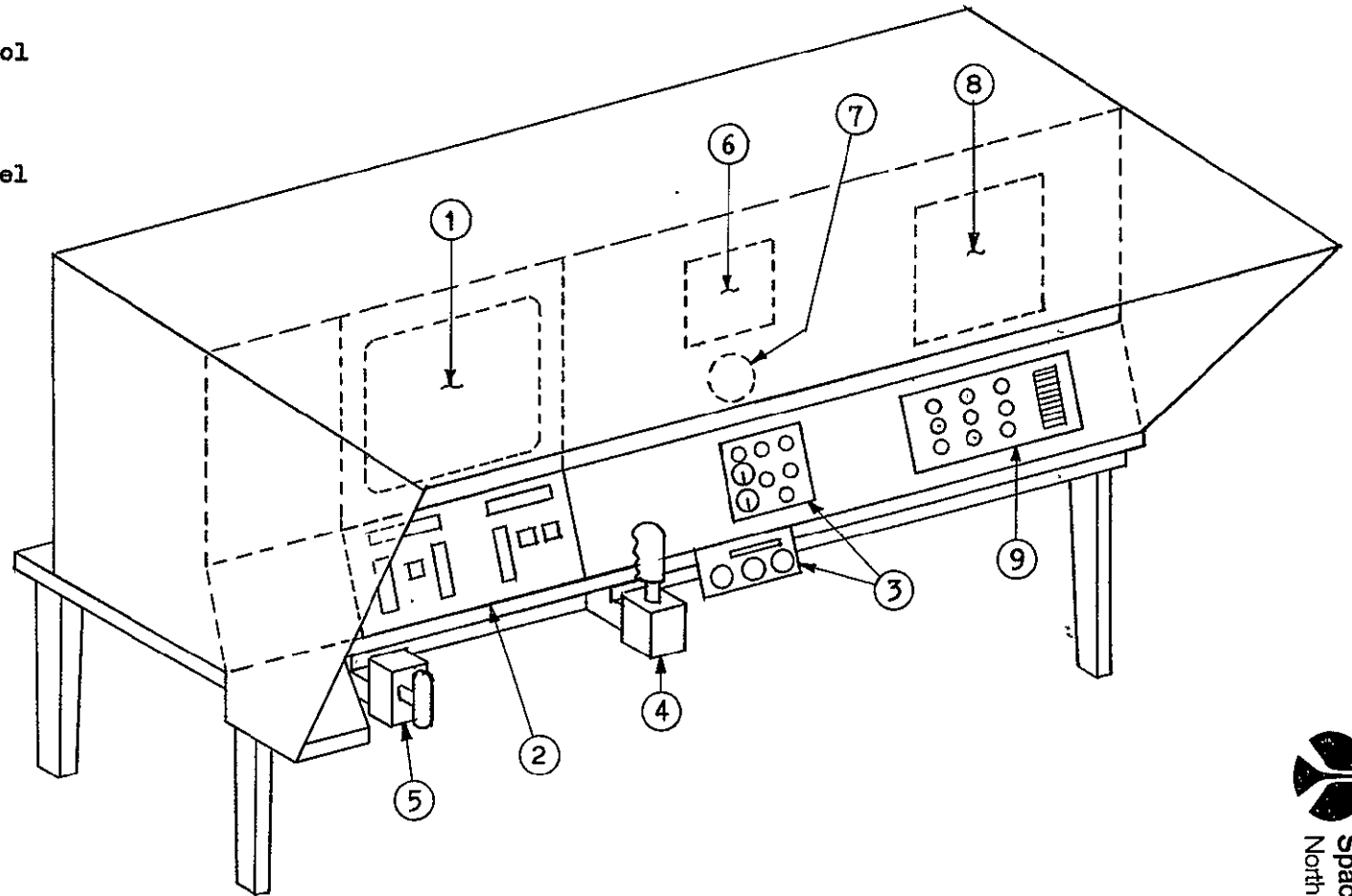
Figure 7-38 Recommended Three-Man Console

8. Rate reset switch (resets trans.rate displays)
9. Pitch yaw attitude display 0-20 degrees
10. X Trans. rate display − 0.5 to + 1.0 ft/sec
11. Y Trans. rate display − 0.1 to + 0.1 ft/sec
12. Z Trans. rate display − 0.1 to + 0.1 ft/sec

Status Engineer Bay

13. Roll gimbal angle display ± 50 degrees
14. Pitch gimbal angle display ± 50 degrees
15. Yaw gimbal angle display ± 50 degrees
16. Roll gimbal angle CMD momentary switch
17. Pitch gimbal angle CMD momentary switch
18. Yaw gimbal angle CMD momentary switch
19. Jet temp monitor (status lights − 12 ea.)
20. Latch status lights (armed, latched, open)
21. Fuel monitor display
22. Latch pressure display
23. Power monitor
24. D.C. Voltmeter with two position switch
25. Mission profile (time) indicator clock

Co-Pilot Bay

26. Event timer (digital stop watch)
27. 1 TV monitor 17-inch 525 line (CONRAC)
28. 1 latch index display (oscilloscope)
29. Derotation optics control

   a. Switch (control switch)
   b. Vernier control (pot)
   c. Spin-despin switch (view switch)

30. Spin cage control

   a. Switch (control switch)
   b. Vernier control (pot)

31. Latch separation switch
32. Latch status lights (armed, latched, open)
33. Latch arm switch
34. TV lens switch (70° FOV 14° FOV)

Visual System Engineer Console

35. 1 TV camera control unit, despin optics, COHU model 3900 (with Dot bar generator)
36. 1 TV camera control unit, RMU camera (dual unit)
37. RMU light status (indicator light for single tube or dual tube operation)
38. Despin optics servo checkout unit
39. D.C. voltmeter with ten position switch for systems monitoring
40. 1 17-inch TV monitor 525 line

7.3.2 System Checkout Console

The system checkout console includes all the test equipment required to perform the basic spacecraft subsystem functional test, subsystem performance test, and spacecraft integration test. The system checkout console is designed to evaluate the performance of the spacecraft command subsystem, telemetry subsystem, communication subsystem, communications antenna and electronics, attitude control subsystem, reaction control subsystem, video/illumination subsystem, and the electrical power subsystem. The system checkout console is composed of a mixture of standard commercial equipment, special NR designed and fabricated equipment, and GFE items. The system checkout console is composed of the following major subsystems:

1. Repeater Test Equipment
2. Telemetry and Command RF Equipment
3. Telemetry and Command Digital Equipment
4. Spacecraft Auxiliary Power Supply Equipment
5. Data Recording Equipment
6. General Purpose Test Equipment

Most of the items for the system checkout console are considered GFE from the ATS program. The major subsystem components of the system checkout console are discussed below:

Repeater Test Equipment – The communication portion of the SCC will quantitatively test the performance of the communication system of the RMU spacecraft. The equipment is capable of measuring the parameters of the repeater and the phased array antenna. The repeater RF test set transmits RF test signals to the spacecraft and monitors the applied signals. When used in conjunction with supplementary commercial equipment, the test set is suitable for making quantitative measurements of the spacecraft return signal to measure the transponder performance. The quality of the test set circuitry insures that quantitative measurements are not limited to test set performance.

Telemetry and Command - The telemetry and command portion of the system check-out console contains the equipment required to test, operate, and calibrate the RMU telemetry and command subsystem. The major components are the telemetry processor, synchronous controller, subsystem simulator, squib monitor, and squib simulator.

Telemetry and Command Digital Equipment - Test signals and measurements obtained during the test of the RMU are automatically recorded and displayed by the data record-ing system. These signals may represent any of several types of data, such as voltage, currents, power, frequency, time, time intervals, etc. In addition to the test equipment outputs, the telemetry VCO and PCM signals, command generator signals, and voice are recorded during each test. The data recording system records all data in analog and digital form. Digital data, which are best presented in analog form, are converted to analog and recorded on graphic records, such as a function of time or as a function of another signal. Additionally, digitized data are recorded on a digital recorder and the magnetic tape reocrder. Essentially all measurements not available in digital form are converted into digital form. The digital data are then time multiplexed in the digital data converter and recorded on the magnetic tape recorder. The recorded digital data can later be restored to their original digital or analog form.

Spacecraft Auxiliary Power Supply Equipment - The spacecraft auxiliary power supply equipment provides the solar power inputs that normally would be supplied during flight by the solar cells during the time the equipment is being subjected to environmental exposures, such as the thermal vacuum test.

General Purpose Test Equipment - The general purpose test equipment includes all of those commercial available items which have been identified and impose no cost upon the program since they are available as NR or NASA furnished equipment. This equipment includes such items as spectro-analyzers, power meters, thermisters, etc.

In conclusion, the system checkout console provides the necessary electrical and electronics test capability for all RMU checkout and control with the following excep-tions: (1) in process continuity, megger and insulation resistance testing which will be conducted by NR meter room items and NR existing Special Test Equipment, and (2) that equipment which is used to provide power control and docking maneuver testing that has been described previously in 7.3.1.

7.3.3 RMU Dolly & Checkout Stand

The RMU dolly/stand is utilized during assembly and testing. The unit is a four-wheeled, self-locking castered assembly with interfacing accommodations to mount the RMU with cover during ground operations and transportation. The design permits position-ing of the RMU both horizontally and vertically for easy assembly, access, and checkout.

7.3.4 RMU Shipping Containers

Containers will be provided for handling and shipping the RMU experiment hardware. The shipping container for the spacecraft will provide contamination control, shock and vibration protection, and humidity control. Container design and selection of container materials will be predicated on shipment preparation operations being performed in a clean room. Container dimensions will be constrained to permit shipment by common carriers (air and truck).

7.3.5 Propulsion Servicing Unit

Currently, the plans for RCS propulsion servicing is to utilize an existing Apollo servicing unit. Basically this approach is cost effective since the Apollo unit is compatible from a propellant standpoint and requires a minimum mod adapter of a vacuum pump and a few valves. The unit conditions the gas received from a facility supply and provides propellant servicing to the RMU propulsion system. The unit incorporates the necessary disconnects to connect to the facility GN_2 and vacuum lines and is equipped with gauges, regulators, valving, test points, flex hoses, and spacecraft connectors.

7.3.6 Miscellaneous

Additional support equipment items that have been identified are:

RMU/Apogee Motor Sling - The RMU/Apogee motor sling is utilized to lift the spacecraft in the vertical position for transferring the spacecraft from the dolly to test fixtures; in addition it utilizes an adapter for loading of the inert or live apogee motors.

RMU Horizontal Sling - The RMU horizontal sling is utilized to lift the RMU in the horizontal position for measurement of longitudinal C.G.

RMU Environmental Test Adapter - This adapter is utilized for mating the spacecraft to test fixtures (vibration, acoustics, spin balance, and thermal vacuum).

Alignment Fixtures - In addition to a theodolite and stand various alignment fixtures are necessary for overall spacecraft alignment and have been identified as jet nozzle mandrel, autocolimating mirrors for sun sensor alignment and dial indicators for alignment set up.

8.0 COST AND SCHEDULE PLAN

DETAILED COST AND SCHEDULE ANALYSES HAVE RESULTED IN A HIGH CON-
FIDENCE THAT A LOW COST, SHORT SCHEDULE RMU MISSION TO DESPIN ATS-V
CAN BE PERFORMED.

8.1 GENERAL

Figure 8-1 illustrates the logic that was utilized in the study to develop realistic
costs and schedules for the ATS-V despin mission. The principal elements of this logic
are (a) the Statement of Work (SOW) and the related work breakdown structure (WBS),
(b) the test matrix, (c) the manufacturing flow, (d) the hardware utilization list (HUL),
and (e) the program management network (PMN). In the following subsections these
items are briefly discussed, and resulting schedule and cost data are presented. The
estimated cost and schedule impact of the four optional alternate mission objectives is
also given.

The schedule and cost estimates were based on the following related ground rules:

1.   Although the timely availability of the Thor–Delta 603 booster and
its booster–to–RMU adapter was verified with McDonnell Douglas,
their cost as well as the booster related launch costs were excluded
from the estimate.

2.   The communications subsystem (except for the new omni antenna),
the T&C subsystem (except for the squib drivers), and the two sun
sensors of the ACS were considered as government–furnished equip–
ment (GFE); all these items are ATS type equipment.

3.   ATS ground support equipment (GSE) items applicable to the RMU
(notably, the system checkout console) were assumed available as
GFE.

4.   The cost and schedule estimates are based on building only one
"all-up" RMU which is utilized for system level qualification and
as the flight article. The cost of fabricating and testing a separate
thermal/structural test vehicle is included, as are costs of RMU–
related launch support, mission support (trained pilot crews) and
post mission data reduction costs.
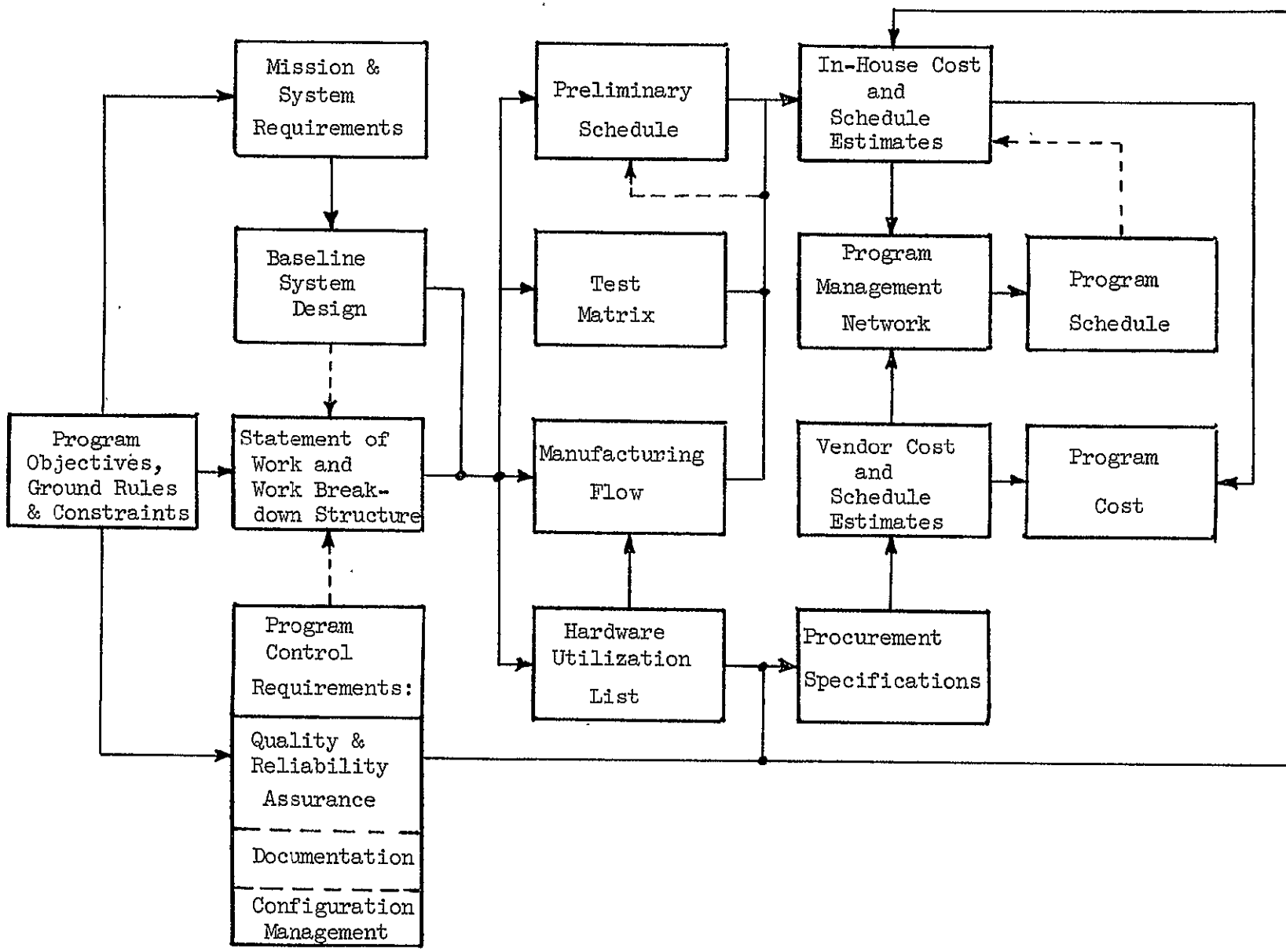
Figure 8-1. Logic for Cost and Schedule Planning

8.2 STATEMENT OF WORK AND WORK BREAKDOWN STRUCTURE

The work breakdown structure utilized in this effort is shown in Figure 8-2; the corresponding summary statement of work is as follows:

Task 1. Program Management

      Provide the effort related to the compilation, review, reproduction and distribution of all program documentation.

      Provide support for program planning and for control of budget, schedule, and technical milestones.

      Provide program technical integration and management effort required for direction of performing functional groups, vendor selection, management/integration of customer interface, liaison meetings, and reporting.

      Provide configuration management for purposes of identifying, accounting, and controlling changes on the program including functional participation on the MRB and CCB.

Task 2. Systems Engineering

      Provide the effort necessary to support and prepare for interface meetings and design reviews, to review changes to interface specifications and interface control drawings, and to supervise, coordinate and regulate subsystem integration efforts.

      Provide for the definition of requirements for the spacecraft and each subsystem. Perform required design analyses, margin evaluation, verification of design and performance adequacy, and continuing analysis of subsystem compatibility.

      Provide the effort necessary to compile, review, approve and update the integrated test plan and schedule; evaluate test reports and flight performance.

Task 3. Design and Breadboard

      Provide the effort, equipment and material required to design the RMU spacecraft and its subsystems, including fabrication and testing of breadboard equipment.

Task 4. Thermal/Structural Model

Design the thermal structural model including thermal/structural mockups of RMU subsystems.

Provide the effort, material and equipment needed to fabricate, assemble and test the thermal/structural model of the spacecraft (Ref. Table 8-2, Hardware Utilization List, Section 8.3)

Evaluate the test results and identify any necessary changes in the spacecraft design established in Task 3.

Task 5. Prototype/Flight Model

Provide the effort, material and equipment needed to fabricate, assemble, qualification/acceptance test, and deliver the prototye/flight model spacecraft, including evaluation of test results and updating and maintenance of the design (Ref.Table 8-2, Hardware Utilization List, Section 8.3)

Task 6. Ground Support Equipment

Provide the effort required to design and fabricate the program-unique equipment needed to perform bench testing, subsystem level, and system level testing of the RMU. Design and fabricate the mission control console needed for command/control of the vehicle in the "piloted" phases of the mission.

Task 7. Field Support

Provide the effort needed at ETR for apogee motor installation, pre-launch RMU/booster integration/checkout and launch support.

Provide the support effort needed during the mission including pilot crew activities at the Rosman, N.C. ground station.

Provide the data reduction effort for post mission evaluation of flight performance.

Task 8. Flight Spares

Provide the effort, material and equipment required for the fabrication, testing, inventory control, and warehousing of flight spares. (Ref.Table 8-2, Hardware Utilization List, Section 8.3).

Task 9. Reliability and Quality Assurance

Provide reliability and quality assurance efforts for the fabrication, assembly, testing and delivery of the RMU and its GSE on the component, subsystem and system level, including vendor surveillance as well as launch site activities.

8.3 TEST MATRIX, MANUFACTURING FLOW AND HARDWARE UTILIZATION LIST

To facilitate realistic assessment of cost and schedule factors a baseline test matrix (see Table 8-1), baseline manufacturing flow (see Figures 8-3 and 8-4), and a preliminary hardware utilization list (See Table 8-2) were developed. Preparation of these items was based on a thorough analysis of the baseline RMU design, the statement of work and programmatic ground rules.

Based on the hardware utilization list preliminary make-buy decisions were made and procurement specifications were prepared for the buy-items. A typical sample of a procurement specification, consisting of the general/environmental requirements specification and a typical specification control drawing, is given in Appendix E.

8.4 PROGRAM MANAGEMENT NETWORK AND PROGRAM SCHEDULE

As a means of defining a realistic program schedule which reflects the constraints imposed by functional interdependance of activities, a program management network (PMN) was developed. The PMN, illustrated in Figure 8-5, was based on schedule estimates of NR functional organizations and vendors of make items; to facilitate a short schedule approach, the PMN allows for procurement of all major buy items at an early stage.

Based on the PMN a program schedule was prepared which, as shown in Figure 8-6, projects a 22 month time span from program go-ahead through RMU launch.

8.5 PROGRAM COSTS

The NR Space Division methodology used for estimating cost was designed to meet the program requirements of credibility, accuracy, and timeliness. Basic estimating by "grass roots" was used. Each functional organization that is to be involved in the subsequent phases of the program estimated their manpower/travel/computer requirements for performing their tasks defined by the statement of work. The estimates were made in accord with the work breakdown structure, the baseline system design, and the program schedule. Costs of buy-items were estimated by prospective vendors based on detailed procurement specifications.

TABLE 8-1   PRELIMINARY RMU TEST MATRIX

Test Item			PERFORMANCE						DEVELOPMENT							QUALIFICATION														ACCEPTANCE						
Unit	Subsystem	System	Inspection	Performance	Mass Properties	Mechanical Alignment	Mech. and Elec. Compatibility	Leak	Thermal	EMI	Static Loads	Modal Vibration	Vibration	Acoustics	Shock	EMI	Temp. (handling and storage)	Temperature Altitude	Humidity	Explosive Atmosphere	Acceleration	Space Simulation	Burst Test	Acoustics	Shock	Continuity, Hi Pot and Res.	Vibration	Thermal–Vacuum	Temp. Cycling	Temperature Altitude	Space Environment Simulation	Vibration	Temp. Cycling	Continuity, Hi Pot and Res.	Proof Pressure	Thermal Vacuum
T-1 RMU Test Spacecraft		x	x	x	x	x	x	x			x	x				x					x					x	x	x								
F-1 RMU Flight Spacecraft		x	x	x	x	x	x	x																						x	x					x
Subsystems																																				
– Reaction Control Subsystem	x		x	x	x	x	x	x																						x		x				x
Fill and Drain Valves	x			x	x	x	x		x																							x					
Tanks	x			x	x	x	x																									x				x	
Filter	x			x	x	x	x																									x					
Pressure Transducer	x			x	x	x	x																									x					
Radioisotope Heater	x			x	x	x	x																									x					
Thrusters	x			x	x	x	x																									x					
– Attitude Control Subsystem		x																																			
Sun Aspect Sensors	x			x	x	x	x	x							x												x	x			x	x					x
Sun Aspect Sensors Electronics	x			x	x	x		x			x																x	x				x					x
Sun Sensors	x			x	x	x	x	x							x												x	x				x					x
Accelerometers	x			x	x	x		x																			x	x				x					x
Electronics Assembly	x			x	x	x		x			x																x	x				x					x
DPG's	x			x	x	x		x		x				x		x	x										x	x				x					x
Housing	x			x	x	x																															
Wheels	x			x	x	x																															
Torquer Motors	x			x	x	x																															

TABLE 8-1 PRELIMINARY RMU TEST MATRIX – continued

Space Division — North American Rockwell

Test Item	TEST ITEM — Unit	Subsystem	System	PERFORMANCE — Inspection	Performance	Mass Properties	Mechanical Alignment	Mech. and Elec. Compatibility	Leak	DEVELOPMENT — Thermal	EMI	Static Loads	Model Vibration	Vibration	Acoustics	Shock	QUALIFICATION — EMI	Temp. (handling and storage)	Temperature Altitude	Humidity	Explosive Atmosphere	Acceleration	Space Simulation	Burst Test	Acoustics	Shock	Continuity, Hi Pot and Res.	Vibration	Thermal-Vacuum	Temp.-Cycling	ACCEPTANCE — Temperature Altitude	Space Environment Simulation	Vibration	Temp. Cycling	Continuity, Hi Pot and Res.	Proof Pressure	Thermal Vacuum
Attitude Control Subsystem (continued)																																					
Gears	x			x	x	x																															
Resolvers	x			x	x	x																															
Despin Drive Assembly	x			x	x	x				x	x						x	x	x									x	x		x						x
Communications Subsystem		x		x	x	x		x																							x	x					x
Omni-Antennas	x			x	x	x	x						x									x				x	x				x						x
Planar Array	x			x	x	x	x	x																													
Antenna Switch (Receiver)	x			x	x	x																															
Antenna Switch Driver	x			x	x	x																															
Antenna Switch (Transmitter)	x			x	x	x																															
Antenna Electronics	x			x	x	x																															
Comm Repeater	x			x	x	x																															
Comm Transmitter	x			x	x	x																															
T&C Subsystem		x		x	x	x		x																							x	x					x
WhipAntenna	x			x	x	x	x																														
Hybrid Balun	x			x	x	x																															
Diplexer	x			x	x	x																															
Command Regulator	x			x	x	x																															

Test Item			Performance						Development							Qualification														Acceptance						
Unit	Subsystem	System	Inspection	Performance	Mass Properties	Mechanical Alignment	Mech. and Elec. Compatibility	Leak	Thermal	EMI	Static Loads	Model Vibration	Vibration	Acoustics	Shock	EMI	Temp. (handling and storage)	Temperature Altitude	Humidity	Explosive Atmosphere	Acceleration	Space Simulation	Burst Test	Acoustics	Shock	Continuity, Hi Pot and Res.	Vibration	Thermal-Vacuum	Temp. Cycling	Temperature Altitude	Space Environment Simulation	Vibration	Temp. Cycling	Continuity, Hi Pot and Res.	Proof Pressure	Thermal Vacuum

T&C Subsystem (continued)

Item	Unit	Subsystem	System	Inspection	Performance	Mass Properties	Mechanical Alignment	Mech. and Elec. Compatibility	Leak	Thermal	EMI	Static Loads	Model Vibration	Vibration	Acoustics	Shock	EMI	Temp. (handling)	Temp. Altitude	Humidity	Explosive Atmosphere	Acceleration	Space Simulation	Burst Test	Acoustics	Shock	Continuity Hi Pot	Vibration	Thermal-Vacuum	Temp. Cycling	Temp. Altitude	Space Env. Sim.	Vibration	Temp. Cycling	Continuity Hi Pot	Proof Pressure	Thermal Vacuum
Command Receiver	x			x	x		x																														
Command Decoder	x			x	x		x																														
Spacecraft Clock	x			x	x		x																														
TM Encoder	x			x	x		x																														
TM Transmitter	x			x	x		x																														
Encoder Regulator	x			x	x		x																														
Signal Conditioner	x			x	x		x																														
Video/Illumination Subsystem			x	x	x	x		x	x	x				x													x	x				x					x
Cameras	x			x	x		x																														
Camera Electronics	x			x	x		x																														
Lense Assembly	x			x	x		x																														
Camera Turret Drive	x			x	x		x																														
Lights	x			x	x		x																														

FOLDOUT FRAME

FOLDOUT FRAME

Test Item	Unit	Subsystem	System	Inspection	Performance	Mass Properties	Mechanical Alignment	Mech. and Elec. Compatibility	Leak	Thermal	EMI	Static Loads	Model Vibration	Vibration	Acoustics	Shock	EMI	Temp. (handling and storage)	Temperature Altitude	Humidity	Explosive Atmosphere	Acceleration	Space Simulation	Burst Test	Acoustics	Shock	Continuity, Hi Pot and Res.	Vibration	Thermal-Vacuum	Temp. Cycling	Temperature Altitude	Space Environment Simulation	Vibration	Temp. Cycling	Continuity, Hi Pot and Res.	Proof Pressure	Thermal Vacuum
				PERFORMANCE						DEVELOPMENT							QUALIFICATION														ACCEPTANCE						
— Docking Subsystem																																					
Latches	x			x	x	x																															
Latch Pneumatics	x			x	x	x																															
— Power Subsystem		x		x	x	x		x		x	x						x			x	x																
Batteries	x			x	x	x																x					x	x			x						x
Solar Panels	x			x	x	x																x					x	x			x						x
Wiring Harnesses	x			x	x	x																x					x	x			x				x		x
Electronics	x			x	x	x																x					x	x			x						x
— Propulsion Subsystem		x		x		x																															
Apogee Motor	x			x		x																															
Squibs	x			x		x																															
— Structure Subsystem		x		x	x	x	x																														

TABLE 8-2. PRELIMINARY HARDWARE UTILIZATION LIST

SUBSYSTEM	ITEM	QUANTITY					DEVELOPMENT STATUS		
		BREADBOARDS	T-1 VEHICLE	F-1 VEHICLE	SPARES	TOTAL	FLOWN OR QUALIFIED	DEVELOPED	NEW
N/A	T-1 TEST SPACECRAFT		X						X
	F-1 PROTO-FLIGHT SPACECRAFT			X					X
REACTION CONTROL SUBSYSTEM	FILL AND DRAIN VALVE	3		3	1	7	X		
	FILTER	1		1	1	3	X		
	PRESSURE TRANSDUCER	1		1	1	3	X		
	THRUSTER ASSEMBLY	3		12	3	18	X		
	PROPELLANT TANK			2	1	3	X		
	MANIFOLDS & DISTRIBUTION	1*	1	1		2+			X
ATTITUDE CONTROL SUBSYSTEM	SOLAR ASPECT SENSOR ASSEMBLY	1*		1	1*	1+	X		
	SUN SENSOR			2	1	3	X		
	ACCELEROMETER			2	1	3	X		
	DPG ASSEMBLY	1		3	1	5		X	
	GYRO ROTOR ASSEMBLY	2		6	2	10	X		
	GIMBAL TORQUER	1		3	1	5	X		
	RESOLVER	1		3	1	5	X		
	HOUSING	1		3	1	5			X
	GEARS	2		6	2	10			X
	BALL BEARING	4		12	4	20	X		
	ELECTRONICS ASSEMBLY	1*		1	1	2+		X	X
	DESPIN DRIVE ASSEMBLY		1*	1	1*	1+			
COMMUNICATIONS SUBSYSTEM	OMNI ANTENNA			1	1	2			X
	PLANAR ARRAY ASSEMBLY			1	1	2	x		
	ANTENNA SWITCH (RECEIVER)			1	1	2	X		
	ANTENNA SWITCH DRIVER			1	1	2	X		
	ANTENNA SWITCH (TRANSMITTER)			1	1	2	X		
	ANTENNA ELECTRONICS			1	1	2	X		
	REPEATER			2	1	3	X		
	TRANSMITTER			1	1	2	X		

* PARTIAL

Space Division
North American Rockwell

TABLE 8-2. PRELIMINARY HARDWARE UTILIZATION LIST (CONTINUED)

SUBSYSTEM	ITEM	QUANTITY					DEVELOPMENT STATUS		
		BREADBOARDS	T-1 VEHICLE	F-1 VEHICLE	SPARES	TOTAL	FLOWN OR QUALIFIED	DEVELOPED	NEW
TELEMETRY & COMMAND SUBSYSTEM	WHIP ANTENNA			8	4	12	X		
	HYBRID BALUN			1	1	2	X		
	DIPLEXER			2	1	3	X		
	COMMAND REGULATOR			1	1	2	X		
	COMMAND RECEIVER			2	1	3	X		
	COMMAND DECODER			1	1	2	X		
	CLOCK			1	1	2	X		
	TM ENCODER			2	1	3	X		
	TM TRANSMITTER			2	1	3	X		
	ENCODER REGULATOR			2	1	3	X		
	SIGNAL CONDITIONER			2	1	3	X		
	SQUIB DRIVER ASSEMBLY			1	1	2			X
VIDEO & ILLUMI-NATION SUBSYSTEM	TV CAMERA AND ELECTRONICS			2	1	3	X		
	LENS ASSEMBLY			1	1	2		X	
	LIGHT ASSEMBLY	1		1	1	3			X
	TURRET ASSEMBLY	1		1		2			X
DOCKING SUBSYSTEM	LATCH ASSEMBLY	3		3	1	7			X
	LATCH PNEUMATIC ASSEMBLY	1		1	1	3		X	
POWER SUBSYSTEM	SOLAR PANEL ASSEMBLY (SET)			1	1	2			X
	SOLAR SUBSTRATES (SET)		1	1	1	3			X
	BATTERY			2	2	4	X		
	ELECTRONICS ASSEMBLY	1*		1	1	2+			X
	REGULATOR	1		1	1	3	X		
	BATTERY CHARGER	1		1	1	3	X		
	STATUS MONITOR	1		2	1	4	X		
	INVERTER	1		1	1	3		X	

* PARTIAL

Space Division
North American Rockwell

TABLE 8-2. PRELIMINARY HARDWARE UTILIZATION LIST (CONTINUED)

SUBSYSTEM	ITEM	BREADBOARDS	QUANTITY				DEVELOPMENT STATUS		
			T-1 VEHICLE	F-1 VEHICLE	SPARES	TOTAL	FLOWN OR QUALIFIED	DEVELOPED	NEW
PROPULSION SUBSYSTEM	APOGEE MOTOR (FLIGHT)			1	1	2	X		
	APOGEE MOTOR (INERT)		1			1	N/A	N/A	N/A
	SQUIBS	2		4	2	8	X		
THERMAL SUBSYSTEM	RADIOISOTOPE HEATER			15	3	18	X		
	PASSIVE ELEMENTS (SET)		1	1	1	3			X
STRUCTURE SUBSYSTEM	PRIMARY STRUCTURE		1	1		2			X
	SECONDARY STRUCTURE		1	1		2			X
	DOCKING CAGE STRUCTURE		1	1		2			X
	MECHANISMS (SET)	1	1	1		3			X

Space Division
North American Rockwell

Appropriate rates and factors (as approved by the cognizant Government Audit Agency) were then applied to these cost elements and a total cost was developed by the contracts and pricing department. Table 8-3 shows the resultant cost breakdown for second level elements of the work breakdown structure and indicates the total estimated cost of the program as 10.488 million dollars.

In addition to the above primary cost estimating methods, a Parametric Cost Analysis was performed on the basis of historical data on prior programs involving spacecraft of similar complexity and size. This data was used for assessing the "grass roots" estimates and substantiated that they are of the proper magnitude.

The alternate (optional) experiments analyzed and described in Section 6.0 were also assessed as to their rough-order-of-matnitude (ROM) impact on the total cost of the baseline program. Referring to Section 6.0, the estimated ROM delta-costs, per optional experiment, are as follows:

Communications Experiments. Two mechanizations are identified in Section 6.0. The first one is suited to performing the "ring-around ranging" experiment only. The delta-cost for implementing this mechanization was estimated at approximately 150K dollars.

The second experiment mechanization allows all three suggested communications experiments to be performed. Assuming (a) that the required L-Band ATS-type gear would be GFE, and (b) that the weight increase will not necessitate a larger booster (Delta 903), the delta cost was estimated as approximately 450K dollars (excluding cost of converting the 40 foot ground antenna to allow operation at L-Band).

Long Term Observation of ATS-V. The impact of implementing this experiment is considered negligible.

Rendezvous with ATS-F/G. Assuming that the weight increase (additional propellant) will not necessitate a larger booster (Delta 903), the cost of this experiment is considered negligible.

Fuel Transfer. Implementation of the fuel transfer experiment was estimated at approximately 225K dollars.

Table 8-3   Program Costs per WBS Element

WBS ELEMENT		ESTIMATED COST (K $)
NO.	DESCRIPTION	
1.0	Program Management	340
2.0	Systems Engineering	1,081
3.0	Design/Breadboard	2,870
4.0	Thermal/Structural Model	1,071
5.0	Prototype/Flight Model	2,955
6.0	Ground Support Equipment	597
7.0	Field Support	253
8.0	Flight Spares	908
9.0	Reliability and Quality Assurance	413
	TOTAL	10,488